Acta Universitatis Tamperensis 2117

HANNA VUORENPÄÄ

Development of Human Cell Based *In Vitro* Vascular and Cardiovascular Models

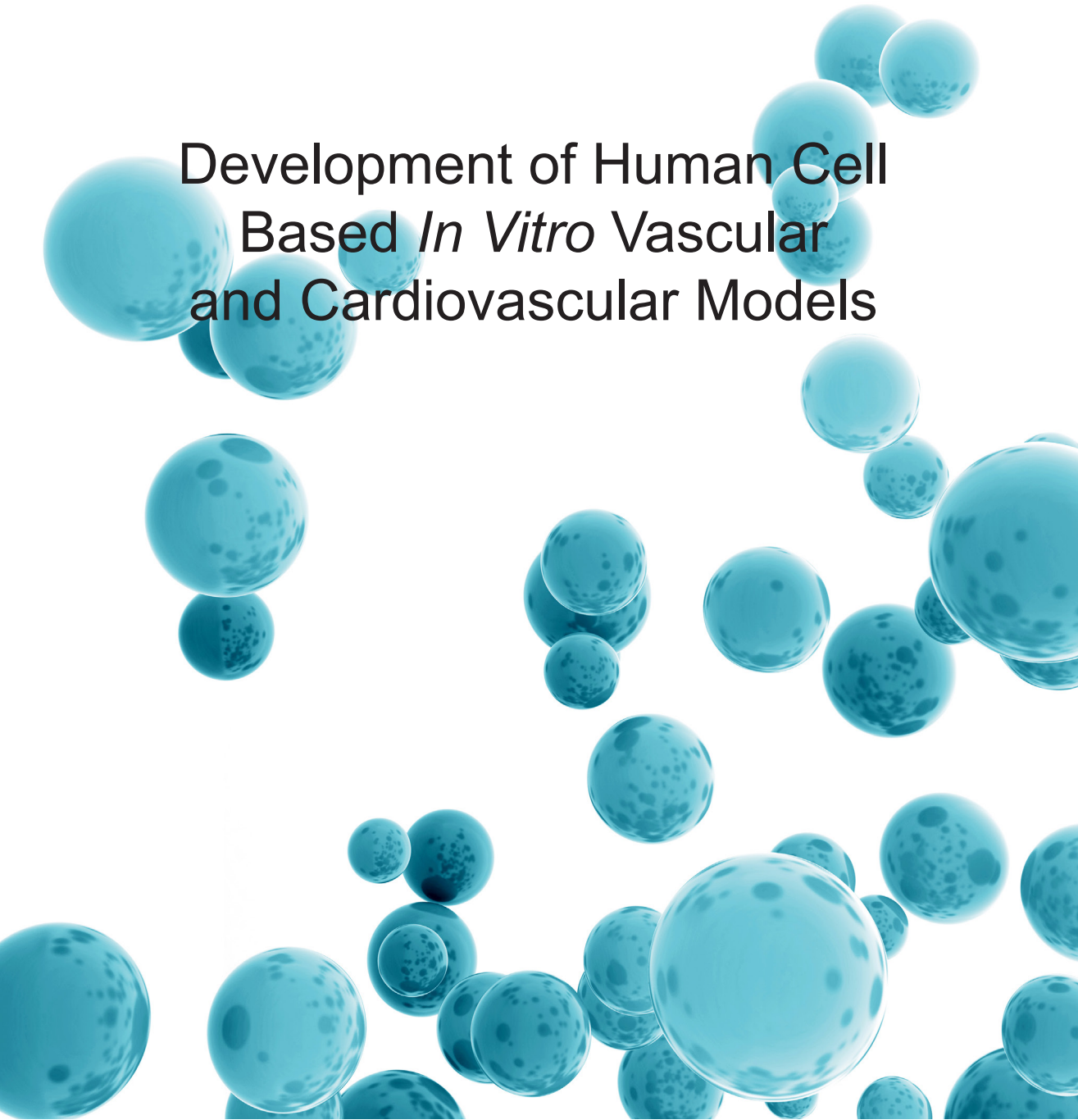

HANNA VUORENPÄÄ

Development of Human Cell Based *In Vitro* Vascular and Cardiovascular Models

ACADEMIC DISSERTATION
To be presented, with the permission of
the Board of the School of Medicine of the University of Tampere,
for public discussion in the small auditorium of building B,
School of Medicine, Medisiinarinkatu 3, Tampere,
on 19 December 2015, at 12 o'clock.

UNIVERSITY OF TAMPERE

HANNA VUORENPÄÄ

Development of Human Cell Based *In Vitro* Vascular and Cardiovascular Models

Acta Universitatis Tamperensis 2117
Tampere University Press
Tampere 2015

UNIVERSITY
OF TAMPERE

ACADEMIC DISSERTATION
University of Tampere, School of Medicine
BioMediTech
Finland

Supervised by
Docent Tuula Heinonen
University of Helsinki and
University of Turku
Finland
PhD Riina Sarkanen
University of Tampere
Finland

Reviewed by
Docent Riikka Kivelä
University of Helsinki
Finland
Professor Petri Lehenkari
University of Oulu
Finland

The originality of this thesis has been checked using the Turnitin OriginalityCheck service in accordance with the quality management system of the University of Tampere.

Cover design by
Mikko Reinikka

Distributor:
verkkokauppa@juvenesprint.fi
https://verkkokauppa.juvenes.fi

Acta Universitatis Tamperensis 2117
ISBN 978-951-44-9976-0 (print)
ISSN-L 1455-1616
ISSN 1455-1616

Acta Electronica Universitatis Tamperensis 1614
ISBN 978-951-44-9977-7 (pdf)
ISSN 1456-954X
http://tampub.uta.fi

Suomen Yliopistopaino Oy – Juvenes Print
Tampere 2015

To All Creatures Great and Small

Abstract

In order to protect human health and environment, safety assessment of drugs and industrial chemicals is mandatory according to the EU legislations. In pharmaceutical industry, lack of efficacy in addition to safety concerns in clinical trials are the main reasons for low success rate in the development of new drugs. Animal biology based test systems have often failed to predict the efficacy in humans and to reveal the adverse effects. In addition to poor predictive value, ethical concerns, high costs, time consuming protocols and low throughput have raised the need to replace animal models and to develop more advanced test systems.

Primary cells are considered as the traditional *in vitro* test systems for safety and efficacy assessment. More recently, human pluripotent stem cells have emerged as a promising source of specific cell types with the possibility for high throughput production with reasonably low costs. Growing data shows that instead of planar monocultures, supportive microenvironment, essential cell types and defined culture conditions are critical in developing more accurate *in vitro* models. Furthermore, before utilization in regulatory safety and efficacy assessment, careful characterization and validation of the developed *in vitro* models is necessary.

The main objective of this thesis was to develop advanced, human cell based tissue models to supplement or, preferably, replace animal tests and to be used in biomedical research. First, *in vitro* vascular models were developed for toxicity and efficacy assessment of pro- or anti- angiogenic compounds. Careful characterization with defined medium was performed to vasculogenesis-angiogenesis model for further intra-laboratory validation and to study the properties of the model as a supportive platform for tissue models. As the second main objective, we combined the vascular model with cardiomyocytes to establish a cardiovascular model for cardiac safety and efficacy assessment of chemicals.

The results showed that an extensive vascular-like network formation with mature tubules was reproducible formed in vasculogenesis-angiogenesis model in six day culture. The characterization with defined, serum-free medium showed that vasculogenesis-angiogenesis model is ready for intra-laboratory validation. Proof-of-concept on the enhanced viability of co-culture of cardiomyocytes and vascular-like network was received with two different vascular platforms. Finally, completely human cell based cardiovascular model was shown to possess more mature structure and response to chemicals than widely used cardiomyocyte monoculture.

It can be concluded that the developed vascular and cardiovascular models provide more advanced test systems for safety and efficacy assessment compared to widely used monocultures with the possibility to supplement or replace part of the tests currently performed with animal models. However, further characterization as well as *in vitro-in vivo* comparison on human cardiovascular model is needed before it may enter into validation.

Tiivistelmä

Lääkkeiden ja teollisuuskemikaalien turvallisuuden arviointi on säädetty EU:ssa pakolliseksi ihmisten terveyden ja ympäristönsuojelun takaamiseksi. Lääketeollisuudessa suurin ongelma uusien lääkeaineiden kehittämisessä on niiden riittämätön teho tai lääkeaineiden ihmisille aiheuttamat haittavaikutukset. Tähän on syynä usein se, että eläinmalleilla ei ole kyetty ennustamaan lääkeaineiden ja kemikaalien tehoa tai turvallisuutta ihmisille. Huonon ennustavuuden lisäksi eettiset syyt, korkeat kustannukset ja alhainen suoritusteho ovat syitä sille, että eläinbiologiaan perustuvat testausmallit halutaan korvata kehittyneemmillä menetelmillä.

Primaarisolut ovat perinteisesti käytettyjä *in vitro* testimenetelmiä lääkeaineiden ja kemikaalien turvallisuuden ja tehon arvioinnissa. Ihmisen pluripotenteista kantasoluista erilaistetut solut tarjoavat uuden mahdollisuuden yksilöllisten, spesifisten solutyyppien monistamiseen suhteellisen edullisin kustannuksin. Viimeaikaiset tutkimukset ovat osoittaneet, että yksisoluviljelmien sijaan kasvuympäristö, muut oleelliset solutyypit ja kontrolloidut kasvuolosuhteet ovat kriittisiä uusien, ennustavampien *in vitro* mallien kehityksessä. Tämän lisäksi *in vitro* mallien huolellinen karakterisointi ja validointi ovat edellytyksenä niiden hyväksymiselle virallisiksi testimenetelmiksi viranomaisohjeistoihin.

Tämän väitöskirjatyön päätavoitteena oli kehittää ihmissolupohjaisia kudosmalleja testimenetelmiksi, joilla voitaisiin täydentää tai korvata eläinkokeita ja saada suoraan ihmisiin sovellettavaa tutkimustietoa. Verisuonimuodostusta jäljittelevi *in vitro* malleja kehitettiin verisuonimuodostusta lisäävien tai estävien yhdisteiden testaamiseen. Vaskulogeneesi-angiogeneesi -verisuonimallin karakterisoinnissa kehitettiin uusi kasvatusliuos tulevaa laboratorion sisäistä validointia varten sekä tutkittiin mallin ominaisuuksia verisuoniverkostoa muodostavana pohjarakenteena. Lopullisena tavoitteena oli yhdistää verisuonimalli sydänlihassoluihin ja kehittää

täysin ihmissolupohjainen sydänmalli lääkeaineiden ja kemikaalien tehon ja turvallisuuden tutkimiseen.

Tulokset osoittivat, että vaskulogeneesi-angiogeneesi -mallissa muodostuu kypsiä verisuonimaisia rakenteita toistettavasti kuuden viljelypäivän aikana. Uusi kasvatusliuos tuki vaskulogeneesi-angiogeneesi -mallin kypsymistä aikuisen kaltaiseksi ja mallin todettiin olevan valmis laboratorion sisäiseen validointiin. Verisuonimallin ja sydänlihassolujen yhdistäminen sydänmalliksi osoitettiin toimivaksi kahdella erilaisella verisuonimaisella pohjarakenteella. Tulokset täysin ihmissolupohjaisesta sydänmallista osoittivat sydänlihassolujen kypsyvän aikuisen kaltaisiksi ja vastaavan kemikaalialtistuksiin yksisoluviljelmää herkemmin. Tämän väitöskirjatyön tulosten perusteella verisuoni- ja sydänmalli tarjoavat kehittyneemmän testausmenetelmän yhdisteiden toksisuuden ja tehon testaamiseen sekä mahdollisuuden korvata osa vastaavista eläinmalleilla suoritettavista testeistä. Sydänmalli vaatii kuitenkin jatkokarakterisointia sekä *in vitro-in vivo* vertailua ennen siirtymistä mallin validointiin.

Contents

List of original publications

The present thesis is based on the following publications that are referred to in the text by their Roman numerals (I-IV)

I Sarkanen JR, **Vuorenpää H**, Huttala O, Mannerström B, Kuokkanen H, Miettinen S, Heinonen T and Ylikomi T (2012). Adipose stromal cell tubule network model provides a versatile tool for vascular research and tissue engineering. Cells Tissues Organs 196: 385-397.

II Huttala O*, **Vuorenpää H***, Toimela T, Uotila J, Kuokkanen H, Ylikomi T, Sarkanen JR and Heinonen T (2015). Human vascular model with defined stimulation medium –a characterization study. ALTEX 32: 125-136. *equal contribution

III **Vuorenpää H***, Ikonen L*, Kujala K, Huttala O, Sarkanen JR, Ylikomi T, Aalto-Setälä K and Heinonen T (2014). Novel in vitro cardiovascular constructs composed of vascular-like networks and cardiomyocytes. In Vitro Cell Dev Biol Anim 50: 275-286. *equal contribution

IV **Vuorenpää H***, Miettinen K*, Pekkanen-Mattila M, Sarkanen JR, Ylikomi T, Aalto-Setälä K and Heinonen T (2015). Vascular-like Network Enhances Structural and Functional Maturation of Human Pluripotent Stem Cell derived Cardiomyocytes in Cardiovascular Construct. Submitted *equal contribution

Author´s contribution

Study I The author contributed to the performance of the practical laboratory work (cell isolation, culture and differentiation), measurements (immunocytochemistry, qRT-PCR, microscopical analyses) and the data analysis. In addition, the author contributed to the manuscript writing with the first author.

Study II The author was responsible for the design of the study and contributed to all laboratory work (cell isolation, culture and differentiation), measurements (immunocytochemistry, qRT-PCR, flow cytometry, confocal and electron microscopy) and the data analysis performed. In addition, the author was the main writer of the manuscript with the first author.

Study III The author was responsible for the design of the study and for all practical laboratory work related to the vascular models utilized in the study. The author also contributed to the performance of the measurements of the cardiovascular constructs (MEA, immunocytochemistry, microscopical analyses) and the data analysis. In addition, the author was the main writer of the manuscript with the second author.

Study IV The author was responsible for the design of the studies and for all laboratory work related to the vascular model utilized in the study. The author also contributed to the measurements of the cardiovascular construct (MEA, calsium imaging, qRT-PCR, immunocytochemistry, confocal microscopy) and the data analysis performed. In addition, the author was the main writer of the manuscript with the second author.

The contribution of co-authors have been significant in all of the studies.

Abbreviations

AA	ascorbic acid
ADRB1	beta-1 adrenergic receptor
Ang-1	angiopoietin 1
Ang-2	angiopoietin 2
ANOVA	analysis of variance
BSA	bovine serum albumin
CACNA1C	calcium channel, voltage-dependent, L type, alpha 1C subunit
cDNA	complementary deoxyribonucleic acid
CD31	platelet endothelial cell adhesion molecule
CD144	vascular endothelial cadherin
CM	cardiomyocytes
COL	collagen
Cx	connexin
DMEM/F12	Dulbecco's modified Eagle's medium nutrient mixture F-12
DNA	deoxyribonucleic acid
EBM-2	endothelial cell basal medium-2
EC	endothelial cell
ECM	extracellular matrix
EGF	epidermal growth factor
EGM-2	endothelial cell growth medium-2
FACS	fluorescence activated cell sorting
FBS	fetal bovine serum
FITC	fluorescein isothiocyanate
FGF	basic fibroblast growth factor
GAPDH	glyceraldehyde-3-phosphate dehydrogenase
GFP	green fluorescence protein
GLP	good laboratory practice
hASC	human adipose stromal cell
hERG	human ether-a-go-go gene
HE	heparin

hESC-CM	human embryonic stem cell derived cardiomyocytes
hPSC	human pluripotent stem cells
hPSC-CM	human pluripotent stem cell derived cardiomyocytes
HS	human serum
HUVEC	human umbilical vein endothelial cell
HY	hydrocortisone (cortisol)
IKr	delayed rectifier potassium current
IGF	insulin-like growth factor
in vitro	outside a living organism in an artificial environment
in vivo	within a living organism
iPSC-CM	induced pluripotent stem cell derived cardiomyocytes
ITS	Insulin, transferrin, Selenic acid medium supplement
KCNJ2	potassium channel, inwardly rectifying subfamily J, member 2
L-glut	L-glutamine
MEA	microelectrode array
mRNA	messenger ribonucleic acid
MSC	mesenchymal stem cell
MYH	myosin heavy chain
NRC	neonatal rat cardiomyocytes
OECD	Organization for Economic Co-operation and Development
PBS	phosphate buffered saline solution
REACH	Registration, Evaluation, Authorization and Restriction of Chemical substances
PDGFR-β	platelet derived growth factor beta
PECAM	platelet endothelial cell adhesion molecule
qRT-PCR	quantitative reverse transcriptase polymerase chain reaction
RNA	ribonucleic acid
RPLP0	ribosomal protein large P0
RT	room temperature
SCN5α	sodium channel, voltage gated, type V alpha subunit
SEM	scanning electron microscopy
SMA	smooth muscle actin
SMMHC	smooth muscle myosin heavy chain
TEM	transmission electron microscopy
TGF	transforming growth factor
TNNT2	cardiac troponin T

TRITC	tetramethyl rhodamine isothiocyanate
VEGF	vascular endothelial growth factor
VEGFR	vascular endothelial growth factor receptor
VSM	Vascular stimulation medium
vWf	von Willebrand factor

1 Introduction

Since animals, especially mammals, are similar to humans in complexity and physiological features, animal testing has been traditionally considered as the most appropriate way to predict human responses. Consequently, various biomedical research areas and the majority of the regulatory guidelines for safety evaluation relies on animal testing. (Heinonen, 2015) However, unreliability related to the translation of the results from animal tests to humans in addition to ethical and economical concerns calls for more advanced test systems (Suter-Dick et al., 2015). Beside general toxicity assessment, high drug attrition rate during clinical phases of drug development has led to an increasing need for test systems that predict clinical outcome better than conventional planar cell culture systems and animal models (Tourovskaia et al., 2014).

Lack of physiologically relevant *in vitro* models is a major obstacle for the implementation of *in vitro* tests systems. Traditionally used primary cell cultures and transformed cell lines often fail to adequately mimic the *in vivo* situation since primary cells tend to lose their differentiated characteristics and genotypic changes take place during the transformation of cell lines. (Suter-Dick et al., 2015). The potential of human pluripotent stem cells (hPSC) to provide differentiated cell models for drug development, safety assessment and regenerative medicine is widely acknowledged (O'Connor, 2013). The utilization of hPSC in improving human safety and, at the same time, following the 3Rs principles of refinement, reduction and replacement of animals, highlights the significant impacts of this field. (Kolaja, 2014)

In vitro models of vasculogenesis and angiogenesis are needed for basic biomedical research as well as for translational research including drug development with screening of pro- and anti-angiogenic compounds (Ucuzian & Greisler, 2007, Folkman, 2007). In addition, drug-induced vascular injury has been challenging pharmaceutical industry causing termination of development of new drug candidates in nonclinical safety assessment (Mikaelian et al., 2014, Morton et al., 2014).

Presently, there are no relevant *in vitro* models available for screening applications to study drug-induced vascular injury (Mikaelian et al., 2014) or embryonic vascular development as part of developmental toxicity assessment (Heinonen, 2015).

Heart has been shown to be particularly prone to toxic effects of drugs that can cause severe adverse effects including decreased cardiac contractility, increased arrhythmia, ischemia and even sudden death (Redfern et al., 2003, Lasser et al., 2002, Lexchin, 2005). Hence, assessment of the risk of a drug to cause cardiac electrophysiological disturbances is regulated as part of the standard preclinical evaluation of new compounds (Braam et al., 2010). Since adverse cardiac effects are the main cause for drug withdrawal from the market and delays in regulatory approval, heart is one of the major target for pharmaceutical industry. For these reasons, relevant test systems for cardiac toxicity assessment are urgently needed (Kettenhofen & Bohlen, 2008).

The objective of this thesis was to develop and characterize vascular model for toxicity and efficacy assessment of pro- and anti-angiogenic compounds and to be used as vascular platform for tissue constructs. Another main objective was to combine the vascular model with cardiomyocytes in order to establish cardiovascular model for cardiac safety and efficacy assessment with human relevance. In the development of these *in vitro* vascular and cardiovascular models, cells mainly of human origin were used, medium was optimized and, furthermore, characterization on structural, gene expression and functional level was performed.

2 Review of the literature

2.1 Development and characteristics of vasculature

Blood vessels arose during evolution to carry oxygen, essential nutrients and waste products to distant organs. In the developing embryo, cardiovascular system is the first organ system developed (Carmeliet, 2005). Blood circulation is crucial to the mammalian embryo when its growth exceeds the limits of oxygen diffusion at about 100–200 μm in size. This occurs in the 3rd week of gestation in humans and 10th day of gestation in rats. (Knudsen & Kleinstreuer, 2011) At the same time, heart starts to beat and vessels of the primary vascular plexus remain either as capillaries or differentiate into arteries or veins (Buschmann & Schaper, 1999). To increase blood transport into growing tissues capillaries sprout and branch into larger, more complex networks. The process of vascular development is most obvious during embryogenesis when the first primitive vascular structures develop. However, similar remodeling processes are thought to be essential for physiological and pathological angiogenesis in adult. (Adams & Alitalo, 2007)

There are several known mechanisms for blood vessel formation. Vasculogenesis is the earliest morphogenetic process of vascularization and takes place during the early embryonic development but also during adult life. (Rivron et al., 2008, Carmeliet & Jain, 2011, Flamme et al., 1997, Drake, 2003) In vasculogenesis, angioblasts, i.e. endothelial precursor cells that share an origin with hematopoietic progenitor cells, differentiate into endothelial cells (EC) and assemble into a primitive vascular plexus (Drake, 2003). Vasculogenesis can be divided into different steps including (1) differentiation of mesodermal cells into angioblast; (2) differentiation of angioblasts into EC; (3) formation of the primary vascular plexus and aggregates that establish cell-cell contacts without lumen; (4) a primary endothelial tube is formed composed of polarized EC; (5) a primary vascular network is formed out of primary endothelial tubes and (6) pericytes and vascular smooth muscle cells are recruited to stabilize the vascular network. (Ko et al., 2007)

In subsequent vessel sprouting, known as angiogenesis, the preexisting vascular network expands, invades to target tissues and gives rise to the vascular system. (Carmeliet & Jain, 2011, Buschmann & Schaper, 1999). Angiogenesis process can be divided into six different steps with (1) vasodilation; (2) basement membrane degradation; (3) cell migration; (4) formation of lumen; (5) synthesis of new basement membrane and (6) recruitment of pericytes or vascular smooth muscle cells to stabilize the vessel. (Ko et al., 2007) During adulthood, most blood vessels are, however, quiescent and angiogenesis occurs mainly in the cycling ovary and in the placenta during pregnancy (Carmeliet, 2005). Tissues can also become vascularized by other mechanisms, e.g. by vessel splitting known as intussusception or tumor cells can take over the existing vasculature. (Carmeliet & Jain, 2011)

De novo formation of vascular structures during embryogenesis begins with the formation of endothelial progenitor cells in the extraembryonic mesoderm allantois (Chen & Zheng, 2014). In humans, this fetoplacental vasculogenesis starts at approximately 21 days after conception by formation of endothelial tubes (Kaufmann et al., 2004). Blood flow to the maternal, fetal and placental units is established during implantation and placentation as the maternal-fetal circulation connects within the placenta (Reynolds & Redmer, 2001). The placental vasculature further expands and extensive vascularization from pre-existing vessels occurs in maternal as well as in fetal site (Chen & Zheng, 2014). Blood flow gradually increases until the mid-gestation and after that according to the rate of the growing fetus (Reynolds & Redmer, 2001). Due to active blood vessel formation, the placenta provides an extensive source of pro- and anti-angiogenic factors (Chen & Zheng, 2014). In addition, umbilical cord blood has been shown to contain high number of hematopoietic stem/progenitor cells (Huss, 2000).

2.1.1 Differentiation and maturation of vascular structures

In order to reach the complex organization, the immature vascular network, formed by vasculogenesis or angiogenesis, must mature at the level of the vessel wall and at the network level. Maturation of the vessel wall involves recruitment of mural cells, development of the surrounding matrix and organ-specific differentiation of EC, mural cells as well as interendothelial junctions, apical-basal polarity and surface

receptors. Maturation of the network involves optimal patterning of the vascular network by branching and expanding to meet the tissue spesific requirements. The timing of these processes may overlap allowing the sustained development of vasculature towards maturation. Each molecule involved in the blood vessel formation has multiple functions in the development of a mature vascular network. (Jain, 2003, Stratman et al., 2009, Risau, 1997).

Maturation involves a transition from an actively growing vascular structures to a quiescent, fully formed and functional network (Adams & Alitalo, 2007). Incomplete maturation is frequently detected in pathological conditions, particularly in the vasculature of tumors. A prominent feature of the maturation is the recruitment of mural cells including pericytes and vascular smooth muscle cells. Pericytes establish direct cell–cell contact with EC and cover capillaries and immature blood vessels. (Aguilera & Brekken, 2014) Vascular smooth muscle cells, on their behalf, cover mature and larger vessels, such as arteries and veins, and are separated from the endothelium by a basement membrane. These mural cell types share a mesenchymal, fibroblast-like morphology. (Adams & Alitalo, 2007) The vessels are stabilized not only by recruiting mural cells but also by generating extracellular matrix (Stratman & Davis, 2012) by controlling the formation of lumen and tubule network formation (Sacharidou et al., 2012, Davis et al., 2011).

2.1.2 Structure of the vascular network

The adult vasculature, with a surface area of ~1,000 m², consists of EC, extracellular matrix (ECM) and supporting mural cells that include pericytes for capillaries and vascular smooth muscle cells for larger vessels (Figure 1). More complex vessel structures may also include fibroblasts. (Rivron et al., 2008, Buschmann & Schaper, 1999) The smallest microvessels are capillaries that consist of lumen with an inner diameter of 4-10 μm and a very thin vessel wall composed of EC. (Ko et al., 2007) Vascular network formation is discussed in detail below.

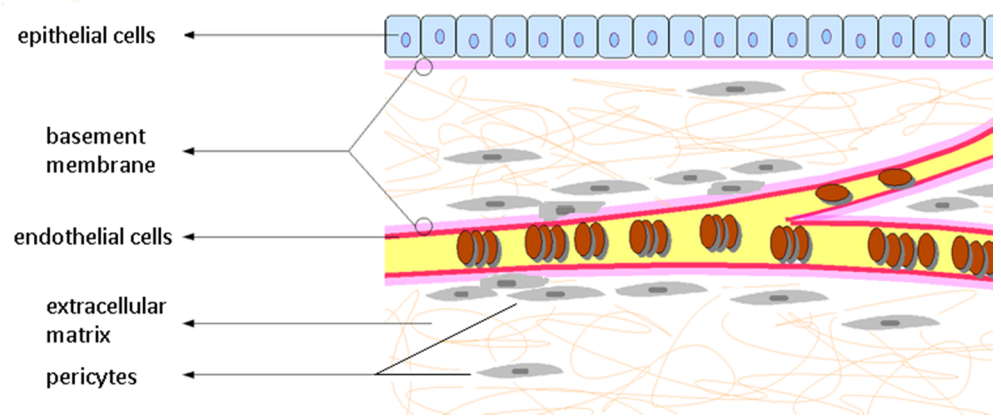

Figure 1. Structure of blood vessel with capillary lining endothelial cells, basement membrane, extracellular matrix and pericytes. Image modified from https://en.wikipedia.org/wiki/Extracellular_matrix

2.1.2.1 Endothelial cells

Endothelial cells are one of the main building blocks of blood vessels with the role in isolating the blood flow from surrounding tissues. EC function as barriers in controlling the infiltration of blood proteins and cells through the vessel wall. (Dejana, 2004) In the angiogenesis process, some EC within the capillary wall, known as the tip cells, are responsible for sprouting. After stimulation with angiogenic factors, the quiescent vessel dilates and the tip cell starts to form branch from the pre-existing vascular structures. (Carmeliet & Jain, 2011) Importantly, EC interact with each other and with variety of other cell types including pericytes, smooth muscle cells and leukocytes as well as extracellular matrix in the formation

of blood vessels and in controlling the infiltration of proteins (Hillen et al., 2006). Turnover time of EC is usually hundreds of days which makes them one of the most quiescent and genetically stable cells in the body. (Kalluri, 2003) EC are widely used to study adverse aspects of EC biology and angiogenesis (Hillen et al., 2006).

Heterogeneous characteristics between EC in different organ sites and vessel types have been detected. For example, studies in humans and in animals have shown that the expression level of von Willebrand Factor in the lung vasculature is higher in larger vessels. (Pusztaszeri et al., 2006) Common EC markers include platelet endothelial cell adhesion molecule (CD31/PECAM), vascular endothelial cadherin (CD144), hematopoietic progenitor cell antigen (CD34), endoglin (CD105), von Willebrand factor (vWf, Factor VIII–related antigen), ecto-5'-nucleotidase (CD73) and intercellular adhesion molecule 2 (ICAM-2, CD102) (Garlanda & Dejana, 1997).

EC express a wide variety of ion channels and show regional heterogeneity including differences in Ca^{2+} signaling as well as in immunological and in metabolic properties. Although EC are nonexcitable cells, the abundance of ion channels in the plasma membrane of them has raised questions about their functional role. Ion channels are involved in controlling intercellular permeability, EC proliferation, and angiogenesis. They might be involved also in the regulation of the traffic of macromolecules, e.g. von Willebrand factor. (Nilius & Droogmans, 2001)

2.1.2.2 Pericytes

Microvessels are composed of EC, surrounded by basal lamina and single pericytes whereas large vessels are covered with multiple layers of smooth muscle cells and collagenous fibers. Smooth muscle cells in large vessels support and regulate blood flow. Although pericytes have been mainly associated with blood vessel stabilization (Bergers & Song, 2005) they have several other relevant functions related to angiogenesis (Gerhardt & Betsholtz, 2003). Pericytes sense the presence of angiogenic stimuli as well as the hemodynamic forces. In the formation of blood vessels, EC and pericytes form a common basement membrane. Furthermore, mature pericytes form umbrella-like contacts with the EC in vascular structures thus covering several capillary structures. (Hall, 2006). Pericytes communicate with EC by direct physical contact through gap junctions and also with paracrine signaling

pathways (Bergers & Song, 2005). Pericytes may contribute to morphogenetic control of capillary diameter through their ability to contract or, perhaps more likely, control capillary diameter by regulating EC proliferation and differentiation. (Gerhardt & Betsholtz, 2003)

Pericytes are multipotent cells with the capacity to differentiate into vascular smooth muscle cells, other mesenchymal cell types and also fibroblasts *in vitro* and *in vivo*. The extent of pericyte coverage in capillaries is tissue specific ranging from 10-50 % thus reflecting the specific functional features of the microvessels in different organs. Pericytes are prevalent at capillary branch points whereas the part of a vessel engaged in the transport of gases and/or nutrients is typically free of pericytes. (Gerhardt & Betsholtz, 2003)

Pericytes express a number of markers of differentiation such as alpha smooth muscle actin (α-SMA), desmin, chondroitin sulfate proteoglycan (NG-2) and platelet-derived growth factor receptor β (PDGFR-β). (Hall, 2006) In addition to these, molecular markers including the regulator of G-protein signaling RGS5 or the reporter transgene X-LacZ4 label only part of the heterogeneous pericyte population and are, moreover, also expressed by vascular smooth muscle cells and other cell types. No single marker is able to identify all pericytes. Furthermore, it remains unclear whether there are other, unidentified and perhaps tissue-specific subsets of mural cells. (Adams & Alitalo, 2007)

2.1.2.3 Extracellular matrix

Extracellular matrix (ECM) and basement membrane have an important role in angiogenesis as EC originate from existing blood vessels, are surrounded by matrix and eventually maturate through basement membrane formation. (Kalluri, 2003). ECM has a mechanical role in supporting and maintaining the tissue architecture. Although the extracellular matrix molecules play an important role in stabilizing blood vessel structures, the components of vascular basement membrane are required also for the initiation of angiogenesis process. (Sottile, 2004) Moreover, ECM regulates migration, proliferation and differentiation of EC in the formation of vascular structures. (Iivanainen et al., 2003)

In resting tissues, interactions between EC and ECM are stable whereas in the presence of angiogenic stimuli EC start to degrade ECM components with matrix metalloproteinases. This change in interaction promotes the process of new blood vessel formation. (Sottile, 2004) ECM is organized into two layers: 1) vascular basement membrane located between EC and vascular smooth muscle cells or pericytes and 2) the interstitial matrix. Basement membrane consists of molecules including collagen IV, laminins and heparin sulfate proteoglycans (e.g. perlecans) whereas typical components of the interstitial matrix are fibrillar collagens and glycoproteins such as fibronectin. (Iivanainen et al., 2003) Type IV collagen is the main component of the vascular basement membrane and the assembly of the type IV collagen scaffold is important for basement membrane integrity and structural organization. Type IV collagen has also been shown to promote vascular elongation, proliferation, and stabilization in a dose-dependent manner. (Bonanno et al., 2000)

Although several cell types are responsible for producing constituents of the basement membrane, fibroblasts are known to secrete the precursor components of ECM. Several studies have shown that cells can sense the three-dimensional organization of fibrillar ECM proteins, and that cell phenotype can be altered by changing the composition or organization of matrix fibrils (Ichii et al., 2001, Sottile, 2004, Sechler & Schwarzbauer, 1998).

2.1.2.4 Junctions

Cell-cell interactions are important for the regulation of tissue integrity and for generation of barriers between different organs (Hillen et al., 2006). Intercellular junctions mediate adhesion and communication between EC and epithelial cells. In the endothelium, cells are connected through tight junctions, adherence junctions and gap junctions. (Bazzoni & Dejana, 2004) The expression and organization of these junctions depends on the type of vessels and the permeability requirements of the organ. During the organization of an EC monolayer into vascular structures, cell-cell connections follow different steps of maturation. (Bazzoni & Dejana, 2004, Dejana, 2004, Nilius & Droogmans, 2001)

Gap junctions are communication structures that control the passage of small molecular weight compounds and ions between neighboring cells (Bazzoni &

Dejana, 2004). They allow direct electrical and metabolic communication between EC, between EC and SMC and also between EC and lymphocytes or monocytes. Various isoforms of connexins are thought to be responsible for these functional cell-cell connections. At least three isoforms including Cx-37, Cx-40, and Cx-43 are expressed in EC. Cx-43 has shown to be more abundant in macrovascular than in microvascular cells whereas coronary artery endothelium expresses Cx-40 and Cx-37 but lacks Cx-43. Gap junctions can be formed between the same or different isoforms of connexins. Expression of connexins depends on the functional state of EC and is modulated by growth factors, inflammatory agents (TNF-α) and by mechanical forces. (Nilius & Droogmans, 2001).

Adherence junctions and tight junctions share the same binding mechanism where adhesion is mediated by transmembrane protein forming a zipper-like structure along the cell border (Hillen et al., 2006). Adherence junctions play an important role in contact inhibition of EC growth and in organization of new vessels. The major functional purpose of tight junctions is to provide a barrier within the membrane by regulating paracellular permeability and maintaining cell polarity by subdividing the plasma membrane into an apical and basolateral side. (Bazzoni & Dejana, 2004) In tight junctions, adhesion is mediated by claudins and occludins whereas at adherence junctions adhesion is mostly promoted by vascular endothelial cadherin. Nectin participates in the organization of tight junctions as well as adherence junctions. Outside these junctional complexes, platelet endothelial cell adhesion molecule (PECAM) contributes to endothelial cell–cell adhesion. (Dejana, 2004)

2.1.3 Functional properties of vasculature

Blood vessels are crucial for organ growth in the embryo and repair of wounded tissue in adults (Carmeliet, 2005). All tissues need to be vascularized in order to develop and survive. Capillaries are the smallest blood vessels with the inner diameter of 4-10 μm. Vascular system contributes also to immune protection by circulating immune cells, it controls temperature and blood pressure and, further, provides a biochemical communication system. (Ko et al., 2007)

Properly functioning vasculature requires branching of vascular structures. It has been shown that vascular patterns produced in the adult are highly variable. The lumenal surface of blood vessels is constantly exposed to hemodynamic forces, primarily to shear stress, created by the blood flow in vivo. Hemodynamic forces play a critical role in the remodeling of vascular network according to tissue specific requirements. (Dor et al., 2003)

2.1.4 Regulation of blood vessel formation

Blood vessel formation is a strictly organized process including vascular initiation, formation, maturation, remodelling and regression that are controlled and modulated to meet the tissue requirements (Figure 2) (Staton et al., 2009). In the regulation of blood vessel formation, important signaling factors include VEGF-A in sprouting vessel formation, Notch/Delta signaling in specification and TGF-beta/Angiopoietin in the stabilization of vessel structures (Knudsen & Kleinstreuer, 2011, Bikfalvi & Bicknell, 2002). Growth factors and signaling pathways related to blood vessel formation are discussed below in detail.

2.1.4.1 VEGF

Vascular Endothelial Growth Factor (VEGF) family consists of six members: VEGF-A, PlGF, VEGF-B, VEGF-C, VEGF-D, and orf virus VEGF (VEGF-E) (Liekens et al., 2001). VEGF (also known as VEGF-A) is the main component of VEGF family stimulating angiogenesis in health and in disease (Carmeliet & Jain, 2011, Tang et al., 2015). VEGF-A exerts its biologic effect through interaction with cell surface receptors, i.e. transmembrane tyrosine kinases. VEGF receptor-1 (VEGFR-1) and VEGFR-2 are mainly expressed on vascular EC and VEGFR-2 appears to be the major receptor mediating the pro-angiogenic effects of VEGF-A. (Otrock et al., 2007) VEGFR-2 deficiency as well as loss of VEGF aborts vascular development. (Carmeliet & Jain, 2011)

VEGF is expressed by many cell types and in different tissues including brain, kidney, liver, and spleen (Liekens et al., 2001). Members of the VEGF family are produced by human fibroblasts and are important in regulating vascular EC

proliferation (Wong et al., 2007). *In vitro*, VEGF stimulates ECM degradation, proliferation, migration, and EC tubule formation as well as expression of MMP-1 (Figure 2). *In vivo*, VEGF has been shown to regulate vascular permeability in the initiation of angiogenesis. During embryogenesis, VEGF promotes differentiation and proliferation of EC and the formation of immature vessels. (Liekens et al., 2001, Domigan et al., 2015) Beside growth factors, VEGF levels are also regulated by tissue oxygen levels as hypoxia induces VEGF expression rapidly and reversibly. On the contrary, normoxia down-regulates VEGF production and causes regression of newly formed blood vessels. With these opposing processes, the vasculature meets the metabolic requirements of the specific tissue. (Liekens et al., 2001)

2.1.4.2 FGF family

The fibroblast growth factor (FGF) family consists of at least 19 members (Liekens et al., 2001) in which heparin-binding protein mitogens acidic and basic fibroblast growth factors (aFGF and FGF-2) play an important role in angiogenesis (Figure 2) (Otrock et al., 2007). FGF-2 induces tubule formation in collagen gels and modulates gap junction communication as well as VEGF up-regulation *in vitro*. FGF-2 is expressed at low levels in almost all tissues with high levels reached in the brain and pituitary. It is found also in many cultured cell types, including fibroblasts, EC, smooth muscle cells and glial cells. (Liekens et al., 2001)

ECM sequesters angiogenic factors, such as FGF-2 and heparin-binding forms of VEGF. Although FGF-2 is not required for angiogenesis, it stimulates EC proliferation and migration and acts synergistically with VEGF to promote angiogenesis *in vivo*. Matrix-bound FGF-2 can be released by proteolysis and induce VEGF expression by EC. Certain heparin-binding isoforms of VEGF can also release matrix-bound FGF-2 suggesting that some of the biological effects of VEGF may be mediated by FGF-2. (Sottile, 2004)

2.1.4.3 Angiopoietins and Tie signaling

Angiopoietins and Tie -receptors play a critical role in angiogenesis. The angiopoietin family consists of three ligands: angiopoietin-1 (Ang-1), angiopoietin-2 (Ang-2) and

angiopoietin-4 (Carmeliet & Jain, 2011). All three angiopoietins bind to Tie-2 while Tie-1 remains an orphan receptor. However, an interaction between Tie-1 and Tie-2 occurs and both receptors translocate to EC cell-cell contacts upon angiopoietin stimulation. (D'Amico et al., 2014) Angiopoietin/Tie signaling is the prominent system to maintain quiescent state in healthy vasculature. Angiopoietin-1 function as a Tie-2 agonist and Ang-2 acts as a competitive antagonist in a context-dependent manner. Ang-1 is expressed by mural and tumor cells whereas Ang-2 is expressed by angiogenic tip cells in the initiation of angiogenic process (Figure 2). (Carmeliet & Jain, 2011) Expression patterns of the two Tie -receptors, are similar to those of VEGF -receptors. Tie-1 mRNA is highly expressed in embryonic vascular endothelium, angioblasts and endocardium whereas it is weakly expressed in an adult endocardium. (Otrock et al., 2007)

Through the Tie-2 receptor Ang-1 induces the remodeling and stabilization of the blood vessels with interaction with the ECM. In an adult vessel, Ang-1 is associated with Tie-2 to keep the vessels in a stable state. (Liekens et al., 2001) Ang-1 promotes mural cell coverage and basement membrane deposition thus promoting vessel tightness. In the presence of angiogenic stimulators, sprouting EC release Ang-2 thus enhancing mural cell detachment, vascular permeability and EC sprouting. (Carmeliet & Jain, 2011). Up-regulation of Ang-2, by hypoxia or VEGF, disrupts the interaction between Ang-1 and Tie-2, resulting in destabilization of the vessels. (Liekens et al., 2001)

2.1.4.4 Platelet-derived growth factor

To obtain an adequate function, vessels must mature and be covered with mural cells (Carmeliet & Jain, 2011). Platelet derived growth factor β (PDGF-B) plays a critical role in the recruitment of pericytes to newly formed vessels as well as in differentiation of smooth muscle cells (Figure 2). (Gerhardt & Betsholtz, 2003, Vikkula et al., 1996) In addition to PDGF-B, PDGF family is composed of two other isoforms including PDGF-A and -C which carry out their biological activities by receptors PDGFR-α and PDGFR-β. (Liu et al., 2014) Sprouting EC secrete PDGF-B signaling through PDGFR-β that is expressed by mural cells during blood vessel formation. Secretion of PDGF-B results in proliferation and migration of mural cells

during vessel maturation. (Armulik et al., 2005) In smooth muscle cells/pericytes PDGF-B has been shown to upregulate Ang-1 expression and to regulate transforming growth factor-β expression (Nishishita & Lin, 2004).

PDGF also functions as one of the key players in pathological processes including cancers and atherosclerosis by regulating cell proliferation, differentiation, apoptosis, angiogenesis and metastasis (Liu et al., 2014). *Pdgfb* and *pdgfrb* knockouts have been shown to lead to lethal phenotype with vascular dysfunction. The primary cause of the phenotype is the lack of pericytes leading to endothelial hyperplasia, abnormal junctions, and excessive luminal membrane folds. (Armulik et al., 2005)

2.1.4.5 Transforming growth factor

The maturation of blood vessels relies partly on transforming growth factor β (TGF-β) signaling. TGF-β stimulates mural cell differentiation, proliferation and migration as well as promotes production of ECM (Figure 2). In humans, mutations in TGF-β receptor 2 (TGFBR2, endoglin) expressed by EC, causes arteriovenous malformations and abnormally remodeled vessel walls (Armulik et al., 2005). TGF-β signaling in EC contributes to vessel maturation by secretion of PAI1 by preventing degradation of the perivascular matrix. (Potente et al., 2011) TGF-β is produced by a variety of cell types including EC and smooth muscle cells (Nishishita & Lin, 2004).

Several studies have shown the importance of TGF-β for vascular smooth muscle cells differentiation *in vitro*. Activation of TGF-β is dependent on EC–pericyte contact and TGF-β signaling in mesenchymal cells is required for their differentiation into the mural cell lineage. Gap junctions between EC and pericytes appear to be involved in the TGF-β activation, and are also required for endothelium-induced mural differentiation, as demonstrated by studies of connexin 43 knockout mice. (Armulik et al., 2005)

2.1.4.6 Notch/Delta signaling

In the vertebrate cardiovascular system, multiple Notch family receptors and ligands are expressed during critical stages of embryonic and postnatal development. Functional studies in mice and fish have shown that the formation of blood vessel network, the proliferation of EC and the differentiation of arteries and veins are controlled by Notch signaling. The Notch pathway is an evolutionary highly conserved signaling pathway with critical role in vascular morphogenesis in almost all vertebrates. Notch receptors are transmembrane proteins with large extracellular domains. (Roca & Adams, 2007) Four Notch molecules (Notch1–Notch4) interact with five ligands, including Delta-like 1, Delta-like 3, Delta-like 4, Jagged1 and Jagged2 (Yan & Plowman, 2007). Delta-like 4 and VEGF are the only known genes where loss of a single allele results in embryonic lethality due to defective vascular development. Hence, blockade of Delta-like 4 may impair remodeling of the tumor vasculature by preventing the progression to stabilized vessels. (Yan & Plowman, 2007)

The Notch pathway is a regulator of cell fate specification, growth and differentiation (Figure 2). Notch/delta is a cell-cell interaction signaling pathway helping similar cells to integrate information. An interaction in several levels between VEGF and Notch/delta pathways is involved in the development of vascular network. VEGF pathway provides signals from surrounding tissues to EC and Notch/delta pathway acts among the EC to respond appropriately to the VEGF signals. (Thurston & Kitajewski, 2008)

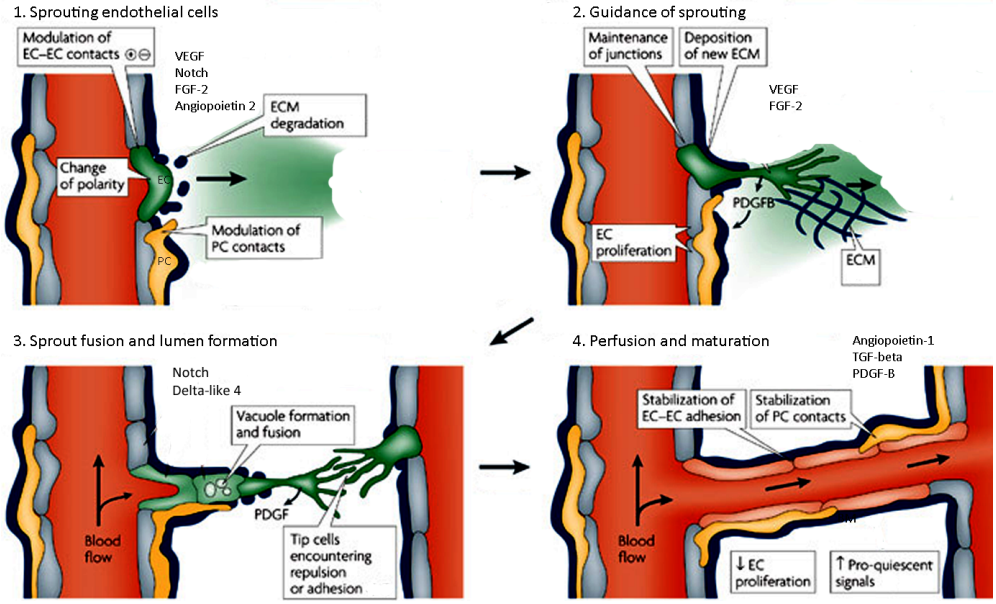

Figure 2. Growth factors related to different steps of blood vessel formation and maturation. 1) Some endothelial cells (EC) within the vessel wall, known as tip cells, lead the growing sprout; 2) EC guidance is controlled by VEGF-A and PDGF-B that promote the recruitment of pericytes (PC); 3) Notch and Delta-like 4 signaling leads to formation of vascular lumen by fusion of vacuoles; 4) The recruitment of pericytes and deposition of extracellular matrix (ECM) proteins into basement membrane (BM) promote vessel maturation. Image modified from Adams&Alitalo (2007).

2.1.5 Disturbances in vascular development

The formation of new blood vessels is essential for organ growth and repair (Carmeliet, 2005). However, angiogenesis is typically quiescent in the adult except in exercise (Kivela et al., 2008), female reproductive system and in pathological conditions (Knudsen & Kleinstreuer, 2011). Imbalance in the blood vessel formation contributes to numerous disorders including cancer, rheumatoid arthritis, cardiac ischemia, retinal disorders, psoriasis, inflammatory bowel disease and infertility (endometriosis) (Liekens et al., 2001, Knudsen & Kleinstreuer, 2011). Inadequate vessel maintenance or decreased growth causes ischemia after myocardial infarction, and neurodegenerative or obesity-associated disorders, whereas excessive vascular growth or abnormal remodelling promotes cancer, inflammatory disorders and retinal disorders (Potente et al., 2011). The process leading to angiogenesis is strictly controlled with positive (inductors) and negative (inhibitors) regulators. The

progress of the process is defined by the balance between these regulators. The mechanism of action of several new drugs used in cancer treatments is to prevent angiogenesis thus inhibit the tumor growth (Staton et al., 2009).

Genetic studies have shown that perturbing embryonic vascular development may cause adverse consequences from benign vascular malformations to embryolethality. Defects in pathways linked to vascular development and angiogenesis, such as VEGF, PDGFR-β, TGF-β and Tie-2, are suggested to play critical role in vascular malformations. (Knudsen & Kleinstreuer, 2011)

2.2 Development and characteristics of heart

Heart is the first organ to form in vertebrates and has a vital role in distributing nutrients and oxygen to the embryo (Buckingham et al., 2005). Formation of heart is a complex process starting at early phase of embryogenesis prior to gastrulation. Cardiac cells originate from the mesodermal germ layer with inductive signals coming from the adjacent cell populations, especially from the endoderm (Verma et al., 2013). The initial form of the heart is the heart tube that results from migration and organization of precursor cells from the cardiac crescent (Figure 3) (Nemer, 2008). In addition to growth of cells within the heart tube, studies in chicken and mouse have shown that further recruitment of heart progenitor cells occurs at the poles of the heart tube referred as the heart fields. The first heart field gives rise to differentiated myocardial cells of the cardiac crescent and early heart tube. The second heart field, located in the heart tube at the outflow tract (ot, Figure 3), has been identified as another source of cells with myocardial potential. (Buckingham et al., 2005) Differentiation process from mesodermal cells into cardiac progenitor cells in the cardiac crescent leads towards immature cardiomyocytes when the cells stop proliferating (Verma et al., 2013). Primitive heart tube starts to beat at approximately 3 weeks of gestation in man (Brand, 2003). Heart tube is composed of a contractile myocardium that is essential for its action as a central pump. Heart tube, formed by the fusion of cardiac crescent, subsequently undergoes looping that is followed by expansion into primitive chambers. After multi-phased regionalization of the myocardium, a four-chambered heart tissue is formed. (Buckingham et al., 2005) Adult human heart has been shown to have some regenerative capacity. Cells isolated from human atrial and ventricular biopsies possess characteristics typical to stem and endothelial progenitor cells and appear to have properties of adult cardiac stem cells (Messina et al., 2004).

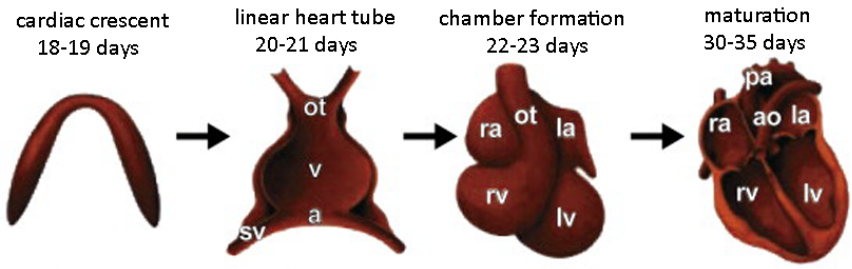

Figure 3. The major stages of human heart development after conception. a=atria; ao=aorta; la=left atrium; lv=left ventricle; ot= outflow tract; pa= pulmonary aorta/trunk; ra= right atrium; rv= right ventricle; sv= sinus venosus; v= ventricle. Image modified from Nemer (2008).

Heart has been shown to be particularly prone to toxic effects of both cardiac and noncardiac drugs. Cardiotoxic substances can cause severe effects on heart functions including decreased contractility, increased arrhythmia and ischemia. (Redfern et al., 2003, Lasser et al., 2002, Lexchin, 2005) The toxicity is typically targeted to the electrophysiological properties of the heart (Andersson et al., 2010).

2.2.1 Differentiation of human pluripotent stem cell derived cardiomyocytes

Human pluripotent stem cells (hPSC), namely embryonic stem cells (hESC) and induced pluripotent stem cells (iPSC), are capable for indefinite self-renewal and differentiation into all somatic cell types. Directed differentiation of hPSC towards cardiomyocytes is commonly based on developmental principles detected in the gastrulation when myocardial mesodermal progenitor cells are formed in the embryo. (Braam et al., 2009) A global gene expression profile of early hPSC-CM is more similar to fetal cardiac tissue than to adult cardiac tissue (Xu et al., 2009). Differences are seen in the number of cardiac ion channel and calcium handling genes highlighting the immature phenotype of hPSC-CM compared to adult heart tissue (Synnergren et al., 2007).

hESC differentiation is classically achieved through spontaneous differentiation as embryoid bodies. Another method used is to co-culture hESC with a mouse visceral endodermal cell line. Differentiation into CM can be performed quite rapidly, in approximately 20 days. However, the reported cardiac differentiation efficiencies of the hESC lines show enormous differences between 8.1-70 %. (Pekkanen-Mattila et al., 2009) Differentiated CM express markers typical for human cardiac cells with properly functioning L-type Ca^{2+} channels and a β-adrenoreceptor system. (Pekkanen-Mattila et al., 2009, Lian et al., 2013)

The use of human embryo derived cells may, however, face ethical concerns that limit the applications of these cells. Moreover, the generation of patient- or disease-specific cells is difficult from hESC. (Takahashi et al., 2007) Yamanaka´s group introduced induction of pluripotent status in somatic cells by direct reprogramming. iPSC can be generated from somatic cells by retroviral transduction with transcription factors Oct3/4, Sox2, Klf4, and c-Myc. The established human iPSC are similar to hESC in morphology, proliferation, surface markers, gene expression, *in vitro* differentiation and teratoma formation. (Takahashi et al., 2007)

2.2.2 Cellular composition of the heart

Heart tissue is a complicated organ having multiple cell types and highly organized structure and function. The major cell types present in the human heart are cardiomyocytes (CM), smooth muscle cells, endothelial cells (EC) and fibroblasts (Nag, 1980, Banerjee et al., 2007, Vidarsson et al., 2010). Cardiomyocytes in the adult heart have highly limited proliferation capacity. Furthermore, they cannot be propagated as a cell line. After birth there is a transition from hyperplastic to hypertrophic growth that increases myocardial mass without CM proliferation. Although CM occupy 80-90 % of the total myocardium mass they constitute only 20-30% of the cells present in the adult heart tissue. The remaining two-thirds are proliferating non-myocytes including EC and fibroblasts. (Soonpaa & Field, 1998, Chien et al., 2008)

From the onset of cardiac development, endothelial cells are prerequisite for myocardial maturation, physiological function and survival (Brutsaert, 2003).

Vascular EC produce several compounds including angiopoietin 2 and nitric oxide that may influence on myocardial growth. Angiopoetin-1 and VEGF are mainly produced by the cardiomyocytes. (Brutsaert, 2003, Leucker et al., 2011). In mature myocardial tissue every CM has a physical contact with at least one capillary. Coronary vasculature is typically generated by angiogenesis in response to specific local demands. (Garzoni et al., 2009) The interactions between vasculature and myocardium are bidirectional (Bhattacharya et al., 2006, Balligand et al., 1997) and active through the adult life affecting to cardiac growth, function and rhythmicity (Brutsaert, 2003). Although cardiomyocytes in adult heart are considered mainly as terminally differentiated cells, they may respond to hypertrophic growth including hypoxia and growth factors. Many signaling factors affecting to myocardial growth have been shown to be produced by adult endothelial cells. *In vitro* co-culture experiments with endothelial cells and cardiomyocytes have shown that depending on the origin of EC, adult cardiomyocytes either maintain their adult phenotype or undergo dedifferentiation. (Brutsaert, 2003)

The myocardial microenvironment is composed of CM and non-myocytes embedded in an aligned and structured ECM which is mainly produced by the cardiac fibroblasts. In the healthy heart, the extracellular matrix guiding cellular orientation facilitates also efficient cell contraction, force transduction and electrical transmission of the cells. The importance of alignment of CM in coordinated contraction is proven by the native cardiac structure, but also in *in vitro* studies. (van Spreeuwel et al., 2014)

2.2.2.1 Morphology and maturation of human Pluripotent Stem Cell-derived Cardiomyocytes

Human pluripotent stem cell-derived cardiomyocytes (hPSC-CM) differ from adult cardiomyocytes with respect to structure, proliferation, metabolism and electrophysiology. (Robertson et al., 2013). Human PSC-CM can be classified into early stage with roughly 3-5 weeks after cardiac differentiation and late stage corresponding to 12–15 weeks of culture after cardiac differentiation. Early stage hPSC-CM have an immature phenotype, reflecting cardiomyocytes in the very early fetal heart including contractility with some proliferative capacity and embryonic like electrophysiology. However, hPSC-CM do show progressive maturation with

duration in culture (Hartman et al., 2015) and adult characteristics, i.e. loss of proliferative capacity and more adult-like electrophysiology, arise in late stages (Robertson et al., 2013). Although the factors affecting maturity remain largely unknown, cell line, time in culture, co-cultured cells and other culture conditions appear to have an effect on the maturity suggesting that after initiation of contraction, genetic and environmental factors interact leading to a more mature phenotype (Robertson et al., 2013).

Differences are seen when the morphology of hPSC-CM is compared to adult CM (Snir et al., 2003). In the adult human heart, ventricular cardiomyocytes are large (~ 130 μm in length) with brick-shaped morphology and sarcomere structures that are readily apparent by phase-contrast microscopy (Hartman et al., 2015) while early hPSC-CM are small and round with approximately 5-10 μm in diameter. Late hPSC-CM (>35 days) develop more oblong morphology (30 μm × 10 μm) but remain small compared to adult. Additionally, most adult CM are bi- or multinucleated with large numbers of mitochondria whereas hPSC-CM are mono-nuclear, have moderate numbers of mitochondria and show smaller sarcomeric regions. Since the extensive t-tubule network present in adult ventricular CM is absent in hPSC-CM, excitation-contraction coupling is slower and calcium primarily enters the cell through the cell membrane instead of releasing from the sarcoplasmic reticulum. However, with increasing time in culture late hPSC-CM develop a more adult-like morphology but do not appear to develop t-tubules or multinucleation. (Robertson et al., 2013)

The expression of mRNAs for cardiac structural proteins myosin light chain 2 ventricular isoform (MLC2v), α-actinin (ACTN2) and α-myosin heavy chain (MYH6) is undetectable or very low in undifferentiated cells but is strongly upregulated in CM at day 18 of differentiation. Immunocytochemical analyses revealed that at day 18 human iPSC- and hESC-CM stain positively for cardiac proteins α-actinin and troponin T and display typical pattern of cross-striations indicative of sarcomeric organization in CM. The highly ordered striated pattern recapitulates the normal architecture of the contractile apparatus in functional CM. (Gupta et al., 2010)

2.2.3 Functional properties of cardiomyocytes

Spontaneous and synchronous contraction is the hallmark of differentiated hPSC-CM and is seen as early as 5 days after the initiation of differentiation. Spontaneous contraction with basal rhythm around 40 beats per minute can be maintained for more than 1 year in culture in strong contrast to adult CM. (Zhang et al., 2009) Responses of α-, β1-, and β2 -adrenoceptors have all been demonstrated in hPSC-CM. As in vivo, isoprenaline has been shown to increase the contraction rate and the amplitude of the calcium transient and decrease the relaxation time. (Brito-Martins et al., 2008)

Important differences in cardiac ion channels and calcium handling genes were seen when hPSC-CM and adult heart tissue were compared. (Robertson et al., 2013) The major ionic currents present in adult CM are expressed also in hPSC-CM although frequently at abnormal levels. Intracellular calcium handling and sarcolemmal ion channels that are necessary for contraction, play a critical role also in functional maturation of hPSC-CM and contribute to their electrical properties (Louch et al., 2015). Signals from neighboring non-cardiomyocytes enhance the electrical maturation of hPSC-CM especially through sarcolemmal ion channel development (Kim et al., 2010).

The cardiac action potential is a combination of different ion channel conductances including Na^+, Ca^{2+} or K^+ currents. In the resting state of the cell, a negative membrane potential exists. In typical action potential, the cell is polarized due to high K^+ conductance as within the cell K^+ remains the main cation and outside it is Na^+. In the rapid depolarization, Na^+ channels open and the membrane potential changes to positive. The plateau phase of the action potential follows when the Ca^{2+} moves in and K^+ out of the cell. As K^+ efflux exceeds Ca^{2+} influx, the cell membrane repolarizes. This rapid repolarization reduces the Ca^{2+} current resulting in contraction (Finlayson et al., 2004) as Ca^{2+} binds to troponin C. For relaxation, Ca^{2+} dissociates from troponin C and turns off the contractile machinery. (Bers, 2000). In the final stage of the action potential, complete repolarization occurs where K^+ channels reopen and flow out of the cell thereby restoring the negative resting potential. Gap junctions enable the spontaneous depolarization and action potential to be proceeded thus allowing coordinated contraction of the heart. (Finlayson et al.,

2004) In early stage hPSC-CM, almost no Ca^{2+} is released from the sarcoplasmic reticulum thus leading to slow, diffusion-limited Ca^{2+} influx. Late stage hPSC-CM perform better but still show slow influx compared to adult CM. The K^+ currents, considered to be responsible for arrhythmias, are expressed in hPSC-CM. (Robertson et al., 2013)

Rate dependence of action potential is a fundamental property of cardiomyocytes. QT interval, measured from the beginning of the QRS complex to the end of the T wave in the electrocardiogram (Figure 4), must be corrected for the cardiac rhythm. In electrocardiogram, the QT interval represents the time from the beginning of ventricular depolarization to the end of ventricular repolarization. (Davila et al., 2004) Thus, the QT interval in the electrocardiogram represents the duration of the ventricular action potential and a prolongation of the QT interval corresponds to a prolongation of the ventricular action potential. A prolonged QT interval, i.e. long QT syndrome, induced by drugs or rare mutations, increases the possibility of developing severe ventricular arrhythmias and sudden death. (Finlayson et al., 2004). When drug responses of hPSC-CM were studied, multielectrode array (MEA) and impedance measurements with 28 cardioactive drugs indicated a strong correlation between *in vitro* and known *in vivo* arrhythmia and QT prolongation effects. Interestingly, although hPSC-CM generally exhibit immature phenotype, hPSC-CM for QT and arrhythmia detection show a strong correlation to adult responses. These results demonstrate the robust utility of hPSC-CM in prediction QT prolongation and arrhythmia thus making them a useful tool for drug discovery and safety pharmacology. (Kolaja, 2014)

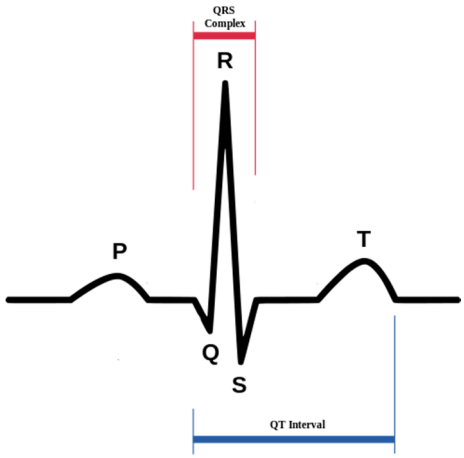

Figure 4. Diagram of QT interval as measured from the beginning of the QRS complex to the end of the T wave in the electrocardiogram. Image modified from https://en.wikipedia.org/wiki/QT_interval

2.2.4 Regulation of heart development

Cardiac development is a complex and highly regulated process controlled by genes and cell–cell interactions. Inductive signals including bone morphogenetic proteins, FGF-2 and Wnt proteins guide the cardiac development in early embryonic stages. (Nemer, 2008) The Wnt signaling pathway is one of the key regulators of cardiogenesis in vivo and *in vitro*. Canonical Wnt ligands direct cell proliferation and cell fate determination during embryonic development. (Lian et al., 2012) In addition, Nkx2.5 and the GATA family of zinc-finger transcription factors are specifically expressed in the heart (Brand, 2003). Also the Notch signaling pathway has been shown to affect in cardiogenesis. Notch1 has a role in the differentiation of cardiac cell types into ventricles. (Chau et al., 2006) Similarly to *in vivo* heart development, *in vitro* cardiogenesis is a dynamic process that is tightly controlled by the chronological expression of several signaling factors (Verma et al., 2013).

2.2.4.1 Vascular growth factors related to heart

VEGF has an important role in the function of heart since mice with cardiomyocyte specific deletion of exon 3 in the VEGF-A results in the loss of all VEGF-A isoforms. The hearts of these mice had fewer coronary microvessels, thinned

ventricular walls, decreased contractile function and an abnormal response to β-adrenergic stimulation. These findings suggest that cardiac myocytes have a critical role as secretory cells and that cardiac muscle is the major source of VEGF in the heart. (Giordano et al., 2001)

In the infarcted myocardium, PDGF-A and PDGF-D are significantly increased as well as receptors PDGFR-α and -β. In an *in vitro* study using cultured cardiac fibroblasts, PDGF-D was shown to promote cardiac fibroblast proliferation and collagen synthesis. Furthermore, it is reported that pretreatment of PDGF-AB promotes angiogenesis in the aging rat hearts after coronary ligation. (Liu et al., 2014)

Angiopoietins have a critical role in cardiovascular biology. Knockout of Ang-1 and Tie-2 leads to embryonic lethal cardiac defects, including impairments in vascular maturation with abnormal recruitment of smooth muscle cells and endocardial formations. (Nishishita & Lin, 2004, Dallabrida et al., 2005) Ang-1 has an indispensable role in coronary vein formation in developing heart presumably by promoting differentiation of immature EC (Arita et al., 2014). Ang-1 levels increase as the cardiovascular development have reached the adult, mature state suggesting that Ang-1 may serve a maintenance function for the vasculature in vivo. (Dallabrida et al., 2005) In the study of Dallabrida et al. 2005 Ang-1 was shown to markedly increase cardiomyocyte survival and protect cardiomyocytes from apoptosis. (Dallabrida et al., 2005)

In the cardiovascular system, FGFs are known to mediate various processes including angiogenesis, embryonic heart development and cardioprotection. However, the role of FGF signaling system in adult heart is poorly understood. FGF-2 has been shown to have beneficial effects when overexpressed in myocardial infarction or ischemia-reperfusion injury studies. Gap junction protein connexin 43 has been proposed to be one of the effectors in FGF-2 mediated cardioprotection. More precisely, FGFs is required for maintenance of cardiomyocyte cell-cell junctions and myocardial integrity *in vitro* and *in vivo*. (Sakurai et al., 2013)

2.3 Tools for development of *in vitro* models

In vitro cell culture was developed to enable observation and manipulation of cells to study the basic biological mechanisms, development and diseases (Shamir & Ewald, 2014). Traditional *in vitro* models are mainly based on utilization of either primary cells isolated from tissues or of transformed cell lines with genetic manipulations (Laustriat et al., 2010). The main limitation of *in vitro* models is their inability to mimic the complexity of the *in vivo* situation. Absorption, distribution, metabolism and excretion processes controlling the exposure of the target tissue are absent in the *in vitro* systems in addition to cross-talk between different organs. (Scanu et al., 2011)

A new kind of innovation for development of *in vitro* models arose in 1998 when the first stem cell lines were established (Laustriat et al., 2010). The enormous potential benefits of stem cells results from their unique properties compared to primary human cells including unlimited proliferation ability, plasticity to generate specific cell types and also easily available sources of human cells (Davila et al., 2004). Human mesenchymal stem cells could replace the currently used transformed cell lines and primary cells and eliminate the limitations related to these test systems thus improving the relevance of predictive *in vitro* assay (Scanu et al., 2011). In addition, the *in vitro* production of differentiated cells, such as cardiomyocytes, from human pluripotent stem cells provides a source of cells for applications in drug discovery, disease modeling, regenerative medicine and toxicity screening (Mordwinkin et al., 2013, Chow et al., 2013). With the iPSC technology it is possible to isolate somatic cells, generate pluripotent iPS cells out of them and genetically engineer these cells for different purposes. Since the pluripotent cells match the donors genetic background, it is possible to generate a variety of somatic cells that are immunological identical to the donor and therefore do not induce immune rejection when transplanted. Furthermore, with reprogramming techniques, it has become possible to generate patient specific iPSC lines from donors independent of sex or age or to use patient specific iPSC to generate disease model-specific iPSC for *in vitro* modeling. (Pfannkuche et al., 2010a, Musunuru et al., 2010)

Stem cell-based systems offer a very promising and innovative alternative to obtain large numbers of cells for early efficacy and higher toxicity screening thus allowing

scientists to improve the selection of lead candidates and, further, the possibility to decrease the adverse effects in clinical phase of drug development (Davila et al., 2004, Lou & Liang, 2011). Since *in vitro* assays should improve the translation of preclinical data into the clinical studies, a critical component is to use physiologically relevant *in vitro* model that mimics the complexity of the clinical situation (Engle & Puppala, 2013). The most relevant cell types used in *in vitro* models and in this study are discussed in detail below.

2.3.1 Primary cells

Natural type of the cells used in *in vitro* models enables to maintain better the structural and biochemical complexity found *in vivo*. Therefore, primary cells are often a preferred choice for *in vitro* studies. However, after being isolated from original tissue, primary cells begin to de-differentiate within hours to days when cultured *in vitro*. Primary cells may also be sensitive to passaging, result in altered phenotypes, possess slow proliferation rates and metabolic capacities, and, additionally, develop early senescence after few expansions. (Astashkina et al., 2012)

Isolation of human primary cardiomyocytes from heart tissue is challenging and the access to the tissue is problematic. At the same time, the process is uncontrolled with respect to donor disease and treatment modalities. (Vidarsson et al., 2010) Furthermore, cardiomyocytes from the adult heart have highly limited proliferation capacity and they cannot be propagated as a cell line. Therefore, repeated isolation of primary tissue is necessary for sustainable *in vitro* studies (Braam et al., 2009).

2.3.1.1 Endothelial cells

Among the most extensively used primary endothelial cells of human origin are human umbilical vein endothelial cells (HUVEC) that can be easily isolated from the umbilical cord and have been successfully cultured since 1973. HUVEC grow as a monolayer with polygonal cell morphology in comparison to long, slender, spindle-shaped and overlapping fibroblasts. (Jaffe et al., 1973). Although all vascular endothelial cells share common functions, it has been shown that considerable heterogeneity exists in the vascular network and between different organs. Evidence

show that endothelial cell heterogeneity develops through interactions with the microenvironment either through soluble factors or cell-cell contacts. Thus, blood vessel type–specific and tissue-specific characteristics of EC are under the control of their microenvironment. (Lacorre et al., 2004) See also chapter 2.1.2.1.

2.3.1.2 Fibroblasts

Fibroblasts are a heterogeneous population of cells with mesenchymal origin that are present in various tissues. Although fibroblasts from different tissues have similar morphology, DNA-microarray studies have demonstrated that they have unique gene expression profiles and characteristic phenotypes. Fibroblasts secrete various growth factors and cytokines with direct effect on cell proliferation, differentiation and formation of extracellular matrix. In neovascularization, fibroblasts contribute to basement membrane formation by producing collagen types IV and VII and have an important paracrine role. (Wong et al., 2007) Human foreskin derived fibroblasts have been widely used to study the basic mechanisms of cell function and signaling, wound repair, topical pharmaceuticals and have been incorporated also into bioengineered skin products (Nahm et al., 2002).

2.3.1.3 Primary cardiomyocytes of animal origin

Animal-derived, adult cardiomyocytes are routinely used *in vitro* models in cardiovascular research. While freshly isolated cardiomyocytes remain functional for 10–12 hours, cultured cardiomyocytes can be used for longer term studies (approximately 5 days). However, while long-term viability is an advantage, the long culture time allows the cells also to adapt to the culture conditions and alter their phenotype. Adult rat cardiomyocytes have shown to undergo critical morphological and functional changes including internalization of intercalated disks, decreased tubule density, altered calcium signaling and reduced contractility in addition to decreased resting membrane potential and L-type calcium current density. (Banyasz et al., 2008)

2.3.2 Immortalized cells

Immortalized cells have their origin in primary cells that have been further genetically modified. Immortalization is the result of oncogene transfection to enable rapid proliferation in culture, resistance to dedifferentiation, improved passaging and greater resilience. As a result of genetic transformations, these cells are no longer primary cells, not phenotypically identical and often only marginally similar to their original primary phenotype. Immortalized cells are typically easy to maintain, can be expanded and stored and are stable for up to 25–50 passages. However, cell behavioral changes upon immortalization are reported when compared to homologous primary cells. Specifically, immortalized cell lines have been shown to possess altered genomic content, abnormal expression of intracellular proteins, lack or significant morphological features such as tight junctions, ligands, transporters, cellular receptors as well as loss of cellular polarity. These changes have to be considered while using immortalized cell lines in *in vitro* models. (Astashkina et al., 2012)

2.3.3 Stem cells

Stem cells can be roughly characterized as embryonic or adult stem cells. Embryonic stem cells from the fertilized oocyte are called totipotent. These totipotent cells are able to specialize and form the blastocyst from which the embryo will develop. Embryonic stem cells from within blastocyst are called pluripotent sine these cells form all three germ layers. In addition, adult tissues and organs contain niche of multipotent adult stem cells that are able to differentiate into varying cell lineages. The key properties for all stem cells are to exhibit unlimited self-renewal and multilineage differentiation potential. (Salem & Thiemermann, 2010)

2.3.3.1 Adult stem cells

Mesenchymal stem cells (MSC) are adult stem cells with capacity for self-renewal and differentiation with a large tissue distribution (Williams & Hare, 2011). MSC, also called mesenchymal stromal cells, are non-hematopoietic cells that originate from the mesoderm and exist in almost all tissues. MSC differentiate into mesoderm

lineages, such as chondrocytes, osteocytes and adipocytes, but also ectodermic cells and endodermic cells. MSC can be easily isolated from the bone marrow, adipose tissue, the umbilical cord, fetal liver, muscle, and lung and further successfully expanded *in vitro*. (Wei et al., 2013) The International Society for Cell Therapy proposed a criteria for MSC identification that include (1) adherence to plastic in standard *in vitro* culture conditions; (2) expression of the surface markers CD73, CD90, CD105 and the absence of CD34, CD45, HLA-DR, CD14 or CD11b, CD79a, or CD19 surface molecules and (3) the ability to differentiate into osteoblasts, adipocytes and chondroblasts *in vitro*. (Williams & Hare, 2011)

The endogenous role for MSC is the maintenance of stem cell niche and contribution to organ homeostasis, wound healing, and successful aging. In regenerative medicine, MSC are emerging as an extremely promising therapeutic tools for tissue regeneration. (Williams & Hare, 2011)

2.3.3.1.1 Adipose tissue derived stromal cells

Previously, research related to adult stem cells has focused on mesenchymal stem cells found within the bone marrow stroma. However, adipose tissue, like bone marrow, is derived from the embryonic mesenchyme and contains a stroma that can be easily isolated. (Zuk et al., 2002) Adipose tissue represents an ideal source of autologous stem cells since it is easy to obtain with minimal patient discomfort, but yet capable for extensive expansion *in vitro*. The stem cell population derived from collagenase-digested human adipose tissue stated as stromal-vascular fraction has been shown to differentiate into multiple cell types including adipocytes, chondrocytes, osteoblasts, myocytes, neuronal cells, endothelial cells, cardiomyocytes and smooth muscle cells. Term human adipose tissue derived stromal cells (hASC) refers to plastic-adherent cell population that includes vascular cells (pericytes and endothelial progenitor cells); adipocyte progenitor cells and adult multipotent mesenchymal stem cells in addition to blood cells, fibroblasts, endothelial cells, smooth muscle cells and immune cells. (Madonna et al., 2009)

The high proliferation and differentiation capacity of hASC makes them an ideal source for vascular modeleling (Madonna et al., 2009, Miranville et al., 2004, Hutton et al., 2012). hASC monocultures have been shown to spontaneously generate vascular structures through the coordination of its subpopulations in the absence of

exogenous ECM proteins (Hutton et al., 2012). Moreover, hASC are shown to exhibit significantly higher potential to stimulate vascular-like network formation compared to smooth muscle cells or fibroblasts (Merfeld-Clauss et al., 2010). Due to putative endothelial progenitor cell population, hASC might represent a tool for vasculogenesis research (Miranville et al., 2004). This is supported by reports stating that endothelial progenitor cells possess high plasticity with the ability to give rise to smooth muscle cells (Moonen et al., 2010), enhance the differentiation of MSC towards pericyte phenotype and increase the ability of MSC to attach to the tubule structures *in vitro* (Goerke et al., 2012). Vasculogenic potential of hASC is suggested to be dependent on direct and reciprocal interaction with EC resulting in secretion of cytokines and ECM proteins (Merfeld-Clauss et al., 2010, Merfeld-Clauss et al., 2015).

hASC are known to secrete several angiogenic and anti-apoptotic growth factors such as VEGF, hepatocyte growth factor (HGF), FGF-2, PDGF-B and TGF-β and matrix metalloproteinases that are known to act in a synergistic manner (Rehman et al., 2004, Rubina et al., 2009, Verseijden et al., 2010b). In the formation of vascular structures, cells originating from hASC contribute to vessel maturation by aligning along the vascular structures thus stabilizing them *in vitro* and *in vivo*. Cell–cell contacts appear to be important in the formation of stable vascular-like structures *in vitro* (Rubina et al., 2009, Traktuev et al., 2008) as direct interaction between hASC and EC shifts hASC paracrine activity from being pro-angiogenic to angiostatic (Merfeld-Clauss et al., 2015, Merfeld-Clauss et al., 2014).

EC and ASC co-culture have been shown to produce vascular structures *in vitro* and *in vivo* (Merfeld-Clauss et al., 2010, Verseijden et al., 2010a, Traktuev et al., 2009, Verseijden et al., 2010b, Rohringer et al., 2014). Vascular-like network formation is shown to be associated with extracellular accumulation of ECM proteins such as fibronectin and collagen IV (Merfeld-Clauss et al., 2010). Preformed vascular structures within *in vitro* constructs can also integrate with the host vascular system and improve the vascularization upon implantation (Verseijden et al., 2010a, Traktuev et al., 2009).

2.3.3.2 Pluripotent stem cells

Human pluripotent stem cells (hPSC) can be isolated from the blastocyst resulting in embryonic stem cells or reprogrammed from somatic cell sources (e.g. fibroblasts) to pluripotent state resulting in induced pluripotent stem cells. Human PSC have raised high degree of interest due to their potential use in applications from basic research to novel cell based therapies and tissue engineering. (Hartman et al., 2015) Although the development of human embryonic stem cells (hESC) and, more recently, human induced pluripotent stem cells (hiPSC) has offered an alternative to human primary cells (Engle & Puppala, 2013), improved methods to derive specific cell subtypes and improvements in their maturation into a more adult-like phenotype is needed (Hartman et al., 2015). Moreover, challenges typical for all *in vitro* systems also apply to utilization of pluripotent stem cells including the phenotypic characterization of the cells, the cell culture conditions, the composition and architecture of the cell culture systems, the time of the experiments and the measurement and interpretation of endpoint results to assess the potential human risk. (Hartman et al., 2015)

Industrial utilization of pluripotent stem cells will require the control of the expansion and differentiation processes as well as large scale expansion of the cells with reasonable costs. The high-throughput production of iPSC have shown to be time-consuming and troubled with batch-to-batch variability. Another specific challenge for iPSC cells with the transcription factor based reprogramming, is the epigenetic memory since their epigenetic profile is related to the tissue of origin and may limit the directed differentiation. However, despite the current technical limitations, the potential of pluripotent stem cells, particularly with iPSC, will certainly contribute to *in vitro* safety assessment in the future. (Suter-Dick et al., 2015)

2.3.3.2.1 Human pluripotent stem cell derived cardiomyocytes

Human pluripotent stem cell derived cardiomyocytes may provide significant advantages over previous cardiac models. Similar to currently available cardiomyocyte models, hPSC-derived cardiomyocytes contract rhythmically and respond appropriately to numerous cardioactive drugs. However, questions of their immaturity complicate their adoption as a new *in vitro* model. (Robertson et al., 2013) hPSC-derived cardiomyocytes can be used to study cellular responses including, but

not limited to, contractile function, cardiac arrhythmia, resistance to apoptosis and protection from ischemia. (Sartipy et al., 2007) See also chapters 2.2.2.1. and 2.2.3.

2.3.4 Cell culture conditions

2.3.4.1 Defined medium

Good cell culture practice guidance is developed to provide common standards for development of *in vitro* methods and use of chemically defined media is part of it. The defined composition of the media used in the study is essential to achieve high experimental reproducibility. Although defined media are commercially available for some cell types, information on the composition of the media provided by the manufacturing companies is often limited. (van der Valk et al., 2010) Cell culture media used in *in vitro* models often do not reflect the *in vivo* situation. Serum concentration in culture media often comprises of 5–10 % of the volume and additional cell nutrients are commonly used. Arguments on the justification for use of a specific cell culture media are rarely provided in published reports. (Astashkina et al., 2012) Since serum is a complex mixture of components with unknown chemical structure and protein binding affinities, serum-free medium is recommended when studying the effects of different chemicals (Shen et al., 2013). For example, serum heparin is needed for the attachment of some growth factors to their cell surface receptors. VEGF121 does not bind to heparin and is freely diffusible while the larger isoforms including VEGF165 contain heparin-binding residues and are bound to the cell surface or sequestered in the ECM (Liekens et al., 2001, Ashikari-Hada et al., 2005).

The concentration of serum in the medium plays an essential role in determining the morphology, growth characteristics and differentiation of the CM. More mitogenic medium stimulates cell proliferation whereas CM cultured in lower serum concentrations (0-5 %) maintain the cell number, phenotype and contractile properties. (Passier et al., 2005, Xu et al., 2006, Li, 2002)

Beside serum, other specific supplements in the medium are important. Adult rat CM in primary culture re-express markers of hypertrophy that are normally

expressed during fetal stage and are down-regulated during maturation. The growth factors FGF-2 and IGF-1 have shown to guide this process into opposite directions. FGF-2 increases the expression of dedifferentiation markers, such as atrial natriuretic factor, α-smooth muscle-actin and myofibrillar organization, while IGF-1 promotes more differentiated CM phenotype. (Montessuit et al., 2004) In *in vitro* vascular models, several growth factors are added to medium to induce vascular-like network formation. VEGF was added to induce vascular structure formation of EC and hASC co-culture in spheroids (Verseijden et al., 2010b). In another study, EC and hASC were co-cultured in the presence of 5 % FBS medium supplemented with VEGF or HGF (Merfeld-Clauss et al., 2010).

2.3.4.2 2D vs 3D culture

Although *in vitro* models have shown to be powerful tools in drug screening and in toxicity assessment, these models are only as good as their ability to recapitulate the *in vivo* physiological processes and specific properties under study. Commonly employed methods of *in vitro* testing include organ explants, organotypic cultures, dissociated 2D cultures and 3D cultures (Figure 5). (Astashkina et al., 2012) Traditional 2D *in vitro* cell culture does not include the complexities of the cellular microenvironment nor the extracellular matrix within tissues *in vivo* (Shamir & Ewald, 2014). Growth on 2D surfaces results in cell flattening and changes in cell morphology and internal cytoskeleton (Knight & Przyborski, 2014, Pontes Soares et al., 2012). These changes have been shown to alter gene expression, affect nuclear shape, cell performance and consequently influence the results of biological assays. (Knight & Przyborski, 2014) Growing evidence show that 3D cell arrangement, co-culture of different cell types and physico-chemical properties lead to improved predictive value of the test system (Shamir & Ewald, 2014, Song et al., 2014, Tourovskaia et al., 2014). Currently, there are a large variety of 3D constructs with different degrees of complexity. Bioreactors, lab on a chips and microtissues comprises the most commonly used 3D constructs. (Suter-Dick et al., 2015)

The 3D culture enables cell-cell and cell-matrix contacts resulting in increased intercellular signaling, facilitating developmental processes and allowing cells to differentiate into more complex and mature structures. The loss of extracellular

matrix-cell interactions and cell-cell communication often results in rapid cell dedifferentiation and poor passaging in *in vitro* cell culture systems. (Astashkina et al., 2012) Tissue-like structures are able to form in 3D environment also through more uniform expression of adhesion molecules. Receptors and adhesion molecules are more naturally and evenly spread over the cell surface in 3D cell culture whereas in 2D culture cells are polarized with binding proteins concentrated on the side where they attach to the cell culture plastic. (Knight & Przyborski, 2014)

Most 3D tissue-engineering strategies rely on the use of exogenous, biocompatible scaffolds as alternatives for extracellular matrix in which cells are seeded and matured (Shimizu et al., 2003, Norotte et al., 2009, Hussain et al., 2013). In myocardial tissue, cell density is high to enable synchronous beating. The use of scaffolds in cardiac constructs has been, however, associated with reduced cell-cell contacts, as well as incorrect deposition and alignment of extracellular matrix thus affecting to the force generation ability of the constructs. (Norotte et al., 2009)

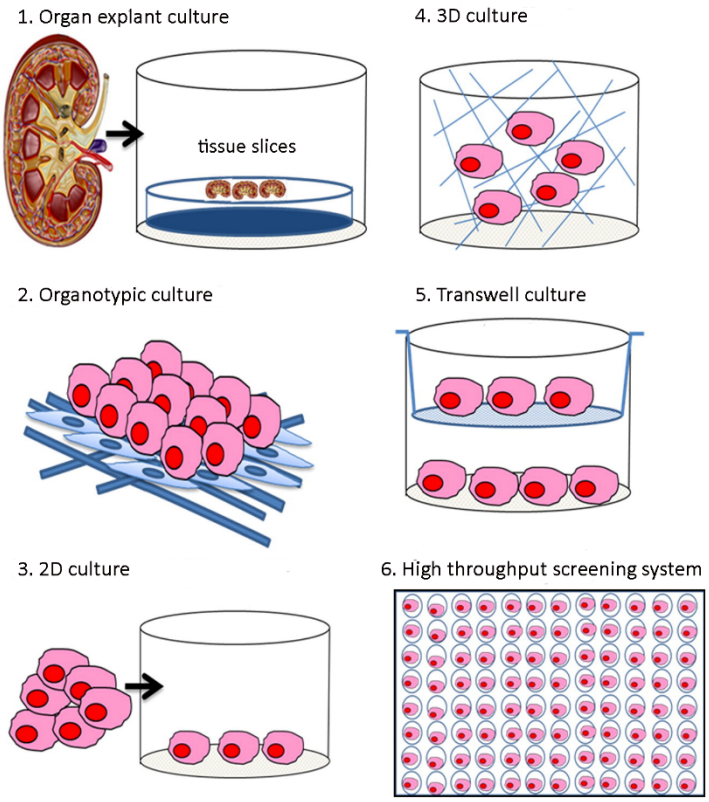

Figure 5. Different methods for *in vitro* modeling. 1) Organ explant cultures maintain whole or partial histological architecture of an isolated organ; 2) In organotypic culture multiple different cell types are used to recapitulate the *in vivo* situation; 3) Dissociated 2D cell cultures on plastic surfaces are the traditional *in vitro* model used; 4) 3D cell culture models enables cell-cell and cell-matrix contacts; 5) Transwell culture system allows co-culture and paracrine activity of different cell types ; 6) *In vitro* models can be optimized for high throughput screening systems to improve the efficiency of the method. Image modified from Astashkina et al. (2012)

2.4 *In vitro* and *in vivo* models of vasculature and heart

2.4.1 Safety and efficacy assessment in respect of 3R´s

In 1959 Russell and Burch introduced the conception of Replacement, Reduction and Refinement (3R´s) of animal testing in the book "The principles of humane experimental technique". They stated that mammalian tissue cultures have become one of the most important replacement techniques for animal experiments. Although Russell and Burch demanded reduction of inhumane animal experiments, they also acknowledge that animal experimentation has brought substantial benefit for medicine and enhanced the development of science knowledge overall. Russell and Burch also pointed out that similar species do not necessarily possess good correlation between each other. (Jennings, 2014, Russell & Burch, 1959)

Presently, animal models are still generally regarded as the most relevant model systems and this is reflected in the regulatory guidelines for safety assessment evaluation worldwide (Suter-Dick et al., 2015). In European Union, the total number on animals used for experimental and other scientific purposes in 2011 was approximately 11.5 million (European Commission, 2013). However, the poor relevance of animal models to humans in addition to ethical, cost and time concerns increases the need for physiologically relevant *in vitro* models for safety and efficacy assessment. European Union has set the final goal to replace animal experiments with non-animal approaches in the Directive 2010/63/EU. (Heinonen, 2015) At 2011-2012, the cause for drug attrition in clinical development phase was mostly due to a lack of efficacy (56%) or to safety issues (28%) (Arrowsmith & Miller, 2013). Hepatotoxicity and cardiotoxicity are the two leading causes of failure in preclinical development of new drugs (Davila et al., 2004). Recently, numerous non-cardiac drugs have had to be withdrawn from the market due to cardiotoxicity concerns. This indicates that the current drug testing strategies have severe limitations. (Feric & Radisic, 2015). Beside drug development, the safety of industrial chemicals stated in REACH (Registration, Evaluation, Authorization and Restriction of Chemical substances) legislation on the evaluation of chemicals reinforce the need to develop a new, robust and economical *in vitro* models (Laustriat et al., 2010).

Food and Drug Adminstration (FDA) and European legislators have identified prolongation of the QT interval as a critical drug safety issue. QT prolongation is most commonly induced when component of a drug molecule binds to hERG ion channel and affects the rapid potassium current (Braam et al., 2010). Block of hERG K^+ channels (I_{Kr}) is a predominant risk factor for drug-induced Torsade de Pointes which is rare but life-threatening type of ventricular arrhythmia associated with the prolongation of the QT interval in humans (Redfern et al., 2003). Several clinically successful drugs in the market have revealed to inhibit hERG and create a concomitant risk of sudden death as a side effect (Finlayson et al., 2004). Consequently, the assessment of the risk for QT interval prolongation is part of the standard preclinical evaluation of new compounds defined by the International Conference of Harmonization (ICH) Expert Working Group in topic S7B (ICH S7B) for all drugs in development (Braam et al., 2010).

Angiogenesis is studied extensively due to its broad importance in medicine. *In vitro* models of blood vessel formation are needed for basic biomedical research as well as for translational research including drug development that needs relevant test systems for screening of pro- and anti-angiogenic compounds. (Ucuzian & Greisler, 2007, Folkman, 2007) In addition, detection of drug-induced vascular injury has been a major challenge for the pharmaceutical industry for decades causing termination of development of new drug candidates in nonclinical safety assessment. Drugs associated with vascular injury include anti-bacterials, anti-malarials, anti-virals, anti-inflammatory agents as well as drugs related to neurologic diseases, cardiovascular diseases and diabetes mellitus (Mikaelian et al., 2014, Morton et al., 2014).

2.4.2 *In vitro* vascular models

An ideal *in vitro* vascular model would be robust, rapid and reproducible with reliable readouts and should include automated computational analysis. In addition, it should include multi-parameter assessment with positive and negative controls and should relate directly to results seen in the clinical studies. Despite the increasing numbers of *in vitro* and *in vivo* assays, a "gold-standard" vascular model does not exist. (Staton et al., 2009) Commonly used *in vitro* vascular models are presented below and in Table 1.

Quantification of EC proliferation with thymidine incorporation is the simplest form of *in vitro* angiogenesis screening. This assay has the advantage of being quantitative, rapid and easy to perform although some steps in the assay protocol may be prone to inter-observer variability. (Friis et al., 2003) Another method for detecting tubule formation *in vitro* includes EC proliferation in a gel composed of collagen, fibronectin or Matrigel (Nicosia & Ottinetti, 1990). However, tubule formation in Matrigel is not specific to EC. Primary human fibroblasts, a metastatic breast cancer cell line, a metastatic prostatic carcinoma cell line and glioblastoma cells are also able to form tubule structures in Matrigel but not when co-cultured with fibroblasts in the absence of Matrigel. (Donovan et al., 2001) Several co-culture models, comprising of EC and stromal cells, mimicking angiogenesis have been developed (Donovan et al., 2001, RW.ERROR - Unable to find reference:41, Merfeld-Clauss et al., 2010, Friis et al., 2003). The advantage of these co-culture assays is the interactions between the EC and stromal cells thus leading to more mature tubule structures (Merfeld-Clauss et al., 2010).

Presently, one of the most specific angiogenesis assays are the ones establishing EC to form 3D tubule structures in different matrices (Auerbach et al., 2003, Peterson et al., 2014, Koh et al., 2008). First 3D *in vitro* angiogenesis assays were established already at 1990´s. In the assay EC were seeded on gelatine coated microcarriers into a 3D fibrin matrix. Each microcarrier gave rise to a limited number of capillaries and the angiogenic response could be easily quantified by determining the average number of capillary-like structures. (Nehls & Drenckhahn, 1995, Nakatsu et al., 2003) Also another 3D angiogenesis assay in type I collagen gel suitable for EC migration studies and to the evaluation of angiogenic compounds have been reported (Vernon & Sage, 1999).

Improvements in iPSC technology, tissue engineering and microfabrication techniques have enabled the development of 3D microphysiological systems that more accurately reflect human biology compared to traditional 2D cell culture systems or animal models (Moya et al., 2013). For modeling the human tissue microenvironment, a microfluidic chip with connecting tubule structures was developed. In the chip, EC are seeded on tubule channels and surrounded by extracellular matrix. Consequently, a perfusable system with connected upstream and downstream fluidic channels is formed. With these chips, models of angiogenesis,

the blood–brain barrier and tumor-cell extravasation can be developed. (Tourovskaia et al., 2014)

Moreover, microfluidic based platforms consisting of co-culture of EC and fibroblasts, pericytes or cancer cells with perfusable microvessels have been developed. An open delivery of nutrients, chemical compounds, biomolecules and cell suspensions as well as flow-induced mechanical stimuli are the main benefits of the perfused microvasculature. This platform provides applications in vascular physiology studies as well as in developing vascularized organ-on-a-chip and human disease models for pharmaceutical screening. (Kim et al., 2013) Also complex combination of microcirculation, the cardiac muscle and a solid tumor integrated into 3D microphysiological system simulating perfused cardiac muscle and solid tumor on a single platform have been developed. This platform provides a new paradigm for accurate drug and toxicity screening with the focus on anti-cancer drugs with minimal cardiotoxicity. (Moya et al., 2013)

2.4.3 *In vivo* vascular models

Animal models mimicing blood vessel formation are considered essential in development of anti- or pro-angiogenic therapeutic treatments (Norrby, 2006, Auerbach et al., 2003). However, although the *in vivo* the complexity can be assessed, these assays are limited with species-to-species differences, administration of the test substances and lack of quantitative analysis (Staton et al., 2009). Among the most commonly used *in vivo* vascular models are chicken chorioallantoic membrane assay (CAM), corneal angiogenesis assay, mouse retinal angiogenesis assay, rat hindlimb ischemia model, Matrigel assay and different tumor models (Table 1) (Auerbach et al., 2003, Staton et al., 2009).

CAM (chicken chorioallantoic membrane) assay was developed by experimental embryologists more than 50 years ago. In the assay, the CAM of 7–9 day old chick embryos is exposed by making a window in the eggshell and tissue grafts, with or without test compounds, are placed directly on the CAM. After that, eggs are reincubated and the grafts recovered after an appropriate length of time and later on scored according to the growth and vascularization. (Auerbach et al., 2003) The

CAM assay is useful in tumor-induced angiogenesis studies since the host immune system is not completely developed. (Norrby, 2006) CAM assays are relative easy and inexpensive to perform, semi high-throughput studies can be executed and monitoring the reaction throughout the study is possible. (Auerbach et al., 2003)

Corneal angiogenesis assay is considered one of the best *in vivo* assays as the cornea itself is avascular and transparent. Thus, blood vessel formation taking place in the cornea is solely due to angiogenic stimulation by tissues or compounds. The method was developed for rabbit eyes but has been adapted also to mice. Briefly, a pocket is made in the cornea and test tumors or tissues with possible test substances are introduced into this pocket. (Auerbach et al., 2003) The advantage of this assay is the ability to monitor progress of angiogenesis as well as the absence of background vasculature. Technical factors, including the surgical procedure, may, however, affect the angiogenesis quantification. The assay is also relatively time consuming thus limiting the application of the assay in high-throughput screening. (Staton et al., 2009)

Widely used mouse retinal angiogenesis assay allows the study of developmental as well as pathological vasculature formation since retinal vascular development occurs postnatally in rodents. With this assay, different stages of formation and regression of blood vessels can be studied in controlled settings. Retinas are usually visualized with whole-mount stainings and *in-situ* hybridization techniques. (Stahl et al., 2010)

In rat ischemic hindlimb model ischemia is created in the left hind limb with the right leg serving as control. In the assay, all left side branches of the aorta distal to the renal arteries and of the iliac artery are ligated. After 5 days, the femoral artery is also ligated. After ligations, growth factors are injected and implanted into the animal. In addition to rat and rabbit ischemic hind-limb model, Cao et al. (2003) used Matrigel assay. In Matrigel assay, growth factor loaded beads were mixed with Matrigel and subcutaneously injected into mice. After 2 weeks, Matrigel pellets were collected and fixed in paraffin. Paraffin sections were stained and quantified to assess the blood vessel formation. (Cao et al., 2003) Matrigel assay is considered one of the best methods for rapid assessment of pro- anti-angiogenic potential of compounds. However, Matrigel assays suffers of high variability between different experiments. (Norrby, 2006)

Several animal models have been established to mimic complex tumor angiogenesis. In experimental tumor models, tumor cells, either genetically identical or of human origin, are implanted into the animal. Tumor angiogenesis is influenced by the organ site or microenvironment and also animal strain of choice or tumor cell line used, thus displaying large heterogeneity in terms of angiogenesis and chemosensitivity. In cancer research, tumor models have an essential role in the assessment of efficacy of novel compounds in preclinical studies. (Staton et al., 2009)

Standard assessment of embryogenesis disruption involves testing of pregnant laboratory animals, typically rats and rabbits, with at least two generations involved in standard test system (Piersma, 2006, Knudsen & Kleinstreuer, 2011). Animals are exposed during the critical organogenesis and evaluated just before term. In the animal models, intrauterine death, fetal growth retardation, structural variations and abnormalities are the main endpoints in the assessment of developmental toxicity. Although the current animal models are used in the assessment of developmental toxicity, they are also low-throughput, slow, costly and ethically questionable. Consequently, the use of animal models in the assessment of developmental toxicity results in a relatively low number of compounds with sufficient *in vivo* data concerning the potential adverse effects on human development. (Knudsen & Kleinstreuer, 2011)

Table 1. Typical characteristics of commonly used *in vitro* and *in vivo* vascular models.

***In vitro* vascular models**	**Cells used**	**End points**	**Applications**
Endothelial cell proliferation assay	endothelial cells of different origin	3H-thymidine incorporation during cell proliferation	studies on cell migration and proliferation
2D and 3D tubule formation assay in biomaterials	rings of rat aorta, human endothelial cells	tubule formation	vascular physiology studies, evaluation of angiogenic compounds
Angiogenesis co-culture assays	human endothelial cells+fibroblasts/pericytes/human adipose stromal cells	tubule formation	vascular physiology studies, evaluation of angiogenic compounds
Microfluidic chips	human endothelial cell monocultures, human endothelial cells+fibroblasts/pericytes/cancer cells	tubule formation, cell migration, permeability	vascular physiology studies, disease model development, evaluation of angiogenic compounds
***In vivo* vascular models**	**Animals used**	**End points**	**Applications**
Chorioallantoic membrane assay	chicken embryo	tubule formation	tumor-induced angiogenesis studies
Corneal angiogenesis assay, **Mouse retinal angiogenesis assay**	rabbit, mouse	tubule formation, structure, morphology	evaluation of angiogenic compounds, developmental, physiological and pathological vascular studies
Rat ischemic hindlimb model	rat, rabbit, mice	tubule formation, histopathology	evaluation of angiogenic compounds, ischemic studies
Tumor angiogenesis models	several species	tubule formation, chemosensitivity, histopathology	cancer research, evaluation of angiogenic compounds
Embryogenesis disruption model	rat, rabbit, other species	intrauterine death, fetal growth retardation, abnormalities	developmental toxicity studies

2.4.4 *In vitro* cardiac models

Currently, *in vitro* screening utilizes mainly cell lines that express human cardiac ion channels, cardiac cell cultures, isolated tissues preparations such as Purkinje fibres and perfused heart preparations. Electrophysiology remains the "gold standard" method to characterize ion channel properties and drug discovery will undoubtedly

benefit from the development of more high-throughput electrophysiological systems. However, despite of the new technology, there is no clear guidelines stating which protocols should be used to study hERG channels *in vitro*. (Finlayson et al., 2004) The most relevant *in vitro* cardiac models are discussed below and presented in Table 2.

Presently, two functional *in vitro* assays are routinely used in the assessment of drug's potential to delay cardiac repolarization. Repolarization assay performed with canine Purkinje fibers characterizes drug-induced changes in the action potential duration of cardiac tissues and ionic current assay evaluates drug-induced block of the hERG current or native I_{Kr} current. In an evaluation of the functionality of these assays with pharmaceuticals, results showed a poor correlation between hERG and repolarization assays suggesting that the hERG assay oversimplifies drug effects on the repolarization process and that neither assay alone adequately predicts pro-arrhythmic risk. (Martin et al., 2004) Another study using human hERG transfected embryonic kidney cells (HEK293) also showed that the hERG assay alone does not adequately identify drugs inducing QT prolongation (Lu et al., 2008).

Rat ventricle myoblasts (H9c2) and mouse atrial HL-1 cells are available for the analysis of compound interaction with cardiac ion channels. (Vidarsson et al., 2010) Rodent cells are widely used in drug-related studies although they exhibit several distinctions from human cells: a shorter action potential, different calcium handling, a higher percentage of alfa-myosin heavy chain isoform, a higher resting heart rate and an inverse force-frequency relationship. In particular, the differences in ion channels and currents complicate the transferability of the data from drug screening and toxicity studies from murine to humans. (Polini et al., 2014)

The voltage-dependent contractile properties of hPSC-CM are necessary to mimic the primary *in vivo* role of cardiomyocytes. For mechanistic toxicological studies, rhythmic perturbations must be assessed as well as the consequences of energy production as they relate to drug-induced cardiotoxicity simultaneously. Using a variety of molecular markers, including mitochondrial membrane potential, endoplasmic reticulum integrity, Ca^{2+} metabolism and membrane permeability beside the assessment of cell viability, hPSC-CM were shown to be more predictive

than primary dog cardiomyocytes and H9c2 cell line when tested with therapeutic concentrations. (Kolaja, 2014)

Presently, there are several cardiac in *vitro* models with scaffolds and cardiomyocytes of animal origin. Garzoni et al (2009) created a 3D tissue-like spheroid model where cardiomyocytes are co-cultured either with EC or mesenchymal stromal cells. In the model, murine fetal cardiomyocytes form 3D contractile structures, couple through gap junctions and form vascular structures in co-culture with HUVEC. Furthermore, human mesenchymal cells were seen to form vascular structures by vasculogenesis. The presence of vascular structures led to long-term survival and contractile capacity of cardiac microtissues. (Garzoni et al., 2009)

Moreover, a 3D *in vitro* cardiac model composed of rat embryonic cardiomyocytes and adult rat bone marrow stromal cells to study myocardial regeneration has been developed. In the system, cells were seeded on 3D tubular scaffold engineered from type I collagen fibers. The 3D co-culture system was shown to maintain the embryonic cardiomyocytes differentiation process and, at the same time, induce the differentiation and maturation of rat bone marrow stromal cells into cardiomyocyte-like cells. (Valarmathi et al., 2010) Another 3D *in vitro* cardiac model was developed to mimic healthy aligned and diseased disorganized cardiac matrix. In the system, neonatal mouse cardiomyocytes and cardiac fibroblasts were suspended in a collagen–matrigel hydrogel and seeded to form microtissues. Cardiomyocytes in aligned matrix were shown to be more elongated and possess aligned sarcomeres. Furthermore, proliferation of the cardiac fibroblasts had an effect on the microtissue contraction rate. (van Spreeuwel et al., 2014)

Simple and robust systems with human embryonic stem cell (hESC) have been created for basic research and preclinical safety assessment. Fibrin based human engineered heart tissue in a 24-well format with cardiomyocytes was developed. Cardiomyocytes formed a dense network of longitudinally oriented, interconnected and cross-striated cells. Furthermore, chronotropic responses to calcium and the β-adrenergic agonist were detected. Well known pro-arrhythmic compounds induced concentration-dependent and reversible decreases in relaxation velocity and, further, an asynchronous beating at concentrations similar to those used in hERG assays. (Schaaf et al., 2011)

Vascularized, implantable tissue constructs are one of the main goals of regenerative medicine. In cell sheet tissue technology, neonatal rat cardiomyocytes were co-cultured with EC of rat origin on temperature sensitive culture dishes. Co-cultured EC formed networks within the cardiomyocyte sheets. Cardiac cell sheets were layered into 3D myocardial tissues and the tissue grafts were transplanted into infarcted rat hearts. As a result, cardiac function could be significantly improved. Moreover, vascular structures from the cardiac tissues were shown to integrate into the infarcted myocardium and to connect with capillaries of the host heart. (Sekine et al., 2008, Sekine et al., 2013)

In the study by Caspi et al (2007) the aim was to form a multicellular tissue construct that enables the generation of highly vascularized human engineered cardiac tissue. In the protocol, hESC-CM were seeded on 3D biodegradable, polymeric scaffolds and co-cultured with EC with or without embryonic fibroblasts. The presence of fibroblasts was shown to decrease EC death and increase EC proliferation. Moreover, the presence of EC derived vascular structures increased cardiomyocyte proliferation without limiting the cardiomyocyte orientation and alignment. This 3D vascularized human cardiac construct is proposed for utilization in studies related to cardiac development, function and tissue replacement therapy. (Caspi et al., 2007)

2.4.5 *In vivo* cardiac models

To assess the potential of a drug to delay ventricular repolarization in safety pharmacology, dogs, monkeys, swine, rabbits, ferrets and guinea pigs are considered as suitable animal models according to ICH guideline S7B. Smaller rodents (adult rat and mice) are excluded due to their markedly different mechanism of repolarization compared to humans.(Food and Drug Administration, 2005) The advantages of *in vivo* experiments is that the effects of anti-arrhytmic compounds, I_f blockers and also effects of non-cardiovascular chemicals can be identified. Moreover, all routes for drug administration can be applied. The disadvantage of animal models include high doses of compounds that may induce side effects on other organs thus increasing the complexity of assessing cardiac toxicity. Moreover, *in vivo* tests are time-consuming, allow only low-throughput and faces ethical problems. (Kettenhofen &

Bohlen, 2008) The most relevant *in vivo* cardiac models and the benefits and disadvantages related to them are discussed below and presented in Table 2.

Explanted hearts of guinea pigs and rabbits, as well as Purkinje fibres of guinea pig or dog origin, are common models in cardiac safety pharmacology studies (Kettenhofen & Bohlen, 2008). Action potential duration and arrhythmogenic effects can be measured using isolated Purkinje fibres and perfused hearts from rabbits. (Lu et al., 2008) These tests belong to the "Gold Standard" of test batteries for the investigation of new chemical entities prior to clinical trials. (Kettenhofen & Bohlen, 2008) However, standardization of these models is difficult due to inter-operator differences and inter-animal variations. Furthermore, the short experimental times severely limit the ability to assess long-term exposure of toxic compounds. (Kettenhofen & Bohlen, 2008)

To study safety pharmacological effects of new chemical entities, the whole animal models with different species are preferred. *In vivo* cardiac safety studies are most commonly performed using dogs. However, none of the animal models used appears to produce Torsade de Pointes with complete reliability. Studies in dogs, whether conscious or anaesthetised, appear to be invaluable in assessing the arrhythmic potential of new chemical entities. Since the dog studies are laborious and costly, alternative models such as the anaesthetised guinea pigs have been used. However, guinea pigs have, at molecular level, heterogeneity in cardiac ion channels that is not detected in rabbits, swine or dogs. (Finlayson et al., 2004)

Although rodent studies are considered inappropriate for assessment of cardiac repolarization, transgenic mouse models with appropriate cardiac ion channel mutations may be useful in identifying of novel arrhythmic mechanisms. (Finlayson et al., 2004)

Table 2. Typical characteristics of commonly used *in vitro* and *in vivo* cardiac models.

***In vitro* cardiac models**	**Cells used**	**End points**	**Applications**
Repolarization assay	dog Purkinje fibers, human pluripotent stem cell-derived cardiomyocytes	action potential duration, arrhythmia	drug development, safety assessment of chemicals, basic research
Ion current assay	transfected cell lines of different origin, rat ventricle myoblasts, mouse atrial cells, human pluripotent stem cell-derived cardiomyocytes	hERG current, IKrcurrent	drug development, safety assessment of chemicals, basic research
3D spheroid models with/without biomaterials	human pluripotent stem cell-derived cardiomyocytes, rodent fetal cardiomyocytes+endothelial cells/stromal cells	electrophysiology, morphology, tubule formation	cardiovascular development studies, disease modeling, drug development
Vascularized cardiac constructs with/without perfusion	human pluripotent stem cell-derived cardiomyocytes/neonatal rat cardiomyocytes+endothelial cells+fibroblasts of different origin	electrophysiology, viability, structure, tubule formation	tissue engineering, regenerative medicine, embryonic heart development, drug development
***In vivo* cardiac models**	**Animal used**	**End points**	**Applications**
Explanted heart	guinea pig, rabbit	action potential duration, arrhythmia	drug development, safety assessment of chemicals, basic research
Whole animal models	dog, guinea pig, swine, transgenic mouse, rabbit	electrophysiology, arrhythmia, histopathology	drug development, safety assessment of chemicals, disease modeling

3 Aims of the study

The aim of this thesis was to develop advanced, human cell based tissue models to supplement or replace animal tests and to be used for biomedical research. First objective was to establish and characterize human vascular models for testing of pro- and anti-angiogenic substances. Second aim was to combine vascular model with cardiomyocytes in order to develop cardiovascular model for cardiac safety and efficacy assessment. The specific aims of this thesis were as follows:

1. To develop and optimize human cell based stromal-vascular and vasculogenesis-angiogenesis models (I)

2. To characterize the human vasculogenesis-angiogenesis model for chemical testing as well as for tissue engineering platform (II)

3. To develop cardiovascular model composed of two different vascular platforms, vasculogenesis-angiogenesis model and angiogenesis model, and neonatal rat cardiomyocytes for a proof-of-concept level (III)

4. To develop functional human cell based cardiovascular model composed of angiogenesis model and human cardiomyocytes (IV)

4 Materials and methods

4.1 Origin of cells and ethical approvals

This study conforms to the principles outlined in the Declaration of Helsinki. Human adipose stromal cells (hASC) used in studies I, II and III were isolated in FICAM from adipose tissue samples that were received as a leftover material from surgeries at Tampere University Hospital, Tampere, Finland with individual written informed consents. Utilization of hASC has received an approval of Joint Municipal Authority of the Pirkanmaa Hospital District with ETL-code R03058.

Human umbilical vein endothelial cells (HUVEC) used in all four studies were isolated in FICAM from human umbilical cords that were received from caesarean sections at Tampere University Hospital, Tampere, Finland with individual written informed consent. Utilization of HUVEC has received an approval of Joint Municipal Authority of the Pirkanmaa Hospital District with ETL-code R08028.

Human foreskin fibroblasts used in studies III and IV were purchased from American Type Culture Collection (CRL-2522; ATCC, Manassas, VA, USA).

Neonatal rat cardiomyocytes (NRC) used in the study III were isolated from one to four-day-old Sprague Dawley rat pups. Rats were obtained from Animal Facilities of University of Tampere and cells were isolated in accordance with the Finnish animal protection laws and accepted by the Department for Social Welfare and Health Services of State Provincial Office of Western Finland. Euthanasia was performed by decapitation, a method approved in Directive 2010/63/EU. The use of NRC does not require permission for animal testing since the animals are being euthanized immediately (animal test level K0).

Human embryonic stem cell derived cardiomyosytes (hESC-CM, cell line H7) used in study III and IV were purchased from WiCell Research Institute (Madison, WI, USA). The induced pluripotent stem cells (iPSCC) used in study IV were derived

from human foreskin fibroblasts. Patient-specific iPSC cell line UTA.04602.WT was established in University of Tampere from healthy control individual as described earlier (Lahti et al., 2012, Takahashi et al., 2007). Results of the characterization of iPSC-derived cardiomyocyte cell line UTA.04602.WT used in study IV has been described earlier (Lahti et al., 2012). The Ethical Committee of Pirkanmaa Hospital District has granted approval for iPSC cells study with ETL-code R08070.

4.2 Development of media (I-IV)

In order to replace the commercial HUVEC medium (Table 3) and to create a completely defined medium, a vascular stimulation medium (VSM, Table 3) was developed to induce optimal vascular-like network formation in vasculogenesis-angiogenesis model (II). For cardiovascular models (III,IV), a universal medium was developed to primarily support CM functionality and maturation and secondarily to induce adequate vascular-like network formation. Development and optimization of media for different *in vitro* models was performed throughout the studies. The cell culture media used in all fours studies are presented in Table 3.

Medium was changed every two to three days to fibroblasts, HUVEC and hASC that were quality-controlled and tested for mycoplasma contamination (MycoAlert® Mycoplasma Detection Kit, Lonza) before experimental use.

In study I, the different test media were: 1) HUVEC medium; 2) HUVEC medium/HS where 2 % FBS was replaced with 2 % HS; 3) HUVEC medium/-serum where serum was excluded and 4) HUVEC medium/-gf where growth factors were excluded and 0,1 % gentamicin, 2 % FBS and 1 mM L-glutamine added to the medium. Detailed description of the media components is presented in Table 3.

In study II, the different test media were: 1) HUVEC medium; 2) HUVEC medium/HS, where 2 % FBS was replaced with 2 % HS; 3) serum free basal medium (SFBM) and 4) vascular stimulation medium (VSM). Detailed description of the media components can be seen in Table 3. In the first, above mentioned media comparison study, the ascorbic acid (AA), hydrocortisone (HY) and heparin (HE) in VSM were received from EGM-2 kit Single Quots -supplements (Lonza) and used

according to manufacturer´s protocol (concentrations of these supplements are not publicly available). After first media comparison study, concentrations of AA, HE (Heparin sodium salt from bovine intestinal mucosa) and HY, all purchased from Sigma, were optimized for VSM. In the concentration optimization study, the tested concentrations of AA were 0, 50, 100, 200, 500, 1000 and 2000 μg/ml; of HY 0, 20 ng/ml, 200 ng/ml, 1 μg/ml and 2μg/ml and of HE 0, 50 ng/ml, 500 ng/ml, 10μg/ml and 50 μg/ml. The concentrations of 10 ng/ml VEGF and 1 ng/ml FGF-2 used for VSM were optimized previously by us (Sarkanen et al., 2011).

In study III, altogether six different media were tested to find out the most optimal medium for rat cardiovascular model. The media were chosen to represent optimal culture media for either NRC (NRC medium 1 and 2, Table 3), angiogenesis model (angiogenic medium 3 and 4, Table 3) or vasculogenesis-angiogenesis model (vasculogenic-angiogenic medium 5 and 6, Table 3). The media 3-6 were chosen according to study II and according to our previous results (Sarkanen et al., 2011). Detailed description of the all test media components can be seen in Table 3. Hydrocortison, ascorbic acid and heparin used in NRC medium 2 were received from Single Quots -supplements (Lonza) with unknown concentrations. All media were tested with NRC monoculture and with rat cardiovascular model.

In study IV, due to our objective to have a low-serum or serum-free culture conditions in human cardiovascular model the minimum serum concentration for human CM monoculture was tested. Altogether five different serum concentrations including 0, 2, 5, 10 and 20 % FBS (Table 3) in EB medium were tested for dissociated human CM. All media were tested with CM monoculture and with human cardiovascular model.

Table 3. List of the cell culture, differentiation and stimulation media used for cell culture studies

Medium	Basal medium	Serum	Supplements	Study
Angiogenic medium 1	EBM-2 (Lonza)	2% FBS	10 ng/ml VEGF, 1 ng/ml FGF-2, 1 % l-glutamine	III
Angiogenic medium 2	EBM-2 (Lonza)	2% HS (Lonza)	10 ng/ml VEGF, 1 ng/ml FGF-2, 1 % l-glutamine	III
Angiogenesis stimulation medium	EBM-2 (Lonza)	2% FBS	1 % l-glutamin, 10 ng/ml VEGF, 1 ng/ml FGF-2	III,IV
EB medium	DMEM/ F-12 (Invitrogen)	0, 2, 5, 10, 20% FBS	1% NEAA (Lonza), glutamax (Invitrogen), 50 U/ml penicillin/streptomycin (Lonza)	IV
Fibroblast medium	MEM	10% FBS	1 % NEAA, 1 % l-glutamin	III, IV
hASC medium	DMEM/ F-12	10% HS (Lonza)	1 % l-glutamin	I-III
HUVEC medium	EBM-2 (Lonza)	2% FBS	Single Quots –supplements (Lonza): VEGF, FGF-2, IGF-I, EGF, hydrocortisone, ascorbic acid, heparin	I-IV
HUVEC medium/HS	EBM-2 (Lonza)	2% HS (Lonza)	Single Quots -supplements (Lonza): VEGF, FGF-2, IGF-I, EGF, hydrocortisone, ascorbic acid, heparin	I
HUVEC medium/- serum	EBM-2 (Lonza)	-	Single Quots -supplements (Lonza): VEGF, FGF-2, IGF-I, EGF, hydrocortisone, ascorbic acid, heparin	I
HUVEC medium/- gf	EBM-2 (Lonza)	2% FBS	0,1 % gentamicin, 1 mM l-glutamine	I
KSR medium	DMEM/ F-12 (Invitrogen)	20% KnockOut serum replacement (Invitrogen)	1% NEAA (Lonza), 2 mM Glutamax (Invitrogen), 50 U/ml penicillin/streptomycin (Lonza), 0.1 mM β-mercaptoethanol (Invitrogen), 7.8 ng/ml FGF-2 (R&D Systems)	IV

Table 3-continued. List of the cell culture, differentiation and stimulation media used for cell culture studies

Medium	Basal medium	Serum	Supplements	Study
NRC medium 1	DMEM/ F-12	-	10 ng/ml VEGF, 1 ng/ml FGF-2, 10 % BSA, 2.8 mM Sodium Pyruvate (Lonza), 2.56 mM L-glutamine, ITS and T3	III
NRC medium 2	DMEM/ F-12	-	10 ng/ml VEGF, 1 ng/ml FGF-2, hydrocortisone, heparin, ascorbic acid, 10 % BSA, 2.8 mM Sodium Pyruvate (Lonza), 2.56 mM L-glutamine, ITS and T3	III
NRC Seeding Medium (NRC-SM)	DMEM/F-12	10% FBS	100 IU/ml Penicillin/0.1 mg/ml Streptomycin, 2.56 mM L-glutamine	III
NRC Serum Free Medium (NRC-SFM)	DMEM/F-12	-	10 % BSA, 2.8 mM Sodium Pyruvate (Lonza), 2.56 mM L-glutamine, ITS and T3	III
Serum free basal medium (SFBM)	DMEM/ F-12	-	10 % BSA, 2.8 mM Sodium Pyruvate (Lonza), 2.56 mM L-glutamine, ITS and T3	II
Vascular stimulation medium (VSM)	DMEM/ F-12	-	10 ng/ml VEGF, 1 ng/ml FGF-2, hydrocortisone, ascorbic acid, heparin, 10 % BSA, 2.8 mM Sodium Pyruvate (Lonza), 2.56 mM L-glutamine, ITS and T3	II
Vasculogenic-angiogenic medium 1	EBM-2 (Lonza)	2% HS (Lonza)	Single Quots -supplements (Lonza): VEGF, FGF-2, IGF, EGF, gentamycin, hydrocortisone, ascorbic acid, heparin	III
Vasculogenic-angiogenic medium 2	EBM-2 (Lonza)	-	Single Quots -supplements (Lonza): VEGF, FGF-2, IGF, hEGF, gentamycin, hydrocortisone, ascorbic acid, heparin	III

Detailed description of the hPSC-derived cardiomyocyte differentiation media is presented in chapter 4.3.8.

All media components without supplier information were purchased from Gibco.

NEAA= non-essential amino acids

BSA= Bovine Serum Albumin (Sigma)

ITS= Insulin– transferrin–sodium selenite media supplement composed of 1 µM insulin, 5.64 µg/ml transferrin and 32 nM selenium (Lonza)

T3= 100 IU/ml P/0.1 mg/ml S 0.1 nM 3,3',5-Triiodo-L-thyronine sodium salt (Sigma)

4.3 Cell isolation, differentiation and culture

All cell culture was performed in incubators at 37 °C, under 5 % CO_2 atmosphere and at constant humidity.

4.3.1 Culture of human foreskin fibroblasts (I,III,IV)

Human foreskin fibroblasts were cultured in fibroblast medium (Table 3). After thawing cells were grown to confluency 2-3 days and used for further experiments.

4.3.2 Isolation and culture of human adipose stromal cells (I-III)

Human adipose tissue specimens were cut into small pieces, enzymatically digested with 0,05% collagenase I (Invitrogen, Paisley, Scotland, UK) in plain DMEM/F12 (Gibco, Invitrogen, Carlsbad, CA, USA) for 60 min at 37°C in a gyratory water bath. The digested tissue was centrifuged at 600 x g for 10 min in room temperature. The digested tissue was filtered through a 100 μm filter (Sarstedt, Nümbrecht, Germany), centrifuged and filtered through a 40 μm filter (Sarstedt). Cells were seeded into 75 cm^2 flasks (Nunc EasyFlask™, Nunc, Roskilde, Denmark) in hASC medium (Table 3). Cells were cultured to confluency and used for further experiments or cryopreserved in liquid nitrogen at passage 0-2 before experimental use.

4.3.3 Isolation and culture of human umbilical vein endothelial cells (I-IV)

HUVEC were isolated from human umbilical cord vein by using enzymatic procedure according to Jaffe et al. (Jaffe et al., 1973) but the process was further optimized by us (Sarkanen et al., 2011). The umbilical cord was separated from the placenta and the umbilical vein was cannulated with a 20G needle. The needle was secured by clamping the cord over the needle with a surgical clamp. The vein was perfused with Umbilical cord Buffer Solution (UBS; 0,1 M phosphate buffer solution containing 0,14 M NaCl , 0,004 M KCl and 0,011 M glucose) to wash out blood. After that the opposing end of the umbilical vein was clamped with a surgical clamp. The vein was infused with 0.05% collagenase I in a water bath at 37 °C up to 20 min.

After incubation, the collagenase I solution containing HUVEC was flushed from the cord by infusing the vein with UBS into 50 ml polypropylene tube. The cells were centrifuged at 250 x g for 10 min, resuspend to HUVEC medium (Table 3) and seeded into 75 cm^2 flasks. Cells were cultured to confluency and cryopreserved in liquid nitrogen at passage 2 before experimental use.

4.3.4 GFP-infection to human umbilical vein endothelial cells

Lentiviral construct pLKO-MISSION-Bright-GFP was purchased from Biomedicum Genomics (BMGen, Biomedicum Helsinki, Helsinki, Finland). The infection was carried out with HUVEC at low passages with 300 µl of pLKO-MISSION-Bright-GFP in 1 ml HUVEC medium (1 U/ml). Virus infection was accelerated with 8 µg/ml hexadimethrine bromide (Sigma). After 24 hours of incubation, medium was replaced with fresh HUVEC medium. Highly fluorescent clones were selected with cloning rings and further selected with dilution cloning to obtain pure GFP-HUVEC-culture. GFP-infected HUVEC were cultured to confluency and used for vasculogenesis-angiogenesis model to assess the origin and ratio of the cells responsible for vascular-like network formation in hASC and HUVEC co-culture.

4.3.5 Isolation and culture of neonatal rat cardiomyocytes (III)

Neonatal rat cardiomyocytes were harvested from one to four-day-old Sprague Dawley rat pups hearts as described by Uusimaa et al. (Uusimaa et al., 1992). Briefly, the hearts were perfused with collagenase solution and cut into 1-2 mm pieces. The heart pieces were incubated at 37 °C for 5 min and the supernatant was discarded. Fresh 5 ml of collagenase solution was added and this step was repeated five times. The supernatants were collected and filtered (100µm) into 20 ml of NRC seeding medium (NRC-SM, Table 3). The cells were preplated for 45 minutes to reduce the number of non-muscle cells and to achieve more pure NRC population. After the preplating, the NRC were collected and seeded in NRC-SM into 48-well plates (Nunc, Thermo Fisher Scientific, USA) at a density of 0,1 – 0,4 x 10^6 cells/cm^2. Serum free medium (NRC-SFM, Table 3) was changed day after plating and thereafter every second or third day.

4.3.6 Establishment of neonatal rat cardiomyocyte monoculture (III)

After preplating, the NRC were collected and seeded in NRC-CM seeding medium at a density of 0,1 – 0,4 x 10^6 cells/cm^2. Serum free medium was changed the day after cell seeding and thereafter every second or third day. NRC monoculture was used as a control to cardiovascular constructs in study III and cultured 7-14 days prior to end point analysis.

4.3.7 Establishment of human iPSC line (IV)

Patient-specific iPSC line UTA.04602.WT (from a 55-year-old female) was established using lentivirus infection followed by retrovirus infection into the primary fibroblasts from adult skin. Primary fibroblasts from a skin biopsy were cultured in Dulbecco's Modified Eagle's Medium (DMEM) (Lonza) containing 10% fetal bovine serum (Lonza), 2 mmol/l L-glutamine and 50 U/ml penicillin/streptomycin. The cells, plasmids and reagents used in the iPSC line establishment included 293FT cells (Invitrogen, Carlsbad, CA), PlatE cells (Cell Biolabs, San Diego, CA), pLenti6/UbC/mSlc7a1 vector (Addgene, Cambridge, MA), ViraPower Packaging Mix (Invitrogen), Lipofectamine 2000 (Invitrogen), pMX retroviral vector (hOCT3/4, hSOX2, hKLF4 or hc-MYC; Addgene) and Fugene 6 (Roche Diagnostics). The protocol for iPSC line establishment has been described previously (Takahashi et al., 2007). 293FT cells were maintained in Dulbecco's Modified Eagle's Medium (DMEM) (Lonza) containing 10% fetal bovine serum (Lonza), 2 mmol/l L-glutamine, 50 U/ml penicillin/streptomycin and 1% non-essential amino acids (Cambrex, East Rutherford, NJ). Plat-E cells, irradiated SNL-76/7 cells and mouse embryonic fibroblasts (MEF; Millipore, Billerica, MA) were cultured without antibiotics.

4.3.8 Differentiation and culture of human cardiomyocytes (IV)

Patient-specific iPSC or hESC differentiation into cardiomyocytes (CM) was carried out with either by co-culturing iPSC/hESC with murine visceral endoderm-like (END-2) cells (Humbrecht Institute, Utrecht, The Netherlands) as described earlier (Mummery et al., 2003) or with small molecule differentiation method via temporal

modulation of canonical Wnt signaling (Lian et al., 2013). In small molecule method pluripotent stem cells were cultured on Geltrex (Life Technologies) coated plates in mTeSR1 (StemCell Tehcnologies) medium for at least 3 passages before initiating the cardiac differentiation. After fully confluent, cells were passaged with Versene (Life Technologies). For differentiation, cells were treated with Accutase (Merck Millipore) at 37 °C for 5 min and single cells were seeded onto Geltrex coated plates at 0,17-0,25 x 10^6 cell/cm^2 in mTeSR1 supplemented with 5 μM ROCK inhibitor (RD Systems) for 4 days. The medium was changed to RPMI/B27 (Life Technologies) without insulin containing a Gsk3 inhibitor CHIR99021 (Miltenyi Biotech) to start differentiation (day 0) and it was changed to RPMI+B27 without insulin on next day (day 1). RPMI/B27 without insulin containing 5 μM IWP-4 was added to cells on day 3. The RPMI/B27 without insulin was changed to cells on day 5 and 7 after which the cells were maintained in the RPMI/B27 starting from day 10, with the medium changed every 3 days. Both differentiation methods resulted in beating cardiomyocyte aggregates. Aggregates were mechanically excised and treated with collagenase A (Roche Diagnostics) to dissociate aggregates to single cell level for further experimental use.

Patient-specific iPSC (UTA.04602.WT) and hESC (H7) were cultured on mitomycin C inactivated mouse embryonic fibroblasts (MEF) in KSR medium (Table 3). The medium was refreshed daily, and the stem cell colonies were passaged onto a new MEF layer once a week using 1 mg/ml collagenase IV (Invitrogen).

4.3.9 Establishment of human cardiomyocyte monoculture (IV)

After dissociation human CM were seeded in EB medium with 5 % FBS (Table 3) at density of 0,01-0,04 x 10^6 cells/cm^2. EB medium with 5 % FBS was changed 1-2 days after cell seeding and thereafter every second or third day. CM monoculture was used as a control to cardiovascular construct in study IV and cultured 6-13 days prior to end point analysis.

4.3.10 Development of tissue models

In this thesis two different vascular models, a stromal-vascular model (study I) and vasculogenesis-angiogenesis model (studies I, II) were developed to mimic embryonic vasculogenesis and adult angiogenesis. In parallel, cardiovascular model based on rat cardiomyocytes mimicking adult heart was develop for a proof-of-concept level (study III). In rat cardiovascular model, neonatal rat cardiomyocytes were combined with vasculogenesis-angiogenesis model and with angiogenesis model that was previously developed and validated in FICAM (Sarkanen et al., 2011). These two different vascular models were tested for their ability to support the viability and contractility of cardiomyocytes. Finally, completely human cell based cardiovascular model with human cardiomyocytes and angiogenesis model (study IV) mimicking adult human heart was developed.

4.3.11 Stromal-vascular model (I)

hASC (six different cell lines from different donors, passages 1-7 were used) were seeded in HUVEC medium at a density of 20 000 cells/cm^2. Cells were cultured for either 3 or 6 days in HUVEC medium to assess vascular-like network formation. HUVEC medium and other test media inducing vascular-like network formation was changed once to cells cultured for 3 days and twice to cells cultured for 6 days.

4.3.12 Vasculogenesis-angiogenesis model (I, II)

hASC were seeded (p1-7) in HUVEC medium (Table 3) into 48-well plates at a density of 20 000 cells/cm^2. After 1-3 hours HUVEC (p4) were seeded on top of hASC at a density of 4000 cells/cm^2 in HUVEC medium. The seeding densities of hASC and HUVEC were chosen in study I. Vasculogenesis-angiogenesis model was cultured 3 or 6 days prior to end point analysis in study I, and 6 days prior to end point analysis in study II. Vasculogenesis-angiogenesis model was cultured for approximately 24 hours prior to utilization in cardiovascular construct used in study III. HUVEC medium and other test media inducing vascular-like network formation was changed once to 3 day culture and twice to 6 day culture.

4.3.13 Rat cardiovascular model (III)

Two different vascular platforms were cultured with neonatal rat cardiomyocytes (NRC) in order to develop an optimal cardiovascular model. NRC were seeded on top of the (1) vasculogenesis-angiogenesis model and (2) angiogenesis model approximately after 24 hours at a density of 0,1-0,4 x 10^6 cells/cm^2 in NRC-SM (Table 3). Angiogenesis model was constructed as described previously by us (Sarkanen et al., 2011). Briefly, fibroblasts (p6-7) were seeded at a density of 20 000 cells/cm^2 in fibroblast medium (Table 3) and grown for 2-3 days to confluency. HUVEC medium was changed and HUVEC were seeded on top of the fibroblast culture at a density of 4000 cells/cm^2 in HUVEC medium (Table 3). Rat cardiovascular models consisted of HUVEC+hASC+NRC and HUVEC+fibroblast+NRC. After approximately 24 hours after NRC seeding serum free medium (NRC-SFM, Table 3) and other test media was changed and thereafter three times in a week. Rat cardiovascular models were cultured 7-14 days prior to end point analysis.

4.3.14 Human cardiovascular model (IV)

EB medium with 5 % FBS (Table 3) was changed to angiogenesis model before seeding of CM. Angiogenesis model was constructed as described previously by us (Sarkanen et al., 2011). Briefly, fibroblasts (p6-7) were seeded at a density of 20 000 cells/cm^2 in fibroblast medium (Table 3) and grown for 2-3 days to confluency. HUVEC medium was changed and HUVEC were seeded on top of the fibroblast culture at a density of 4000 cells/cm^2 in HUVEC medium (Table 3). Angiogenic stimulation medium (ASM, Table 3) inducing vascular-like network formation was changed the day after cell seeding and thereafter twice. Dissociated human iPSC- or hESC-derived CM were seeded on top of the angiogenesis model at day 6, when the vascular-like network was already formed, at a density of 0,01-0,04 x 106 cells/cm^2 in EB medium with 5 % FBS. 1-2 days after CM seeding first EB medium with 5 % FBS change was performed and thereafter three times in a week. Human cardiovascular model was cultured 6-12 days prior to end point analysis.

4.4 Flow cytometric analysis (I,II)

Characterization of individual cells was performed to the building blocks, i.e. hASC and HUVEC, of vasculogenesis-angiogenesis model. hASC (p1) and HUVEC (p3) were analysed for surface and intracellular marker expression using a BD FACSCanto II and FACSAria flow cytometers (both BD Biosciences, Erembodegem, Belgium). The markers used in the analysis are listed in Table 4. The analysis was performed using 5 000-10 000 cells per sample. Isotype controls and unstained cell samples were used to eliminate background fluorescence. Compensation was performed using compensation particles (BDTM CompBeads, BD Biosciences). The results were analyzed using BD FACSDivaTM Software (BD Biosciences).

Table 4. Surface and intracellular* markers used in flow cytometric analysis

Cell	Marker	Target
hASC	vWf*-APC	von Willebrand factor
	CD144-FITC	vascular endothelial cadherin
	eNOS*-PE	endothelial nitric oxide synthase
	CD140b-PE	platelet derived growth factor receptor beta
	CD45-PE	leukocyte common antigen
	CD14-FITC	surface antigen expressed on monocytes/macrophages
	CD68-FITC	glycoprotein expressed on monocytes/macrophages
	CD309-PE	vascular endothelial growth factor receptor 2
	CD31-V450	platelet endothelial cell adhesion molecule
	NG2-PE	chondroitin proteoglycan expressed on pericytes
	CD90-FITC	mesenchymal stem cells, T cells
	CD105-V450	endoglin expressed on mesenchymal stem cells
	CD73-PE-CY7	ecto-5'-nucleotidase
	CD34-APC	sialomucin-like adhesion molecule expressed on hematopoietic progenitor cells
HUVEC	vWf*-APC/PE	von Willebrand Factor
	CD144-FITC/PE	vascular endothelial cadherin
	CD309-PE	vascular endothelial growth factor receptor 2
	CD73-PE-CY7	ecto-5'-nucleotidase
	CD68-FITC	glycoprotein expressed on monocytes/macrophages
	eNOS*-PE	endothelial nitric oxide synthase
	CD105-V450	endoglin expressed on mesenchymal stem cells
	CD34-APC	sialomucin-like adhesion molecule expressed on hematopoietic progenitor cells
	CD31-V450/FITC	platelet endothelial cell adhesion molecule
	CD140b-PE	platelet derived growth factor receptor beta
	NG2-PE	chondroitin proteoglycan expressed on pericytes
	CD13-PE	aminopeptidase N
	CD44-FITC	hyaluronate, homing cell adhesion molecule (HCAM)
	CD117-APC	receptor tyrosine kinase protein, mast/stem cell growth factor receptor
	CD 133-PE	glycoprotein prominin-1 expressed in endothelial progenitor cells
	CD202b	angiopoietin receptor Tie-2
	CD63-PE	tetraspanin expressed in basophils
	VEGFR2	vascular endothelial growth factor receptor 2

4.5 Immunocytochemical analysis (I-IV)

For immunocytochemical stainings, cells were washed two to three times with PBS, fixed with ice-cold 70 % ethanol or 4 % paraformaldehyde for 20 minutes, permeabilized with 0,5 % Triton X-100 (JT Baker, Phillipsburg, NJ, USA) for 15 minutes and blocked for unspecific staining with 10 % bovine serum albumin (BSA, Sigma) for 30 minutes. After blocking, the cells were incubated with the primary antibodies at 1 hour at RT or in + 4 °C o/n. After primary antibody incubation, cells were washed three times with PBS and incubated 30 min with secondary antibody. Fluorescence was visualized with Nikon Eclipse Ti-S microscope (Nikon, Tokyo, Japan) or with confocal laser scanning microscope Zeiss LSM 700 (Zeiss LSM 700 on the Axio Observer, Carl Zeiss Microimaging GmbH, Jena, Germany) and the images were processed with Zen2009 (confocal images, Carl Zeiss) and with Adobe Photoshop software 7.0 (Adobe Systems, San Jose, CA, USA) and Corel Draw software 10.0 (Corel Corporation, Ottawa, ON, Canada). A complete list of primary and secondary antibodies used in immunocytochemical stainings is shown in Table 5.

Table 5. List of antibodies used in studies (I-IV)

Primary antibody	Target	Dilution	Origin	Secondary antibody	Supplier of prim. ab
von Willebrand factor	endothelial cells	1:100	rabbit	IgG-TRITC, IgG A568	Sigma-Aldrich
collagen IV	basement membrane	1:500	mouse	IgG-FITC	Sigma-Aldrich
calponin	contractile smooth muscle cells	1:800	mouse	IgG-FITC	Sigma-Aldrich
α-smooth muscle actin	smooth muscle actin pericytes	1:200	mouse	IgG-FITC	DAKO
smooth muscle myosin heavy chain	vascular smooth muscle cells	1:800	mouse	IgG-FITC	Sigma-Aldrich
platelet derived growth factor receptor β	pericytes, smooth muscle cell progenitors	1:800	mouse	IgG-FITC	Sigma-Aldrich
vascular endothelial cadherin	endothelial cell junctions	1:50	mouse	IgG-FITC	BD Biosciences
occludin	endothelial cell junctions	1:300	mouse	IgG-FITC	Sigma-Aldrich
troponin t	cardiomyocytes	1:1500 1:500	goat mouse	IgG Alexa Fluor 488 IgG Alexa Fluor 568 IgG-FITC	Abcam Abcam
α-actin	cardiomyocytes	1:1500	mouse	IgG-FITC	Sigma-Aldrich
connexin-43	cardiomyocyte gap junctions	1:1000	mouse rabbit	IgG-FITC IgG-TRITC	Sigma-Aldrich

4.6 Microscopical analysis (I-IV)

4.6.1 Analysis of cardiomyocyte contractility (III, IV)

NRC contractility was estimated visually as weak (10-30 % beating cardiomyocytes per cm^2), moderate (30-50 % of the cardiomyocytes beating per cm^2) or strong (50-70 % synchronously beating cardiomyocytes per cm^2).

Human CM viability and functionality was microscopically observed three to five times in a week under phase contrast microscope. In the assessment of human CM contractility, the size of the areas of beating CM, beating frequency and synchronization were visually observed.

4.6.2 Analysis of vascular-like network formation

In studies I and II, the vascular-like network formation, i.e. vWf-positive tubule structures, were analysed with Nikon Eclipse TS100 microscope (Nikon, Tokyo, Japan) from with 40x magnification (study I, II) or using Cell-IQ (Chipman tech., Tampere, Finland) with 10x objective and 5x5 grid (study II). The analysis and grading was based on the length and the branches of the tubules. After Cell-iQ imaging, the quantitation of the area of the vascular-like network was performed using ImageJ software (National institutes of health, NIH, Maryland, USA). The total vascular-like network area was calculated as the total number of pixels in images.

In study III, the vascular-like network formation in rat cardiovascular model in different media were analysed visually using Nikon Eclipse TS100 microscope and compared to a control medium that gave value of 100 % vascular-like network formation. In rat cardiovascular model composed of hASC+HUVEC+NRC, the control media was HUVEC medium and in rat cardiovascular model composed of fibroblast+HUVEC+NRC the control medium was angiogenesis stimulation medium (Table 5). The analysis was based on vascular-like network formation, i.e. the length and the branches of tubules.

4.7 Electron microscopical analysis (II)

To study the microstructure of vascular-like network, the vasculogenesis-angiogenesis model was cultured in 24 well UpCell plate (ThermoFisher) for transmission electron microscopy (TEM) and on glass cover slip coated with 0,1 % Gelatin for scanning electron microscopy (SEM). Culture was maintained for 6 days and washed twice with PBS prior to fixation.

SEM specimens were fixed in 2 % glutaraldehyde in 0.1 M phosphate buffer after which the SEM samples were dehydrated in alcohol and dried in Baltec critical point dryer (Baltec, CPD030, Balzers, Liechtenstein). A layer of platinum was sputtered on the specimens with a sputter coater (Agar Scientific, Stansted, England). Specimens were examined in a Zeiss Ultra Plus scanning electron microscope, (Carl Zeiss MT- Nanotechnology System Division, Carl Zeiss NTS Gmbtt, Oberkochen, Germany) using 5 kV as an accelerating voltage.

TEM specimens were detached from temperature sensitive 24 well UpCell plate and transferred to fixative with 1 % glutaraldehyde 4 % formaldehyde mixture in 0.1 M phosphate buffer for 10 minutes. The cell sheet was immersed in 2% Agarose in distilled water and postfixed in 1% osmiumtetroxide, dehydrated in acetone and embedded in Epon LX 112 (Ladd Research Industries, Vermont, USA). Thin sections were cut with Leica Ultracut UCT ultramicrotome, stained in uranyl acetate and lead citrate and examined in Cm 100 transmission electron microscope. Images were captured by Morada CCD camera (Olympus Soft Imaging Solutions GMBH, Munster Germany).

4.8 Gene expression studies (I,II,IV)

Quantitative reverse-transcriptase polymerase chain- reaction (qRT-PCR) was performed to stromal-vascular model (d3 and d6, study I), vasculogenesis-angiogenesis model (d3 and d6, studies I and II), angiogenesis model (d1, d6 and d18, study IV), human cardiomyocyte monoculture (d7 and d18, study IV) and human cardiovascular model (d7 and d18, study IV). The total RNA was extracted using TRIzol® (Invitrogen, study I), RNAeasy minikit (Qiagen, studies II and IV)

or PureLink RNA Mini Kit (Life Technologies, study IV) following the manufacturer's protocol. The concentration and purity of RNA was assessed using spectrophotometry (GeneQuant II RNA/DNA calculator, Pharmacia Biotech GE Healthcare UK Ltd and microplate reader in Varioskan Flash Spectrophotometer, ThermoScientific) before further use. Reverse transcription of the total RNA to cDNA was performed using High-Capacity cDNA Reverse Transcriptase Kit (Life Technologies, study I), RT² First Strand Kit (Qiagen, study II) or iScript cDNA synthesis kit (Bio-Rad, study IV) following manufacturer's instructions. qRT-PCR was performed according to standard protocols on Abi Prism 7000 sequence detector (Applied Biosystems, study I) or on Bio-rad CFX96 Real Time System (BioRad Laboratories, USA, studies II and IV).

Human Angiogenesis RT² Profiler™ PCR Array (Qiagen) was used to profile the expression of 84 key human angiogenesis-related genes (study II). A comprehensive list of genes included in the array can be found in http://www.sabiosciences.com. Additionally, the expression of human angiogenesis related genes including VEFG-A, FGF-2, PDGF-β, TGF-β1, angiopoietin-1, angiopoietin-2, caldesmon, PECAM and human cardiac related genes including CACNA1C, TNNT2, KCNJ2, CX-43, MYH-6, MYH-7, ADRB1 and SCN5a were studied (Table 6). Reference genes for human RPLP0 and GAPDH were used for data normalization. 1-50 ng of total cDNA and 300 nM primer pairs were used in each PCR reaction, except for human angiogenesis RT² Profiler™ PCR Array (study II) 980 ng of total cDNA was used. Relative RNA expression was calculated in comparison to reference gene RNA expression using the Pfaffl method (Pfaffl, 2001). Ratio of relative expression= $(E_{target})^{\Delta CP \text{ target (control-sample)}} / (E_{reference})^{\Delta CP \text{ reference (control-sample)}}$

Table 6. The list of human SYBR-green primers and Taqman primer-probe sets* used in qRT-PCR

Gene	Forward primer	Reverse primer	Study
VEFG-A	AGGGCAGAATCATCACGAAGT	AGGGTCTCGATTGGATGGCA	IV
FGF-2	AGAAGAGCGACCCTCACATCA	CGGTTAGCACACACTCCTTTG	IV
PDGFβ	CTCGATCCGCTCCTTTGATGA	CGTTGGTGCGGTCTATGAG	IV
TGFβ1	CAATTCCTGGCGATACCTCAG	GCACAACTCCGGTGACATCAA	IV
Angiopoietin1	AGCGCCGAAGTCCAGAAAAC	TACTCTCACGACAGTTGCCAT	IV
	AGCTACCACCAACAACAGTG	CAAAGATTGACAAGGTTGTGG	I
Angiopoietin2	ACCCCACTGTTGCTAAAGAAGA	CCATCCTCACGTCGCTGAATA	IV
CACNA 1C	TGACATCGAGGGAGAAAACT	ACATTAGACTTGACTGCGGC	IV
TNNT2	TTCACCAAAGATCTGCTCCTCGCT	TTATTACTGGTGTGGAGTGGGTGTGG	IV
KCNJ2	GAGCACAGCTCCTCAAATCC	TTCCACTGTCAAACCCAACA	IV
CX-43	GGTCTGAGTGCCTGAACTTGCCT	TGCCTGGGCACCACTCTTTTGC	IV
MYH6	AGGGATAACCAGGGGAAGCACC	TGCGAATGTCAAAGGGCCGGG	IV
MYH7	GGCAAGACAGTGACCGTGAAG	CGTAGCGATCCTTGAGGTTGTA	IV
PECAM	TCATTTCTGGGATCC ATATG A	TGGGTGTAGAGAAGGATTCCGT	I
caldesmon	AAGAATCCTTGGGACAGGTGAC	GTGGTGGTTGTCTTGGCCTC	I
RPLP0	AATCTCCAGGGGCACCATT	CGCTGGCTCCCACTTTGT	I
ADRB1*	Hs02330048_s1		IV
SCN5A*	Hs00165693_m1		IV
RPLP0*	Hs04189669_g1		IV
GAPDH*	Hs02758991_g1		IV

4.9 Functional studies

4.9.1 Microelectrode array (MEA) measurements

The electrophysiological properties, especially field potentials, and conductance of cardiovascular constructs were analyzed using the MEA system (Multi Channel Systems MCS GmbH, Reutlingen, Germany). Cells were grown on top of the electrodes on MEA well with which the field potential can be measured (Reppel et al., 2004). The MEA wells (8x8 standard MEAs or 6-well MEAs) were first hydrophilized with FBS for 30 min at RT and then coated with 0.1 % gelatin type A (Sigma-Aldrich) for 1 hour at RT.

In rat cardiovascular model (study III), the MEA measurements were performed as described in Kujala et al. (Kujala et al., 2011). Briefly, an MEA1060-Inv-BC amplifier, a 20 kHz sampling rate and MC_Rack software (all from Multi Channel Systems MCS GmbH) was used. The recordings were performed at room atmosphere keeping the temperature at +37 °C with MEA amplifier's heating element. To maintain the sterility of the cultures the MEAs were covered with a gas-permeable membrane (ALA Scientific). The field potential signals were recorded twice during each culture and for three minutes at a time. The measurements were performed with MC_Rack, files converted with MC_DataTool and signals analyzed with AxoScope.

In human cardiovascular model (study IV), field potentials were recorded at + 37°C and signals were recorded for 2 min. The sampling frequency was 20 kHz. Field potentials were recorded during spontaneous baseline beating, and with 1μM adrenaline (Sigma-Aldrich) or 300nM E-4031 (Sigma-Aldrich). Drugs were diluted and measurements performed in EB medium with 5 % FBS. A wash-in time of two to five minutes was allowed for the drugs before measurement. The field potentials were recorded with MC_Rack v.4.5.7 software (Multi Channel Systems MCS GmbH). Signals were analyzed with Cardiomyocyte MEA Data Analysis (CardioMDA) software (Pradhapan et al., 2013).

4.9.2 Analysis of Ca^{2+} cycling

Human cardiovascular model (study IV) was loaded with 4 μmol/L Fura-2 AM (Invitrogen, Molecular Probes) for 30 minutes in HEPES based medium. Measurements were performed in 37°C and the extracellular solution and consisted of (in mmol/L): 137 NaCl, 5 KCl, 0.44 KH_2PO_4, 20 HEPES, 4.2 $NaHCO_3$, 5 D-glucose, 2 $CaCl_2$, 1.2 $MgCl_2$ and 1 Na-pyruvate (pH was adjusted to 7.4 with NaOH). Ca_{2+} measurements were conducted on an inverted IX70 microscope (Olympus Corporation, Hamburg, Germany) where spontaneously beating CM were visualized with a UApo/340 x 20 air objective (Olympus). Images were acquired with an ANDOR iXon 885 CCD camera (Andor Technology, Belfast, Northern Ireland) synchronized with a Polychrome V light source by a real time DSP control unit and TILLvisION software (TILL Photonics, Munich, Germany). Fura-2 in CM was

excited at 340 nm and 380 nm light and the emission was recorded at 505 nm. For Ca^{2+} analysis, areas of interests were selected for spontaneously beating cells and background noise was subtracted before further processing. The Ca^{2+} levels are presented as ratiometric values of F340/F380. The changes in Ca^{2+} were recorded during spontaneous baseline beating and spontaneous beating during 1μM adrenaline (Sigma-Aldrich) perfusion.

4.10 Statistical analysis (I-IV)

In study I, statistical analyses were performed and graphs processed with GraphPadPrism 5.0 (GraphPad Software, Inc., San Diego, CA, USA). Analysis of vascular-like network formation and qRT-PCR results were subjected to One-way ANOVA followed by Dunnett's and Bonferroni's post-tests. The results were reported as mean ± SD and differences were considered significant when $p<0.05$*, $p<0.01$** and $p<0.001$***.

In study II, PCR results were analyzed using the PCR Array Data Analysis Web Portal (http://www.SABiosciences.com/pcrarraydataanalysis.php). Two fold change compared to housekeeping gene GAPDH was considered significant. Statistical analyses were performed and graphs processed with GraphPad Prism 5.0 (GraphPad Software, Inc., San Diego, CA, USA). The results concerning vascular-like network formation were subjected to One-way ANOVA followed by Dunnett's and Bonferroni's post-tests. The results were reported as mean ± SD and differences were considered significant when $p<0.05$*, $p<0.01$** and $p<0.001$***.

In study III, a linear mixed-effect model was used to assess differences in vascular-like network formation in control versus other media. A linear mixed-effect model with estimation as a dependent variable was fitted separately for angiogenesis model and vasculogenesis-angiogenesis model using function lme in R (Software environment for statistical computing and graphics, version 2.13.0, The R Foundation for Statistical Computing). Experiments and media were used as independent variables. Random intercept for parallel wells was used together with independent random errors.

In study IV, comparative ΔΔCt method (Livak & Schmittgen, 2001) was used in gene expression studies to analyze the relative expression levels of angiogenesis and cardiac related genes. qPCR data is expressed as mean values +/- SD. Statistical analysis for the qPCR data was performed by IBM SPPS Statistics 22-software and by using Mann-Whitney U-test for independent samples. Bon ferroni -correction was included when more than two groups were analyzed. A p-value less than 0.05 was considered statistically significant.

In MEA and Ca^{2+} imaging data, the significance of differences between the two groups (CM monoculture and cardiovascular construct) was evaluated with the unpaired Student's t-test. The significance of changes within a group was evaluated with the paired Student's t-test. MEA and Ca^{2+} imaging data are expressed as average ± S.E.M. In Ca^{2+} imaging data n refers to the number of cells and in MEA data n refers to number of MEA chips. A p-value less than 0.05 was considered statistically significant.

5 Results

5.1 Development of *in vitro* vascular models (I,II)

Two different human cell based *in vitro* vascular models, a stromal-vascular model and a vasculogenesis-angiogenesis model, were developed. Stromal-vascular model consisted of hASC monoculture and vasculogenesis-angiogenesis model consisted of hASC and HUVEC co-culture (Figure 6). In vasculogenesis-angiogenesis model simultaneous seeding of hASC and HUVEC was shown to produce an optimal vascular-like network.

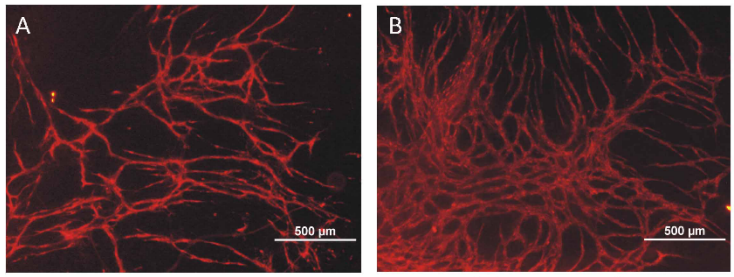

Figure 6. The *in vitro* (A) stromal-vascular model and (B) vasculogenesis-angiogenesis model developed in this study at day 6. Anti-von Willebrand factor staining, scale bars 500 µm.

5.1.1 Vascular-like network formation in *in vitro* vascular models (I)

The vascular-like network formation capacity of the stromal-vascular model and vasculogenesis-angiogenesis model was compared in two different time points (day 3 and day 6). The results showed that vasculogenesis-angiogenesis model produced more extensive vascular-like network with high reproducibility compared to stromal-vascular model (Figure 6). Vascular-like network formation in vasculogenesis-angiogenesis model was independent of the cell line or passage number (p1-7 were tested) whereas in stromal-vascular model induction to vascular-like network formation was not seen repeatedly. With passage dependent manner, less than 50 %

of the tested hASC lines (six lines, p1-7) produced a vascular-like network in some degree. Although vascular-like network was produced in vasculogenesis-angiogenesis model already at day 3, a significantly higher ($p<0.001$) vascular-like network formation with multilayered tubules was seen at day 6.

Immunocytochemical staining with anti-collagen IV, a marker of the basement membrane, was widely used in this study to assess the stability and maturity of vascular-like network. Basement membrane covering the tubules was intact in vasculogenesis-angiogenesis model at day 6 whereas in stromal-vascular model the development of basement membrane was incomplete. As a conclusion, further characterization including medium development was performed to vasculogenesis-angiogenesis with 6 day culture.

5.1.2 Optimal medium for vasculogenesis-angiogenesis model (II)

First, commercial HUVEC medium (Table 3) was used to induce vascular-like network formation for vasculogenesis-angiogenesis model. In order to replace the commercial HUVEC medium and to create a completely defined medium, a vascular stimulation medium (VSM) was developed for vasculogenesis-angiogenesis model. VSM was shown to produce evenly distributed vascular-like network with connected branches and less cell aggregates compared to vascular-like network formed in HUVEC medium. Moderate differences in the expression of angiogenesis-related genes were detected between HUVEC medium and VSM. In VSM, nine genes were upregulated (Angpt1, F3, FIGF, IGF-1, LEP, MDK, MMP2, MMP9, PGF) and nine genes (CCL11, CXCL9, FN1, IL6, IL8, SERPINE1, TGFB2, THBS2, TIMP1) were down-regulated compared to gene expression in HUVEC medium.

5.1.2.1 Impact of serum (II)

In the HUVEC medium, the effect of human serum (HUVEC medium/HS, Table 3), fetal bovine serum (HUVEC medium, Table 3) and the absence of serum (HUVEC medium/-serum, Table 3) on vascular-like network formation capacity of vasculogenesis-angiogenesis model was studied. The results showed that FBS could be replaced with HS without significant effect on the vascular-like network

formation as tested with one-way ANOVA. Also in the absence of serum an extensive vascular-like network formation similar to HS induction was detected.

In the development of VSM, a low serum (2 %) and serum-free medium enabled stable cell attachment and induced a dense, connected vascular-like network with intact tubule walls. The presence of HS in the medium was found to induce denser and more connected vascular-like network than presence of FBS (see Figure 1 in the original publication II).

5.1.2.2 Growth factor optimization (II)

Before developing VSM, vascular-like network formation in the vasculogenesis-angiogenesis model and in the stromal-vascular model was induced in the HUVEC medium in the presence of angiogenic growth factors and substances including vascular endothelial growth factor (VEGF), fibroblast growth factor (FGF-2), epidermal growth factor (EGF), insulin-like growth factor (IGF), heparin (HE), hydrocortisone (HY) and ascorbic acid (AA). In the absence of growth factors (HUVEC medium/-gf, Table 3), the vascular-like network formation was markedly decreased in vasculogenesis-angiogenesis model.

In the development of VSM for vasculogenesis-angiogenesis model, concentrations of 10 ng/ml VEGF and 1 ng/ml FGF-2 were used according to our previous study (Sarkanen et al., 2011). Concentrations of heparin, hydrocortisone and ascorbic acid were optimized by comparing the vascular-like network formed in HUVEC medium. An optimal vascular-like network formation was received with ascorbic acid concentration 100 μg/ml and heparin concentration 0-500 ng/ml. The results showed that vascular-like network was formed in the absence of heparin supplement with minor morphological differences. However, low concentration of heparin (50 ng/ml) increased the total area of vascular-like network significantly compared to HUVEC medium. An optimal hydrocortison concentration was shown to be 0.2 μg/ml.

5.1.3 Maturation of vasculogenesis-angiogenesis model (I-IV)

An intact basement membrane was detected in tubule structures formed in VSM as detected in collagen IV immunocytochemical staining. Additionally, smooth muscle actin (SMA), smooth muscle myosin heavy chain (SMM) and contractile smooth muscle calponin positive cells were seen to surround the tubule structures (Figure 7.A-C). The presence of platelet derived growth factor receptor-β (PDGFR-β) positive cells were also detected (Figure 7.D).

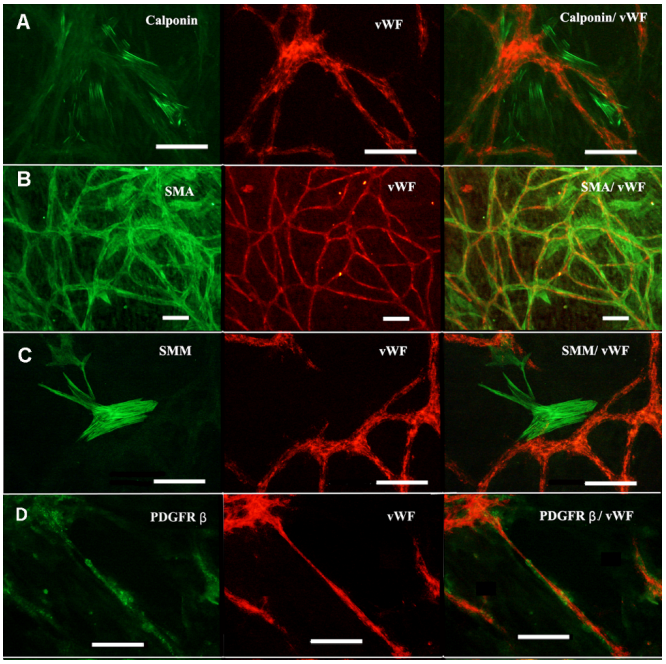

Figure 7. Vascular-like network formed in VSM showed properties of vascular maturation. Anti- von Willebrand factor -staining shown in red in all figures. (A) Calponin -; (B) SMA - and (C) SMM -positive cells surrounding the vascular-like network. (D) α-PDGFR-β stained pericytes are located along the tubules. Scale bars 100 µm.

Analysis of 84 angiogenesis-related genes was performed to study the maturation of vasculogenesis-angiogenesis model in VSM compared to HUVEC medium that was used as a control (study II). The expression of angiopoietin 1, a marker for maturated tubules, was significantly high ($p<0.05$) in vasculogenesis-angiogenesis model in VSM at day 6. VEGF-A and FGF-2, indicators of the early stage of angiogenesis, were moderately down-regulated in VSM but not in statistically significant manner.

TGF-β1, a marker for tubule maturation, was slightly down-regulated. An up-regulation of MMP-2 and MMP-9, enzymes that are involved in degradation of the ECM in the early stages of angiogenesis, were detected.

5.1.4 Morphology and microstructure of vasculogenesis-angiogenesis model (I,II)

Confocal laser scanning microscopical analysis showed approximately 196 μm thickness and three-dimensional structure with overlaying tubules in the vasculogenesis-angiogenesis model cultured in HUVEC medium (Figure 8.A-B). Basement membrane marker collagen IV was widely expressed and covered the tubule structures (Figure 8.B). With electron microscopy, the microstructure of the tubules formed in VSM was studied. The analysis showed the presence of lumen, basement membrane and adherence junctions. Moreover, the electron microscopic as well as immunocytochemical analysis showed that vasculogenesis-angiogenesis model actively produces extracellular matrix components including basement membrane, fibrillins and collagens (Figure 8.C). Immunocytochemical staining with VE-Cadherin and occludin confirmed the presence of adherence junctions between endothelial cells (Figure 8.C). The 3D structure of the vascular-like network and shape of the tubules can be seen in the close-up image (Figure 8.D).

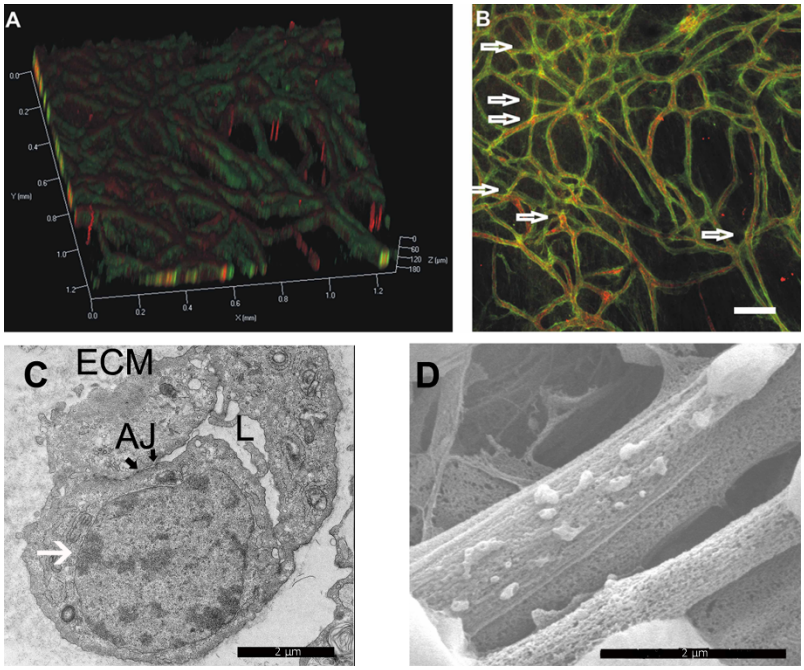

Figure 8. Structure of vascular-like network in vasculogenesis-angiogenesis model. (A) 3D projection of the vascular-like network; (B) multilayered tubule formation with intact basement membrane, some of the crossing points of the tubules are indicated with arrows. Anti-von Willebrand factor antibody (red) and anti-collagen IV (green); (C)Transmission electron microscopy image of tubule in earlier stage of vascular development showing endothelial cell with large nucleus (white arrow), lumen (L), adherence junctions (AJ) and ECM. Scale bar 2 µm; (D) scanning electron microscopy image shows the 3D structure and the tubule shape of the vascular-like network. Scale bar 2µm.

5.1.5 Vasculogenic properties of vasculogenesis-angiogenesis model (I,II)

Stromal-vascular model (hASC monoculture) had a passage and donor dependent differentiation capacity towards endothelial cells. hASC monoculture typically forms short cords with less than 50 % of the tested hASC lines (six lines, p1-7) producing a vascular-like network in some degree (study I).

hASC and GFP-infected HUVEC co-culture model was created to evaluate the origin of the cells responsible for the tubule formation in vasculogenesis-angiogenesis model. The results showed that co-culture stained with anti-vWf was mostly mosaic and consisted of two different populations of vWf-positive cells. Approximately half of the vWf-positive cells was GFP-infected and the other half

of was GFP-negative cells (see Figure 2 in the original publication I). In addition, the expression of endothelial cell marker PECAM-1 was significantly increased in hASC monoculture from day 3 to day 6 ($p<0.05$).

We analyzed whether population of endothelial progenitor cells capable for vasculogenesis resides inside hASC population. In FACS analysis, high expression of CD90 and a moderate expression of CD34 was seen. The expression levels of mature endothelial cell markers CD31 and CD144 in hASC population were very low. However, another endothelial progenitor cell marker CD309 (VEGFR2) showed very low expression in all six hASC lines that were analyzed (study II).

5.2 Development of *in vitro* cardiovascular models (III,IV)

In this thesis, two different *in vitro* cardiovascular models were developed. Rat cardiovascular model consisted of human angiogenesis model and human vasculogenesis-angiogenesis model combined with neonatal rat cardiomyocytes (fibroblast+HUVEC+NRC and hASC+HUVEC+NRC, respectively) (Figure 9.A-B). Human cardiovascular model composed of human angiogenesis model and human pluripotent stem cell derived cardiomyocytes (fibroblast+HUVEC+hESC/iPS-CM) (Figure 9.C).

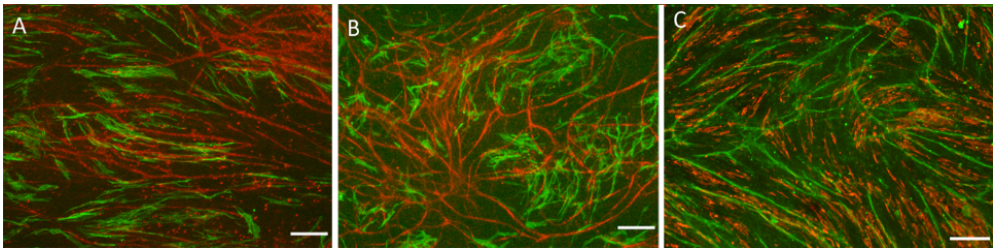

Figure 9. *In vitro* cardiovascular models developed in this study. Rat cardiovascular model with (A) fibroblast+HUVEC+NRC and with (B) hASC+HUVEC+NRC stained with anti-troponin T (green, cardiomyocytes) and anti-vWf (red, vascular-like network). Human cardiovascular model with (C) fibroblast+HUVEC+human pluripotent stem cell derived cardiomyocytes stained with anti-troponin t (red, cardiomyocytes) and anti-collagen IV (green, vascular-like network). Scale bars 300µm.

5.2.1 Optimal media for cardiovascular models (III,IV)

For cardiovascular models, a universal medium was developed to primarily support cardiomyocyte functionality and maturation and secondarily to induce adequate vascular-like network formation. Of the six different medium, serum free medium supplemented with 10 ng/ml VEGF and 1 ng/ml FGF (NRC medium 1, Table 3) supported most efficiently the viability and contractility of rat cardiovascular models as an entity. NRC medium 1 provided 50-70% contractility of NRC and the vascular-like network formation was 34.7 % in hASC+HUVEC+NRC co-culture and 68.9 % in fibroblast+HUVEC+NRC co-culture. Although additional supplements in NRC medium 2 (AA, HE and HY, Table 3) were seen to increase vascular-like network formation, cardiomyocyte contractility was decreased to 30–70 %. Due to

stronger and more repeatable cardiac contractility, NRC medium 1 was chosen for further experiments.

The optimal medium for human cardiovascular model was EB medium without addition of exogenous growth factors (Table 3). VEGF and FGF-2 were used to induce vascular-like network formation in angiogenesis model until day 6 and removed before seeding of human CM. An optimal serum concentration for human cardiovascular model was assessed by studying the effect of different serum concentrations on the morphology of human CM. In low serum (2%) and serum-free medium the size of the human CM was small compared to CM cultured in control medium supplemented with 20 % FBS. In concentrations of 5, 10 or 20 % FBS there were no differences between human CM in size or growth of the cells. Therefore, EB medium with 5 % FBS was chosen for further studies with human cardiovascular model.

5.2.2 Vascular-like network formation in cardiovascular models (III,IV)

In rat and human cardiovascular models, the vascular-like network formation was shown to be dependent on the culture media, serum concentration and growth factor composition (see chapter 5.2.1.). The vascular-like network formation capacity of vasculogenesis-angiogenesis model and angiogenesis model in rat cardiovascular model was evaluated. Differences in the formation of vascular-like structures were seen with more dense and branching network in co-culture of HUVEC+hASC+NRC (Figure 9.B) whereas orientation of vascular-like structures was more parallel in co-culture of HUVEC+fibroblast+NRC (Figure 9.A). Importantly, both vascular platforms supported cardiomyocyte viability and functionality.

Although mature vascular structures are formed in angiogenesis model in the presence of VEGF and FGF-2 prior to seeding of human CM at day 6 (Figure 9.C), the vascular-like network starts to regress after CM seeding. Basement membrane in tubules becomes less intact and tubules becomes shorter due to absence of supporting growth factors in EB medium (Table 3).

Expression levels of angiogenesis related genes including VEGF, FGF-2, TGF-β, PDGF-β, angiopoietin-1 and angiopoietin-2 in time points 0, 6 and 18 days were analysed in human cardiovascular model and in angiogenesis model that was considered as a control. The expression levels of the FGF-2, TGF-β, angiopoietin-1 were at the similar level in cardiovascular model and in angiogenesis model. However, the expression levels for VEGF and PDGF-β were significantly higher in the cardiovascular model ($p<0.05$). On the contrary, the expression level of Angiopoietin-2 was significantly lower in the cardiovascular model compared to angiogenesis model ($p<0.05$).

5.2.3 Morphology, orientation and maturation of cardiomyocytes (III,IV)

Human CM morphology and orientation in the absence and presence of vascular-like network was studied to assess the maturation state and structure of the human cardiovascular model. As a result, structural maturation of the CM was detected with oblong, brick-shaped phenotype of mature CM in the presence of vascular-like structures (Figure 10.C-D). Moreover, 2D (Figure 10.F) as well as 3D projection (Figure 10.E) showed that CM co-localized mostly longitudinally and parallel around the tubule structures. On the contrary, CM in the monoculture remained rounded, less organized and orientation of the cells could not be detected (Figure 10.A-B). Similar results were seen in rat cardiovascular model. NRC were distributed throughout the dense, branching vascular-like network without organization into any major direction in hASC+HUVEC+NRC co-culture (see Figure 9.B) whereas a parallel organization of vascular-like and co-localization of cardiomyocytes was seen in fibroblast+HUVEC+NRC co-culture (see Figure 9.A).

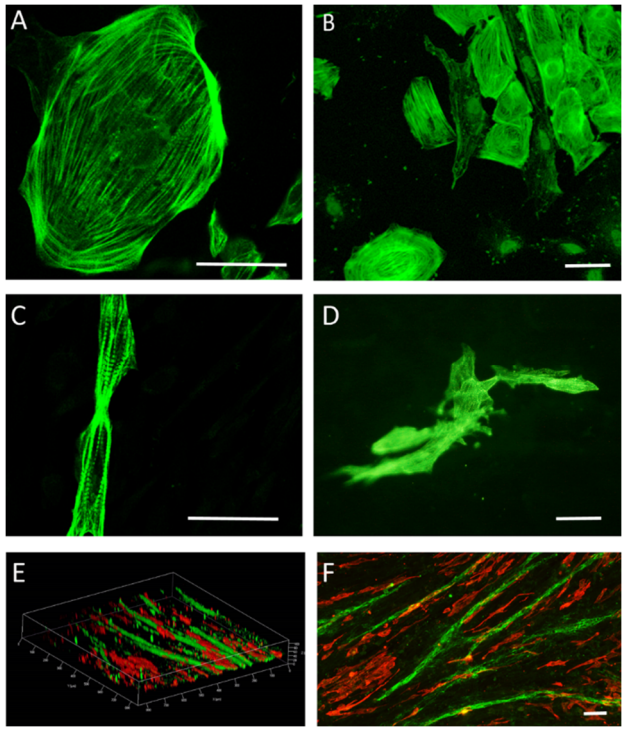

Figure 10. (A-B) Human pluripotent stem cell derived cardiomyocytes in monoculture show round morphology whereas (C-D) cardiomyocytes cultured with vascular-like network in human cardiovascular model possess oblong phenotype. Stained with anti-troponin t (green). (E) 3D and (F) 2D projections show the alignment of human stem cell derived cardiomyocytes (anti-troponin t, red) with vascular-like network (anti-collagen IV, green) in human cardiovascular model. Scale bars 50 µm.

Human CM maturation was detectable also in gene expression level. Expression levels of cardiac structure related genes in time points 0, 6 and 18 days were analysed in human cardiovascular model and in human CM monoculture that was considered as a control. As a result, levels of cardiac muscle myosin transcripts MYH6, MYH7 and troponin t were seen to increase markedly throughout the culture in cardiovascular model whereas they remained constant in CM monoculture. Also expression level of gap junction marker connexin 43 was shown to increase significantly in cardiovascular model while remaining low in CM monoculture (Figure 11).

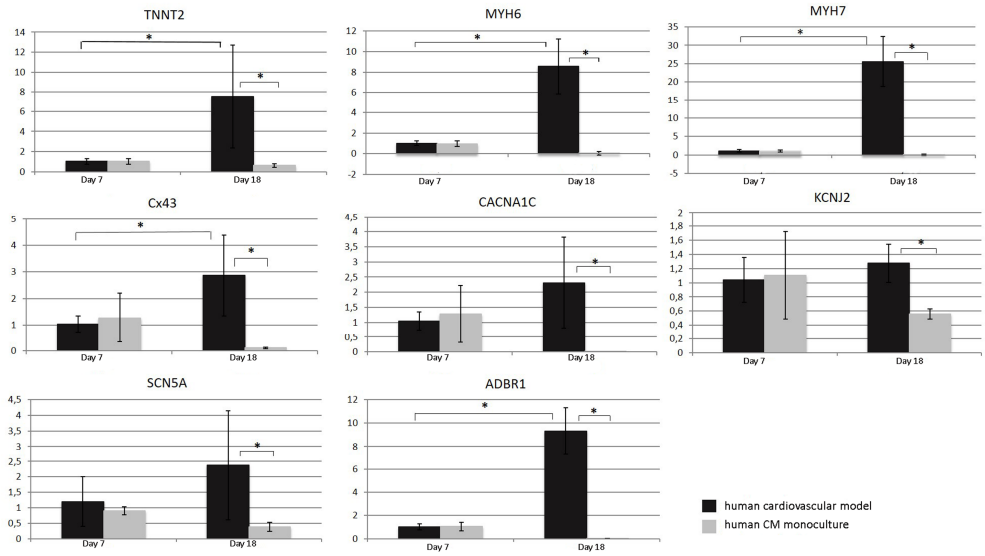

Figure 11. Expression of levels of cardiac related genes troponin t (TNNT2), cardiac muscle myosins (MYH6, MYH7), connexin 43 (Cx43), calcium channel (CACNA1C), potassium channel (KCNJ2), sodium channel (SCN5A) and beta-1-adrenergic receptor (ADBR1) at day 7 and day 18 in human cardiomyocyte monoculture and in human cardiovascular model.* $p<0.05$ indicates statistically significant difference between the groups.

5.2.4 Electrophysiological properties of the cardiovascular models (III,IV)

Microelectrode array (MEA) was used to analyse the electrophysiological properties and conductivity of the both cardiovascular models. The results showed that rat as well as human cardiovascular model conducted the electrical signal of cardiomyocytes and the electrical activity was detectable in MEA despite of the thick cell layer. Microscopical analysis and MEA measurements showed that the contractility of cardiomyocytes in rat as well as in human cardiovascular model was synchronous. Furthermore, there were no differences detected in the baseline beating frequency of cardiomyocytes in monoculture compared to cardiomyocytes in either cardiovascular model.

The capability of two different vascular-like networks to support the functionality of NRC was compared to NRC monoculture. In NRC monoculture, the cardiomyocytes were contractile approximately for seven days in any of the tested media (Table 3) whereas in the presence of vascular-like network the NRC

maintained their contractile capacity for at least 14 days. Differences in duration of contractility were not detected between hASC+HUVEC+NRC and fibroblast+HUVEC+NRC cultures and a synchronized contractility was visually observed in both models. In addition, the number of NRC was less critical when they were cultured with the vascular-like network compared to NRC monoculture as the contractility was stronger even with a fewer number of NRC (study III).

Functionality of human cardiovascular model was analyzed with adrenalin and potassium channel-blocker E-4031 exposure. Adrenaline increased the beating frequency of human CM thus decreasing the field potential duration (FPD) in cardiovascular model as well as in CM monoculture. The increase in beating frequency and decrease in FPD was statistically significant ($p<0.05$) between baseline and adrenaline perfusion only in cardiovascular model (Figure 12.A-B).

E-4031, a hERG blocker, was shown to significantly prolong ($p<0.05$) the FPD in human cardiovascular model and in CM monoculture compared to the baseline (Figure 12.B-C). However, there was no statistically significant difference between CM monoculture and cardiovascular model (Figure 12.D). Prolongation of FPD due to E-4031 exposure resulted in additional adverse effects including pausing beating and/or arrhythmias. These adverse effects were seen in CM monoculture as well as in cardiovascular model.

Expression levels of transcripts related to cardiac ion channels in time points the day after CM seeding (day 6) and at the end of co-culture (day 18) were analysed to assess the electrophysiological properties of human cardiovascular model. An increase in the expression level of sodium channel SCN5A and in calcium channel CACNA1C was detected while potassium channel KCNJ2 remained constant in the cardiovascular model (Figure 11). Moreover, the expression of beta-1 adrenergic receptor, ADRB1, was shown to increase markedly from day 1 to day 13 in cardiovascular model (Figure 11). In human CM monoculture, used as a control, expression levels of SCN5A, CACNA1C, KCNJ2 and ADRB1 remained constant (Figure 11).

5.2.5 Calcium metabolism in human cardiovascular model (IV)

Ca^{2+} transients of the human cardiovascular model was detectable with Ca^{2+} imaging method. Human cardiovascular model and human CM monoculture were shown to respond similarly to adrenaline exposure. In cardiovascular model, adrenaline caused significant increase in the frequency of calcium cycling and significant decrease in amplitude compared to CM monoculture (Figure 12.E).

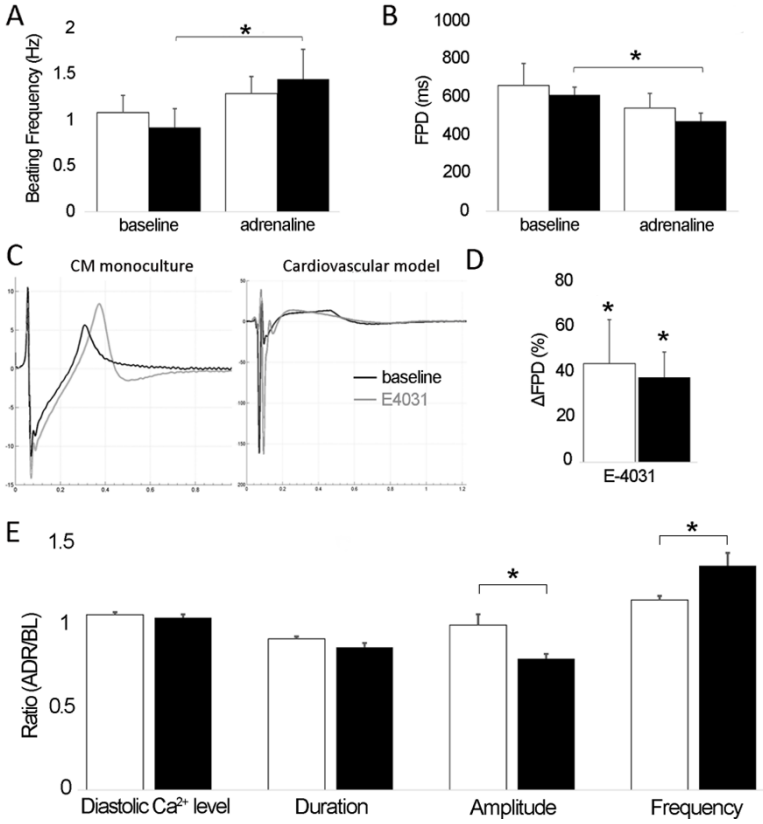

Figure 12. Electrophysiological and calcium cycling analysis of human cardiovascular model (black columns) and human cardiomyocyte monoculture (white columns). Statistical analysis of (A) beating frequencies and (B) field potential durations (FPD) in MEA measurements show significant difference between baseline and adrenaline exposure in human cardiovascular model, * $p<0.05$. (C) Overlay plot show the effect of 300nM E-4031 on field potential duration; (D) significant difference between baseline and E-4031 responses of 300nM E-4031 in human CM monoculture (n=6) and in human cardiovascular model (n=7) were detected. Difference was calculated as relative change from the baseline, * $p<0.05$; (E) significant difference between human cardiomyocyte monoculture and human cardiovascular model was detected in amplitude and frequency of calcium cycling. Analysis was performed separately for each cell as the ratio of adrenaline response divided by baseline response. CM monoculture n=16, cardiovascular model n=26, * $p<0.05$.

6 Discussion

Presently, the main test systems for the assessment of safety of chemicals for regulatory purposes as well as for efficacy testing in drug development are based on animal biology. However, it has been widely shown that animals are poor predictors of human situation resulting in false negative and false positive predictions. The use of animal models has been recognized as a contributing factor to low success rate in drug development. (Heinonen, 2015) Furthermore, it has been hypothesized that a major obstacle in the identification of adverse effects in safety assessment is the lack of relevant *in vitro* test systems (Suter-Dick et al., 2015).

Commonly used *in vitro* assays consist of primary cells and transformed cell lines that often fail to predict the *in vivo* situation (Suter-Dick et al., 2015). However, specific cell types differentiated from human mesenchymal and pluripotent stem cells could replace the currently used assays and improve the relevance by recapitulating more closely the essential physiological structure and function of the target tissue (Scanu et al., 2011, Pfannkuche et al., 2010a). In addition, appropriately engineered cell culture environment could improve the predictive value of a test system (Knight & Przyborski, 2014). The main benefit of implementing advanced *in vitro* methods will be the reduction and/or replacement of animal testing, enhanced prediction of specific adverse effects and the reduction of costs and time required for the toxicity assessment. However, careful characterization, thorough validation and *in vitro–in vivo* comparison is needed before stem cell based test systems can provide a valid alternative to the current toxicity test systems. (Suter-Dick et al., 2015, O'Connor, 2013) Growing evidence show that three-dimensional cell arrangement and co-culture of different cell types leads to improved predictive value of the test system. Moreover, a key element in all tissue microenvironments is the presence of vasculature. (Tourovskaia et al., 2014)

In vitro models of both vasculogenesis and angiogenesis are needed for basic biomedical research as well as for translational research including pharmaceutical

development that needs relevant test systems for screening of pro- and anti-angiogenic compounds. (Ucuzian & Greisler, 2007, Folkman, 2007) In addition, drug-induced vascular injury has been a difficult problem for the pharmaceutical industry causing termination of development of new drug candidates in nonclinical assessment of safety (Mikaelian et al., 2014, Morton et al., 2014). Presently, there are no relevant *in vitro* models available for screening applications to study drug-induced vascular injury (Mikaelian et al., 2014) or embryonic vascular development as part of developmental toxicity assessment (Heinonen, 2015).

Heart has been shown to be particularly prone to toxic effects of drugs that can cause severe adverse effects including decreased cardiac contractility, increased arrhythmia, ischemia and sudden death. (Redfern et al., 2003, Lasser et al., 2002, Lexchin, 2005) Hence, assessment of the risk of a drug to cause cardiac electrophysiological disturbances, mainly ventricular arrhythmia detected as QT interval prolongation in electrocardiogram, is regulated as part of the standard preclinical evaluation of new compounds (Braam et al., 2010). Since adverse cardiac effects are the main cause for drug withdrawal from the market and delays in regulatory approval, heart is one of the major target for pharmaceutical industry. For these reasons, relevant test systems for cardiac toxicity assessment are urgently needed.(Kettenhofen & Bohlen, 2008)

In this thesis *in vitro* vascular models (studies I, II) and cardiovascular models (studies III, IV) were developed. Artificial scaffolds were not used in the development of these *in vitro* test systems. Instead, vascular-like network formed in vascular models served as a natural, supporting and interactive scaffold in cardiovascular models. In addition, throughout this thesis, development of an optimal media was part of the process of establishing defined *in vitro* models.

6.1 Development of *in vitro* vascular models (I,II)

In this thesis, two different vascular models, a stromal-vascular model and vasculogenesis-angiogenesis model, were developed for safety and efficacy assessment of pro- and anti-angiogenic compounds, for biomedical research and for utilization in tissue constructs as a vascular platform.

hASC were used as building blocks in vascular models due to their human origin, availability, ability to differentiate into several vascular cell types (Madonna et al., 2009, Miranville et al., 2004) and due to the ability to secrete several angiogenic and anti-apoptotic compounds (Rehman et al., 2004, Rubina et al., 2009, Verseijden et al., 2010b). HUVEC, on their behalf, are among the most extensively used primary endothelial cells of human origin and can also be easily isolated from the umbilical cord (Jaffe et al., 1973). As hASC, HUVEC can be easily expanded *in vitro* and freezed for further experimental use as a cell banks.

Marked differences between the stromal-vascular model (hASC monoculture) and vasculogenesis-angiogenesis model (hASC and HUVEC co-culture) were detected. The vascular-like network formation capacity of the vasculogenesis-angiogenesis model was shown to be more reproducible, more extensive and independent of the cell line or passage number compared to stromal-vascular model. Immature tubule structures were formed in stromal-vascular model detected as incomplete formation of the basement membrane. In addition, in stromal-vascular model, less than 50 % of the tested hASC lines were shown to form short cords and produce a vascular-like network in some degree. Although donor-to-donor variability is a well known characteristic related to hASC, the ability of four different donors of hASC to give rise to similar vascular structures has been reported (Hutton et al., 2012).

Our findings suggest that hASC monoculture may not provide a relevant vascular model for screening of angiogenic compounds due its low reproducibility but it might, however, provide an inductive platform for tissue constructs. Due to high proliferation and differentiation capacity (Madonna et al., 2009, Miranville et al., 2004) and the ability to secrete several angiogenic and anti-apoptotic factors (Rehman et al., 2004, Rubina et al., 2009, Verseijden et al., 2010b), hASC could provide promising source for development of stromal-vascular platform for complex tissue constructs. In the present study, further characterization towards routine test system was performed to vasculogenesis-angiogenesis model due to its higher reproducibility, more mature structure and indepence of donor-to-donor variability.

6.1.1 Development of optimal medium for *in vitro* vascular models

Mammalian cells are generally cultured under controlled conditions in humidified incubators typically at 37 °C and in gas mixture consisting of 5 % CO_2 and 95% O_2. For longer cell cultivations, the basal medium must be supplemented with various factors including serum. (van der Valk et al., 2010) The concentration of serum in the medium plays an essential role in determining the morphology and differentiation of the cardiomyocytes as mitogenic medium stimulates cell proliferation whereas CM cultured in lower serum concentrations (0-5 %) maintain the cell number, phenotype and contractile properties. (Passier et al., 2005, Xu et al., 2006) In order to achieve high reproducibility within an *in vitro* test system, the defined composition of the medium is essential. However, commercial media producing companies do not necessarily publish the specific compositions of their media. (van der Valk et al., 2010) Our objective was to create low-serum or serum-free culture conditions for *in vitro* models in order to provide physiologically relevant environment and improve the predictive capacity of the test systems.

We developed a defined vascular stimulation medium (VSM) for vasculogenesis-angiogenesis model. This was important for thorough characterization of the model and, additionally, critical for utilization in chemical testing since medium components may interact with test compounds. Serum was excluded from the VSM as we detected that network formation increased and tubule walls remained intact in serum-free environment. This was beneficial for the model compared to similar study from Merfeld-Clauss et al. where they reported use of 5 % FBS in the culture medium (Merfeld-Clauss et al., 2010).

Our results showed that with specific concentrations of VEGF, FGF-2, ascorbic acid, hydrocortisone and heparin in VSM, an extensive vascular-like network was created with high reproducibility. Moreover, genetic analysis of 84 angiogenesis-related genes between VSM and commercial HUVEC medium (Table 3) confirmed an improved maturation of the vasculogenesis-angiogenesis model in VSM. We conclude that VSM provides a valid, inductive medium for *in vitro* vascular models with the benefits of being serum-free and completely defined by its composition compared to commercial HUVEC medium with unknown growth factors concentrations. Hence, our results suggest that VSM could be used also

commercially in the development of different *in vitro* vascular models. Furthermore, defined medium was an important developmental advantage for future intra-laboratory validation of the vasculogenesis-angiogenesis model.

6.1.2 Characterization of vasculogenesis-angiogenesis model (I,II)

6.1.2.1 Vasculogenic properties of vasculogenesis-angiogenesis model (I,II)

In addition to model adult angiogenesis (Sarkanen et al., 2011), our objective was to develop a relevant vascular model mimicking vasculogenesis, i.e. embryonic *de novo* production of vasculature. First, we wanted to find out whether population of endothelial progenitor cells capable for vasculogenesis resides in human adipose stromal cell (hASC) population. As a result, high expression of two known progenitor markers, CD90 and CD34, was detected. In addition, we saw very low expression levels of mature endothelial cell markers CD31 and CD144 indicating that mature endothelial cells were removed during the hASC isolation process. Similar results were reported by Miranville et al (2004) showing the presence of the endothelial progenitor cell phenotype in the stromal-vascular fraction of isolated human adipose tissue characterized as CD34+/CD31− cells (Miranville et al., 2004). Our results suggest that endothelial progenitor cells capable for vasculogenesis does exist in hASC population indicating that our vasculogenesis-angiogenesis model have the potential to be used also as a test system to mimic vasculogenesis.

To further study the vasculogenic properties of vasculogenesis-angiogenesis model, GFP-infection was performed to human umbilical vein endothelial cells (HUVEC) in order to track the cells responsible for tubule formation. The results showed that hASC and HUVEC co-culture was mostly mosaic and consisted of two different populations indicating that hASC as well as HUVEC contribute to tubule formation. Hence, our results suggest that vasculogenesis-angiogenesis model is a suitable test system to study both vasculogenesis and angiogenesis. However, further studies are needed to confirm the predictive capacity of the model by testing a set on known chemicals that interfere the process of vasculogenesis and angiogenesis.

6.1.2.2 Maturation and structure of vascular-like network (I,II)

In order to mimic adult blood vessel formation, the vascular-like network must mature. Maturation involves formation of adherence junctions and branching of the vascular network to meet the tissue-spesific requirements (Jain, 2003, Stratman et al., 2009, Risau, 1997). In addition, an essential feature of the maturation is the recruitment of mural cells including pericytes and vascular smooth muscle cells (Aguilera & Brekken, 2014). Our results showed that vascular-like network formation in vasculogenesis-angiogenesis was significantly increased from day 3 to day 6. Pericyte receptors were detected in cells surrounding the tubules as well as cells expressing several smooth muscle markers showing the presence of supporting mural cells around the tubules. In addition, vascular endothelial cadherin and occludin stainings confirmed the presence of adherence junctions. In mature vasculature, endothelial cells and pericytes form a common basement membrane (Hall, 2006). In our vasculogenesis-angiogenesis model, an intact basement membrane was repeatedly seen in the vascular structures formed in vasculogenesis-angiogenesis model. These markers indicated the maturated state of vasculogenesis-angiogenesis model can be received in 6 day culture. Maturation was confirmed by genetic studies showing an up—regulation of angiopoietin-1 and contractile smooth muscle caldesmon at day 6.

The structure of the vascular-like network was shown to be thick and three-dimensional with overlapping tubules and lumen thus resembling the morphology of native vessels. However, tubules in different stages of development were detected in electronmicroscopical as well as in genetic analysis indicating the ongoing process of network formation. It has been reported that timing of maturation processes may overlap thus allowing the sustained development of vasculature towards maturation (Jain, 2003, Stratman et al., 2009, Risau, 1997).

Production of extracellular matrix (ECM) is part of the maturation process (Stratman & Davis, 2012). ECM components including basement membrane, fibrillins and collagens were shown to be produced in vasculogenesis-angiogenesis model thus providing a natural, *in vivo*-like microenvironment. ECM has a mechanical role in supporting the tissue architecture and stabilizing blood vessel structures (Sottile, 2004) with accumulation of ECM proteins such as collagen IV (Merfeld-Clauss et

al., 2010). Thus, with the production of extracellular matrix components and inductive growth factors (Rehman et al., 2004, Rubina et al., 2009, Verseijden et al., 2010b), vasculogenesis-angiogenesis model can be used as a supporting and interactive platform in different tissue constructs. Presently, several angiogenesis assays are based on the utilization of different scaffolds (Auerbach et al., 2003, Peterson et al., 2014, Koh et al., 2008) such as fibrin matrix (Nehls & Drenckhahn, 1995, Nakatsu et al., 2003) or collagen gel (Vernon & Sage, 1999) as alternatives to *in vivo* ECM. However, the use of scaffolds has been shown to interfere cell-cell contacts and affecting to the force generation ability in cardiac constructs (Norotte et al., 2009). In the third study of this thesis, we published, for the first time, the utilization of vasculogenesis-angiogenesis model in tissue construct with cardiomyocytes. Our study showed that beside mechanical support and production of angiogenic and anti-apoptotic growth factors, another advantage of the vascular platform is the absence of artificial scaffold.

The utilization of vasculogenesis-angiogenesis model with human pluripotent stem cell derived cardiomyocytes is presently under study. Although high proliferation and differentiation capacity of hASC makes them an ideal source for vascular models (Madonna et al., 2009, Miranville et al., 2004, Hutton et al., 2012), it also increases the detachment of the thick cell layer especially when contractile cells are included into the co-culture as detected in our ongoing studies. Although not tested yet, the use of additional scaffold is one possibility to prevent the detachment. Nonetheless, this is an issue that needs to be solved before vasculogenesis-angiogenesis model can be utilized in tissue construct for long term studies.

6.2 Development of *in vitro* cardiovascular models (III, IV)

In this thesis two different *in vitro* cardiovascular models were developed. Rat cardiovascular model consisted of neonatal rat cardiomyocytes combined with angiogenesis model (fibroblast+HUVEC+NRC) and with vasculogenesis-angiogenesis model (NRC+hASC+HUVEC). Human cardiovascular model consisted of human pluripotent stem cell derived cardiomyocytes and angiogenesis model (fibroblast+HUVEC+hPSC-CM). Intra-laboratory validated angiogenesis model consisting of co-culture of HUVEC and fibroblast, previously developed by

us, was used as a platform in development of cardiovascular models due to its stable structure and ability to mimic adult vasculature. Furthermore, since fibroblasts are known to give mechanical support by producing ECM components and enhance alignment of cardiomyocytes (Pfannkuche et al., 2010b) the use of fibroblasts might improve functional properties of the cardiovascular models.

First objective was to test the ability of two different vascular platforms to support the viability and contractility of NRC and to establish a proof-on-concept for the *in vitro* cardiovascular model. NRC were used due to their availability, ability for spontaneous contraction for several days and also since rodent cardiomyocytes are a routinely used *in vitro* models in cardiovascular research (Banyasz et al., 2008). As a final goal, we developed a completely human cell based cardiovascular model for cardiotoxicity and efficacy assessment that is urgently needed especially for drug development and testing of new chemical entities. hPSC-CM provide number of advantages over previous cardiac models with the benefit of being human origin, the ability to contract rhythmically and respond appropriately to numerous cardioactive drugs (Robertson et al., 2013). Cardiomyocytes in monoculture were used in parallel with cardiovascular models throughout these studies as a control to provide a baseline for analyzed parameters.

6.2.1 Development of optimal media for cardiovascular models

The concentration of serum in the medium had a significant impact on the functionality and structure of cardiovascular models. In both cardiovascular models, a universal medium was developed to primarily support CM functionality and maturation and secondarily to induce adequate vascular-like network formation. CM cultured in medium with low serum concentrations (0-5 %) have been shown to maintain the cell number, phenotype and contractile properties (Li, 2002). Our results showed that optimal medium for rat cardiovascular model was serum-free medium with angiogenic growth factors VEGF and FGF-2. Since serum was not needed to support NRC contractility, our results suggest that *in vitro* models with different primary cell types can be maintained in serum-free conditions that supports the functionality of the cells. This might be due to beneficial microenvironment similar to native tissue. Moreover, although FGF-2 have been shown to increase the

expression of dedifferentiation markers, such as atrial natriuretic factor, α-smooth muscle-actin and myofibrillar organization, in adult rat cardiomyocytes (Montessuit et al., 2004) we detected more mature phenotype of NRC in the presence of vascular-like network compared to NCR in monoculture.

In human cardiovascular model, VEGF and FGF-2 were excluded from the medium due to unknown effects on hPSC-CM differentiation and maturation. In addition, 5 % concentration of FBS was needed to maintain physiologically relevant phenotype and growth of the human CM. hPSC-CM have been, however, successfully cultured in serum-free medium at least in monoculture (Stancescu et al., 2015). Hence, further optimization of the medium components might be needed for human cardiovascular model especially when combining vasculogenesis-angiogenesis model with hPSC-CM.

6.2.2 Rat cardiovascular model

The importance of endothelial cells and hASC to the viability of primary CM has been reported earlier (Sadat et al., 2007, Narmoneva et al., 2004). However, the effects of vascular-like network on CM viability and contractility without artificial scaffold was studied here for the first time. Our results showed that the contractility of NRC could be maintained twice as long in culture with vascular-like network compared to NRC monoculture. The increased functionality provides a significant advantage for the model and enables long term use or repeated dose toxicity studies. We detected that vascular-like network provides mechanical support and inductive growth factors for cardiovascular model thus acting as a natural scaffold. Hence, our results highlight the importance of relevant microenvironment and supportive, essential cell types for the viability and functionality of *in vitro* models as suggested also by others (Suter-Dick et al., 2015, Knight & Przyborski, 2014). This should be taken into consideration in the development of all *in vitro* cell- and tissue models including tissue constructs aimed for regenerative medicine. Since the angiogenesis model possessed more stable platform with parallel co-localization of NRC, it was chosen for further development of completely human cell based cardiovascular model.

The microelectrode array (MEA) is a robust, widely used method to analyse the electrophysiological properties of CM. Our results showed that rat cardiovascular model conducted the electrical signal and electrophysiology of the construct was detectable with MEA. This is essential if the model is to be used for screening of cardiotoxic compounds that often affect on the electrophysiological properties of CM. In addition, vascular-like structures in cardiovascular model might assist in the formation of cell-cell contacts and gap junctions between the cardiomyocytes thus enhancing the conduction of electrical signals. Due to critical differences in electrophysiological properties of human and rat cardiomyocytes, especially in the response to rapid delayed rectifier potassium current (Hirt et al., 2014), chemical tests were not performed to rat cardiovascular model. However, proof-of-concept on the cardiovascular model was received.

6.2.3 Human cardiovascular model

Myocardium is composed of cardiomyocytes and non-myocytes embedded in ECM guiding cellular organization and facilitating efficient cell contraction and electrical transmission of the cells (van Spreeuwel et al., 2014). Previous *in vitro* studies have shown that cell alignment improves CM calcium handling and contractile properties when compared to randomly oriented CM monocultures (Pong et al., 2011, Feinberg et al., 2012). However, since the use of scaffolds in cardiac constructs has been associated with reduced cell-cell contacts as well as incorrect deposition and alignment of extracellular matrix (Norotte et al., 2009), we used vascular-like network to support and orientate CM. Genetic analysis showed that stable tubule structures were formed before seeding of CM thus providing a supportive platform for CM orientation and maturation in human cardiovascular model. In addition, our result demonstrated that seeding of CM to stable vascular-like network orientates the cells mostly parallel but also surrounding the vascular structures thus resembling the architecture of *in vivo* myocardium.

Although regression of vascular structures after seeding of CM was seen in the absence of VEGF and FGF-2, it did not seem to have effect on the human CM viability or contractility as detected in the MEA and calcium metabolism measurements. These results suggests that cell-cell as well as cell-matrix interactions,

instead of completely developed vascular structures, are critical for CM viability and contractility.

Although immature rodent cardiomyocytes have been used as model systems for decades, mature human cardiomyocytes are likely to reflect the physiology of the adult heart more closely and present more relevant *in vitro* model system for humans. In addition, electrical and mechanical properties of hPSC-CM should resemble native myocardium. (Yang et al., 2014) One of the main objective of this thesis was to develop cardiovascular model using hPSC-CM to mimic adult human heart. However, it is widely acknowledged that hPSC-CM possess fetal-like characteristics that may limit their use as a relevant test systems (Robertson et al., 2013). Long-term culture, 3D tissue engineering, electric stimulation and modulation of substrate stiffness are suggested to contribute to the maturation of hPSC-CM (Yang et al., 2014). Therefore, we were interested to know whether vascular-like network with 3D properties enhances the maturation of hPSC-CM and improves the utilization of hPSC-CM as a models of adult human heart.

We detected that in culture with vascular-like structures hPSC-CM obtained more mature phenotype compared to CM monoculture. Cardiac gene expression analysis confirmed the structural maturation in cardiovascular model. These results suggest a significant improvement in the structural maturation of fetal-like hPSC-CM towards more adult phenotype in co-culture with vascular-like structures. With the orientating and maturating benefits, the present cardiovascular construct provides more advanced *in vitro* model for adult human cardiotoxicity assessment compared to CM monoculture.

6.2.3.1 Electrophysiological properties of human cardiovascular model (IV)

The measurement of electrophysiological parameters is essential in characterizing critical ion channel properties of cardiomyocytes (Finlayson et al., 2004). In this study, Ca^{2+} imaging and MEA, two critical methods to assess functionality of cardiomyocytes, were used to study the electrophysiological properties and calcium metabolism of human cardiovascular model.

Since several clinically successful drugs may inhibit hERG channel and lead to potentially fatal long QT syndrome (Finlayson et al., 2004), our especial interest was in detecting drug-induced QT prolongation in human cardiovascular model. hERG blocker E-4031 exposure was performed to cardiovascular model to analyze the effects of an antiarrhythmic drug to field potential duration including the QT interval. The MEA measurements showed that E-4031 increased significantly the field potential duration and arrhythmogenicity of the cardiovascular model. Similar effect was detected in CM monoculture as has already been reported (Caspi et al., 2009, Braam et al., 2008). These results indicate that the *in vitro* cardiovascular model is a responsive test system and that drugs affecting to field potential duration and rhythmicity can be tested with this system.

Although the major ionic currents normally present in adult CM are expressed also in hPSC-CM (Robertson et al., 2013), differences are seen in the number of cardiac ion channel and calcium handling genes (Synnergren et al., 2007). Our genetic analysis showed that in the presence of vascular-like network the expression of transcripts of sodium and calcium channels were increased in the cardiovascular model. This in an important finding since intracellular calcium handling and sarcolemmal ion channels have been shown to play critical role in functional maturation of CM and contribute to their electrical properties (Kim et al., 2010). These results support the earlier findings and confirm the maturation of CM in human cardiovascular model thus bringing the model one step closer towards adult characteristics.

Since intracellular Ca^{2+} is the key regulator of cardiac contractility, alterations in cardiomyocyte Ca^{2+} regulation may be critical in mechanical dysfunction and in arrhythmia (Bers, 2000). Calcium imaging analysis showed that Ca^{2+} transients were detectable and adrenaline responses evident in the cardiovascular model. As in native heart, adrenaline was shown to increase the diastolic Ca^{2+} level in cardiovascular construct. Interestingly, we detected that adrenaline increased significantly the beating frequency of cardiovascular model when compared to CM monoculture as detected both in MEA and Ca^{2+} cycling measurements. Neighboring non-myocytes could enhance the electrical maturation of CM in cardiovascular construct, especially through sarcolemmal ion channel development, as also suggested by Kim et al. (2010) (Kim et al., 2010).

These result showing more sensitive response to adrenaline in cardiovascular model compared to CM monoculture was confirmed by genetic analysis. In CM, adrenaline binds to β1-adrenoreceptors and mediates the catecholamine-induced activation of the cells. We detected a higher expression of the transcripts of β1-adrenoreceptors in cardiovascular model suggesting that due to higher number of β1-adrenoreceptors, adrenaline increases the beating frequency more in the model compared to CM monoculture. Since it is crucial to provide the CM the microenvironment that supports their viability, adhesion and structural maturation (Pfannkuche et al., 2010b), the present cardiovascular construct could serve as a more mature and responsive test systems in cardiac safety and efficacy assessment. However, more extensive characterization with cardiotoxic and antiarrhythmic drugs is needed before entering into validation.

6.3 Future perspectives

Ever since establishment of modern cell culture techniques, *in vitro* models have been used in basic biomedical research, and, more recently, in drug development, regenerative medicine and in safety assessment. Traditionally, animal models have been considered as the most relevant surrogates for humans for their apparent similarity. However, most animals do not naturally develop human disorders, such as Alzheimer's disease, and genetically modified animals have been shown to poorly mimic human situation (Engle & Puppala, 2013, Seok et al., 2013). In the drug development, predictive capacity of animal models to assess human toxicity ranges between 43-71 % (Olson et al., 2000, Heinonen, 2015). The lack of human relevance in addition to ethical concerns and high costs have raised the need for more relevant model systems. Although drug screening requires miniaturized and automated test systems with high throughput, the major argument to use human 3D tissue assays is their human relevance. (Hirt et al., 2014)

Beside regenerative medicine and other fields that directly benefit human health, human mesenchymal stem cell and pluripotent stem cell derived model systems have an emerging potential in implicating the 3R principles of Refinement, Reduction and Replacement of animals. Moreover, with reprogramming technology, patient-

specific cells differentiated into tissues of interest may, in the future, assess chemical safety and efficacy prior to exposing a human.

Although a lot of emphasis has been put in the development of elegant *in vitro* models by numerous research groups worldwide, the development of valid *in vitro* test systems to supplement or replace corresponding animal tests is challenging. Replacement of an animal test reclaims several surrogate *in vitro* and/or *in silico* tests for different parameters of interest. In addition, a paradigm change in toxicity assessment is needed towards the identification of human adverse outcome pathways instead of traditional histopathological findings of an animal tissue.

In the present thesis, *in vitro* models of human vasculature and heart were developed. Unlike similar *in vitro* models described in chapters 2.4.2.-2.4.5., the main purpose for the development of the models in this thesis was to use them in reducing or replacing corresponding animal tests. To come closer to this objective, careful characterization was performed to these models beyond the previously published ones. In contrast to similar studies, a defined procedure for development, characterization and, finally, validation of the model was applied in order to establish an *in vitro* vascular model that could be used as a test system for regulatory purposes. Hence, after development and characterization of vasculogenesis-angiogenesis model, an intra-laboratory validation was performed. As a result, the model is presently used in the safety and efficacy assessment of pro- and anti-angiogenic compounds. Similar method development process was applied to human cardiovascular model.

The result of this thesis suggest that the vasculogenesis-angiogenesis model as well as human cardiovascular model could serve as a relevant test systems in biomedical research as well as in safety and efficacy assessment of compounds. This thesis also provides understanding on the method development procedure that is essential for the establishment of alternative *in vitro* methods to animal testing. In the thesis, more advanced model systems compared to previously used cell monocultures were developed in order to produce relevant data that is applicable to humans. However, more detailed characterization with chemical tests and *in vitro-in vivo* comparison is needed before human cardiovascular model may enter into validation.

7 Conclusions

The aim of this study was to develop relevant *in vitro* models of human vasculature and heart.

Based on the four studies the main findings and conclusions are as follows:

- Co-culture of human umbilical vein endothelial cells (HUVEC) and human adipose stromal cells (hASC) forms extensive and reproducible vascular-like network in six day culture.
- In further characterization of HUVEC and hASC co-culture model properties of mature, 3D vascular structures were detected. Serum-free vascular stimulation medium with specific growth factor concentrations was developed to produce completely defined vascular model for further intra-laboratory validation.
- In the HUVEC and hASC co-culture model, vasculogenic properties in addition to angiogenic network formation were detected suggesting that vasculogenesis-angiogenesis model can be used to study both vasculogenesis and angiogenesis. Thus, the model has the potential to be used as a test system for toxicity and efficacy assessment of angiogenic compounds and, additionally, platform for tissue models.
- Two different vascular models were combined with neonatal rat cardiomyocytes (NRC) to study the ability of these vascular-like networks to support cardiomyocyte viability and contractility. We detected twofold increase in the time of viability of NRC in rat cardiovascular model compared to NRC monoculture. Consequently, proof-of-concept was established with the ability to measure electrophysiological properties of the cardiovascular construct.
- A completely human cell based cardiovascular model consisting of HUVEC+fibroblast+human pluripotent stem cell derived cardiomyocytes (hPSC-CM) aimed for cardiac safety and efficacy assessment of chemicals was developed. In the human cardiovascular model, hPSC-CM were seen to align with vascular-like network and show more mature morphology compared to hPSC-CM monoculture.

- Electrophysiological and calcium handling properties of the hPSC-CM in human cardiovascular model were seen to resemble adult human heart. In addition, responses to chronotropic and arrhythmic compounds were physiologically normal including the prolongation of QT interval. It can be concluded that the present cardiovascular model provides an advanced test system for cardiotoxicity assessment with human relevance.

8 Acknowledgements

This study was performed in the Finnish Centre for Alternative Methods (FICAM), School of Medicine in University of Tampere at 2010-2015. Part of the study was carried out in the BioMediTech, a joint institute of the University of Tampere and Tampere University of Technology. I am grateful to FinPharma Doctoral Program for providing me scientific education, peer support as well as financial support for my studies, several conferences and research visit. This study was financially supported by Ida Montin Foundation, Finnish Cultural Foundation, Juliana von Wendt Foundation, City of Tampere and Orion Pharma.

My deepest gratitude goes to my supervisors Adjunct Professor Tuula Heinonen and PhD Riina Sarkanen who lead me all the way from B.Sc. to Ph.D. I want to thank Tuula for introducing me to the field of alternative methods to animal testing that is a true interest of mine. I am grateful for the opportunity to do my thesis specifically in FICAM and for the example of determination that you gave. I want to thank Riina for her support and valuable point of views during all these years. You showed that obstacles are to be overcome and scientists should be open-minded. I also want to thank Professor Timo Ylikomi for his support and innovative thinking as part of my thesis committee. I admire and am grateful to Professor Emerita Hanna Tähti for her ongoing interest into the *in vitro* methods as alternatives to animal tests and support during my way.

My thesis was reviewed by Professor Petri Lehenkari and Docent Riikka Kivelä. I want to thank both of them for their constructive comments that were valuable for my thesis. Your positive comments meant a lot to me.

My sincere thanks go to my closest co-authors M.Sc.s Liisa Ikonen, Kirsi Penttinen and Outi Huttala who shared the difficulties of this work. I want to thank for your support and say that it was a privilege to work with you ladies. As individual thinking is always limited, the best ideas and results come from co-operation.

I want to thank Professor Katriina Aalto-Setälä and the Heart Group in BioMediTech for your co-operation and resilience regarding to the cardiovascular model. Your contribution and knowledge was indispensable for the project.

I want to thank all co-authors especially in FICAM. The door of PhD Tarja Toimela is always open and I want to thank her for the support and assistance. M.Sc. Pauliina Salonen and FICAMs excellent laboratory personnel including Mirja Hyppönen, Hilkka Mäkinen, Paula Helpiölä and Sari Leinonen are thanked for their help. I want to thank Marika Mannerstöm and Maaret Vaani for introducing me to the world of GLP and keeping me always updated with it. I learned a lot from you all and I really enjoyed working in a place where everyone is allowed to be him/herself. MD, PhD Jukka Uotila and MD, PhD Hannu Kuokkanen are thanked for providing the tissue samples from Tampere University Hospital that were essential for this study. I also want to thank PhD Mari Pekkanen-Mattila for her knowledge and support.

I would like to say thank you for my deceased grandmother Tyyne Vuorenpää who said that I should find myself a husband with a docentship. Maybe she did not think I could be one myself. She was always reminding of the importance of an education and an important contributor for me. Also my other grandparents Toivo Vuorenpää, Aarno Kaakkurivaara and Annikki Kaakkurivaara were always supportive during my way from elementary school to university.

Thank you does not seem to be enough for my parents Aino and Jouko Vuorenpää who have been there for me all the way. I am truly grateful for the support and love of you and my dear siblings Maria, Anne and Mikko. Special thank goes to my sister Anne who I can share everything with. Finally, I want to thank Niko and Calle, the amazing cat of ours. Niko, you have remained persistent in your support and I thank you for your love and for sharing me the life that I want to live.

Tampere, 10th of November 2015

Hanna Vuorenpää

9 References

Adams RH, Alitalo K. 2007. Molecular regulation of angiogenesis and lymphangiogenesis. Nat Rev Mol Cell Biol 8:464-478.

Aguilera KY, Brekken RA. 2014. Recruitment and retention: factors that affect pericyte migration. Cell Mol Life Sci 71:299-309.

Andersson H, Steel D, Asp J, Dahlenborg K, Jonsson M, Jeppsson A, Lindahl A, Kagedal B, Sartipy P, Mandenius CF. 2010. Assaying cardiac biomarkers for toxicity testing using biosensing and cardiomyocytes derived from human embryonic stem cells. J Biotechnol 150:175-181.

Arita Y, Nakaoka Y, Matsunaga T, Kidoya H, Yamamizu K, Arima Y, Kataoka-Hashimoto T, Ikeoka K, Yasui T, Masaki T, Yamamoto K, Higuchi K, Park JS, Shirai M, Nishiyama K, Yamagishi H, Otsu K, Kurihara H, Minami T, Yamauchi-Takihara K, Koh GY, Mochizuki N, Takakura N, Sakata Y, Yamashita JK, Komuro I. 2014. Myocardium-derived angiopoietin-1 is essential for coronary vein formation in the developing heart. Nat Commun 5:4552.

Armulik A, Abramsson A, Betsholtz C. 2005. Endothelial/pericyte interactions. Circ Res 97:512-523.

Arrowsmith J, Miller P. 2013. Trial watch: phase II and phase III attrition rates 2011-2012. Nat Rev Drug Discov 12:569.

Ashikari-Hada S, Habuchi H, Kariya Y, Kimata K. 2005. Heparin regulates vascular endothelial growth factor165-dependent mitogenic activity, tube formation, and its receptor phosphorylation of human endothelial cells. Comparison of the effects of heparin and modified heparins. J Biol Chem 280:31508-31515.

Astashkina A, Mann B, Grainger DW. 2012. A critical evaluation of in vitro cell culture models for high-throughput drug screening and toxicity. Pharmacol Ther 134:82-106.

Auerbach R, Lewis R, Shinners B, Kubai L, Akhtar N. 2003. Angiogenesis assays: a critical overview. Clin Chem 49:32-40.

Balligand J, Kelly RA, Smith TW. 1997. Cardiac endothelium and tissue growth. Prog Cardiovasc Dis 39:351-360.

Banerjee I, Fuseler JW, Price RL, Borg TK, Baudino TA. 2007. Determination of cell types and numbers during cardiac development in the neonatal and adult rat and mouse. Am J Physiol Heart Circ Physiol 293:H1883-91.

Banyasz T, Lozinskiy I, Payne CE, Edelmann S, Norton B, Chen B, Chen-Izu Y, Izu LT, Balke CW. 2008. Transformation of adult rat cardiac myocytes in primary culture. Exp Physiol 93:370-382.

Bazzoni G, Dejana E. 2004. Endothelial cell-to-cell junctions: molecular organization and role in vascular homeostasis. Physiol Rev 84:869-901.

Bergers G, Song S. 2005. The role of pericytes in blood-vessel formation and maintenance. Neuro Oncol 7:452-464.

Bers DM. 2000. Calcium fluxes involved in control of cardiac myocyte contraction. Circ Res 87:275-281.

Bhattacharya S, Macdonald ST, Farthing CR. 2006. Molecular mechanisms controlling the coupled development of myocardium and coronary vasculature. Clin Sci (Lond) 111:35-46.

Bikfalvi A, Bicknell R. 2002. Recent advances in angiogenesis, anti-angiogenesis and vascular targeting. Trends Pharmacol Sci 23:576-582.

Bonanno E, Iurlaro M, Madri JA, Nicosia RF. 2000. Type IV collagen modulates angiogenesis and neovessel survival in the rat aorta model. In Vitro Cell Dev Biol Anim 36:336-340.

Braam SR, Tertoolen L, van de Stolpe A, Meyer T, Passier R, Mummery CL. 2010. Prediction of drug-induced cardiotoxicity using human embryonic stem cell-derived cardiomyocytes. Stem Cell Res 4:107-116.

Braam SR, Passier R, Mummery CL. 2009. Cardiomyocytes from human pluripotent stem cells in regenerative medicine and drug discovery. Trends Pharmacol Sci 30:536-545.

Braam SR, Denning C, Matsa E, Young LE, Passier R, Mummery CL. 2008. Feeder-free culture of human embryonic stem cells in conditioned medium for efficient genetic modification. Nat Protoc 3:1435-1443.

Brand T. 2003. Heart development: molecular insights into cardiac specification and early morphogenesis. Dev Biol 258:1-19.

Brito-Martins M, Harding SE, Ali NN. 2008. Beta(1)- and Beta(2)-Adrenoceptor Responses in Cardiomyocytes Derived from Human Embryonic Stem Cells: Comparison with Failing and Non-Failing Adult Human Heart. Br J Pharmacol 153:751-759.

Brutsaert DL. 2003. Cardiac endothelial-myocardial signaling: its role in cardiac growth, contractile performance, and rhythmicity. Physiol Rev 83:59-115.

Buckingham M, Meilhac S, Zaffran S. 2005. Building the mammalian heart from two sources of myocardial cells. Nat Rev Genet 6:826-835.

Buschmann I, Schaper W. 1999. Arteriogenesis Versus Angiogenesis: Two Mechanisms of Vessel Growth. News Physiol Sci 14:121-125.

Cao R, Brakenhielm E, Pawliuk R, Wariaro D, Post MJ, Wahlberg E, Leboulch P, Cao Y. 2003. Angiogenic synergism, vascular stability and improvement of hind-limb ischemia by a combination of PDGF-BB and FGF-2. Nat Med 9:604-613.

Carmeliet P, Jain RK. 2011. Molecular mechanisms and clinical applications of angiogenesis. Nature 473:298-307.

Carmeliet P. 2005. Angiogenesis in life, disease and medicine. Nature 438:932-936.

Caspi O, Itzhaki I, Kehat I, Gepstein A, Arbel G, Huber I, Satin J, Gepstein L. 2009. In vitro electrophysiological drug testing using human embryonic stem cell derived cardiomyocytes. Stem Cells Dev 18:161-172.

Caspi O, Lesman A, Basevitch Y, Gepstein A, Arbel G, Habib IH, Gepstein L, Levenberg S. 2007. Tissue engineering of vascularized cardiac muscle from human embryonic stem cells. Circ Res 100:263-272.

Chau MD, Tuft R, Fogarty K, Bao ZZ. 2006. Notch signaling plays a key role in cardiac cell differentiation. Mech Dev 123:626-640.

Chen DB, Zheng J. 2014. Regulation of placental angiogenesis. Microcirculation 21:15-25.

Chien KR, Domian IJ, Parker KK. 2008. Cardiogenesis and the complex biology of regenerative cardiovascular medicine. Science 322:1494-1497.

Chow M, Boheler KR, Li RA. 2013. Human pluripotent stem cell-derived cardiomyocytes for heart regeneration, drug discovery and disease modeling: from the genetic, epigenetic, and tissue modeling perspectives. Stem Cell Res Ther 4:97.

Dallabrida SM, Ismail N, Oberle JR, Himes BE, Rupnick MA. 2005. Angiopoietin-1 promotes cardiac and skeletal myocyte survival through integrins. Circ Res 96:e8-24.

D'Amico G, Korhonen EA, Anisimov A, Zarkada G, Holopainen T, Hagerling R, Kiefer F, Eklund L, Sormunen R, Elamaa H, Brekken RA, Adams RH, Koh GY, Saharinen P, Alitalo K. 2014. Tie1 deletion inhibits tumor growth and improves angiopoietin antagonist therapy. J Clin Invest 124:824-834.

Davila JC, Cezar GG, Thiede M, Strom S, Miki T, Trosko J. 2004. Use and application of stem cells in toxicology. Toxicol Sci 79:214-223.

Davis GE, Stratman AN, Sacharidou A, Koh W. 2011. Molecular basis for endothelial lumen formation and tubulogenesis during vasculogenesis and angiogenic sprouting. Int Rev Cell Mol Biol 288:101-165.

Dejana E. 2004. Endothelial cell-cell junctions: happy together. Nat Rev Mol Cell Biol 5:261-270.

Domigan CK, Warren CM, Antanesian V, Happel K, Ziyad S, Lee S, Krall A, Duan L, Torres-Collado AX, Castellani LW, Elashoff D, Christofk HR, van der Bliek AM, Potente M, Iruela-Arispe ML. 2015. Autocrine VEGF maintains endothelial survival through regulation of metabolism and autophagy. J Cell Sci 128:2236-2248.

Donovan D, Brown NJ, Bishop ET, Lewis CE. 2001. Comparison of three in vitro human 'angiogenesis' assays with capillaries formed in vivo. Angiogenesis 4:113-121.

Dor Y, Djonov V, Keshet E. 2003. Making vascular networks in the adult: branching morphogenesis without a roadmap. Trends Cell Biol 13:131-136.

Drake CJ. 2003. Embryonic and adult vasculogenesis. Birth Defects Res C Embryo Today 69:73-82.

Engle SJ, Puppala D. 2013. Integrating human pluripotent stem cells into drug development. Cell Stem Cell 12:669-677.

European Commission. 2013. Seventh report on the statistics on the number of animals used for experimental and other scientific purposes in the member states of the european union 7

Feinberg AW, Alford PW, Jin H, Ripplinger CM, Werdich AA, Sheehy SP, Grosberg A, Parker KK. 2012. Controlling the contractile strength of engineered cardiac muscle by hierarchal tissue architecture. Biomaterials 33:5732-5741.

Feric NT, Radisic M. 2015. Towards adult-like human engineered cardiac tissue: Maturing human pluripotent stem cell-derived cardiomyocytes in human engineered cardiac tissues. Adv Drug Deliv Rev

Finlayson K, Witchel HJ, McCulloch J, Sharkey J. 2004. Acquired QT interval prolongation and HERG: implications for drug discovery and development. Eur J Pharmacol 500:129-142.

Flamme I, Frolich T, Risau W. 1997. Molecular mechanisms of vasculogenesis and embryonic angiogenesis. J Cell Physiol 173:206-210.

Folkman J. 2007. Angiogenesis: an organizing principle for drug discovery?. Nat Rev Drug Discov 6:273-286.

Food and Drug Administration. 2005. The International Conference on Harmonisation of Technical Requirements for Registration of Pharmaceuticals for Human Use. Guideline S7B: The non-clinical evaluation of the potential for delayed ventricular repolarization (QT interval prolongation) by human pharmaceuticals. Federal Register 70:61133-61134.

Friis T, Kjaer Sorensen B, Engel A, Rygaard J, Houen G. 2003. A quantitative ELISAbased co-culture angiogenesis and cell proliferation assay. APMIS 111:658-668.

Garlanda C, Dejana E. 1997. Heterogeneity of endothelial cells. Specific markers. Arterioscler Thromb Vasc Biol 17:1193-1202.

Garzoni LR, Rossi MID, de Barros APDN, Guarani V, Keramidas M, Balottin LBL, Adesse D, Takiya CM, Manso PP, Otazú IB, Meirelles MdN, Borojevic R. 2009. Dissecting coronary angiogenesis: 3D co-culture of cardiomyocytes with endothelial or mesenchymal cells. Exp Cell Res 315:3406-3418.

Gerhardt H, Betsholtz C. 2003. Endothelial-pericyte interactions in angiogenesis. Cell Tissue Res 314:15-23.

Giordano FJ, Gerber HP, Williams SP, VanBruggen N, Bunting S, Ruiz-Lozano P, Gu Y, Nath AK, Huang Y, Hickey R, Dalton N, Peterson KL, Ross J,Jr, Chien KR, Ferrara N. 2001. A cardiac myocyte vascular endothelial growth factor paracrine pathway is required to maintain cardiac function. Proc Natl Acad Sci U S A 98:5780-5785.

Goerke SM, Plaha J, Hager S, Strassburg S, Torio-Padron N, Stark GB, Finkenzeller G. 2012. Human endothelial progenitor cells induce extracellular signal-regulated kinase-dependent differentiation of mesenchymal stem cells into smooth muscle cells upon cocultivation. Tissue Eng Part A 18:2395-2405.

Gupta MK, Illich DJ, Gaarz A, Matzkies M, Nguemo F, Pfannkuche K, Liang H, Classen S, Reppel M, Schultze JL, Hescheler J, Saric T. 2010. Global transcriptional profiles of beating clusters derived from human induced pluripotent stem cells and embryonic stem cells are highly similar. BMC Dev Biol 10:98-213X-10-98.

Hall AP. 2006. Review of the pericyte during angiogenesis and its role in cancer and diabetic retinopathy. Toxicol Pathol 34:763-775.

Hartman ME, Dai DF, Laflamme MA. 2015. Human pluripotent stem cells: Prospects and challenges as a source of cardiomyocytes for in vitro modeling and cell-based cardiac repair. Adv Drug Deliv Rev

Heinonen T. 2015. Better science with human cell-based organ and tissue models. Altern Lab Anim 43:29-38.

Hillen F, Melotte V, van Beijnum JR, Griffioen AW. 2006. Endothelial Cell Biology. In: Staton CA, Lewis CE, Bicknell R editors: Angiogenesis Assays. A critical appraisal of current techniques:John Wiley & Sons, Ltd. p 1-38

Hirt MN, Hansen A, Eschenhagen T. 2014. Cardiac tissue engineering: state of the art. Circ Res 114:354-367.

Huss R. 2000. Isolation of primary and immortalized CD34-hematopoietic and mesenchymal stem cells from various sources. Stem Cells 18:1-9.

Hussain A, Collins G, Yip D, Cho CH. 2013. Functional 3-D cardiac co-culture model using bioactive chitosan nanofiber scaffolds. Biotechnol Bioeng 110:637-647.

Hutton DL, Logsdon EA, Moore EM, Mac Gabhann F, Gimble JM, Grayson WL. 2012. Vascular morphogenesis of adipose-derived stem cells is mediated by heterotypic cell-cell interactions. Tissue Eng Part A 18:1729-1740.

Ichii T, Koyama H, Tanaka S, Kim S, Shioi A, Okuno Y, Raines EW, Iwao H, Otani S, Nishizawa Y. 2001. Fibrillar collagen specifically regulates human vascular smooth muscle cell genes involved in cellular responses and the pericellular matrix environment. Circ Res 88:460-467.

Iivanainen E, Kahari VM, Heino J, Elenius K. 2003. Endothelial cell-matrix interactions. Microsc Res Tech 60:13-22.

Jaffe EA, Nachman RL, Becker CG, Minick CR. 1973. Culture of human endothelial cells derived from umbilical veins. Identification by morphologic and immunologic criteria. J Clin Invest 52:2745-2756.

Jain RK. 2003. Molecular regulation of vessel maturation. Nat Med 9:685-693.

Jennings P. 2014. "The future of in vitro toxicology". Toxicol in Vitro

Kalluri R. 2003. Basement membranes: structure, assembly and role in tumour angiogenesis. Nat Rev Cancer 3:422-433.

Kaufmann P, Mayhew TM, Charnock-Jones DS. 2004. Aspects of human fetoplacental vasculogenesis and angiogenesis. II. Changes during normal pregnancy. Placenta 25:114-126.

Kettenhofen R, Bohlen H. 2008. Preclinical assessment of cardiac toxicity. Drug Discov Today 13:702-707.

Kim C, Majdi M, Xia P, Wei KA, Talantova M, Spiering S, Nelson B, Mercola M, Chen HS. 2010. Non-cardiomyocytes influence the electrophysiological

maturation of human embryonic stem cell-derived cardiomyocytes during differentiation. Stem Cells Dev 19:783-795.

Kim S, Lee H, Chung M, Jeon NL. 2013. Engineering of functional, perfusable 3D microvascular networks on a chip. Lab Chip 13:1489-1500.

Kivela R, Silvennoinen M, Lehti M, Jalava S, Vihko V, Kainulainen H. 2008. Exercise-induced expression of angiogenic growth factors in skeletal muscle and in capillaries of healthy and diabetic mice. Cardiovasc Diabetol 7:13-2840-7-13.

Knight E, Przyborski S. 2014. Advances in 3D cell culture technologies enabling tissue-like structures to be created in vitro. J Anat

Knudsen TB, Kleinstreuer NC. 2011. Disruption of embryonic vascular development in predictive toxicology. Birth Defects Res C Embryo Today 93:312-323.

Ko HC, Milthorpe BK, McFarland CD. 2007. Engineering thick tissues--the vascularisation problem. Eur Cell Mater 14:1-18; discussion 18-9.

Koh W, Stratman AN, Sacharidou A, Davis GE. 2008. In vitro three dimensional collagen matrix models of endothelial lumen formation during vasculogenesis and angiogenesis. Methods Enzymol 443:83-101.

Kolaja K. 2014. Stem cells and stem cell-derived tissues and their use in safety assessment. J Biol Chem 289:4555-4561.

Kujala VJ, Jimenez ZC, Vaisanen J, Tanskanen JM, Kerkela E, Hyttinen J, Aalto-Setala K. 2011. Averaging in vitro cardiac field potential recordings obtained with microelectrode arrays. Comput Methods Programs Biomed 104:199-205.

Lacorre DA, Baekkevold ES, Garrido I, Brandtzaeg P, Haraldsen G, Amalric F, Girard JP. 2004. Plasticity of endothelial cells: rapid dedifferentiation of freshly isolated high endothelial venule endothelial cells outside the lymphoid tissue microenvironment. Blood 103:4164-4172.

Lahti AL, Kujala VJ, Chapman H, Koivisto AP, Pekkanen-Mattila M, Kerkela E, Hyttinen J, Kontula K, Swan H, Conklin BR, Yamanaka S, Silvennoinen O, Aalto-Setala K. 2012. Model for long QT syndrome type 2 using human iPS cells demonstrates arrhythmogenic characteristics in cell culture. Dis Model Mech 5:220-230.

Lasser KE, Allen PD, Woolhandler SJ, Himmelstein DU, Wolfe SM, Bor DH. 2002. Timing of new black box warnings and withdrawals for prescription medications. JAMA 287:2215-2220.

Laustriat D, Gide J, Peschanski M. 2010. Human pluripotent stem cells in drug discovery and predictive toxicology. Biochem Soc Trans 38:1051-1057.

Leucker TM, Bienengraeber M, Muravyeva M, Baotic I, Weihrauch D, Brzezinska AK, Warltier DC, Kersten JR, Pratt Jr. PF. 2011. Endothelial–cardiomyocyte crosstalk enhances pharmacological cardioprotection. J Mol Cell Cardiol 51:803-811.

Lexchin J. 2005. Drug withdrawals from the Canadian market for safety reasons, 1963-2004. CMAJ 172:765-767.

Li R. 2002. Cardiomyocytes. In: Palsson BO, Masters JRW editors: Human Cell Culture: Primary Mesenchymal Cells:Kluwer Academic Publishers Group. p 118-119

Lian X, Zhang J, Azarin SM, Zhu K, Hazeltine LB, Bao X, Hsiao C, Kamp TJ, Palecek SP. 2013. Directed cardiomyocyte differentiation from human pluripotent stem cells by modulating Wnt/beta-catenin signaling under fully defined conditions. Nat Protoc 8:162-175.

Lian X, Hsiao C, Wilson G, Zhu K, Hazeltine LB, Azarin SM, Raval KK, Zhang J, Kamp TJ, Palecek SP. 2012. Robust cardiomyocyte differentiation from human pluripotent stem cells via temporal modulation of canonical Wnt signaling. Proc Natl Acad Sci U S A 109:E1848-57.

Liekens S, De Clercq E, Neyts J. 2001. Angiogenesis: regulators and clinical applications. Biochem Pharmacol 61:253-270.

Liu C, Zhao W, Meng W, Zhao T, Chen Y, Ahokas RA, Liu H, Sun Y. 2014. Platelet-derived growth factor blockade on cardiac remodeling following infarction. Mol Cell Biochem 397:295-304.

Livak KJ, Schmittgen TD. 2001. Analysis of relative gene expression data using real-time quantitative PCR and the 2(-Delta Delta C(T)) Method. Methods 25:402-408.

Lou YJ, Liang XG. 2011. Embryonic stem cell application in drug discovery. Acta Pharmacol Sin 32:152-159.

Louch WE, Koivumaki JT, Tavi P. 2015. Calcium signalling in developing cardiomyocytes: implications for model systems and disease. J Physiol 593:1047-1063.

Lu HR, Vlaminckx E, Hermans AN, Rohrbacher J, Van Ammel K, Towart R, Pugsley M, Gallacher DJ. 2008. Predicting drug-induced changes in QT interval and arrhythmias: QT-shortening drugs point to gaps in the ICHS7B Guidelines. Br J Pharmacol 154:1427-1438.

Madonna R, Geng YJ, De Caterina R. 2009. Adipose tissue-derived stem cells: characterization and potential for cardiovascular repair. Arterioscler Thromb Vasc Biol 29:1723-1729.

Martin RL, McDermott JS, Salmen HJ, Palmatier J, Cox BF, Gintant GA. 2004. The utility of hERG and repolarization assays in evaluating delayed cardiac repolarization: influence of multi-channel block. J Cardiovasc Pharmacol 43:369-379.

Merfeld-Clauss S, Lupov IP, Lu H, March KL, Traktuev DO. 2015. Adipose Stromal Cell Contact with Endothelial Cells Results in Loss of Complementary Vasculogenic Activity Mediated by Induction of Activin A. Stem Cells

Merfeld-Clauss S, Lupov IP, Lu H, Feng D, Compton-Craig P, March KL, Traktuev DO. 2014. Adipose stromal cells differentiate along a smooth muscle lineage pathway upon endothelial cell contact via induction of activin A. Circ Res 115:800-809.

Merfeld-Clauss S, Gollahalli N, March KL, Traktuev DO. 2010. Adipose tissue progenitor cells directly interact with endothelial cells to induce vascular network formation. Tissue Eng Part A 16:2953-2966.

Messina E, De Angelis L, Frati G, Morrone S, Chimenti S, Fiordaliso F, Salio M, Battaglia M, Latronico MV, Coletta M, Vivarelli E, Frati L, Cossu G, Giacomello A. 2004. Isolation and expansion of adult cardiac stem cells from human and murine heart. Circ Res 95:911-921.

Mikaelian I, Cameron M, Dalmas DA, Enerson BE, Gonzalez RJ, Guionaud S, Hoffmann PK, King NM, Lawton MP, Scicchitano MS, Smith HW, Thomas RA, Weaver JL, Zabka TS, Vascular Injury Working Group of the Predictive Safety Consortium. 2014. Nonclinical safety biomarkers of drug-induced vascular injury: current status and blueprint for the future. Toxicol Pathol 42:635-657.

Miranville A, Heeschen C, Sengenes C, Curat CA, Busse R, Bouloumie A. 2004. Improvement of postnatal neovascularization by human adipose tissue-derived stem cells. Circulation 110:349-355.

Montessuit C, Rosenblatt-Velin N, Papageorgiou I, Campos L, Pellieux C, Palma T, Lerch R. 2004. Regulation of glucose transporter expression in cardiac myocytes: p38 MAPK is a strong inducer of GLUT4. Cardiovasc Res 64:94-104.

Moonen JR, Krenning G, Brinker MG, Koerts JA, van Luyn MJ, Harmsen MC. 2010. Endothelial progenitor cells give rise to pro-angiogenic smooth muscle-like progeny. Cardiovasc Res 86:506-515.

Mordwinkin NM, Burridge PW, Wu JC. 2013. A review of human pluripotent stem cell-derived cardiomyocytes for high-throughput drug discovery, cardiotoxicity screening, and publication standards. J Cardiovasc Transl Res 6:22-30.

Morton D, Houle CD, Tomlinson L. 2014. Perspectives on drug-induced vascular injury. Toxicol Pathol 42:633-634.

Moya M, Tran D, George SC. 2013. An integrated in vitro model of perfused tumor and cardiac tissue. Stem Cell Res Ther 4 Suppl 1:S15.

Mummery C, Ward-van Oostwaard D, Doevendans P, Spijker R, van den Brink S, Hassink R, van der Heyden M, Opthof T, Pera M, de la Riviere AB, Passier R, Tertoolen L. 2003. Differentiation of human embryonic stem cells to cardiomyocytes: role of coculture with visceral endoderm-like cells. Circulation 107:2733-2740.

Musunuru K, Domian IJ, Chien KR. 2010. Stem cell models of cardiac development and disease. Annu Rev Cell Dev Biol 26:667-687.

Nag AC. 1980. Study of non-muscle cells of the adult mammalian heart: a fine structural analysis and distribution. Cytobios 28:41-61.

Nahm WK, Zhou L, Falanga V. 2002. Sustained ability for fibroblast outgrowth from stored neonatal foreskin: a model for studying mechanisms of fibroblast outgrowth. J Dermatol Sci 28:152-158.

Nakatsu MN, Sainson RC, Aoto JN, Taylor KL, Aitkenhead M, Perez-del-Pulgar S, Carpenter PM, Hughes CC. 2003. Angiogenic sprouting and capillary lumen formation modeled by human umbilical vein endothelial cells (HUVEC) in fibrin gels: the role of fibroblasts and Angiopoietin-1. Microvasc Res 66:102-112.

Narmoneva DA, Vukmirovic R, Davis ME, Kamm RD, Lee RT. 2004. Endothelial cells promote cardiac myocyte survival and spatial reorganization: implications for cardiac regeneration. Circulation 110:962-968.

Nehls V, Drenckhahn D. 1995. A novel, microcarrier-based in vitro assay for rapid and reliable quantification of three-dimensional cell migration and angiogenesis. Microvasc Res 50:311-322.

Nemer M. 2008. Genetic insights into normal and abnormal heart development. Cardiovasc Pathol 17:48-54.

Nicosia RF, Ottinetti A. 1990. Modulation of microvascular growth and morphogenesis by reconstituted basement membrane gel in three-dimensional cultures of rat aorta: a comparative study of angiogenesis in matrigel, collagen, fibrin, and plasma clot. In Vitro Cell Dev Biol 26:119-128.

Nilius B, Droogmans G. 2001. Ion channels and their functional role in vascular endothelium. Physiol Rev 81:1415-1459.

Nishishita T, Lin PC. 2004. Angiopoietin 1, PDGF-B, and TGF-beta gene regulation in endothelial cell and smooth muscle cell interaction. J Cell Biochem 91:584-593.

Norotte C, Marga FS, Niklason LE, Forgacs G. 2009. Scaffold-free vascular tissue engineering using bioprinting. Biomaterials 30:5910-5917.

Norrby K. 2006. In vivo models of angiogenesis. J Cell Mol Med 10:588-612.

O'Connor MD. 2013. The 3R principle: advancing clinical application of human pluripotent stem cells. Stem Cell Res Ther 4:21.

Olson H, Betton G, Robinson D, Thomas K, Monro A, Kolaja G, Lilly P, Sanders J, Sipes G, Bracken W, Dorato M, Van Deun K, Smith P, Berger B, Heller A. 2000. Concordance of the toxicity of pharmaceuticals in humans and in animals. Regul Toxicol Pharmacol 32:56-67.

Otrock ZK, Mahfouz RA, Makarem JA, Shamseddine AI. 2007. Understanding the biology of angiogenesis: review of the most important molecular mechanisms. Blood Cells Mol Dis 39:212-220.

Passier R, Oostwaard DW, Snapper J, Kloots J, Hassink RJ, Kuijk E, Roelen B, de la Riviere AB, Mummery C. 2005. Increased cardiomyocyte differentiation from human embryonic stem cells in serum-free cultures. Stem Cells 23:772-780.

Pekkanen-Mattila M, Kerkela E, Tanskanen JM, Pietila M, Pelto-Huikko M, Hyttinen J, Skottman H, Suuronen R, Aalto-Setala K. 2009. Substantial variation in the cardiac differentiation of human embryonic stem cell lines derived and propagated under the same conditions--a comparison of multiple cell lines. Ann Med 41:360-370.

Peterson AW, Caldwell DJ, Rioja AY, Rao RR, Putnam AJ, Stegemann JP. 2014. Vasculogenesis and Angiogenesis in Modular Collagen-Fibrin Microtissues. Biomater Sci 2:1497-1508.

Pfaffl MW. 2001. A new mathematical model for relative quantification in real-time RT-PCR. Nucleic Acids Res 29:e45.

Pfannkuche K, Hannes T, Khalil M, Noghabi MS, Morshedi A, Hescheler J, Droge P. 2010a. Induced pluripotent stem cells: a new approach for physiological research. Cell Physiol Biochem 26:105-124.

Pfannkuche K, Neuss S, Pillekamp F, Frenzel LP, Attia W, Hannes T, Salber J, Hoss M, Zenke M, Fleischmann BK, Hescheler J, Saric T. 2010b. Fibroblasts

facilitate the engraftment of embryonic stem cell-derived cardiomyocytes on three-dimensional collagen matrices and aggregation in hanging drops. Stem Cells Dev 19:1589-1599.

Piersma AH. 2006. Alternative methods for developmental toxicity testing. Basic Clin Pharmacol Toxicol 98:427-431.

Polini A, Prodanov L, Bhise NS, Manoharan V, Dokmeci MR, Khademhosseini A. 2014. Organs-on-a-chip: a new tool for drug discovery. Expert Opin Drug Discov 9:335-352.

Pong T, Adams WJ, Bray MA, Feinberg AW, Sheehy SP, Werdich AA, Parker KK. 2011. Hierarchical architecture influences calcium dynamics in engineered cardiac muscle. Exp Biol Med (Maywood) 236:366-373.

Pontes Soares C, Midlej V, de Oliveira ME, Benchimol M, Costa ML, Mermelstein C. 2012. 2D and 3D-organized cardiac cells shows differences in cellular morphology, adhesion junctions, presence of myofibrils and protein expression. PLoS One 7:e38147.

Potente M, Gerhardt H, Carmeliet P. 2011. Basic and therapeutic aspects of angiogenesis. Cell 146:873-887.

Pradhapan P, Kuusela J, Viik J, Aalto-Setala K, Hyttinen J. 2013. Cardiomyocyte MEA data analysis (CardioMDA)--a novel field potential data analysis software for pluripotent stem cell derived cardiomyocytes. PLoS One 8:e73637.

Pusztaszeri MP, Seelentag W, Bosman FT. 2006. Immunohistochemical expression of endothelial markers CD31, CD34, von Willebrand factor, and Fli-1 in normal human tissues. J Histochem Cytochem 54:385-395.

Redfern WS, Carlsson L, Davis AS, Lynch WG, MacKenzie I, Palethorpe S, Siegl PK, Strang I, Sullivan AT, Wallis R, Camm AJ, Hammond TG. 2003. Relationships between preclinical cardiac electrophysiology, clinical QT interval prolongation and torsade de pointes for a broad range of drugs: evidence for a provisional safety margin in drug development. Cardiovasc Res 58:32-45.

Rehman J, Traktuev D, Li J, Merfeld-Clauss S, Temm-Grove CJ, Bovenkerk JE, Pell CL, Johnstone BH, Considine RV, March KL. 2004. Secretion of angiogenic and antiapoptotic factors by human adipose stromal cells. Circulation 109:1292-1298.

Reppel M, Pillekamp F, Lu ZJ, Halbach M, Brockmeier K, Fleischmann BK, Hescheler J. 2004. Microelectrode arrays: a new tool to measure embryonic heart activity. J Electrocardiol 37 Suppl:104-109.

Reynolds LP, Redmer DA. 2001. Angiogenesis in the placenta. Biol Reprod 64:1033-1040.

Risau W. 1997. Mechanisms of angiogenesis. Nature 386:671-674.

Rivron NC, Liu JJ, Rouwkema J, de Boer J, van Blitterswijk CA. 2008. Engineering vascularised tissues in vitro. Eur Cell Mater 15:27-40.

Robertson C, Tran DD, George SC. 2013. Concise review: maturation phases of human pluripotent stem cell-derived cardiomyocytes. Stem Cells 31:829-837.

Roca C, Adams RH. 2007. Regulation of vascular morphogenesis by Notch signaling. Genes Dev 21:2511-2524.

Rohringer S, Hofbauer P, Schneider KH, Husa AM, Feichtinger G, Peterbauer-Scherb A, Redl H, Holnthoner W. 2014. Mechanisms of vasculogenesis in 3D fibrin matrices mediated by the interaction of adipose-derived stem cells and endothelial cells. Angiogenesis 17:921-933.

Rubina K, Kalinina N, Efimenko A, Lopatina T, Melikhova V, Tsokolaeva Z, Sysoeva V, Tkachuk V, Parfyonova Y. 2009. Adipose stromal cells stimulate angiogenesis via promoting progenitor cell differentiation, secretion of angiogenic factors, and enhancing vessel maturation. Tissue Eng Part A 15:2039-2050.

Russell WMS, Burch RL. 1959. The Principles of Humane Experimental Technique. London:Methuen

Sacharidou A, Stratman AN, Davis GE. 2012. Molecular mechanisms controlling vascular lumen formation in three-dimensional extracellular matrices. Cells Tissues Organs 195:122-143.

Sadat S, Gehmert S, Song YH, Yen Y, Bai X, Gaiser S, Klein H, Alt E. 2007. The cardioprotective effect of mesenchymal stem cells is mediated by IGF-I and VEGF. Biochem Biophys Res Commun 363:674-679.

Sakurai T, Tsuchida M, Lampe PD, Murakami M. 2013. Cardiomyocyte FGF signaling is required for Cx43 phosphorylation and cardiac gap junction maintenance. Exp Cell Res 319:2152-2165.

Salem HK, Thiemermann C. 2010. Mesenchymal stromal cells: current understanding and clinical status. Stem Cells 28:585-596.

Sarkanen JR, Mannerstrom M, Vuorenpaa H, Uotila J, Ylikomi T, Heinonen T. 2011. Intra-Laboratory Pre-Validation of a Human Cell Based in vitro Angiogenesis Assay for Testing Angiogenesis Modulators. Front Pharmacol 1:147.

Sartipy P, Bjorquist P, Strehl R, Hyllner J. 2007. The application of human embryonic stem cell technologies to drug discovery. Drug Discov Today 12:688-699.

Scanu M, Mancuso L, Cao G. 2011. Evaluation of the use of human Mesenchymal Stem Cells for acute toxicity tests. Toxicol in Vitro 25:1989-1995.

Schaaf S, Shibamiya A, Mewe M, Eder A, Stohr A, Hirt MN, Rau T, Zimmermann WH, Conradi L, Eschenhagen T, Hansen A. 2011. Human engineered heart tissue as a versatile tool in basic research and preclinical toxicology. PLoS One 6:e26397.

Sechler JL, Schwarzbauer JE. 1998. Control of cell cycle progression by fibronectin matrix architecture. J Biol Chem 273:25533-25536.

Sekine H, Shimizu T, Sakaguchi K, Dobashi I, Wada M, Yamato M, Kobayashi E, Umezu M, Okano T. 2013. In vitro fabrication of functional three-dimensional tissues with perfusable blood vessels. Nat Commun 4:1399.

Sekine H, Shimizu T, Hobo K, Sekiya S, Yang J, Yamato M, Kurosawa H, Kobayashi E, Okano T. 2008. Endothelial cell coculture within tissue-engineered cardiomyocyte sheets enhances neovascularization and improves cardiac function of ischemic hearts. Circulation 118:S145-52.

Seok J, Warren HS, Cuenca AG, Mindrinos MN, Baker HV, Xu W, Richards DR, McDonald-Smith GP, Gao H, Hennessy L, Finnerty CC, Lopez CM, Honari S, Moore EE, Minei JP, Cuschieri J, Bankey PE, Johnson JL, Sperry J, Nathens AB, Billiar TR, West MA, Jeschke MG, Klein MB, Gamelli RL, Gibran NS, Brownstein BH, Miller-Graziano C, Calvano SE, Mason PH, Cobb JP, Rahme LG, Lowry SF, Maier RV, Moldawer LL, Herndon DN, Davis RW, Xiao W, Tompkins RG, Inflammation and Host Response to Injury, Large Scale Collaborative Research Program. 2013. Genomic responses in mouse models poorly mimic human inflammatory diseases. Proc Natl Acad Sci U S A 110:3507-3512.

Shamir ER, Ewald AJ. 2014. Three-dimensional organotypic culture: experimental models of mammalian biology and disease. Nat Rev Mol Cell Biol 15:647-664.

Shen Q, Wang L, Zhou H, Jiang HD, Yu LS, Zeng S. 2013. Stereoselective binding of chiral drugs to plasma proteins. Acta Pharmacol Sin 34:998-1006.

Shimizu T, Yamato M, Kikuchi A, Okano T. 2003. Cell sheet engineering for myocardial tissue reconstruction. Biomaterials 24:2309-2316.

Snir M, Kehat I, Gepstein A, Coleman R, Itskovitz-Eldor J, Livne E, Gepstein L. 2003. Assessment of the ultrastructural and proliferative properties of human embryonic stem cell-derived cardiomyocytes. Am J Physiol Heart Circ Physiol 285:H2355-63.

Song HH, Park KM, Gerecht S. 2014. Hydrogels to model 3D in vitro microenvironment of tumor vascularization. Adv Drug Deliv Rev 79-80:19-29.

Soonpaa MH, Field LJ. 1998. Survey of studies examining mammalian cardiomyocyte DNA synthesis. Circ Res 83:15-26.

Sottile J. 2004. Regulation of angiogenesis by extracellular matrix. Biochim Biophys Acta 1654:13-22.

Stahl A, Connor KM, Sapieha P, Chen J, Dennison RJ, Krah NM, Seaward MR, Willett KL, Aderman CM, Guerin KI, Hua J, Lofqvist C, Hellstrom A, Smith LE. 2010. The mouse retina as an angiogenesis model. Invest Ophthalmol Vis Sci 51:2813-2826.

Stancescu M, Molnar P, McAleer CW, McLamb W, Long CJ, Oleaga C, Prot JM, Hickman JJ. 2015. A phenotypic in vitro model for the main determinants of human whole heart function. Biomaterials 60:20-30.

Staton CA, Reed MWR, Brown NJ. 2009. A critical analysis of current in vitro and in vivo angiogenesis assays. Int J Exp Pathol 90:195-221.

Stratman AN, Davis GE. 2012. Endothelial cell-pericyte interactions stimulate basement membrane matrix assembly: influence on vascular tube remodeling, maturation, and stabilization. Microsc Microanal 18:68-80.

Stratman AN, Malotte KM, Mahan RD, Davis MJ, Davis GE. 2009. Pericyte recruitment during vasculogenic tube assembly stimulates endothelial basement membrane matrix formation. Blood 114:5091-5101.

Suter-Dick L, Alves PM, Blaauboer BJ, Bremm KD, Brito C, Coecke S, Flick B, Fowler P, Hescheler J, Ingelman-Sundberg M, Jennings P, Kelm JM, Manou I, Mistry P, Moretto A, Roth A, Stedman D, van de Water B, Beilmann M. 2015. Stem cell-derived systems in toxicology assessment. Stem Cells Dev 24:1284-1296.

Synnergren J, Giesler TL, Adak S, Tandon R, Noaksson K, Lindahl A, Nilsson P, Nelson D, Olsson B, Englund MC, Abbot S, Sartipy P. 2007. Differentiating human embryonic stem cells express a unique housekeeping gene signature. Stem Cells 25:473-480.

Takahashi K, Tanabe K, Ohnuki M, Narita M, Ichisaka T, Tomoda K, Yamanaka S. 2007. Induction of pluripotent stem cells from adult human fibroblasts by defined factors. Cell 131:861-872.

Tang JM, Luo B, Xiao JH, Lv YX, Li XL, Zhao JH, Zheng F, Zhang L, Chen L, Yang JY, Guo LY, Wang L, Yan YW, Pan YM, Wang JN, Li DS, Wan Y, Chen SY. 2015. VEGF-A promotes cardiac stem cell engraftment and myocardial repair in the infarcted heart. Int J Cardiol 183:221-231.

Thurston G, Kitajewski J. 2008. VEGF and Delta-Notch: interacting signalling pathways in tumour angiogenesis. Br J Cancer 99:1204-1209.

Tourovskaia A, Fauver M, Kramer G, Simonson S, Neumann T. 2014. Tissue-engineered microenvironment systems for modeling human vasculature. Exp Biol Med (Maywood) 239:1264-1271.

Traktuev DO, Prater DN, Merfeld-Clauss S, Sanjeevaiah AR, Saadatzadeh MR, Murphy M, Johnstone BH, Ingram DA, March KL. 2009. Robust functional vascular network formation in vivo by cooperation of adipose progenitor and endothelial cells. Circ Res 104:1410-1420.

Traktuev DO, Merfeld-Clauss S, Li J, Kolonin M, Arap W, Pasqualini R, Johnstone BH, March KL. 2008. A population of multipotent CD34-positive adipose stromal cells share pericyte and mesenchymal surface markers, reside in a periendothelial location, and stabilize endothelial networks. Circ Res 102:77-85.

Ucuzian AA, Greisler HP. 2007. In vitro models of angiogenesis. World J Surg 31:654-663.

Uusimaa PA, Hassinen IE, Vuolteenaho O, Ruskoaho H. 1992. Endothelin-induced atrial natriuretic peptide release from cultured neonatal cardiac myocytes: the role of extracellular calcium and protein kinase-C. Endocrinology 130:2455-2464.

Valarmathi MT, Goodwin RL, Fuseler JW, Davis JM, Yost MJ, Potts JD. 2010. A 3-D cardiac muscle construct for exploring adult marrow stem cell based myocardial regeneration. Biomaterials 31:3185-3200.

van der Valk J, Brunner D, De Smet K, Fex Svenningsen A, Honegger P, Knudsen LE, Lindl T, Noraberg J, Price A, Scarino ML, Gstraunthaler G. 2010. Optimization of chemically defined cell culture media--replacing fetal bovine serum in mammalian in vitro methods. Toxicol in Vitro 24:1053-1063.

van Spreeuwel AC, Bax NA, Bastiaens AJ, Foolen J, Loerakker S, Borochin M, van der Schaft DW, Chen CS, Baaijens FP, Bouten CV. 2014. The influence of matrix (an)isotropy on cardiomyocyte contraction in engineered cardiac microtissues. Integr Biol (Camb) 6:422-429.

Verma V, Purnamawati K, Manasi, Shim W. 2013. Steering signal transduction pathway towards cardiac lineage from human pluripotent stem cells: a review. Cell Signal 25:1096-1107.

Vernon RB, Sage EH. 1999. A Novel, Quantitative Model for Study of Endothelial Cell Migration and Sprout Formation within Three-Dimensional Collagen Matrices. Microvasc Res 57:118-133.

Verseijden F, Posthumus-van Sluijs SJ, Farrell E, van Neck JW, Hovius SE, Hofer SO, van Osch GJ. 2010a. Prevascular structures promote vascularization in engineered human adipose tissue constructs upon implantation. Cell Transplant 19:1007-1020.

Verseijden F, Posthumus-van Sluijs SJ, Pavljasevic P, Hofer SO, van Osch GJ, Farrell E. 2010b. Adult human bone marrow- and adipose tissue-derived stromal cells support the formation of prevascular-like structures from endothelial cells in vitro. Tissue Eng Part A 16:101-114.

Vidarsson H, Hyllner J, Sartipy P. 2010. Differentiation of human embryonic stem cells to cardiomyocytes for in vitro and in vivo applications. Stem Cell Rev 6:108-120.

Vikkula M, Boon LM, Carraway KL,3rd, Calvert JT, Diamonti AJ, Goumnerov B, Pasyk KA, Marchuk DA, Warman ML, Cantley LC, Mulliken JB, Olsen BR. 1996. Vascular dysmorphogenesis caused by an activating mutation in the receptor tyrosine kinase TIE2. Cell 87:1181-1190.

Wei X, Yang X, Han ZP, Qu FF, Shao L, Shi YF. 2013. Mesenchymal stem cells: a new trend for cell therapy. Acta Pharmacol Sin 34:747-754.

Williams AR, Hare JM. 2011. Mesenchymal stem cells: biology, pathophysiology, translational findings, and therapeutic implications for cardiac disease. Circ Res 109:923-940.

Wong T, McGrath JA, Navsaria H. 2007. The role of fibroblasts in tissue engineering and regeneration. Br J Dermatol 156:1149-1155.

Xu C, He JQ, Kamp TJ, Police S, Hao X, O'Sullivan C, Carpenter MK, Lebkowski J, Gold JD. 2006. Human embryonic stem cell-derived cardiomyocytes can be maintained in defined medium without serum. Stem Cells Dev 15:931-941.

Xu XQ, Soo SY, Sun W, Zweigerdt R. 2009. Global expression profile of highly enriched cardiomyocytes derived from human embryonic stem cells. Stem Cells 27:2163-2174.

Yan M, Plowman GD. 2007. Delta-like 4/Notch signaling and its therapeutic implications. Clin Cancer Res 13:7243-7246.

Yang X, Pabon L, Murry CE. 2014. Engineering adolescence: maturation of human pluripotent stem cell-derived cardiomyocytes. Circ Res 114:511-523.

Zhang J, Wilson GF, Soerens AG, Koonce CH, Yu J, Palecek SP, Thomson JA, Kamp TJ. 2009. Functional cardiomyocytes derived from human induced pluripotent stem cells. Circ Res 104:e30-41.

Zuk PA, Zhu M, Ashjian P, De Ugarte DA, Huang JI, Mizuno H, Alfonso ZC, Fraser JK, Benhaim P, Hedrick MH. 2002. Human adipose tissue is a source of multipotent stem cells. Mol Biol Cell 13:4279-4295.

Original publications

Original Paper

Cells Tissues Organs

Cells Tissues Organs
DOI: 10.1159/000336679

Accepted after revision: January 17, 2012
Published online: June 27, 2012

Adipose Stromal Cell Tubule Network Model Provides a Versatile Tool for Vascular Research and Tissue Engineering

Jertta-Riina Sarkanen[a, b, d] Hanna Vuorenpää[b] Outi Huttala[b]
Bettina Mannerström[c, d, g] Hannu Kuokkanen[e] Susanna Miettinen[c, d, g]
Tuula Heinonen[b] Timo Ylikomi[a, b, f]

[a]Department of Cell Biology, [b]FICAM, Finnish Center for Alternative Methods, School of Medicine, and
[c]Adult Stem Cells, Institute of Biomedical Technology, University of Tampere, [d]Science Center, Departments of
[e]Plastic Surgery and [f]Clinical Chemistry, Tampere University Hospital, and [g]BioMediTech, Tampere, Finland

Key Words
Angiogenesis · Endothelial cells · In vitro differentiation · Mesenchymal stem cells

Abstract
The current limitation in designing three-dimensional tissue models is the lack of adequate vascularization with mature and stable vessels. Adipose tissue is known to secrete several angiogenic factors, and human adipose stromal cells (hASC) are known to promote vessel growth, maturation and stabilization. In this study, hASC were induced to angiogenesis with growth factor-enriched medium either in monoculture or in coculture with human umbilical vein endothelial cells (HUVEC) and analyzed for vascular, pericytic and smooth muscle cell markers. hASC and HUVEC cocultures showed an accelerated proliferation rate and the cells self-assembled, independent of the cell passage number, into multilayered three-dimensional tubular networks. The networks of hASC and HUVEC expressed endothelial markers, a complete basement membrane and vessel-supporting cells with contractile properties. A hASC and green fluorescence protein-HUVEC-infection model revealed that cocultures consisted of a mosaic of von Willebrand factor-positive cells derived from both cell populations – hASC and HUVEC. hASC monoculture had passage- and donor-dependent ability to form tubular networks, with half of the cultures presenting tubule structures and basement membrane formation. Pericytic and smooth muscle cell markers were expressed in hASC monoculture even when tubules were absent. By combining the potential properties of hASC and features from the present angiogenesis assays, we generated a natural-like, xeno-free, prevascular-like network in vitro model with excellent reproducibility and minimal limitations in technical performance. This tubular network model is an excellent tool for studying cell interactions during vascular development, for chemical and drug testing and for developing natural-like, multilayered, vascularized, scaffold-free tissue models.

Introduction

The current major limitation in designing three-dimensional vascularized tissue models and implantable tissue constructs is the lack of adequate vascularization in the construct and especially the maturation and stabilization of the vasculature [Moon and West, 2008; Rivron et

KARGER
Fax +41 61 306 12 34
E-Mail karger@karger.ch
www.karger.com

1422–6405/12/0000–0000$38.00/0

Accessible online at:
www.karger.com/cto

Dr. Jertta-Riina Sarkanen
Finnish Center for Alternative Methods and Department of Cell Biology
Medical School, University of Tampere
FI–33014 Tampere (Finland)
Tel. +35 84 0190 4105, E-Mail riina.sarkanen@uta.fi

Abbreviations used in this paper

bFGF	basic fibroblast growth factor
COLIV	collagen IV
EGM-2	endothelial cell growth medium-2
GFP	green fluorescence protein
hASC	human adipose stromal cells
HS	human serum
HUVEC	human umbilical vein endothelial cells
IGF-I	insulin-like growth factor-I
PDGFRβ	platelet-derived growth factor receptor-β
PECAM-1	platelet/endothelial cell adhesion molecule-1
RPLP0	ribosomal protein large P0
αSMA	α-smooth muscle actin
SMMHC	smooth muscle myosin heavy chain
VEGF	vascular endothelial growth factor
vWf	von Willebrand factor

al., 2008]. The vascular network with stable and functional vessels [Abramsson et al., 2002] is essentially needed to meet the nutritional and functional demands of the organ [Gerhardt and Betsholtz, 2003]. The vessel engineering should optimally produce natural-like and xeno-free vascular constructs. Preferably, no animal components or unnatural scaffold materials should be allowed in the tissue culture, the cultures should contain only growth factors and proteins that occur in tissue naturally, and vessels forming in culture should have features of maturing vessels, i.e. in addition to tubule structures, the pericyte recruitment, basement membrane formation and vessel-supporting layer of smooth muscle cells should appear.

Adipose tissue, an active endocrine organ, is known to secrete several angiogenic and adipogenic cytokines and growth factors such as vascular endothelial growth factor (VEGF), basic fibroblast growth factor (bFGF) and insulin-like growth factor-I (IGF-I) [Gimeno and Klaman, 2005; Rehman et al., 2004; Rubina et al., 2009; Sadat et al., 2007; Verseijden et al., 2009]. Moreover, human adipose stromal cells (hASC), isolated as a stromal-vascular fraction from the adipose tissue specimens, are known to have developmental plasticity both in vitro and in vivo [Planat-Benard et al., 2004; Rehman et al., 2004] and have the capacity to differentiate into multiple cell phenotypes such as adipose [Gimble and Guilak, 2003b; Zuk et al., 2001], smooth muscle [Traktuev et al., 2008] and endothelial cells [Miranville et al., 2004; Oswald et al., 2004; Pittenger et al., 1999; Planat-Benard et al., 2004; Wosnitza et al., 2007; Wu et al., 2007]. hASC are known to promote vessel growth, maturation and stabilization in vivo [Amos et al., 2008; Cai et al., 2009; Covas et al., 2008; Traktuev et al., 2008; Zannettino et al., 2007] by secreting angiogenic factors and by differentiating into vessel lining supporting cells with pericytic properties [Amos et al., 2008; Kilroy et al., 2007; Traktuev et al., 2008]. The high proliferation and differentiation capacity of hASC makes them an ideal component for angiogenesis modeling, and the use of abundant adipose tissue as a source of endothelial cells would also be attractive for vessel engineering [Merfeld-Clauss et al., 2010; Miranville et al., 2004; Planat-Benard et al., 2004; Wu et al., 2007]. Moreover, understanding the role of angiogenesis in adipose tissue is important, as vasculature regulates both the adipose tissue mass development and adipose tissue reduction, and is also suggested to have an impact on regulating the mass of other adult tissues [Rupnick et al., 2002].

The angiogenic potential of hASC has widely been studied [Cao et al., 2005; Planat-Benard et al., 2004; Traktuev et al., 2008; Verseijden et al., 2009], alone or in coculture with endothelial cells, in the presence of a supporting scaffold, e.g. collagen I, Matrigel or fibrin [Dietrich and Lelkes, 2006; Lai et al., 2009; Miranville et al., 2004; Oswald et al., 2004; Pittenger et al., 1999; Planat-Benard et al., 2004; Rubina et al., 2009; Verseijden et al., 2010; Wosnitza et al., 2007]. However, in general, in the previous methods, the capillary tubule formation has been quite modest or the test has contained animal-derived components. Moreover, several previous methods have focused only on the role of endothelial cell migration and proliferation during angiogenesis, i.e. tubule formation. However, as pericytes have a crucial role in the regulation of the microvessel growth, maturation and stabilization during angiogenesis [Amos et al., 2008; Benjamin et al., 1998], the endothelial tubule formation alone is not a sufficient measure of vascular growth and differentiation. The recruitment of pericytes along vascular tubules is an essential step in vessel maturation, needed to induce basement membrane formation and to prevent vessel regression [Gerhardt and Betsholtz, 2003]. The failure of the endothelial cells to establish mature structures in vitro is often due to an absence of stabilizing mural cells [Merfeld-Clauss et al., 2010]. Coculture models that have been used in several studies [Bishop et al., 1999; Donovan et al., 2001; Friis et al., 2003, 2005; Merfeld-Clauss et al., 2010; Montesano et al., 1993; Nicosia and Ottinetti, 1990] provide a useful method for studying angiogenesis in controlled conditions in vitro, with the advantage of being able to replicate some tissue-derived signaling [Rubina et al., 2009]. However, only a few studies [Merfeld-Clauss et al., 2010; Traktuev et al., 2008] have

characterized hASC and human umbilical vein endothelial cells (HUVEC) scaffold-free cocultures and their angiogenic properties or hASC monoculture angiogenic properties [Miranville et al., 2004].

Our specific aim was to develop a completely human-based, simplified and improved angiogenesis model, a prevascular-like network with properties of maturing vessels, that could be used for studying angiogenesis in vitro, and that would aid in the development of tissue models by improving target cell proliferation, survival and differentiation. In this prevascular-like network model, cells are induced with natural growth factors and allowed to self-assemble into tubular network and vascular supporting structures. We studied the hASC+HUVEC coculture model by combining some properties and analyses from previous studies [Friis et al., 2003; Merfeld-Clauss et al., 2010] and the fibroblast-HUVEC coculture angiogenesis assay previously validated in our laboratory [Sarkanen et al., 2011]. We induced the hASC+HUVEC coculture or hASC monoculture with naturally occurring angiogenic growth factors; epidermal growth factor, VEGF, bFGF and IGF-I [Mehta and Besner, 2007]. We evaluated the cultures for expression of vascular, pericytic and smooth muscle cell markers by immunocytochemistry and quantitative RT-PCR. We also studied the endothelial differentiation capacity of hASC in both hASC monoculture and a hASC and green fluorescence protein (GFP)-HUVEC-infection model. We produced an improved assay that, due to growth factor addition, induces a multilayered prevascular-like network with properties of maturing vessels that do not regress over time. We also showed that hASC, at low passages, are able to differentiate into endothelial-like cells alone and in hASC+HUVEC coculture. This improved and easy tubular network model is an excellent tool for studying cell interactions during vascular development, in drug and chemical screening, and most significantly, in designing vascularized tissue models in vitro or, as it is xeno-free, for creating vascularized tissue constructs for implantation.

Materials and Methods

The study was conducted in accordance with the Ethics Committee of the Pirkanmaa Hospital District, Tampere, Finland (R03058, R08028). The adipose tissue samples were obtained from surgical operations and the human umbilical cords from scheduled cesarean sections with informed consents at the Tampere University Hospital, Tampere, Finland. The experiments complied with the current laws of Finland.

Isolation and Culture of hASCs

Stem cell isolation procedure was performed as described previously [Gimble and Guilak, 2003a; Hong et al., 2005; Niemela et al., 2007]. Briefly, human adipose tissue specimens were cut into small pieces, enzymatically digested with 0.05% collagenase I (Invitrogen, Paisley, UK) in Dulbecco's Modified Eagle's Medium Nutrient Mixture F-12 (Gibco, Invitrogen, Carlsbad, Calif., USA) for 60 min at 37°C in a gyratory water bath. The digested tissue was centrifuged at 600 *g* for 10 min at room temperature. The digested tissue was filtered through a 100-μm filter (Sarstedt, Nümbrecht, Germany), centrifuged and filtered again through a 40-μm filter (Sarstedt). Cells were seeded into 75-cm^2 flasks (Nunc EasyFlask™, Nunc, Roskilde, Denmark) in Dulbecco's Modified Eagle's Medium Nutrient Mixture F-12 supplemented with 1% L-glutamine (Gibco), 1% antibiotic-antimycotic mixture (Gibco) and 15% human serum (HS; Cambrex, East Rutherford, N.J., USA). The next day, cells were washed several times with PBS. The cells were maintained at 37°C under a 5% CO_2 air atmosphere at a constant humidity and medium was changed every 2–3 days. After having grown to confluency, cells were divided in a ratio of 1:2 to 1:3, or further used for cell culture studies.

Isolation and Culture of HUVEC

The HUVEC were isolated from human umbilical cord veins as described previously [Jaffe et al., 1973; Sarkanen et al., 2011]. Briefly, the cord was separated from the placenta and the umbilical vein was cannulated with a 20G needle and the needle was secured by clamping the cord over the needle with a surgical clamp. The vein was perfused with PBS to wash out blood and then the opposing end of the umbilical vein was clamped with a surgical clamp. Subsequently, the vein was infused with 0.05% collagenase I. The umbilical cord was incubated in a water bath at 37°C for 15 min. After incubation, the collagenase I solution containing HUVEC was flushed from the cord by perfusion with PBS into a 50 ml polypropylene tube (Sarstedt). The cells were centrifuged at 200 *g* for 10 min, washed once with medium, centrifuged again and resuspended in endothelial growth cell medium-2 (EGM-2), BulletKit medium (Lonza Group Ltd., Basel, Switzerland) and seeded into 75 cm^2 flasks. Medium was changed every 2–3 days and cells were divided when confluent. For assay controls, HUVEC were plated at 4,000 cells/cm^2 and cultured in EGM-2 BulletKit medium.

Flow Cytometric Surface Marker Expression Analysis of HUVEC

The HUVEC were harvested at passage 3 and analyzed with a fluorescence-activated cell sorter (FACSAria, BD Biosciences, Erembodegem, Belgium). Monoclonal antibodies against CD13-PE (BD Biosciences), CD31-FITC, CD34-APC and CD44-FITC (Immunotools GmbH Friesoythe, Germany), CD117-APC and CD133-PE (Miltenyi Biotech, Bergisch Gladbach, Germany), CD144-PE, CD202b and VEGFR2 (R&D Systems Inc., Minn., USA) and CD63-PE (Abcam, Cambridge, UK) were used. Monoclonal antibodies against von Willebrand factor (vWF, Abcam) were conjugated with IgG-PE (CalTag Laboratories, Calif., USA). Ten thousand cells were analyzed per sample and the positive expression was defined as the level of fluorescence greater than 99% of the corresponding unstained cell sample.

Table 1. Oligonucleotide sequences used for RT-PCR experiments

Gene	Primer
Human *RPLP0*	Forward 5′-AATCTCCAGGGGCACCATT-3′ Reverse 5′-CGCTGGCTCCCACTTTGT-3′
Human *PECAM-1* (CD31)	Forward 5′-TCATTTCTGGGATCCATATGCA-3′ Reverse 5′-TGGGTGTAGAGAAGGATTCCGT-3′
Human *Angiopoietin 1*	Forward 5′-AGCTACCACCAACAACAGTG-3′ Reverse 5′-CAAAGATTGACAAGGTTGTGG-3′
Human *Caldesmon*	Forward 5′-AAGAATCCTTGGGACAGGTGAC-3′ Reverse 5′-GTGGTGGTTGTCTTGGCCTC-3′

Lentivirus Infection

Lentiviral construct pLKO-MISSION-Bright-GFP was purchased from Biomedicum Genomics (BMGen, Biomedicum Helsinki, Helsinki, Finland). The infection was carried out with HUVEC at low passages with 300 μl of pLKO-MISSION-Bright-GFP in 1 ml EGM-2 BulletKit medium (1 U/ml). Virus infection was accelerated with 8 μg/ml hexadimethrine bromide (Sigma). After 24 h of incubation, medium was replaced with fresh EGM-2 medium. Highly fluorescent clones were selected with cloning rings and further selected with dilution cloning to obtain pure GFP-HUVEC culture. After expanding the infected HUVEC, they were used for hASC and HUVEC coculture assay as described below.

hASC Monoculture Assay

hASC (six different cell lines derived from different donors, passages 1–7 used) were seeded in EGM-2 BulletKit medium into 48-well plates (Nunclon™ Multidishes, Nunc, Roskilde, Denmark) at a density of 20,000 cells/cm^2. Cells were induced for either 3 or 6 days in EGM-2 BulletKit medium, a commercially available growth factor-enriched medium containing epidermal growth factor, VEGF, bFGF, IGF-I, ascorbic acid, heparin, 0.1% gentamicin/amphotericin-B and 2% FBS, or in DMEM/F-12 medium supplemented with 15% HS, 1 mM L-glutamine and 1% antibiotic-antimycotic mixture. Medium was changed and the treatments applied once to cells cultured for 3 days and twice to cells cultured for 6 days.

hASC and HUVEC Coculture Assay

hASC (21 different cell lines derived from different donors, passages 1–7 used) were seeded in EGM-2 BulletKit (Lonza) culture medium into 48-well plates (Nunclon™ Multidishes, Nunc, Roskilde, Denmark) or for confocal imaging into 8-well slides (IbiTreat, Ibidi Gmbh, Martinsried, Germany) at a density of 20,000 cells/cm^2. HUVEC, cultured as above (24 different cell lines derived from different donors, passages 1–6 used), were immediately carefully seeded on top of hASC at a density of 4,000 cells/cm^2. The seeding densities of hASC and HUVEC were chosen according to previous studies by us and others [Donovan et al., 2001; Friis et al., 2003; Sarkanen et al., 2011]. The day after plating, the differentiation treatments were applied to hASC+HUVEC coculture. Treatments were (all in duplicate wells): (1) EGM-2 BulletKit medium (composition as described above in hASC monoculture assay); (2) EGM-2 BulletKit – medium in which 2% FBS was replaced with 2% HS; (3) EGM-2 BulletKit – medium without serum, and (4) endothelial cell basal medium-2 (Lonza) containing no growth factors, supplemented with 0.1% gentamicin, 2% FBS and 1 mM L-glutamine. Cells were cultured for either 3 or 6 days prior to immunocytochemistry or quantitative RT-PCR. Medium was changed and the treatments applied once to cells cultured for 3 days and twice to cells cultured for 6 days.

Quantitative RT-PCR

The primers used for angiogenesis and blood vessel maturation genes – platelet/endothelial cell adhesion molecule-1 (*PECAM-1*, also referred to as CD31); the blood vessel stabilizing signal molecule angiopoietin 1 *(Angiopoietin 1)*; the smooth muscle cell microfilament protein regulating cell contraction, caldesmon *(Caldesmon)*; and reference gene ribosomal protein large P0 (*RPLP0*; all oligonucleotides from Oligomer Oy, Helsinki, Finland) – are shown in table 1. The total RNA from hASC or hASC+HUVEC was extracted from 3 or 6 days differentiated confluent cultures using TRIzol® (Invitrogen, Carlsbad, Calif., USA) following the manufacturer's protocol. cDNA was synthetized using High Capacity cDNA Reverse Transcriptase Kit (Applied Biosystems, Foster City, Calif., USA) according to manufacturer's instructions. Quantitative RT-PCR analysis was performed in a 96-well optical reaction plate using an ABI Prism 7000 sequence detector (Applied Biosystems). As the expression of RPLP0 gene was stable between experimental conditions, we used this gene as the reference for data normalization. hASC grown in hASC culture medium were used as controls for gene expression for *Angiopoietin 1* and *Caldesmon* and HUVEC grown in EGM-2 for *PECAM-1*. Reactions were performed using SYBR Green PCR Master Mix kit (Applied Biosystems), 50 ng cDNA sample and 10 μM primers. The PCR conditions were as follows: 10 min at 95°C, followed by 40 cycles of 15 s at 95°C and 60 s at 60°C. The target and reference genes were amplified in separate wells. All reactions were performed in duplicate. Relative RNA expression was calculated in comparison to RPLP0 RNA expression for cell culture experiments using the Pfaffl method [Pfaffl, 2001]:

$$\text{ratio of relative expression} = (E_{\text{target}})^{\Delta CP \text{ target (control-sample)}} / (E_{\text{ref}})^{\Delta CP \text{ ref (control-sample)}}$$

Immunocytochemistry

The tubule formation was visualized with endothelial cell-specific antibody to vWf (anti-vWf primary antibody produced in rabbit, 1:500, Sigma). To evaluate human adipose stromal cell differentiation, parallel double immunofluorescence staining with α-vWf was performed. Primary antibody against either common pericytic marker α-smooth muscle actin (monoclonal anti-αSMA clone 1A4, 1:200, Sigma), vascular smooth muscle cell marker smooth muscle myosin heavy chain (anti-SMMHC, 1:800, Sigma), contractile smooth muscle cell marker calponin (anti-calponin, 1:800, Sigma), pericytic and smooth muscle cell progenitor marker platelet-derived growth factor receptor-β (anti-PDGFRβ 1:800) or basement membrane marker collagen IV (anti-COLIV, 1:500, Sigma) was combined with anti-vWf. Cells were washed three times with PBS, fixed with ice-cold 70% ethanol for 20 min, permeabilized with 0.5% Triton X-100 (JT Baker, Phillipsburg, N.J., USA) for 15 min and blocked for unspecific staining with 10% bovine serum albumin (Sigma) for 30 min. After blocking, cells were incubated with the primary antibody pairs for 1 h at room temperature. Cells were washed three times with PBS, incubated for 30 min with secondary antibody polyclonal anti-rabbit IgG TRITC (1:100, Sigma) for anti-vWf and polyclonal anti-mouse IgG FITC (1:100, Sigma) for anti-αSMA, anti-COLIV, anti-PDGFRβ and anti-SMMHC. Cell nuclei were stained with Hoechst 33258 (1 μg/ml, Sigma) for 5 min and washed 5 times with PBS. For anti-GFP staining, the primary antibody pair was mouse monoclonal antibody to GFP (1:100, Abcam, Cambridge, UK) and anti-vWf, secondary antibodies being anti-mouse IgG TRITC (1:100, Sigma) and polyclonal antibody to rabbit IgG FITC (1:500, Acris Antibodies GmbH, Hiddenhausen, Germany), respectively. Fluorescence was visualized with a Nikon Eclipse Ti-S microscope (Nikon, Tokyo, Japan) or with a confocal laser scanning microscope Zeiss LSM 700 (Zeiss LSM 700 on the Axio Observer, Carl Zeiss Microimaging GmbH, Jena, Germany) and the images were processed with Zen2009 (confocal images, Carl Zeiss), with Adobe Photoshop software 7.0 (Adobe Systems, San Jose, Calif., USA) and Corel Draw software 10.0 (Corel Corporation, Ottawa, Ont., Canada).

Microscopic Analysis of Tubule Formation

After immunocytochemical staining, the tubules were analyzed with Nikon Eclipse TS100 microscope (Nikon, Tokyo, Japan) from 48-well plate wells with 40× magnification. The extent of tubules in different cultures was quantified visually by using a semiquantitative grading scale from 0 to 10. The grading was based on tubule formation, the length and the branches of tubules, as described in our previous study [Sarkanen et al., 2011].

Statistical Analysis

Statistical analyses were performed and graphs processed with GraphPadPrism 5.0 (GraphPad Software Inc., San Diego, Calif., USA). Tubule formation and RT-PCR results were subjected to one-way ANOVA followed by Dunnett's and Bonferroni's post-hoc tests when applicable. The results were reported as mean ± SD and differences were considered significant with $p < 0.05$, $p < 0.01$ and $p < 0.001$.

Results

The Tubule Network Formation Is Induced in hASC Monoculture and in hASC+HUVEC Coculture in the Presence of Inductive Growth Factors

The tubule formation capacity and anti-vWf-positive endothelial tubule structures of hASC monoculture or hASC+HUVEC coculture were evaluated and compared at two different time points (day 3 and day 6) when grown in the growth factor-enriched EGM-2 BulletKit medium (fig. 1a). hASC+HUVEC coculture showed an extremely accelerated proliferation rate that was shown at day 6 as a massive, dense, multilayered prevascular-like network formation. hASC+HUVEC coculture tubular network formation was very extensive early (day 3) in vitro, always reproducible and not dependent on the cell line or passage number of cells. In hASC monoculture, the induction towards angiogenesis was not seen repeatedly between different experiments, only approximately half of the cultures showed tubule formation in some degree and dense tubular network formation, as seen in figure 1a, was seen less often. When the tubule formation was semiquantitatively evaluated (fig. 1b, tubule formation), hASC+HUVEC had significantly more tubules at day 6 than at day 3 ($p < 0.001$) and significantly more tubules than hASC monoculture at day 3 ($p < 0.01$) and at day 6 ($p < 0.01$). The two controls, hASC+HUVEC grown without growth factors and HUVEC alone, both grown in growth factor-enriched EGM-2 medium, showed only mild tubule formation or no tubule formation, respectively (fig. 1c). The surface marker characterization of control HUVEC is shown in table 2. We also studied the hASC+HUVEC tubule formation in EGM-2 when FBS was replaced with 2% human serum (hASC+HUVEC EGM-2, 2% HS, fig. 1d) or when FBS was completely removed (hASC+HUVEC, without serum, fig. 1d). We were able to replace FBS without significant effect on the tubule formation capacity of hASC+HUVEC coculture as tested with one-way ANOVA.

In order to further evaluate which cells were responsible for the massive tubule network formation in hASC+HUVEC coculture and to see whether hASC induce the proliferation and tubule formation of HUVEC or also differentiate into endothelial-like cells, as seemed to be the case according to hASC monoculture studies, we created a hASC and GFP-infected HUVEC coculture (hASC+GFP-HUVEC, fig. 2). The anti-vWf-stained cocultures (fig. 2, vWf) were mostly mosaic and consisted of two different populations of vWf-positive cells, approximately half of the cells being GFP infected (fig. 2,

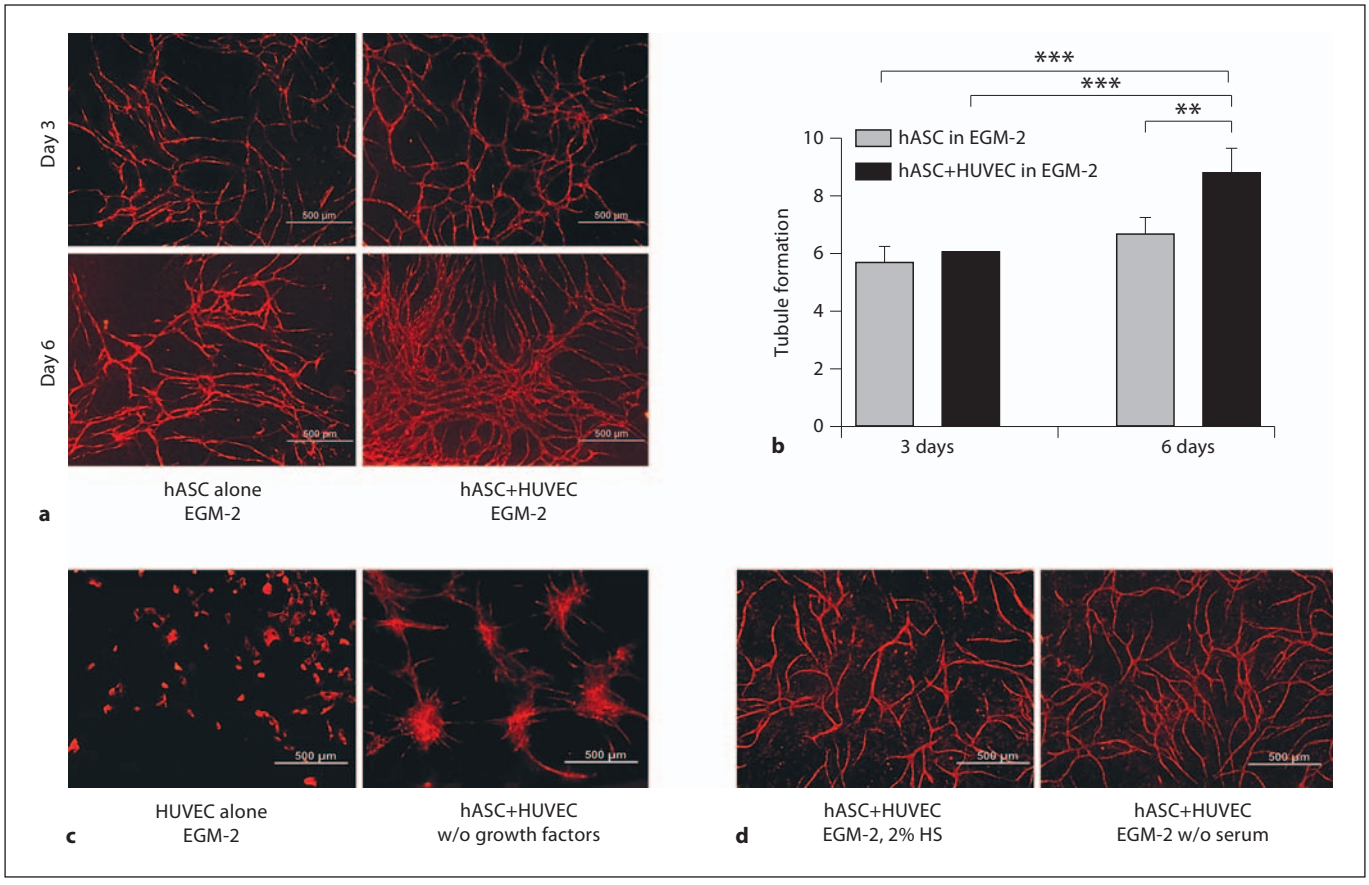

Fig. 1. The tubule formation of hASC monoculture and hASC+HUVEC coculture. Cells were stained with vWf antibody (anti-vWf, 1:500, Sigma; red fluorescence shown with TRITC-conjugated secondary antibody, 1:100, Sigma). **a** Comparison of tubule formation of hASC monoculture and hASC+HUVEC coculture. Cells were cultured and induced to angiogenesis for 3 or 6 days in growth factor-enriched EGM-2 BulletKit medium. **b** Semi-quantitative analysis of the tubule formation between different treatments. hASC monoculture and hASC+HUVEC coculture were compared to each other at 3 and 6 days. Semiquantitative scale according to Sarkanen et al. [2011]. The results are reported as mean ± SD and differences considered significant when ** $p < 0.01$ and *** $p < 0.001$. **c** The controls shown at day 6 in vitro. HUVEC were plated at 4,000 cells/cm^2 and grown in growth factor-enriched EGM-2 and hASC+HUVEC cocultured without exogenous addition of growth factors. **d** hASC+HUVEC were cultured in the growth factor-enriched EGM-2 with human serum (EGM-2, 2% HS) or without serum (EGM-2 w/o serum).

Table 2. Surface protein expression of HUVEC

Antigen	Surface protein	HUVEC
CD 13	Aminopeptidase N	99.4
CD 31	PECAM	94.5
CD 34	Glycoprotein	3.9
CD 44	Hyaluronate, HCAM	44.5
CD 63	Tetraspanin	8.5
CD 117	c-kit, SCFR	8.4
CD 133	AC133	1.1
CD 144	VE-Cadherin	0.9
CD 202b	Tie-2/TEK	31.9
	VEGFR2	0.4
	vWF/factor VIII	14.5

GFP), and the other half of the anti-vWf-positive cells being GFP negative. Moreover, several GFP-negative and vWf-negative cells were surrounding the tubules as seen with Hoechst staining (fig. 2, merged).

Genes That Indicate Differentiation of Cells and Maturation of Tubule Structures Are Upregulated in hASC Monoculture and in hASC+HUVEC Coculture

hASC and hASC+HUVEC, both cultured in EGM-2 BulletKit medium, were further tested for their maturation stage with several pericytic and smooth muscle markers. The relative mRNA expression of *PECAM-1*, *Angiopoietin 1* and *Caldesmon* were studied both in

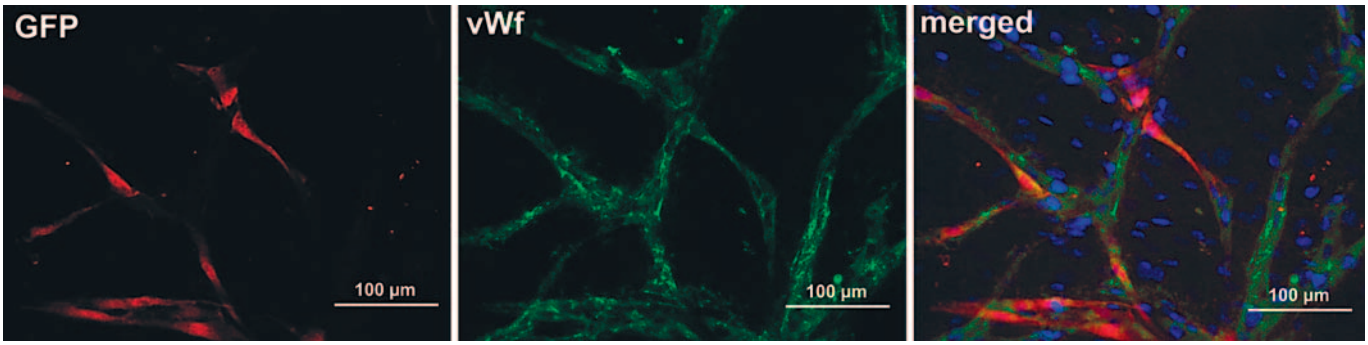

Fig. 2. hASC+GFP-HUVEC coculture model. Cells were cultured for 6 days in the growth factor-enriched EGM-2 medium and immunostained with anti-GFP (GFP, 1:100, Abcam; TRITC-conjugated secondary antibody, 1:100, Sigma) and anti-vWf (1:100, Sigma; FITC-conjugated secondary antibody, 1:500, Acris Antibodies). Cell nuclei were visualized with Hoechst staining (shown in the merged image, 1 μg/ml, Sigma).

hASC monoculture and in hASC+HUVEC coculture at days 3 and 6 (fig. 3). As a control, hASC, grown in their normal culture media, were used. By day 3, only *Caldesmon* showed significant activity, when compared to the control. *Angiopoietin 1* and *Caldesmon* expressions were significantly increased by day 6 with hASC and with hASC+HUVEC by days 3 and 6 ($p < 0.05$ and $p < 0.001$, respectively) when compared to the control hASC. The *PECAM-1* expression was significantly increased with hASC grown in growth factor-enriched medium by day 6 ($p < 0.05$) when compared to the control hASC, and moreover, also between days 3 and 6 ($p < 0.05$). *PECAM-1* expression was also seen to increase with hASC+HUVEC, but due to high variation, the result was not statistically significant. *Caldesmon* expression was increased between days 3 and 6 with hASC and with hASC+HUVEC ($p < 0.01$ and $p < 0.001$, respectively). It seemed that the *PECAM-1* expression was lower with hASC+HUVEC than with the control hASC monoculture. However, the *PECAM-1* expression was very low at day 3 in all treatments, which has probably caused an error in the normalization of the data.

Induced Extracellular Matrix Production in Culture and Differentiation of hASC into Vessel Lining Cells

hASC monoculture and hASC+HUVEC coculture were also subjected to immunocytochemical staining. The results from day 6 are shown in figure 4, except for PDGFRβ expression in hASC+HUVEC which is shown from day 3. PDGFRβ expression was most intense in hASC+HUVEC at day 3, seen as dot-like structures evenly surrounding the developing tubules. At day 6, PDGFRβ was seen in some extent in both hASC and hASC+HUVEC, but the expression was not changed with hASC+HUVEC between days. COLIV, showing the development of a basement membrane, was remarkably widely expressed in hASC+HUVEC. The expression was colocalized with the developing tubules covering the tubules. αSMA- and SMMHC-positive cells were expressed quite often in hASC and widely in hASC+HUVEC at day 6, often localized in the branching points of tubular structures and between the tubules. SMMHC expression was increased between days 3 and 6, especially in hASC+HUVEC. In hASC monoculture, vessel-supporting pericytic and smooth muscle cell markers were expressed, even despite the lack of capillary formation at the area. COLIV was also expressed in hASC monoculture at the sites of tubule formation, but not elsewhere. The confocal laser scanning microscopy of basement membrane (COLIV) and tubule network (vWf) staining showed the multilayered nature of the tubule network (fig. 5). The transparent three-dimensional projection of the Z-stack shown in figure 5a was merged from 28 single layers, the distance between layers being 7 μm. Therefore, the thickness of the tubule network was 196 μm. The close-up of the tubule network (fig. 5b) shows multilayered tubules crossing each other. Some of the crossing points are indicated with arrows.

Discussion

We developed an inductive prevascular-like network support based on adipose stromal cells and endothelial cells for in vitro tissue models and for tissue engineering constructs. Our specific aim was to develop a completely

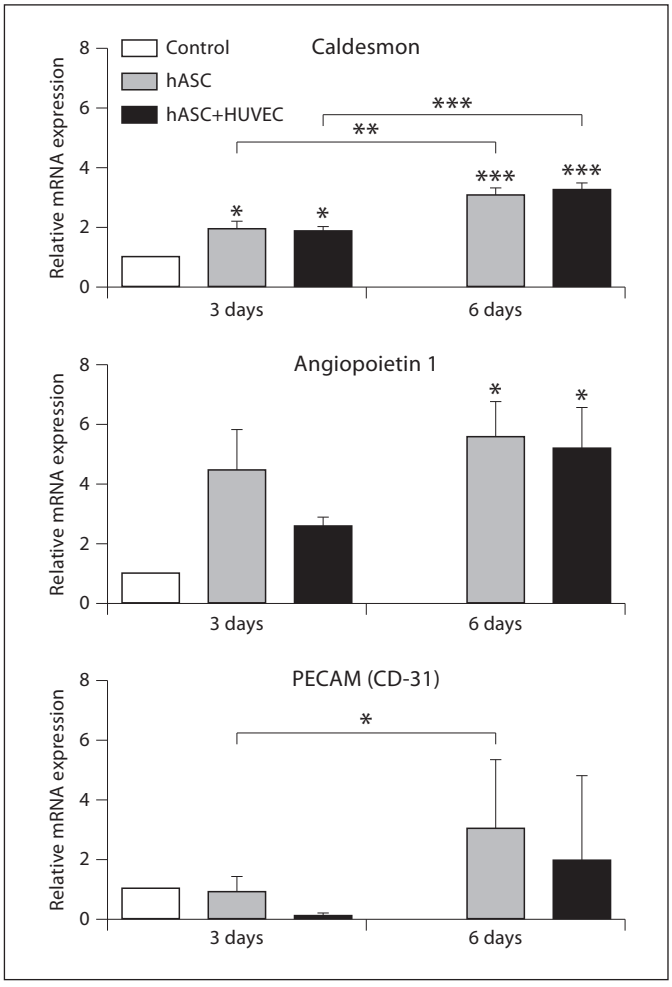

Fig. 3. The relative mRNA expression of *PECAM-1*, *Caldesmon* and *Angiopoietin 1* in hASC monoculture or hASC-HUVEC coculture at 3 and 6 days after angiogenesis induction with growth factor-enriched EGM-2 medium. The expressions were compared to their respective control (hASC, plated at 20,000 cells/cm^2, grown in hASC culture medium). The statistical analysis was performed with one-way ANOVA. The results are reported as mean ± SD and differences considered significant when * $p < 0.05$, ** $p < 0.01$ and *** $p < 0.001$.

human-based, simplified and improved angiogenesis model, a tubular network with properties of maturing vessels, which could be used for studying angiogenesis in vitro, and that would aid in the development of tissue models by improving target cell proliferation, survival and differentiation. In this tubular network model cells are induced with natural growth factors and allowed to self-assemble into a prevascular-like network and vascular supporting structures. We studied a hASC+HUVEC coculture model by combining some properties and analyses from the previously described model [Merfeld-Clauss et al., 2010] and the fibroblast-HUVEC coculture angiogenesis assay previously validated in our laboratory [Sarkanen et al., 2011]. The maturity of the developed model was evaluated with markers that indicated the maturation of the tubules by quantitative RT-PCR and immunocytochemical staining. We also studied whether hASC alone could be induced to endothelial cell differentiation and tubule formation with the addition of these naturally occurring stimulating growth factors.

Merfeld-Clauss et al. [2010] created a similar hASC+HUVEC coculture model with no exogenous growth factors added in cell culture. Contrary to their study, we specifically wanted to investigate tubule formation in a similar coculture system by adding growth factors that are secreted in vivo and that naturally stimulate angiogenesis, e.g. in adipose tissue [Hausman and Richardson, 2004; Mehta and Besner, 2007]. This selection of growth factors would provide a close to natural-like cell culture environment and presumably therefore favor the tubule network induction and allow sustained vessel formation and long-term stability of the tubular network, a feature that is often required in the development of complex tissue or organ models.

When hASC were combined with HUVEC (hASC+HUVEC) and cultured in EGM-2, a remarkable enhancement in cell proliferation, capillary formation and induction of maturation was seen with both cells. However, if the hASC were allowed to attach and proliferate in culture for a prolonged time period prior to HUVEC seeding, only modest tubule formation was seen (data not shown). Therefore, only simultaneous plating of cells effectively induced the self-assembly of the multilayered tubule network. The growth factor stimulation induced tubule formation that seemed not to be passage dependent (up to passage 7 tested) with either HUVEC or hASC, a result contrary to previous studies on these cell types cultured alone by us [Sarkanen et al., 2011] and others [Heydarkhan-Hagvall et al., 2008] that have shown that the differentiation capability is passage dependent.

hASC monoculture, on its behalf, had clearly passage and donor-dependent differentiation capacity towards endothelial-like cells despite the use of the growth factor-enriched medium. hASC alone often formed short cords in culture, but only occasionally massive tubule network formation. In addition to the current study, the tubule formation in hASC monoculture has only been shown previously by Miranville et al. [2004] and Heydarkhan-Hagvall et al. [2008]. Several groups have reported cord formation of hASC in Matrigel for example, but it has also been re-

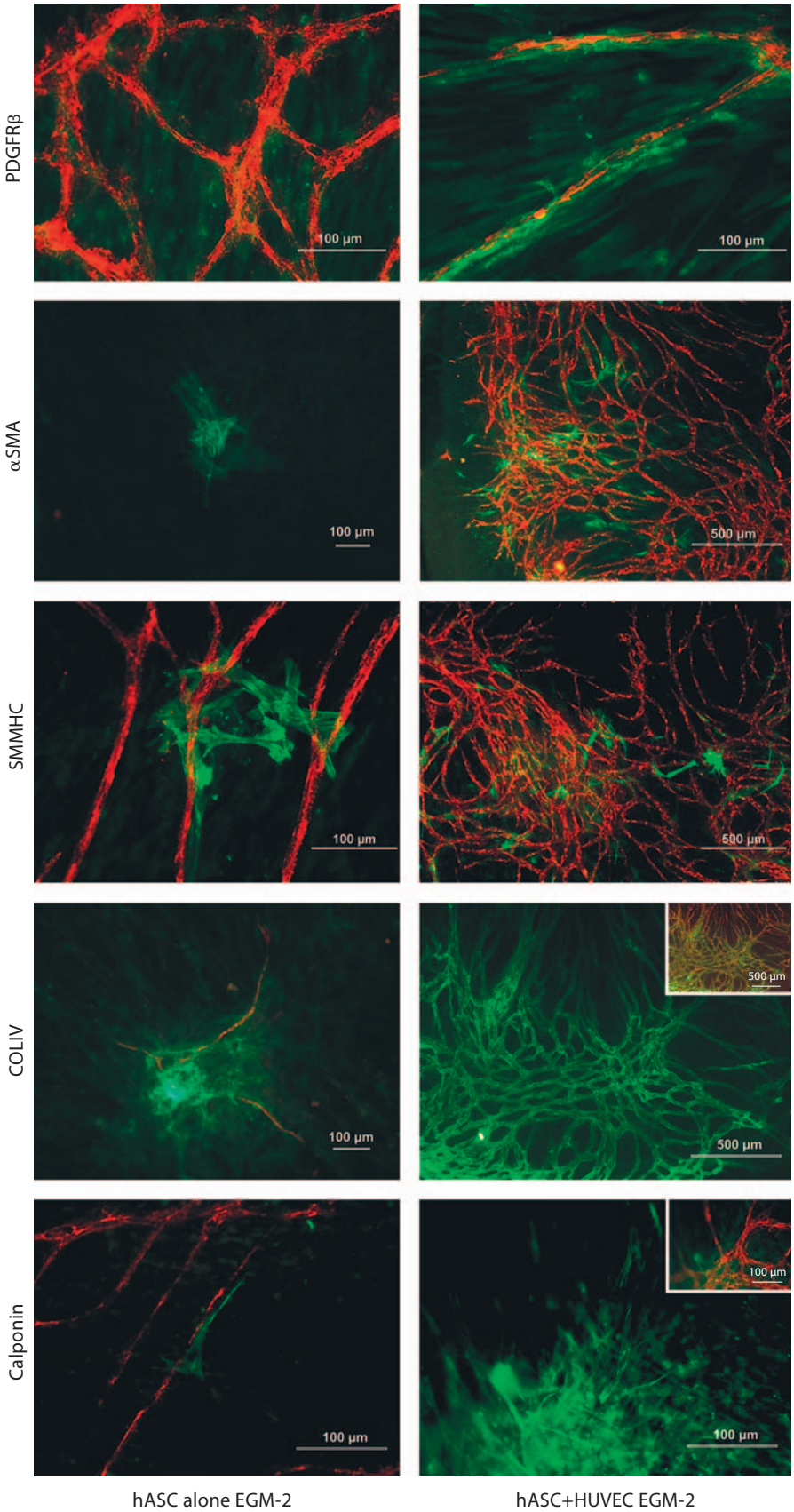

Fig. 4. The expression of pericytic and smooth muscle cell differentiation markers in tubule structures after angiogenic induction with growth factor-enriched EGM-2 medium. For detection of tubule formation, cell cultures were immunostained with vWf antibody (anti-vWf, 1:500, Sigma; red fluorescence shown with TRITC-conjugated secondary antibody, 1:100, Sigma). For detection of tubule maturation, cultures were immunostained with either anti-αSMA (1:200, Sigma), anti-COLIV (1:500, Sigma), anti-PDGFRβ (1:500, Sigma), anti-SMMHC (1:800, Sigma) or anti-calponin (1:800, Sigma), all of these green fluorescence, FITC-conjugated secondary antibody (1:100, Sigma). The images shown are merged images of double immunofluoresence at day 6, except for anti-PDGFRβ, which is at day 3, and except for anti-COLIV and anti-calponin for which both the merged image of staining (**insets**) and the FITC-conjugated secondary antibody – anti-COLIV/anti-calponin staining – are shown.

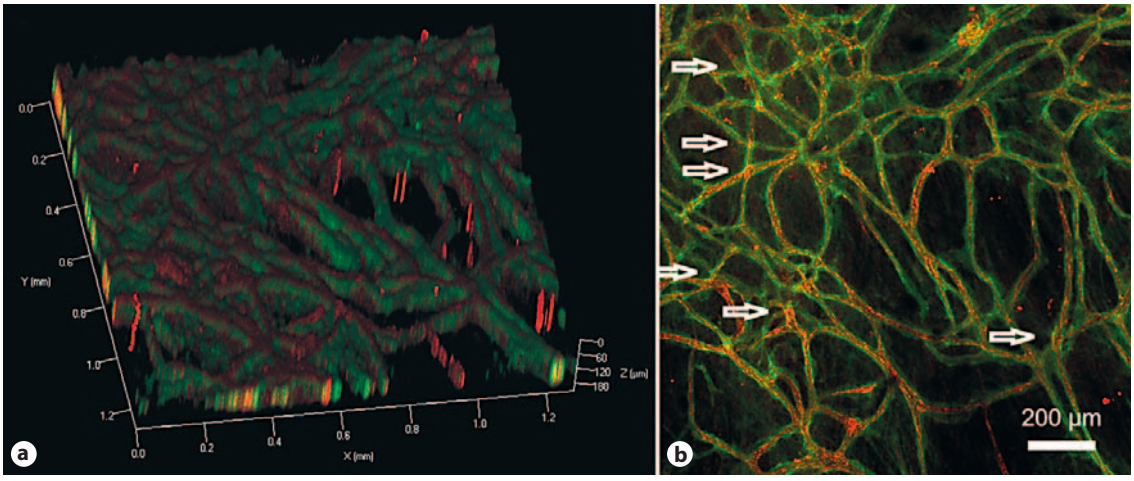

Fig. 5. The confocal laser scanning microscopy of a multilayered precapillary-like tubule network. For detection of the tubule formation, the hASC+HUVEC cocultures were immunostained with vWf antibody (anti-vWf, 1:500, red fluorescence, shown with TRITC-conjugated secondary antibody, 1:100, Sigma). For detection of basement membrane, cultures were immunostained with anti-COLIV (1:500, Sigma green fluorescence, FITC-conjugated secondary antibody, 1:100, Sigma). The images shown are merged images of double immunofluoresence at day 6. **a** Transparent three-dimensional projection of the Z-stack built from 28 layers with a threshold of 13; distance between layers: 7 um; scale bar = 200 µm. **b** A close-up of the tubule network, multilayered tubule formation seen in several areas, some of the crossing points of the tubules are indicated with arrows.

ported that the cord formation observed by different cells in Matrigel is an unspecific phenomenon [Donovan et al., 2001] and, therefore, not a reliable or comparable endothelial tubule formation assay to coculture assays.

To further evaluate which cells contribute to the tubule formation and whether the hASC mainly stimulate endothelial cell proliferation or take part in the endothelial cell differentiation itself, we created a GFP-infection model. In the hASC+GFP-HUVEC coculture, the tubules were seen to consist of a mosaic of GFP-HUVEC and of other cells that were GFP-negative, although vWf-positive. This finding, with our other result that hASC monoculture is able to form tubular networks, suggests that hASC not only stimulate the tubule formation and maturation, but also differentiate into endothelial-like cells in this system. Moreover, the significant increase in the expression of the endothelial marker *PECAM-1* in hASC monoculture between days 3 and 6 supports this finding.

Although freshly isolated hASC, or more precisely, stromal-vascular fraction cells, may contain microvascular endothelial cells [Rehman et al., 2004; Wosnitza et al., 2007], we have previously thoroughly characterized hASC [Lindroos et al., 2009, 2010] and shown that hASC, cultured in several different proliferation media, lack the expression of hematopoietic and angiogenic markers such as CD31, CD106 and CD146 (surface marker expression 0.6 ± 0.7, 0.7 ± 0.7 and 0.4 ± 0.2, respectively). However, the extent whereby hASC differentiate into endothelial-like cells in this model, especially in higher passages, and the functional and metabolic competency of these differentiated endothelial-like cells need careful further evaluation and characterization. In our opinion, the advantage of this current coculture model is, in fact, the heterogeneity of the hASC, creating and inducing a natural-like environment for the formation of a self-assembling tubule network.

The HUVEC isolated from umbilical cords and used in the assay were previously carefully quality controlled for their tubule formation capacity with low variation between cell batches [Sarkanen et al., 2011], and the surface marker expression profile of HUVEC that has been characterized here corresponds with previous reports [Fukasawa et al., 2006; Ichikawa et al., 2006; Korbling et al., 2006; Schmidt et al., 2006]. However, the flow cytometry results indicate low expression of VE-cadherin (0.9%) and relatively low expression of vWf (14.5%). VE-cadherin is reported to be low in HUVEC in normal cell culture, whereas significantly upregulated in HUVEC during tubule network formation [Kiran et al., 2011]. vWf expression, on its behalf, is reported to be heterogeneous in endothelial cells and to show regional variations in mRNA levels [Zanetta et al., 2000]. Expression of vWf is reported to be upregulated by the angiogenic growth fac-

tors bFGF and VEGF [Zanetta et al., 2000], which may explain the difference in our flow cytometry and immunofluoresence results.

Blood vessel formation involves not only endothelial tubule formation, but also the maturation of vessels by basement membrane formation and pericyte and vascular smooth muscle cell recruitment and differentiation [Kalluri, 2003]. Therefore, the maturation stage of hASC-induced vascular structures was evaluated. Our study supports the earlier studies [Merfeld-Clauss et al., 2010; Planat-Benard et al., 2004; Rubina et al., 2009; Traktuev et al., 2008] and demonstrates that hASC are able to contribute to vessel formation maturation in vitro by differentiating into vessel supporting structures with pericytic and smooth muscle cell properties. PDGFRβ, an important receptor in pericytic cell recruitment to developing tubules [Nishishita and Lin, 2004], was already extensively seen at 3 days in hASC+HUVEC. In contrast to a previous study [Merfeld-Clauss et al., 2010], we detected that hASC monoculture expressed COLIV colocalized with the tubules expressing vWf. hASC also widely expressed αSMA and occasionally other markers, even when capillaries were not present, which is well in line with the known vessel supporting role of hASC [Verseijden et al., 2010]. COLIV, an important basement membrane component defining integrity, stability and functionality of the basement membrane [Bonanno et al., 2000; Poschl et al., 2004], was intensively expressed in hASC+HUVEC, both at days 3 and 6, and surrounded all of the tubules completely, indicating well-formed basement membrane. COLIV staining also revealed the multilayered structures where the tubules were organized into three-dimensional networks (fig. 4 and fig. 5). hASC+HUVEC also expressed widely αSMA and SMMHC, the major contractile proteins in smooth muscle cells [Frid et al., 1992]. *Angiopoietin 1*, a molecule regulating blood vessel stabilization [Nishishita and Lin, 2004] and indicating late stages of tubule maturation and stabilization, as well as *Caldesmon,* a smooth muscle cell contraction regulator indicating higher differentiation of smooth muscle cells [Frid et al., 1992], were significantly expressed in both hASC and hASC+HUVEC at day 6. Another regulator of muscle cell contraction, calponin, was rarely seen in hASC monoculture, but often in hASC+HUVEC at the sites of the tubule formation. However, the maturation stage of the tubule networks needs further study, especially with endothelial nitric oxide synthase, an important regulator of angiogenesis, as well as by testing the VEGF independency of the formed tubule network.

Most tissue-engineered constructs are limited in thickness to 1–2 mm due to inadequate vascularization [Norotte et al., 2009]. However, scaffolds, which are often used to create multilayered tissue constructs, may interfere with the cell-to-cell interactions and the cell assembly [Norotte et al., 2009]. The growth factor induction induced a high proliferation of both cell types in hASC+HUVEC coculture. Therefore, this supporting prevascular-like network model could allow for the creation of multilayered, yet scaffold-free, soft tissue constructs. The three-dimensional nature of hASC+HUVEC coculture could be seen in confocal scanning microscopy three-dimensional projection, where the total thickness of the tubule network was nearly 200 μm. This network model would be especially suitable for engineering tissue constructs that need an intense tubular network. Moreover, due to a high proliferation rate, the cell number used in our study was only one fourth of the number used by Merfeld-Clauss et al. [2010], for example. A lower cell number provides a higher capacity, e.g. for in vitro drug screening studies. The xeno-free modification of hASC+HUVEC coculture allows the use of this tubular network culture model in tissue engineering applications. As suggested by Merfeld-Clauss et al. [2010], the endothelial cells could possibly be replaced with any tissue-specific endothelial cells (e.g. microvascular endothelial cells in adipose tissue) with no effect on tubule formation capability. Therefore, we can suspect that this developed tubular network platform is easily modified to be suitable in several different tissue model applications where a dense tubular network is needed. However, when this coculture system is aimed at human use in tissue constructs, the origin of endothelial cells must meet the need of the target tissue. Moreover, if hASC monoculture tubule network induction could be improved to be repeatable, this would allow an even more simplified tubular network model. However, the tubule formation of hASC alone in growth factor-enriched medium needs further study and more optimization, e.g. through an increase in cell seeding density.

By combining the present knowledge of potential properties of hASC in angiogenesis induction and features from the presently available tubule network assays, we could generate a natural-like angiogenesis in vitro with an excellent prevascular-like network formation capability, reproducibility and stability, and minimal limitations in technical performance (i.e. passaging and culture conditions). The tubule network had morphological and genetic features of maturing capillaries. This tubular network model mimics especially well the naturally oc-

curring angiogenesis in adipose tissue. The hASC monoculture or hASC+HUVEC coculture model provides an ideal platform for tissue engineering applications, both for developing tissue models in vitro or for the development of implantable tissue structures. Clinically relevant in vitro angiogenesis models are also valuable tools for investigating the in vivo angiogenesis process [Lai et al., 2009; Ucuzian and Greisler, 2007], e.g. for the treatment of cancer, macular degeneration or peripheral and coronary vascular diseases [Nillesen et al., 2007; Ucuzian and Greisler, 2007].

Acknowledgements

We thank Ms. Paula Helpiölä, Ms. Mirja Hyppönen and Ms. Hilkka Mäkinen for excellent technical assistance. Hannu Uusitalo, MD, PhD and Ulla Aapola, PhD from the SILK Research and Development Center for Ophthalmic Innovations at Tampere University Hospital are thanked for use of the confocal microscope facilities. Funding for the project was provided by Pirkanmaa Centers for Economic Development, Transport and the Environment, City of Tampere, Ministry of Education and Culture, Ministry of Agriculture and Forestry, Competitive research funding of the Pirkanmaa Hospital District (EVO9G189, EVO9H212) and Pirkanmaa Cultural Foundation.

References

Abramsson, A., O. Berlin, H. Papayan, D. Paulin, M. Shani, C. Betsholtz (2002) Analysis of mural cell recruitment to tumor vessels. Circulation *105:* 112–117.

Amos, P.J., H. Shang, A.M. Bailey, A. Taylor, A.J. Katz, S.M. Peirce (2008) IFATS collection: the role of human adipose-derived stromal cells in inflammatory microvascular remodeling and evidence of a perivascular phenotype. Stem Cells *26:* 2682–2690.

Benjamin, L.E., I. Hemo, E. Keshet (1998) A plasticity window for blood vessel remodelling is defined by pericyte coverage of the preformed endothelial network and is regulated by PDGF-B and VEGF. Development *125:* 1591–1598.

Bishop, E.T., G.T. Bell, S. Bloor, I.J. Broom, N.F. Hendry, D.N. Wheatley (1999) An in vitro model of angiogenesis: basic features. Angiogenesis *3:* 335–344.

Bonanno, E., M. Iurlaro, J.A. Madri, R.F. Nicosia (2000) Type IV collagen modulates angiogenesis and neovessel survival in the rat aorta model. In Vitro Cell Dev Biol Anim *36:* 336–340.

Cai, L., B.H. Johnstone, T.G. Cook, J. Tan, M.C. Fishbein, P.S. Chen, K.L. March (2009) IFATS collection: human adipose tissue-derived stem cells induce angiogenesis and nerve sprouting following myocardial infarction, in conjunction with potent preservation of cardiac function. Stem Cells *27:* 230–237.

Cao, Y., Z. Sun, L. Liao, Y. Meng, Q. Han, R.C. Zhao, (2005) Human adipose tissue-derived stem cells differentiate into endothelial cells in vitro and improve postnatal neovascularization in vivo. Biochem Biophys Res Commun *332:* 370–379.

Covas, D.T., R.A. Panepucci, A.M. Fontes, W.A. Silva Jr., M.D. Orellana, M.C. Freitas, L. Neder, A.R. Santos, L.C. Peres, M.C. Jamur, M.A. Zago (2008) Multipotent mesenchymal stromal cells obtained from diverse human tissues share functional properties and gene-expression profile with CD146+ perivascular cells and fibroblasts. Exp Hematol *36:* 642–654.

Dietrich, F., P.I. Lelkes (2006) Fine-tuning of a three-dimensional microcarrier-based angiogenesis assay for the analysis of endothelial-mesenchymal cell co-cultures in fibrin and collagen gels. Angiogenesis *9:* 111–125.

Donovan, D., N.J. Brown, E.T. Bishop, C.E. Lewis (2001) Comparison of three in vitro human 'angiogenesis' assays with capillaries formed in vivo. Angiogenesis *4:* 113–121.

Frid, M.G., B.V. Shekhonin, V.E. Koteliansky, M.A. Glukhova (1992) Phenotypic changes of human smooth muscle cells during development: late expression of heavy caldesmon and calponin. Dev Biol *153:* 185–193.

Friis, T., A.M. Engel, B.M. Klein, J. Rygaard, G. Houen (2005) Levamisole inhibits angiogenesis in vitro and tumor growth in vivo. Angiogenesis *8:* 25–34.

Friis, T., B. Kjaer Sorensen, A.M. Engel, J. Rygaard, G. Houen (2003) A quantitative ELISA-based co-culture angiogenesis and cell proliferation assay. Apmis *111:* 658–668.

Fukasawa, K., H. Fujii, Y. Saitoh, K. Koizumi, Y. Aozuka, K. Sekine, M. Yamada, I. Saiki, K. Nishikawa (2006) Aminopeptidase N (APN/CD13) is selectively expressed in vascular endothelial cells and plays multiple roles in angiogenesis. Cancer Lett *243:* 135–143.

Gerhardt, H., C. Betsholtz (2003) Endothelial-pericyte interactions in angiogenesis. Cell Tissue Res *314:* 15–23.

Gimble, J., F. Guilak (2003a) Adipose-derived adult stem cells: isolation, characterization, and differentiation potential. Cytotherapy *5:* 362–369.

Gimble, J.M., F. Guilak (2003b) Differentiation potential of adipose derived adult stem (ADAS) cells. Curr Top Dev Biol *58:* 137–160.

Gimeno, R.E., L.D. Klaman (2005) Adipose tissue as an active endocrine organ: recent advances. Curr Opin Pharmacol *5:* 122–128.

Hausman, G.J., R.L. Richardson (2004) Adipose tissue angiogenesis. J Anim Sci *82:* 925–934.

Heydarkhan-Hagvall, S., K. Schenke-Layland, J.Q. Yang, S. Heydarkhan, Y. Xu, P.A. Zuk, W.R. MacLellan, R.E. Beygui (2008) Human adipose stem cells: a potential cell source for cardiovascular tissue engineering. Cells Tissues Organs *187:* 263–274.

Hong, Y.H., D. Hishikawa, H. Miyahara, H. Tsuzuki, Y. Nishimura, C. Gotoh, K.C. Choi, Y. Hokari, Y. Takagi, H.G. Lee, K.K. Cho, S.G. Roh, S. Sasaki (2005) Up-regulation of adipogenin, an adipocyte plasma transmembrane protein, during adipogenesis. Mol Cell Biochem *276:* 133–141.

Ichikawa, Y., T. Ishikawa, N. Momiyama, M. Kamiyama, H. Sakurada, R. Matsuyama, S. Hasegawa, T. Chishima, Y. Hamaguchi, S. Fujii, S. Saito, K. Kubota, S. Hasegawa, H. Ike, S. Oki, H. Shimada (2006) Matrilysin (MMP-7) degrades VE-cadherin and accelerates accumulation of beta-catenin in the nucleus of human umbilical vein endothelial cells. Oncol Rep *15:* 311–315.

Jaffe, E.A., R.L. Nachman, C.G. Becker, C.R. Minick (1973) Culture of human endothelial cells derived from umbilical veins. Identification by morphologic and immunologic criteria. J Clin Invest *52*: 2745-2756.

Kalluri, R. (2003) Basement membranes: structure, assembly and role in tumour angiogenesis. Nat Rev Cancer *3:* 422–433.

Kilroy, G.E., S.J. Foster, X. Wu, J. Ruiz, S. Sherwood, A. Heifetz, J.W. Ludlow, D.M. Stricker, S. Potiny, P. Green, Y.D. Halvorsen, B. Cheatham, R.W. Storms, J.M. Gimble (2007) Cytokine profile of human adipose-derived stem cells: expression of angiogenic, hematopoietic, and pro-inflammatory factors. J Cell Physiol *212:* 702–709.

Kiran M.S., R.I. Viji, S.V. Kumar, A.A. Prabhakaran, P.R. Sudhakaran (2011) Changes in expression of VE-cadherin and MMPs in endothelial cells: Implications for angiogenesis. Vasc Cell *3*: 6.

Korbling, M., J.M. Reuben, H. Gao, B.N. Lee, D.M. Harris, D. Cogdell, S.A. Giralt, I.F. Khouri, R.M. Saliba, R.E. Champlin, W. Zhang, Z. Estrov (2006) Recombinant human granulocyte-colony-stimulating factor-mobilized and apheresis-collected endothelial progenitor cells: a novel blood cell component for therapeutic vasculogenesis. Transfusion *46:* 1795–1802.

Lai, N., A. Jayaraman, K. Lee (2009) Enhanced proliferation of human umbilical vein endothelial cells and differentiation of 3T3-L1 adipocytes in coculture. Tissue Eng Part A *15:* 1053–1061.

Lindroos, B., S. Boucher, L. Chase, H. Kuokkanen, H. Huhtala, R. Haataja, M. Vemuri, R. Suuronen, S. Miettinen (2009) Serum-free, xeno-free culture media maintain the proliferation rate and multipotentiality of adipose stem cells in vitro. Cytotherapy *11*: 958-972.

Lindroos, B., K.L. Aho, H. Kuokkanen, S. Räty, H. Huhtala, R. Lemponen, O. Yli-Harja, R. Suuronen, S. Miettinen (2010) Differential gene expression in adipose stem cells cultured in allogeneic human serum versus fetal bovine serum. Tissue Eng Part A *16*: 2281-2294.

Mehta, V.B., G.E. Besner (2007) HB-EGF promotes angiogenesis in endothelial cells via PI3-kinase and MAPK signaling pathways. Growth Factors *25:* 253–263.

Merfeld-Clauss, S., N. Gollahalli, K.L. March, D.O. Traktuev (2010) Adipose tissue progenitor cells directly interact with endothelial cells to induce vascular network formation. Tissue Eng Part A *16:* 2953–2966.

Miranville, A., C. Heeschen, C. Sengenes, C.A. Curat, R. Busse, A. Bouloumie (2004) Improvement of postnatal neovascularization by human adipose tissue-derived stem cells. Circulation *110:* 349–355.

Montesano, R., M.S. Pepper, L. Orci (1993) Paracrine induction of angiogenesis in vitro by Swiss 3T3 fibroblasts. J Cell Sci *105:* 1013–1024.

Moon, J.J., J.L. West (2008) Vascularization of engineered tissues: approaches to promote angio-genesis in biomaterials. Curr Top Med Chem *8:* 300–310.

Nicosia, R.F., A. Ottinetti (1990) Growth of microvessels in serum-free matrix culture of rat aorta: a quantitative assay of angiogenesis in vitro. Lab Invest *63:* 115–122.

Niemela, S.M., S. Miettinen, Y. Konttinen, T. Waris, M. Kellomaki, N.A. Ashammakhi, T. Ylikomi, (2007) Fat tissue: views on reconstruction and exploitation. J Craniofac Surg *18:* 325–335.

Nillesen, S.T., P.J. Geutjes, R. Wismans, J. Schalkwijk, W.F. Daamen, T.H. van Kuppevelt (2007) Increased angiogenesis and blood vessel maturation in acellular collagen-heparin scaffolds containing both FGF2 and VEGF. Biomaterials *28:* 1123–1131.

Nishishita, T., P.C. Lin (2004) Angiopoietin 1, PDGF-B, and TGF-beta gene regulation in endothelial cell and smooth muscle cell interaction. J Cell Biochem *91:* 584–593.

Norotte, C., F.S. Marga, L.E. Niklason, G. Forgacs (2009) Scaffold-free vascular tissue engineering using bioprinting. Biomaterials *30:* 5910–5917.

Oswald, J., S. Boxberger, B. Jorgensen, S. Feldmann, G. Ehninger, M. Bornhauser, C. Werner (2004) Mesenchymal stem cells can be differentiated into endothelial cells in vitro. Stem Cells *22:* 377–384.

Pfaffl, M.W. (2001) A new mathematical model for relative quantification in real-time RT-PCR. Nucleic Acids Res *29:* e45.

Pittenger, M.F., A.M. Mackay, S.C. Beck, R.K. Jaiswal, R. Douglas, J.D. Mosca, M.A. Moorman, D.W. Simonetti, S. Craig, D.R. Marshak (1999) Multilineage potential of adult human mesenchymal stem cells. Science *284:* 143–147.

Planat-Benard, V., J.S. Silvestre, B. Cousin, M. Andre, M. Nibbelink, R. Tamarat, M. Clergue, C. Manneville, C. Saillan-Barreau, M. Duriez, A. Tedgui, B. Levy, L. Penicaud, L. Casteilla (2004) Plasticity of human adipose lineage cells toward endothelial cells: physiological and therapeutic perspectives. Circulation *109:* 656–663.

Poschl, E., U. Schlotzer-Schrehardt, B. Brachvogel, K. Saito, Y. Ninomiya, U. Mayer (2004) Collagen IV is essential for basement membrane stability but dispensable for initiation of its assembly during early development. Development *131:* 1619–1628.

Rehman, J., D. Traktuev, J. Li, S. Merfeld-Clauss, C.J. Temm-Grove, J.E. Bovenkerk, C.L. Pell, B.H. Johnstone, R.V. Considine, K.L. March (2004) Secretion of angiogenic and antiapoptotic factors by human adipose stromal cells. Circulation *109:* 1292–1298.

Rivron, N.C., J.J. Liu, J. Rouwkema, J. de Boer, C.A. van Blitterswijk (2008) Engineering vascularised tissues in vitro. Eur Cell Mater *15:* 27–40.

Rubina, K., N. Kalinina, A. Efimenko, T. Lopatina, V. Melikhova, Z. Tsokolaeva, V. Sysoeva, V. Tkachuk, Y. Parfyonova (2009) Adipose stromal cells stimulate angiogenesis via promoting progenitor cell differentiation, secretion of angiogenic factors, and enhancing vessel maturation. Tissue Eng Part A *15:* 2039–2050.

Rupnick, M.A., D. Panigrahy, C.Y. Zhang, S.M. Dallabrida, B.B. Lowell, R. Langer, M.J. Folkman (2002) Adipose tissue mass can be regulated through the vasculature. Proc Natl Acad Sci USA *99:* 10730–10735.

Sadat, S., S. Gehmert, Y.H. Song, Y. Yen, X. Bai, S. Gaiser, H. Klein, E. Alt (2007) The cardioprotective effect of mesenchymal stem cells is mediated by IGF-I and VEGF. Biochem Biophys Res Commun *363:* 674–679.

Sarkanen, J.-R., M. Mannerström, H. Vuorenpää, J. Uotila, T. Ylikomi, T. Heinonen (2011) Intra-laboratory pre-validation of a human cell based in vitro angiogenesis assay for testing angiogenesis modulators. Front Pharmacol *1:* 147.

Schmidt, D., L.M. Asmis, B. Odermatt, J. Kelm, C. Breymann, M. Gossi, M. Genoni, G. Zund, S.P. Hoerstrup (2006) Engineered living blood vessels: functional endothelia generated from human umbilical cord-derived progenitors. Ann Thorac Surg *82:* 1465–1471.

Traktuev, D.O., S. Merfeld-Clauss, J. Li, M. Kolonin, W. Arap, R. Pasqualini, B.H. Johnstone, K.L. March (2008) A population of multipotent CD34-positive adipose stromal cells share pericyte and mesenchymal surface markers, reside in a periendothelial location, and stabilize endothelial networks. Circ Res *102:* 77–85.

Ucuzian, A.A., H.P. Greisler (2007) In vitro models of angiogenesis. World J Surg *31:* 654–663.

Verseijden, F., H. Jahr, S.J. Posthumus-van Sluijs, T.L. Ten Hagen, S.E. Hovius, A.L. Seynhaeve, J.W. van Neck, G.J. van Osch, S.O. Hofer (2009) Angiogenic capacity of human adipose-derived stromal cells during adipogenic differentiation: an in vitro study. Tissue Eng Part A *15:* 445–452.

Verseijden, F., S.J. Posthumus-van Sluijs, P. Pavljasevic, S.O. Hofer, G.J. van Osch, E. Farrell (2010) Adult human bone marrow- and adipose tissue-derived stromal cells support the formation of prevascular-like structures from endothelial cells in vitro. Tissue Eng Part A *16:* 101–114.

Wosnitza, M., K. Hemmrich, A. Groger, S. Graber, N. Pallua (2007) Plasticity of human adipose stem cells to perform adipogenic and endothelial differentiation. Differentiation *75:* 12–23.

Wu, Y., L. Chen, P.G. Scott, E.E. Tredget (2007) Mesenchymal stem cells enhance wound healing through differentiation and angiogenesis. Stem Cells *25:* 2648–2659.

Zanetta, L., S.G. Marcus, J. Vasile, M. Dobryansky, H. Cohen, K. Eng, P. Shamamian, P. Mignatti (2000) Expression of Von Willebrand factor, an endothelial cell marker, is up-regulated by angiogenesis factors: a potential method for objective assessment of tumor angiogenesis. Int J Cancer *85*: 281–288.

Zannettino, A.C., S. Paton, A. Kortesidis, F. Khor, S. Itescu, S. Gronthos (2007) Human mulipotential mesenchymal/stromal stem cells are derived from a discrete subpopulation of STRO-1^{bright}/CD34^{-}/CD45^{-}/glycophorin-A-bone marrow cells. Haematologica *92:* 1707–1708.

Zuk, P.A., M. Zhu, H. Mizuno, J. Huang, J.W. Futrell, A.J. Katz, P. Benhaim, H.P. Lorenz, M.H. Hedrick (2001) Multilineage cells from human adipose tissue: implications for cell-based therapies. Tissue Eng *7:* 211–228.

Research Article

Human Vascular Model with Defined Stimulation Medium – A Characterization Study

*Outi Huttala [*1], Hanna Vuorenpää [*1], Tarja Toimela [1], Jukka Uotila [2], Hannu Kuokkanen [3], Timo Ylikomi [1,4], Jertta-Riina Sarkanen [1,4] and Tuula Heinonen [1]*

[1]FICAM, Finnish Centre for Alternative Methods, School of Medicine, University of Tampere, Tampere, Finland; [2]Department of Obstetrics and Gynecology, Tampere University Hospital, Tampere, Finland; [3]Department of Plastic Surgery, Tampere University Hospital, Tampere, Finland; [4]Department of Cell Biology, School of Medicine, University of Tampere, Tampere, Finland

Summary

The formation of blood vessels is a vital process in embryonic development and in normal physiology. Current vascular modelling is mainly based on animal biology leading to species-to-species variation when extrapolating the results to humans. Although there are a few human cell based vascular models available, these assays are insufficiently characterized in terms of culture conditions and developmental stage of vascular structures. Therefore, well characterized vascular models with human relevance are needed for basic research, embryotoxicity testing, development of therapeutic strategies and for tissue engineering.

We have previously shown that the *in vitro* vascular model based on co-culture of human adipose stromal cells (hASC) and human umbilical vein endothelial cells (HUVEC) is able to induce an extensive vascular-like network with high reproducibility. In this work we developed a defined serum-free vascular stimulation medium (VSM) and performed further characterization in terms of cell identity, maturation and structure to obtain a thoroughly characterized *in vitro* vascular model to replace or reduce corresponding animal experiments.

The results showed that the novel vascular stimulation medium induced an intact and evenly distributed vascular-like network with morphology of mature vessels. Electron microscopic analysis assured the three-dimensional microstructure of the network containing lumen. Additionally, elevated expression levels of the main human angiogenesis-related genes were detected.

In conclusion, with the newly defined medium the vascular model can be utilized as a characterized test system for chemical testing as well as in creating vascularized tissue models.

Keywords: serum-free media, angiogenesis, mesenchymal stromal cells, coculture techniques

1 Introduction[#]

The formation of the blood vessel network is a vital process in growth and organ development (Carmeliet and Jain, 2011; Carmeliet, 2005). In the embryo, endothelial precursor cells form new vessels that differentiate into a primitive vascular network (vasculogenesis) (Carmeliet and Jain, 2011). Subsequent vessel sprouting (angiogenesis) creates a network of arteries and veins as well as capillaries that facilitate the exchange of gases and metabolites (Carmeliet and Jain, 2011; Adams and Alitalo, 2007). To reach this level of complex organization, the immature vascular network must mature at the level of the vessel wall

*Authors contributed equally to this work.

[#]Abbreviations

AA, ascorbic acid; APC, allophycocyanin; BSA, bovine serum albumin; CD144, vascular endothelial cadherin; EGF, epidermal growth factor; EGM-2, endothelial cell growth medium-2; FBS, fetal bovine serum; FITC, fluorescein isothiocyanate; FGF-2, basic fibroblast growth factor; hASC, human adipose stromal cells; HE, heparin sodium salt; HS, human serum; HUVEC, human umbilical vein endothelial cells; HY, hydrocortisone (cortisol); IGF-I, insulin-like growth factor I; PBS, phosphate buffered saline; RT, room temperature; PDGFRβ, platelet derived growth factor beta; PE, phycoerythrin; PE-CY7, phycoerythrin-cyanine; SFM, basal serum-free medium; αSMA, alpha smooth muscle actin; TRITC, tetramethyl rhodamine isothiocyanate; VEGF, vascular endothelial growth factor; VSM, vascular stimulation medium; vWf, von Willebrand factor

Received November 27, 2014;
Accepted February 25, 2015;
Epub March 2, 2015;
http://dx.doi.org/10.14573/altex.1411271

morphology and as a whole network. Morphological maturation involves recruitment of mural cells, deposition of extracellular matrix and organ-specific specialization of cells, such as inter-endothelial junctions and surface receptors. Maturation of the network involves branching and expanding the network to meet local, tissue-specific demands (Jain, 2003).

Since the formation and maintenance of the vascular network is a complex process, problems related to its regulation are common (Ucuzian and Greisler, 2007). Inadequate vessel maintenance or growth causes ischemia in myocardial infarction and neurodegenerative or obesity-associated disorders, whereas excessive vascular growth or abnormal remodeling promotes cancer, inflammatory disorders and eye diseases (Potente et al., 2011). Moreover, genetic studies have shown that perturbing embryonic vascular development can have adverse consequences from benign vascular malformation to embryolethality and congenital defects (Knudsen and Kleinstreuer, 2011).

Angiogenesis models are important tools for studying the mechanisms of angiogenesis and the therapeutic strategies to modulate neovascularization (Ucuzian and Greisler, 2007). Due to an increasing amount of compounds affecting the vascular system, accurate vasculogenesis and angiogenesis models are needed for chemical safety testing and for drug development (Sarkanen et al., 2011; Bishop et al., 1999). Currently, preclinical animal models are dominantly used for angiogenesis testing although they are not considered optimal in efficacy or relevance to humans. The most commonly used *in vivo* angiogenesis assays include the chick chorioallantoic membrane (CAM) assay, Matrigel plug assay, zebrafish embryo system, corneal micropocket assay, rat/mouse hind limb ischemia model and rat aortic ring assay (Norrby, 2006; Auerbach et al., 2003). Despite the advantage of providing more information on complex cellular interactions compared to *in vitro* models, animal models are burdened by several disadvantages, such as variability, animal-specificity and ethical concerns (Norrby, 2006). Human cell based models have the potential to be valuable tools in predicting effects in man. However, the human relevance of these *in vitro* models needs to be confirmed in terms of cell identity, physiological architecture and functionality (Bale et al., 2014; Hartung, 2011). In addition, the developmental stage of the model system and a defined medium composition are critical, especially when toxicological applications are considered. Serum-free medium with xeno-free and defined supplements is considered essential for *in vitro* models to decrease the variation between experiments due to unknown components in the medium, and further, unknown binding properties of these components (Shen et al., 2013; Brunner et al., 2010; van der Valk et al., 2010). Currently, culture media are still commonly supplemented with serum, although it has a highly uncharacterized composition, including various cytokines and growth factors, as well as a lot-to-lot variability (Lindroos et al., 2011; Brunner et al., 2010).

We and others have shown that adipose stromal cells and umbilical vein endothelial cells are capable of self-assembling into a dense, three-dimensional vascular-like network (Sarkanen et al., 2012; Merfeld-Clauss et al., 2010; Verseijden et al., 2010). While adipose stromal cells secrete factors that induce endothelial cell (EC) sprouting and lumen formation (Rubina et al., 2009; Traktuev et al., 2008; Rehman et al., 2004; Kilroy et al., 2007; Bishop et al., 1999), the supporting stromal cells also enhance vascular basement membrane and lumen formation (Merfeld-Clauss et al., 2010; Newman et al., 2013; Stratman et al., 2009).

The aim of this study was to develop a defined medium and further characterize the *in vitro* vascular model developed by us, which is composed of human adipose stromal cells (hASC) and human umbilical vein endothelial cells (HUVEC) (Sarkanen et al., 2012). Our results showed that the new vascular stimulation media (VSM) developed in this study produces an extensive vascular-like network with mature properties and provides a valid alternative to commercial EGM-2 medium when comparing vascular-like network formation capacity. This vascular model has the potential to be used in the safety and efficacy assessment of angiogenic compounds. In addition, the vascular-like network combined with target cells, such as cardiomyocytes (Vuorenpää et al., 2014), can be used as a tissue engineering platform to create vascularized tissue models.

2 Materials and methods

This study conforms to the principles outlined in the Declaration of Helsinki. The human adipose tissue samples were obtained from surgical operations and human umbilical cords were received from caesarean sections with individual written informed consent at Tampere University Hospital, Tampere, Finland. The use of hASC and HUVEC were approved by the Ethics Committee of the Pirkanmaa Hospital District, Tampere, Finland with permit numbers R03058 and R08028, respectively.

Isolation and culture of human adipose stromal cells

hASC were isolated from human adipose tissue by using a mechanical and enzymatic procedure described previously (Sarkanen et al., 2012). Briefly, human adipose tissue specimens were mechanically cut into small pieces and enzymatically digested with 0.15% collagenase I (Invitrogen, Paisley, Scotland, UK) in Dulbecco's Modified Eagle's Medium Nutrient Mixture F-12 (DMEM/F12, Gibco, Invitrogen, Carlsbad, CA, USA). hASC were cultured in DMEM/F12 supplemented with 10% human serum (HS, Lonza Group Ltd, Basel, Switzerland) and 1% L-Glutamine (Gibco). The cells were tested for mycoplasma contamination (MycoAlert® Mycoplasma Detection Kit, Lonza Group Ltd) before experimental use.

Isolation and culture of human umbilical vein endothelial cells

HUVEC were isolated from human umbilical cord veins using 0.05% collagenase I as described previously (Sarkanen et al., 2011). The cells were cultured in EGM™-2 Endothelial Cell Growth Medium-2 (EGM-2, Lonza Group Ltd). Before use the cells were tested for mycoplasma contamination (MycoAlert® Mycoplasma Detection Kit, Lonza).

Establishment of the co-culture forming the vascular-like network

Co-culture of hASC and HUVEC was established as described previously (Sarkanen et al., 2012). Briefly, hASC were seeded in

Tab. 1: Stimulation media tested in vascular model

Acronym	Basal medium	Serum	Growth factors	Supplementation
EGM-2	EBM-2	2% FBS	VEGF, FGF-2, IGF-I, epidermal growth factor	hydrocortisone, ascorbic acid, heparin, GA-1000
EGM-2/HS	EBM-2	2% HS	VEGF, FGF-2, IGF-I, epidermal growth factor	hydrocortisone, ascorbic acid, heparin, GA-1000
basal SFM	DMEM/F12	–		ITS, BSA, NaP, L-glutamine, T3,
VSM	DMEM/F12	–	VEGF, FGF-2	ITS, BSA, NaP, L-glutamine, T3, hydrocortisone, ascorbic acid, heparin sodium salt

0.1% ITS (insulin-transferrin-sodium selenite media supplement), 1.28 mM L-glutamine, 1% BSA (bovine serum albumin), 2.8 mM NaP (sodium pyruvate), 100 IU/ml P/0.1 mg/ml S, 0.1 nM T3 (3,3',5-triiodo-L-thyronine sodium salt), HS (human serum), FBS (fetal bovine serum), VEGF (vascular endothelial growth factor A), FGF-2 (fibroblast growth factor 2), IGF-I (insulin-like growth factor I), GA-1000 (30 μg/ml gentamicin and 15 ng/ml amphotericin), VSM (vascular stimulation medium), SFM (serum free medium)

EGM-2 (Lonza) at 20,000 cells/cm^2. After 1-3 h HUVEC were seeded on top of hASC at 4,000 cells/cm^2. The hASC were used at passage 2 and HUVEC at passage 4 in the co-culture (passage number increased at seeding). The day after plating, the stimulation media were applied to the co-culture (see Tab. 1): 1) EGM-2 containing epidermal growth factor, vascular endothelial growth factor A (VEGF), fibroblast growth factor 2 (FGF-2), insulin-like growth factor I (IGF-I), ascorbic acid (AA), heparin, hydrocortisone (HY), antibiotic mix: 30 μg/ml gentamicin and 15 ng/ml amphotericin and 2% fetal bovine serum (FBS); 2) EGM-2/HS, where 2% FBS was replaced with 2% HS; 3) serum free basal medium (SFM); 4) Vascular stimulation medium (VSM).

In this first media comparison study, the AA, HY and heparin in VSM were taken from the EGM-2 kit and used according to the manufacturer's protocol (concentrations of these are not publicly available). After that, concentrations of AA, heparin sodium salt from bovine intestinal mucosa (HE) and HY purchased from Sigma were optimized for VSM. In the concentration optimization study the tested concentrations of AA were 0, 50, 100, 200, 500, 1000 and 2000 μg/ml; of HY 0, 20, 200, 1000, and 2000 ng/ml and of HE 0, 50, 500, 10,000 and 50,000 ng/ml. The concentrations of 10 ng/ml VEGF and 1 ng/ml FGF-2, used for VSM, had been optimized in our previous study (Sarkanen et al., 2012). The co-cultures were grown for 6 days prior to immunocytochemistry or quantitative real-time PCR (qPCR) processing. Stimulation medium was changed once during the 6 day culture.

Quantitative real-time PCR

Genes activated in co-culture of hASC and HUVEC in EGM-2 medium versus co-culture in VSM were analyzed by qPCR. Total RNA was extracted at day 6 using the RNAeasy minikit (Qiagen) following the manufacturer's protocol. A step to eliminate genomic DNA contamination was included in the isolation and performed with RNase-free DNase set (Qiagen). Reverse transcription of total RNA to cDNA was performed using RT^2 First Strand Kit (Qiagen) following the manufacturer's instructions.

Human Angiogenesis RT^2 *Profiler™* PCR Array (Qiagen, Valencia, California, USA) was used to profile the expression of 84 key angiogenesis-related genes (the comprehensive list of genes included in the array can be found in http://www.sabiosciences.com). The array was performed according to the manufacturer's protocol using BioRad CFX96 Real Time System (BioRad Laboratories, USA). The array contained five housekeeping genes and controls, including genomic DNA control, Reverse Transcription Control and Positive PCR controls. The co-culture of hASC and HUVEC grown in EGM-2 medium was used as a control. Three independent experiments with the array were performed using the same cells.

Immunocytochemistry

To analyze the vascular-like network formation and different cell types present in hASC and HUVEC co-culture, immunocytochemical staining was performed. In primary antibody staining, endothelial cell specific antibody for rabbit anti-human von Willebrand factor IgG (anti-VWF, 1:100, F3520, Sigma) with common pericytic marker α-human smooth muscle actin (monoclonal anti-SMA clone 1A4, 1:200, M0851, DAKO), vascular smooth muscle cell marker smooth muscle myosin heavy chain (anti-SMMHC, clone hSM-V, 1:800, M7786, Sigma), contractile smooth muscle cell marker calponin (anti-calponin, clone hCP, 1:800, C2687, Sigma), pericytic and smooth muscle cell progenitor marker platelet derived growth factor receptor-β (anti-PDGFRβ, clone PDGFR-B2, 1:800, P7679, Sigma), vascular endothelial cadherin (CD144,Clone 55-7H1, 1:50, 555661, BD Pharmingen), monoclonal occludin (clone 1G7, 1:300, WH0004950M1, Sigma) or basement membrane marker collagen IV (anti-COLIV, clone COL-94, 1:500, C1926, Sigma), all anti-human and all produced in mouse, except vWf, were used. Co-culture was fixed with 70% ethanol at day 6. After fixation, the cells were permeabilized with 0.5% Triton-X100 (MP Biochemicals, Ohio, USA) and non-specific binding sites were blocked with 10% bovine serum albumin (BSA, Roche Diagnostics Corporation, Indianapolis, USA). Primary antibody in 1% BSA was applied to the cells. Secondary antibodies used were polyclonal goat anti-rabbit IgG tetramethylrhodamine (TRITC, 1:50, T6778 Sigma), anti-rabbit IgG A568 (1: 400, A11011, Invitrogen) and anti-mouse IgG fluorescein isothiocyanate (FITC, 1:100, F4143, Sigma). After immunocytochemical staining the

vascular-like network was analyzed and photographed with Nikon Eclipse TS100 inverted fluorescence microscope (Nikon, Tokyo, Japan) and Nikon digital sight DS-U2 camera (Nikon). Images were further processed with NIS Elements (Nikon, Tokyo, Japan) and Adobe Photoshop CS3-software (Adobe Systems Incorporated, San Jose, CA, United States).

Flow cytometric surface marker expression analysis of HUVEC and hASC

hASC were cultured in hASC medium (passage 1) for 6-7 days and HUVEC were cultured in EGM-2 medium (passage 3) for 3 days prior to surface marker expression analysis using a BD FACSCanto II flow cytometer (BD Biosciences, Erembodegem, Belgium). For the flow cytometry analysis cells were divided into 5 ml polystyrene round bottom FACS tubes (BD, New Jersey, USA) at 250,000 cells per tube. The cells were washed once with warm staining buffer (1% BSA in PBS) and centrifuged at 131 x g for 5 min, after which they were stained either for surface markers or for intracellular markers.

Fixation and permeabilization were only performed for staining of intracellular markers. The fixation was conducted by incubating the samples for 30 min in 2% paraformaldehyde in PBS at room temperature (RT). The cells were then centrifuged at 500 x g for 5 min. Permeabilization of the cells was performed by 10 min incubation in 0.1% Triton-X100 in PBS at RT after which the cells were centrifuged at 500 x g for 5 min and washed once or twice with staining buffer before addition of antibodies.

The labelled mouse anti-human antibodies used were intracellular vWf-A2-allophycocyanin IgG2b (APC, #IC27641A) and eNOS- phycoerythrin IgG1 (PE, #560103), and surface markers CD144-FITC IgG1 (#560411), CD73-Phycoerythrin-Cyanine IgG1 (PE-CY7, #561258), CD309-PE IgG1 (#560872), CD68-FITC IgG2b (#562117), NG2-PE IgG1 (#FAB2585P), CD90-FITC IgG1 (#561969), CD105-V450 IgG1 (#561447), CD34-APC IgG1 (#561209), CD140b-PE IgG2a (#558821), CD31-V450 IgG1 (#561653), CD45-PE IgG1 (#560975), CD14-FITC IgG1 (#561712). Isotype controls mouse IgG2b-APC (#IC0041A), Mouse IgG1-PE-CY7 (#557872), mouse IgG1-PE (#559320), mouse IgG1-FITC (#555748), mouse IgG2b-FITC (#556655), mouse IgG1-V450-(#642268), mouse IgG1-APC (#550854), mouse IgG2a-PE (#551438). All antibodies and their corresponding isotype controls used in the flow cytometry analysis were purchased from BD except NG2, vWf and IgG2b-APC, which were purchased from R&D Systems.

Labelled antibodies were added into cell suspension in cold staining buffer and incubated on ice for 30 min in the dark. After incubation the cells were washed once with staining buffer and twice with PBS. Surface marker stained cells were centrifuged at 200 x g for 5 min and intracellular marker stained cells were centrifuged for 5 min at 500 x g.

Flow cytometry analysis was performed with cells suspended in ice cold PBS and 5,000 events were analyzed per sample. Compensation was done with compensation particles, i.e., BD™ CompBeads (BD) according to the manufacturer's instructions. The results were analyzed with BD FACSDiva™ Software (BD). The positive expression was obtained by gating 98% of the events isotype control results and then inverting the gate to obtain a percentage of positively stained cells in the samples. The results were calculated as percentages with SD.

Electron microscopy

hASC and HUVEC co-culture was performed in 24-well UpCell plates (ThermoFisher) for transmission electron microscopy (TEM) and on glass cover slips coated with 0.1% gelatin for scanning electron microscopy (SEM). Co-culture was maintained for 6 days and washed twice with PBS prior to fixation.

SEM specimens were fixed in 2% glutaraldehyde in 0.1 M phosphate buffer after which the SEM samples were dehydrated in alcohol and dried in Baltec critical point dryer (Baltec, CPD030, Balzers, Liechtenstein). A layer of platinum was sputtered onto the specimens with a sputter coater (Agar Scientific, Stansted, England). Specimens were examined in a Zeiss Ultra Plus scanning electron microscope, (Carl Zeiss MT – Nanotechnology System Division, Carl Zeiss NTS GmbH, Oberkochen, Germany) using 5 kV as an accelerating voltage.

TEM specimens were detached from the temperature sensitive 24-well UpCell plate and transferred to fixative with 1% glutaraldehyde, 4% formaldehyde mixture in 0.1 M phosphate buffer for 10 min. The cell sheet was immersed in 2% agarose in distilled water and postfixed in 1% osmiumtetroxide, dehydrated in acetone and embedded in Epon LX 112 (Ladd Research Industries, Vermont, USA). Thin sections were cut with Leica Ultracut UCT ultramicrotome, stained in uranyl acetate and lead citrate and examined in a Philips CM100 transmission electron microscope. Images were captured by a Morada CCD camera (Olympus Soft Imaging Solutions GMBH, Munster Germany).

Quantitative analysis of vascular-like network formation

Vascular-like networks, i.e., vWf-positive tubule structures formed in different stimulation media, were imaged using CellIQ (Chipman tech., Tampere, Finland) with 10x objective and 5x5 grid. The quantitation of the area of the vascular-like network was performed using ImageJ software (National institutes of health, NIH, Maryland, USA) for the image analysis. Images were first converted to 8-bit gray scale, then background was subtracted and finally the binary threshold function was adjusted to obtain the best contrast of the vascular-like network against the background. With these settings, the total area of vascular-like network was calculated as the total number of pixels in images with set threshold.

Statistical analysis

Statistical analyses were performed and graphs processed with GraphPad Prism 5.0 (GraphPad Software, Inc., San Diego, CA, USA). The results concerning vascular-like network formation were subjected to one-way ANOVA followed by Dunnett's post-test when applicable. The results were reported as total area ± SD and differences were considered significant when $p < 0.05$*, $p < 0.01$** and $p < 0.001$***.

PCR results were analyzed with the PCR Array Data Analysis Web Portal (http://www.SABiosciences.com/pcrarraydataanalysis.php). The following formula was used to calculate the relative amount of the transcripts of the co-culture of hASC and

Tab. 2: Phenotypic characterization of human adipose stromal cells (hASC p1) and human umbilical vein endothelial cells (HUVEC p3)
The expression of surface and intracellular markers was analysed by flow cytometry (5000 events per sample). Results are shown as percentage of positive cells.

Cells	Protein	Antigen	Positive cells %	SD	*n*
hASC	vWf	von Willebrand factor	7.5	4.3	11
	CD144	vascular endothelial cadherin	1.4	2.9	9
	eNOS	endothelial nitric oxide synthase	0.7	1.1	8
	CD140b	PDGF Receptor b	52.8	16.0	6
	CD45	leukocyte common antigen	16.4	14.9	6
	CD14	expressed on monocytes/macrophages	0.7	0.8	7
	CD68	expressed on macrophages and monocytes	1.1	1.4	8
	CD309	VEGF receptor 2	1.2	3.5	6
	CD31	platelet endothelial cell adhesion molecule	0.9	3.1	6
	NG2	chondroitin proteoglycan	31.8	29.1	8
	CD90	Thy-1	82.9	15.5	10
	CD105	endoglin	64.1	27.1	7
	CD73	ecto-5'-nucleotidase	88.8	6.7	12
	CD34	sialomucin-like adhesion molecule	40.9	34.3	10
HUVEC	vWf	von Willebrand Factor	45.6	13.2	13
	CD144	vascular endothelial cadherin	70.6	14.7	17
	CD309	VEGF receptor2	31.4	17.0	10
	CD73	ecto-5'-nucleotidase	68.7	17.1	14
	CD68	expressed on macrophages and monocytes	1.9	10.1	11
	eNOS	endothelial nitric oxide synthase	48.4	18.4	13
	CD105	endoglin	57.4	26.6	9
	CD34	sialomucin-like adhesion molecule	43.1	18.6	9
	CD31	platelet endothelial cell adhesion molecule	81.3	13.7	8
	CD140b	PDGF Receptor b	7.2	8.7	8
	NG2	chondroitin proteoglycan	2.0	1.1	7

HUVEC in the VSM compared to transcripts of the co-culture in EGM-2 medium: $\Delta\Delta CT = \Delta CT$ (VSM) – ΔCT (EGM-2). A two-fold change compared to housekeeping gene *GAPDH* was considered significant.

3 Results

3.1 Phenotypic characterization

Phenotypic characterization of the cells used in the vascular model was performed by analyzing the surface and intracellular markers of hASC and HUVEC separately (Tab. 2). The mesenchymal stem cell markers CD73, CD90 and CD105 were highly expressed (> 64%) in hASC. Also, pericyte marker PDGFR-β (CD140b) was strongly expressed (> 52%) in the hASC population. Hematopoietic marker CD34 was moderately expressed (< 40%), whereas the expression levels of endothelial markers CD144 and CD31 and macrophage/monocyte markers CD68 and CD14 were very low (< 1.4%).

HUVEC were shown to express endothelial marker CD31 and a specialized vascular endothelial marker CD144 at a high level (> 70%). Angiogenic endothelial marker CD105 and cell surface enzyme CD73 were found in the HUVEC population (57-68%). Markers for macrophages/monocytes (CD68) and mural cells (NG2) were low (≤ 2%).

3.2 VSM induced optimal vascular-like network formation

Of the different stimulation media (Tab. 1), VSM induced an optimal vascular-like network formation (Fig. 1). The imaging analysis showed morphological differences in the vascular-like network in VSM compared to EGM-2 medium. VSM produced a uniformly distributed vascular-like network with connected branches and fewer cell aggregates. Low serum (2%) and se-

rum-free medium enabled stable cell attachment and induced a dense, connected vascular-like network with intact tubule walls. Human serum was found to induce a denser and more connected vascular-like network than FBS (Fig. 1).

In the supplement optimization several different concentrations of ascorbic acid, heparin sodium salt and hydrocortisone were tested and compared to vascular-like network formed in EGM-2 medium. An optimal vascular-like network formation was obtained with the AA concentration 100 μg/ml (Fig. 2A), HE concentration 0-500 ng/ml (Fig. 2B) and HY concentration 0.2 μg/ml (Fig. 2C). The results showed that a vascular-like network was formed in the absence of HE supplement with minor morphological differences. However, low concentrations of HE (50-500 ng/ml) increased the total area of the vascular-like network significantly compared to EGM-2 medium (Fig. 2B).

3.3 Expression of angiogenesis-related genes in VSM compared to EMG-2

Expression of 84 angiogenesis-related genes was analyzed from a vascular-like network formed in co-culture of hASC and HUVEC in EGM-2 medium (control) and in VSM. Moderate differences in the expression of angiogenesis-related genes were detected between EGM-2 and VSM. In VSM, nine genes were up-regulated (*Angpt1, F3, FIGF, IGF-I, LEP, MDK, MMP2, MMP9, PGF*) and nine (*CCL11, CXCL9, FN1, IL6, IL8, SERPINE1, TGFB2, THBS2, TIMP1*) were down-regulated in comparison to EGM-2 medium. Fold changes and statistical significances of the up- and down-regulated angiogenesis-related genes are shown in Table 3.

3.4 Maturation stage, extracellular matrix production and 3D properties of the vascular-like network formed in VSM

Immunocytochemical staining of the vascular-like network formed in VSM showed the presence of platelet derived growth factor receptor-β (PDGFRβ) positive cells (Fig. 3D). Also, smooth muscle actin (SMA), smooth muscle myosin heavy chain (SMMHC) and contractile smooth muscle calponin positive cells surrounded the tubule structures (Fig. 3A-C). CD144 and occludin positive staining indicated the presence of adherence junctions between endothelial cells (Fig. 3E-F).

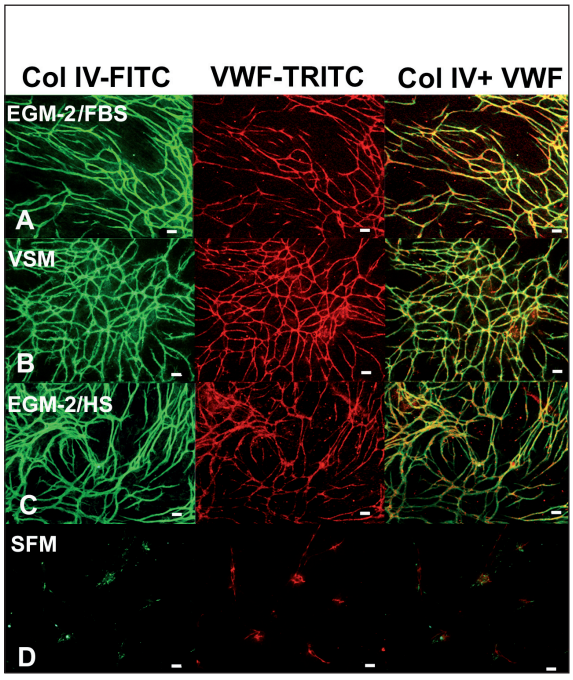

Fig. 1: Morphology of vascular-like network in different stimulation media with different serum concentrations

Vascular-like networks were stained against Col IV (FITC, green) and vWf (TRITC, red). Co-localization is shown in the merged image. Vascular-like network formed in (A) commercial EGM-2 medium with 2% FBS, (B) serum-free VSM, (C) EGM-2 with 2% HS and (D) basal SFM. Scale bars 100 μm in each figure. Col IV= collagen type IV, VWF= von Willebrand factor, VSM= vascular stimulation medium, FBS= fetal bovine serum, HS= human serum, SFM=basal serum free medium.

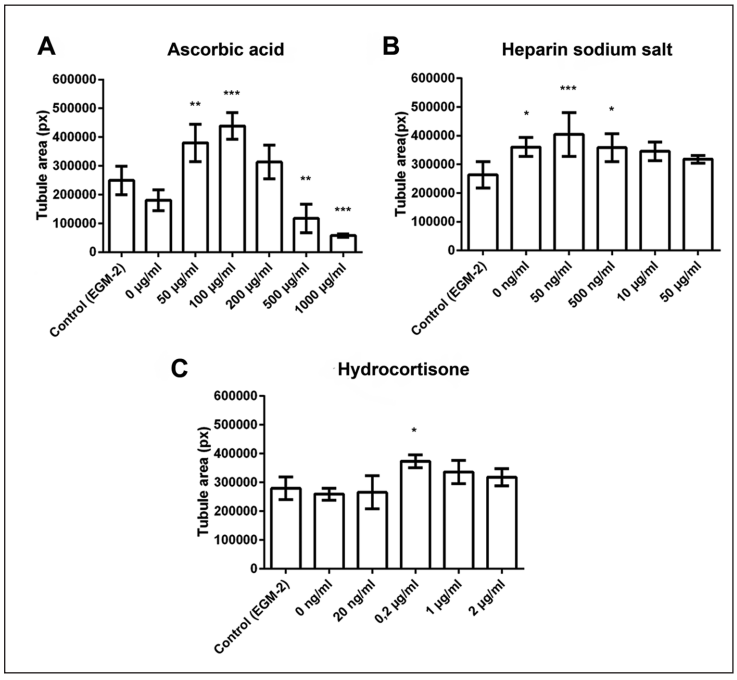

Fig. 2: Vascular-like network formation (area in pixels) in different concentrations of (A) ascorbic acid, (B) heparin sodium salt and (C) hydrocortisone in VSM

Vascular-like network formed in VSM supplemented with different concentrations of ascorbic acid, heparin sodium salt or hydrocortisone were compared to EGM-2 medium and differences presented as follows: $p < 0.05$*, $p < 0.01$** and $p < 0.001$***. An optimal vascular-like network formation was obtained with 100 μg/ml ascorbic acid and 0.2 μg/ml hydrocortisone. Heparin sodium salt could be used in concentrations 0-500ng/ml. Results are depicted as total area with standard deviations, n = 5 in each supplement and concentration.

Tab. 3: Fold changes and statistical significance of expression of angiogenesis-related genes in vascular-like network formed in VSM compared to EGM-2 medium

Genes	Target	Fold change 2^(- ΔΔCT)	Statistical significance
Up-regulated genes			
ANGPT1	angiopoietin 1	2.964	*
F3	coagulation factor III	3.255	*
FIGF	vascular endothelial growth factor D	3.043	ns
IGF-I	insulin-like growth factor I	16.555	ns
LEP	leptin	2.932	ns
MDK	neurite growth-promoting factor 2	2.06	ns
MMP2	matrix metallopeptidase 2	2.011	*
MMP9	matrix metallopeptidase 9	3.919	*
PGF	placental growth factor	2.319	*
ANGPT2	angiopoietin 2	1.769	**
Down-regulated genes			
CCL11	chemokine ligand 11	2.613	ns
CXCL9	chemokine ligand 9	2.197	ns
FN1	fibronectin 1	2.295	*
IL6	interleukin 6	2.331	ns
IL8	interleukin 8	2.546	ns
SERPINE1	serpin peptidase inhibitor	3.465	**
TGFB2	transforming growth factor beta 2	2.080	ns
THBS2	thrombospondin 2	2.085	**
TIMP1	TIMP metallopeptidase inhibitor 1	5.01	**
VEFG-A	vascular endothelial growth factor A	1.804	ns
TGFβ1	transforming growth factor beta 1	1.807	*
FGF-2	fibroblast growth factor 2	1.917	ns

Electron microscopic analysis confirmed the microstructure of the tubules formed in VSM. Tubules were shown to have a lumen, basement membrane and junctions (Fig. 4A-C). The three dimensional structure of the vascular-like network and shape of the tubules can be seen in the close-up image Figure 4D.

4 Discussion

Present chemical safety testing and non-clinical drug development rely mainly on animal biology although relevant safety testing data should be of human origin. Further, *in vitro* test systems should be thoroughly characterized in their human relevance and functionality. In this study, we developed a novel vascular stimulation medium (VSM) and further characterized the *in vitro* human vascular model developed by us (Sarkanen et al., 2012). This defined *in vitro* vascular model has the potential to be used for safety assessment of compounds and for tissue engineering applications.

The phenotypic analysis of the building blocks of the vascular model, i.e., the hASC and HUVEC, was performed using flow cytometry. HUVEC showed a strong expression of CD105 (endoglin), suggesting an active rather than quiescent state of the cells (Bernabeu et al., 2009). Interestingly, a recent study reported a minor role of endoglin in vasculogenesis whereas VEGF-induced angiogenesis was severely impaired in an *endoglin* deficient mouse embryonic stem cell model (Liu et al., 2014). The high expression of CD144 and CD31 supports the active status of HUVEC in the formation of intercellular junctions. The level of CD73, a 5'-ectonucleotidase that normally suppresses pro-inflammatory responses in human endothelial cells (Grunewald and Ridley, 2010) was high in our HUVEC analysis. Pericyte markers NG2 and CD140b (PDGFRβ) were low, indicating the absence of mural cells in the HUVEC population.

This study confirms the earlier results shown by us (Sarkanen et al., 2012) and others (Lindroos et al., 2010; Traktuev et al., 2008) that the stromal-vascular fraction extracted from adipose tissue is heterogenic. hASC expressed mesenchymal stem cell markers CD90, CD105 and CD73 at high levels, showing the

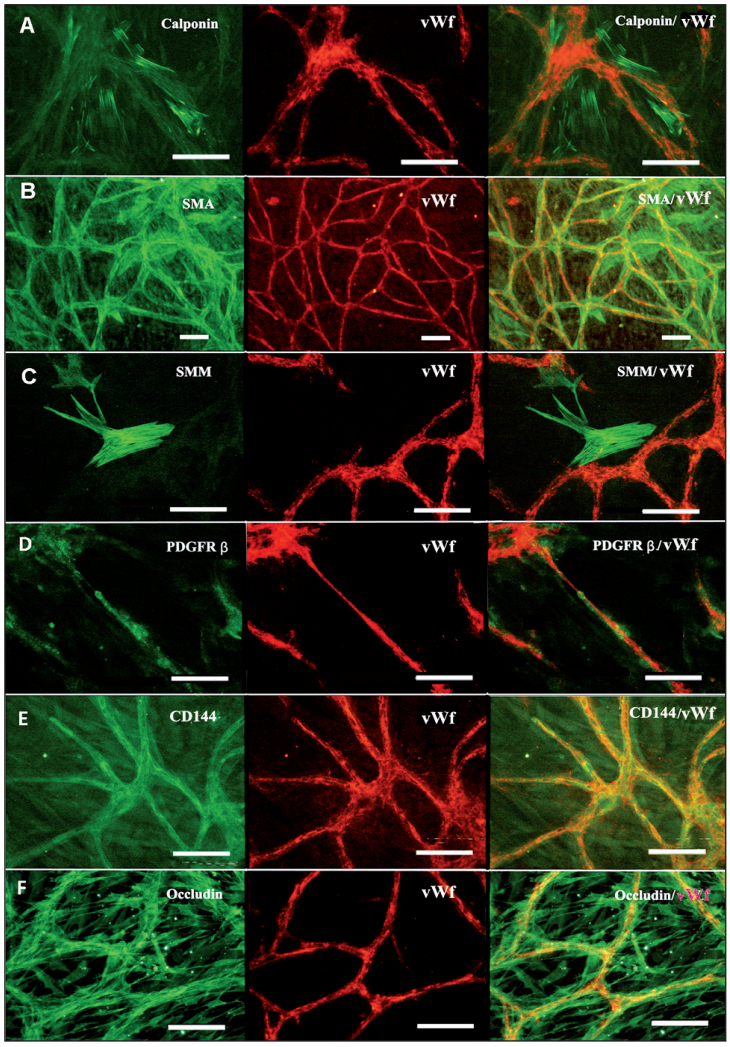

Fig. 3: Vascular-like network formed in serum-free VSM shows vascular maturation markers at day 6

α-vWf-staining is shown in red in all figures. (A) Calponin-, (B) SMA- and (C) SMM-positive cells surrounding the vascular-like network. (D) α-PDGFRβ stained pericytes are located along the tubules. (E) CD144- and (F) occludin-positive junctions can be found in the tubule structures. Scale bar 100 µm in each image. VSM= vascular stimulation medium, vWf = von Willebrand factor, SMA = smooth muscle actin, SMM = smooth muscle myosin heavy chain, PDGFRβ = platelet derived growth factor receptor β, CD144 = vascular endothelial cadherin.

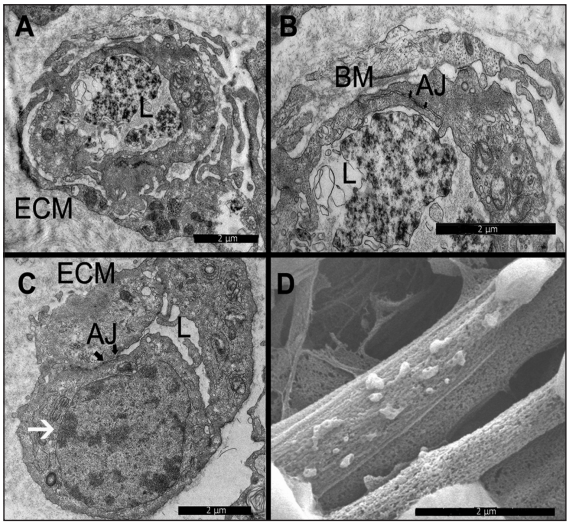

Fig. 4: Transmission (A, B, C) and scanning (D) electron microscopy images of the vascular-like network cultured in VSM

(A) Mature tubule with lumen = L and extracellular matrix = ECM. The lumen is filled with debris from the apoptotic cells. Scale bar 2 *µ*m. (B) Close-up image with basement membrane = BM, adherence junction = AJ and lumen of the vascular-like tubules. Scale bar 2 *µ*m. (C) Tubule in earlier stage of vascular development showing endothelial cell with large nucleus (white arrow), lumen, adherence junctions and ECM. Scale bar 2 *µ*m. D) Scanning electron microscopy image shows the 3D structure and the tubule shape of the vascular-like network. Scale bar 2 *µ*m. VSM = vascular stimulation medium.

presence of a cell population with multilineage differentiation potential. Pericyte markers CD140b (PDGFRβ) and NG2 were expressed at high to moderate level, supporting the finding that pericytes from the hASC population are lining the vascular-like network in our model.

We also analyzed whether the population of endothelial progenitor cells capable of vasculogenesis could be found in hASC as suggested by some earlier reports (Sarkanen et al., 2012; Miranville et al., 2004; Heydarkhan-Hagvall et al., 2008). The results showed that, in addition to the high expression of CD90, there is a moderate expression of CD34; these are markers for mesenchymal stem cells and endothelial progenitors. A hASC population of CD90+/CD34+ cells was shown to be capable of differentiating into endothelial cells and form capillary-like structures (De Francesco et al., 2009).

The expression of mature endothelial cell markers CD31 and CD144 in the hASC population was very low. Interestingly, there is a report suggesting that adipose stromal cells may enhance endothelial differentiation of progenitor cells (Rubina et al., 2009). However, another essential marker for endothelial progenitor cells, CD309 (VEGFR2) (Yoder, 2012), showed very low expression in the six hASC lines that were analyzed in this study. Therefore, the presence of an endothelial progenitor cell population in the stromal-vascular fraction needs to be studied further.

Serum-free VSM was shown to produce a reproducible, extensive mature vascular-like network and provide a suitable alternative to the commercial EGM-2 medium (previously used in the model, containing 2% FBS). Serum had a strong correlation with vascular-like network formation. At higher serum (10%) concentrations the network was shorter with broken tubule walls, and random detachment of the cell layer occurred (data not shown). In low- or serum free (0-2%) environment,

network formation increased, tubules were highly branched and tubule walls remained intact. In serum-free conditions we detected thinner and more branched tubules as also reported by Yang and Xiong (Yang and Xiong, 2012). Serum-free medium is ideal for use in drug development, since serum is a complex mixture of components with unknown composition and protein binding affinities (Shen et al., 2013). Furthermore, a tissue construct aimed for clinical therapy should be cultured in human serum or, preferably, in a serum-free environment to avoid the risk of infection and severe immune reactions in the recipient (Patrikoski et al., 2013; Lindroos et al., 2011, 2010; Holm et al., 2010).

Fetal bovine serum (FBS), although being the most widely used growth supplement, holds ambiguous, unknown effects for cell culture and also raises ethical concerns due to the number of bovine fetuses needed for serum production (Gottipamula et al., 2013; Brunner et al., 2010). In this study, microscopical analysis showed that HS was more inductive for vascular-like network formation than FBS. Replacement of FBS with HS has been reported to support equal or higher proliferation rates and differentiation capacity of adipose stromal cells (Lindroos et al., 2011; Brunner et al., 2010). Furthermore, human mesenchymal stem cells have been shown to maintain their immunophenotype and multilineage potential in serum-free medium (Patrikoski et al., 2013; Mark et al., 2013).

In this study we developed a defined vascular stimulation medium since commercial media producing companies do not necessarily publish the specific composition of their media. This might complicate the use of commercial media in toxicological studies as medium components may interact with test compounds. In addition to commonly used VEGF and FGF-2 defined by us earlier (Sarkanen et al., 2011), we found that the network formation can be further improved by addition of AA, HE and HY. Ascorbic acid (vitamin C) is an essential nutrient for human endothelial cells necessary for their effective migration and for the synthesis of collagen type IV, an important component of basement membrane (Telang et al., 2007). In this study, the formation of basement membrane around the tubules was impaired in the absence of AA (data not shown). However, AA inhibited angiogenesis at high concentrations (1000-2000 μg/ml) as reported previously (Mikirova et al., 2008). Therefore, AA is essential for collagen IV formation in basement membrane at low concentrations.

Although HE is needed for the attachment of some growth factors to their cell surface receptors (Ashikari-Hada et al., 2005) and was found to be beneficial for the network formation, it did not induce a significant advantage to the morphology or branching of the tubules. Since HE is an animal derived substance it should rather be avoided where clinical applications are concerned. The lack of need for added HE can be explained by the secretion of perlecan by HUVEC (Murikipudi et al., 2013; Schlessinger et al., 2000). Our results correlate with earlier studies (Khorana et al., 2003; Jung et al., 2001) showing that HE inhibits vascular-like network formation at high concentrations.

Hydrocortisone, although not pro-angiogenic itself, has a beneficial effect on angiogenesis (Goding, 2009). In this study, hydrocortisone increased the number of branches in the vascular-like network. However, it produced cell aggregates at high concentrations whereas a lack of hydrocortisone induced a sparse vascular-like network. Our results suggest that hydrocortisone acts as a mitogen in the vascular model. Other supplements of the VSM included ITS (insulin, transferrin, selenic acid medium supplement), BSA, sodium pyruvate, L-glutamine and T3 (3,3',5-triiodo-L-thyronine). The concentrations of these supplements were reported earlier by us (Vuorenpää et al., 2014) and were used in this study with minor modifications.

Lumen formation is critical for the transformation of cords into a perfusable vascular system (Charpentier and Conlon, 2014). Electron microscopic analysis assured the formation of 3D vascular microstructure including lumen in the novel VSM. Tubules at different stages of lumen development were detected, indicating the ongoing process of network formation at day 6. The initiation of lumen development is triggered by apical-basal polarity of the endothelial cells in which CD144 plays a critical role in promoting the localization of polarity markers (Charpentier and Conlon, 2014). The electron microscopic analysis as well as immunocytochemistry results of this study showed that hASC and HUVEC co-culture actively produces extracellular matrix (ECM) components, including fibrillins, thus creating natural 3D scaffold around them. The reciprocal interaction between ECM stroma and vascular network is important in directing vessel growth (Hoying et al., 2014; Du et al., 2014). The hASC and HUVEC co-culture gives mechanical support for other target cells, e.g., cardiomyocytes, and, additionally, the microenvironment formed by the co-culture enhances target cell viability as reported previously (Vuorenpää et al., 2014). This 3D vascular model provides a more *in vivo*-like test system without an artificial scaffold that may interfere with the cell-cell interactions or affect the toxicological applications of the model.

In the genotypic analysis 84 human angiogenesis-related genes were studied. Nine genes were down-regulated and nine genes up-regulated in VSM compared to EGM-2 medium. The expression of *angiopoietin 1*, a marker for mature tubules, was significantly higher in VSM compared to EGM-2 medium, whereas *angiopoietin 2*, a marker for the early stage, i.e., sprouting angiogenesis, was slightly upregulated in VSM. *VEGF-A* and *FGF-2*, indicators of early stage angiogenesis, were moderately yet not significantly down-regulated in VSM compared to EGM-2. Since both media included VEGF and FGF-2, the expression of these growth factors was apparently unnecessary for the cells. On the contrary, *placental growth factor* (PGF) showed modest up-regulation in VSM. PGF and its receptor VEGFR-1 are minimally expressed in adult quiescent vasculature, but are markedly up-regulated during pathological conditions (Carmeliet et al., 2001). *TGFβ1*, a marker for tubule maturation, was slightly down-regulated in VSM. Vessel maturation relies partly on TGF-β signaling and TGF-β stimulates mural cell proliferation and migration and production of ECM (Potente et al., 2011). The gene expression analysis confirms the finding that VSM enhances the maturation of the vascular-like network.

Interestingly, the expression of *insulin like growth factor* (IGF-I) showed the highest up-regulation in VSM. IGF-I treatment in myocardial infarction has been shown to increase circulating angiogenic growth factors, thus providing protection

against myocardial ischemia in rats (Mathews et al., 2011). *In vitro* IGF-I stimulates migration and tube-forming activity of endothelial cells (Shigematsu et al., 1999; Nakao-Hayashi et al., 1992). Also leptin, a hormone secreted by adipocytes, was found to be up-regulated. Leptin signaling acts as a link between adipocytes and the vasculature (Sierra-Honigmann et al., 1998). It also increases the production of VEGF and enhances the expression of *MMP-2* and *MMP-9* (matrix metallopeptidases) in HUVEC (Park et al., 2001). This was seen as an up-regulation of *MMP-2* and *MMP-9* enzymes that are involved in degradation of the ECM at the early stages of angiogenesis (Kasper et al., 2007; Cornelius et al., 1998).

In vivo studies in mice have revealed that the adult quiescent vasculature becomes less dependent on VEGF for its maintenance (Gerber et al., 1999). However, during pathological conditions – such as ischemia, inflammation or malignancy – angiogenic endothelial cells are stimulated by increased VEGF levels (Carmeliet et al., 2001). The VEGF signaling pathways have been conclusively identified as central for the processes of vasculogenesis, angiogenesis and lymphangiogenesis. VEGF-D induces sprouting lymphangiogenesis when overexpressed in transgenic mice and also in various tumor models (Lohela et al., 2009). The up-regulation of *vascular endothelial growth factor D (FIGF)* as a marker for lymphangiogenesis suggests the versatile modifications of our vascular model. In future applications, it may be possible to replace HUVEC with lymphatic endothelial cells to form a lymphangiogenesis model.

5 Conclusion

The vascular model characterized in this study forms a vascular-like network with mature properties. The developed novel medium provides a valid alternative to commercial EGM-2 medium and benefits the use of the model in toxicological studies as well as in efficacy studies in drug development. This characterized vascular model is currently under intra-laboratory validation that is performed according to OECD guidance document No. 34 (OECD, 2005) to verify the reliability and human relevance of the test system with known reference chemicals. The validated vascular model will be used in toxicity testing and can be combined with other target cell types from different tissues to create complex, vascularized tissue models.

References

Auerbach, R., Lewis, R., Shinners, B. et al. (2003). Angiogenesis assays: a critical overview. *Clin Chem 49*, 32-40. http://dx.doi.org/10.1373/49.1.32

Adams, R. H. and Alitalo, K. (2007). Molecular regulation of angiogenesis and lymphangiogenesis. *Nat Rev Mol Cell Biol 8*, 464-478. http://dx.doi.org/10.1038/nrm2183

Ashikari-Hada, S., Habuchi, H., Kariya, Y. and Kimata, K. (2005). Heparin regulates vascular endothelial growth factor165-dependent mitogenic activity, tube formation, and its receptor phosphorylation of human endothelial cells. *J Biol Chem 280*, 31508-31515. http://dx.doi.org/10.1074/jbc.M414581200

Bale, A. S., Kenyon, E., Flynn, T. J. et al. (2014). Correlating in vitro data to in vivo findings for risk assessment. *ALTEX 31*, 79-90. http://dx.doi.org/10.14573/altex.1310011

Bernabeu, C., Lopez-Novoa, J. M. and Quintanilla, M. (2009). The emerging role of TGF-beta superfamily coreceptors in cancer. *Biochim Biophys Acta 1792*, 954-973. http://dx.doi.org/10.1016/j.bbadis.2009.07.003

Bishop, E. T., Bell, G. T., Bloor, S. et al. (1999). An in vitro model of angiogenesis: Basic features. *Angiogenesis 3*, 335-344. http://dx.doi.org/10.1023/A:1026546219962

Brunner, D., Frank, J., Appl, H. et al. (2010). Serum-free cell culture: The serum-free media interactive online database. *ALTEX 27*, 53-62. http://www.altex.ch/All-issues/Issue.50.html?iid=112&aid=4

Carmeliet, P., Moons, L., Luttun, A. et al. (2001). Synergism between vascular endothelial growth factor and placental growth factor contributes to angiogenesis and plasma extravasation in pathological conditions. *Nat Med 7*, 575-583. http://dx.doi.org/10.1038/87904

Carmeliet, P. (2005). Angiogenesis in life, disease and medicine. *Nature 438*, 932-936. http://dx.doi.org/10.1038/nature04478

Carmeliet, P. and Jain, R. K. (2011). Molecular mechanisms and clinical applications of angiogenesis. *Nature 473*, 298-307. http://dx.doi.org/10.1038/nature10144

Charpentier, M. S. and Conlon, F. L. (2014). Cellular and molecular mechanisms underlying blood vessel lumen formation. *Bioessays 36*, 251-259. http://dx.doi.org/10.1002/bies.201300133

Cornelius, L. A., Nehring, L. C., Harding, E. et al. (1998). Matrix metalloproteinases generate angiostatin: Effects on neovascularization. *J Immunol 161*, 6845-6852. Print ISSN: 0022-1767, Online ISSN: 1550-6606

De Francesco, F., Tirino, V., Desiderio, V. et al. (2009). Human CD34/CD90 ASCs are capable of growing as sphere clusters, producing high levels of VEGF and forming capillaries. *PLoS One 4*, e6537. http://dx.doi.org/10.1371/journal.pone.0006537

Du, P., Subbiah, R., Park, J. H. and Park, K. (2014). Vascular morphogenesis of human umbilical vein endothelial cells on cell-derived macromolecular matrix microenvironment. *Tissue Eng Part A 20*, 2365-2377. http://dx.doi.org/10.1089/ten.tea.2013.0693

Gerber, H. P., Hillan, K. J., Ryan, A. M. et al. (1999). VEGF is required for growth and survival in neonatal mice. *Development 126*, 1149-1159. http://dev.biologists.org/content/126/6/1149.long

Goding, A. M. (2009). The effect of hydrocortisone on angiogenesis. *BIOS 80*, 59-65. http://dx.doi.org/10.1893/011.080.0202

Gottipamula, S., Muttigi, M. S., Kolkundkar, U. and Seetharam, R. N. (2013). Serum-free media for the production of human mesenchymal stromal cells: A review. *Cell Prolif 46*, 608-627. http://dx.doi.org/10.1111/cpr.12063

Grunewald, J. K. and Ridley, A. J. (2010). CD73 represses pro-inflammatory responses in human endothelial cells. *J Inflamm*

7, 10. http://dx.doi.org/10.1186/1476-9255-7-10

Hartung, T. (2011). From alternative methods to a new toxicology. *Eur J Pharm Biopharm 77*, 338-349. http://dx.doi.org/10.1016/j.ejpb.2010.12.027

Heydarkhan-Hagvall, S., Schenke-Layland, K., Yang, J. Q. et al. (2008). Human adipose stem cells: A potential cell source for cardiovascular tissue engineering. *Cells Tissues Organs 187*, 263-274. http://dx.doi.org/10.1159/000113407

Holm, F., Ström, S., Inzunza, J. et al. (2010). An effective serum- and xeno-free chemically defined freezing procedure for human embryonic and induced pluripotent stem cells. *Hum Reprod 25*, 1271-1279. http://dx.doi.org/10.1093/humrep/deq040

Hoying, J. B., Utzinger, U. and Weiss, J. A. (2014). Formation of microvascular networks: Role of stromal interactions directing angiogenic growth. *Microcirculation 21*, 278-289. http://dx.doi.org/10.1111/micc.12115

Jain, R. K. (2003). Molecular regulation of vessel maturation. *Nat Med 9*, 685-693. http://dx.doi.org/10.1038/nm0603-685

Jung, S. P., Siegrist, B., Wade, M. R. et al. (2001). Inhibition of human angiogenesis with heparin and hydrocortisone. *Angiogenesis 4*, 175-186. http://dx.doi.org/10.1023/A:1014089706107

Kasper, G., Dankert, N., Tuischer, J. et al. (2007). Mesenchymal stem cells regulate angiogenesis according to their mechanical environment. *Stem Cells 25*, 903-910. http://dx.doi.org/10.1634/stemcells.2006-0432

Khorana, A. A., Sahni, A., Altland, O. D. and Francis, C. W. (2003). Heparin inhibition of endothelial cell proliferation and organization is dependent on molecular weight. *Arterioschler Thromb Vasc Biol 23*, 2110-2115. http://dx.doi.org/10.1161/01.ATV.0000090671.56682.D7

Kilroy, G. E., Foster, S. J., Wu, X. et al. (2007). Cytokine profile of human adipose-derived stem cells: Expression of angiogenic, hematopoietic, and pro-inflammatory factors. *J Cell Physiol 212*, 702-709. http://dx.doi.org/10.1002/jcp.21068

Knudsen, T. B. and Kleinstreuer, N. C. (2011). Disruption of embryonic vascular development in predictive toxicology. *Birth Defects Res C Embryo Today 93*, 312-323. http://dx.doi.org/10.1002/bdrc.20223

Lindroos, B., Aho, K. L., Kuokkanen, H. et al. (2010). Differential gene expression in adipose stem cells cultured in allogeneic human serum versus fetal bovine serum. *Tissue Eng Part A 16*, 2281-2294. http://dx.doi.org/10.1089/ten.TEA.2009.0621

Lindroos, B., Suuronen, R. and Miettinen, S. (2011). The potential of adipose stem cells in regenerative medicine. *Stem Cell Rev 7*, 269-291. http://dx.doi.org/10.1007/s12015-010-9193-7

Liu, Z., Lebrin, F., Maring, J. A. et al. (2014). Endoglin is dispensable for vasculogenesis, but required for vascular endothelial growth factor-induced angiogenesis. *PLoS One 9*, e86273. http://dx.doi.org/10.1371/journal.pone.0086273

Lohela, M., Bry, M., Tammela, T. and Alitalo, K. (2009). VEGFs and receptors involved in angiogenesis versus lymphangiogenesis. *Curr Opin Cell Biol 21*, 154-165. http://dx.doi.org/10.1016/j.ceb.2008.12.012

Mark, P., Kleinsorge, M., Gaebel, R. et al. (2013). Human mesechymal stem cells display reduced expression of CD105 after culture in serum-free medium. *Stem Cells Int 2013*, 698076. http://dx.doi.org/10.1155/2013/698076

Mathews, L., Nagaraja, H. and Chakravarthi, S. (2011). Insulin-like growth factor-1 (IGF-1) reduces ischemic changes and increases circulating angiogenic factors in experimentally – induced myocardial infarction in rats. *Vasc Cell 3*, 13. http://dx.doi.org/10.1186/2045-824X-3-13

Merfeld-Clauss, S., Gollahalli, N., March, K. L. and Traktuev, D. O. (2010). Adipose tissue progenitor cells directly interact with endothelial cells to induce vascular network formation. *Tissue Eng Part A 16*, 2953-2966. http://dx.doi.org/10.1089/ten.TEA.2009.0635

Mikirova, N. A., Ichim, T. E. and Riordan, N. H. (2008). Anti-angiogenic effect of high doses of ascorbic acid. *J Transl Med 6*, 50. http://dx.doi.org/10.1186/1479-5876-6-50

Miranville, A., Heeschen, C., Sengenès, C. et al. (2004). Improvement of postnatal neovascularization by human adipose tissue-derived stem cells. *Circulation 110*, 349-355. http://dx.doi.org/10.1161/01.CIR.0000135466.16823.D0

Murikipudi, S., Methe, H. and Edelman, E. R. (2013). The effect of substrate modulus on the growth and function of matrix-embedded endothelial cells. *Biomaterials 34*, 677-684. http://dx.doi.org/10.1016/j.biomaterials.2012.09.079

Nakao-Hayashi, J., Ito, H., Kanayasu, T. et al. (1992). Stimulatory effects of insulin and insulin-like growth factor I on migration and tube formation by vascular endothelial cells. *Atherosclerosis 92*, 141-149. http://dx.doi.org/10.1016/0021-9150(92)90273-J

Newman, A. C., Chou, W., Welch-Reardon, K. M. et al. (2013). Analysis of stromal cell secretomes reveals a critical role for stromal cell-derived hepatocyte growth factor and fibronectin in angiogenesis. *Arterioscler Thromb Vasc Biol 33*, 513-522. http://dx.doi.org/10.1161/ATVBAHA.112.300782

Norrby, K. (2006). In vivo models of angiogenesis. *J Cell Mol Med10*, 588-612.http://dx.doi.org/10.1111/j.1582-4934.2006.tb00423.x

OECD (2005). Guidance document No. 34 on the validation and international acceptance of new or updated test methods for hazard assessment. http://www.oecd.org/officialdocuments/publicdisplaydocumentpdf/?doclanguage=en&cote=env/jm/mono%282005%2914

Park, H. Y., Kwon, H. M., Lim, H. J. et al. (2001). Potential role of leptin in angiogenesis: Leptin induces endothelial cell proliferation and expression of matrix metalloproteinases in vivo and in vitro. *Exp Mol Med. 33*, 95-102. http://dx.doi.org/10.1038/emm.2001.17

Patrikoski, M., Juntunen, M., Boucher, S. et al. (2013). Development of fully defined xeno-free culture system for the preparation and propagation of cell therapy-compliant human adipose stem cells. *Stem Cell Res Ther 4*, 27. http://dx.doi.org/10.1186/scrt175

Potente, M., Gerhardt, H. and Carmeliet, P. (2011). Basic and therapeutic aspects of angiogenesis. *Cell 146*, 873-887. http://dx.doi.org/10.1016/j.cell.2011.08.039

Rehman, J., Traktuev, D., Li, J. et al. (2004). Secretion of angiogenic and antiapoptotic factors by human adipose stromal cells. *Circulation 109*, 1292-1298. http://dx.doi.org/10.1161/01.CIR.0000121425.42966.F1

Rubina, K., Kalinina, N., Efimenko, A. et al. (2009). Adipose stromal cells stimulate angiogenesis via promoting progenitor cell differentiation, secretion of angiogenic factors, and enhancing vessel maturation. *Tissue Eng Part A 15*, 2039-2050. http://dx.doi.org/10.1089/ten.tea.2008.0359

Sarkanen, J. R., Mannerström, M., Vuorenpää, H. et al. (2011). Intra-laboratory pre validation of a human cell based in vitro angiogenesis assay for testing angiogenesis modulators. *Front Pharmacol 1*, 147. http://dx.doi.org/10.3389/fphar.2010.00147

Sarkanen, J. R., Vuorenpää, H., Huttala, O. et al. (2012). Adipose stromal cell tubule network model provides a versatile tool for vascular research and tissue engineering. *Cells Tissues Organs 196*, 385-397. http://dx.doi.org/10.1159/000336679

Schlessinger, J., Plotnikov, A. N., Ibrahimi, O. A. et al. (2000). Crystal structure of a ternary FGF-FGFR-heparin complex reveals a dual role for heparin in FGFR binding and dimerization. *Mol Cell 6*, 743-750. http://dx.doi.org/10.1016/S1097-2765(00)00073-3

Shen, Q., Wang, L., Zhou, H. et al. (2013). Stereoselective binding of chiral drugs to plasma proteins. *Acta Pharmacol Sin 34*, 998-1006. http://dx.doi.org/10.1038/aps.2013.78

Shigematsu, S., Yamauchi, K., Nakajima, K. et al. (1999). IGF-1 regulates migration and angiogenesis of human endothelial cells. *Endocr J 46, Suppl S*, 59-62. http://dx.doi.org/10.1507/endocrj.46.Suppl_S59

Sierra-Honigmann, M. R., Nath, A. K., Murakami, C. et al. (1998). Biological action of leptin as an angiogenic factor. *Science 281*, 1683-1686. http://dx.doi.org/10.1126/science.281.5383.1683

Stratman, A. N., Malotte, K. M. and Mahan, R. D. (2009). Pericyte recruitment during vasculogenic tube assembly stimulates endothelial basement membrane matrix formation. *Blood 114*, 5091-5101. http://dx.doi.org/10.1182/blood-2009-05-222364

Telang, S., Klem, A. L., Eaton, J. W. and Chesney, J. (2007). Depletion of ascorbic acid restricts angiogenesis and retards tumor growth in a mouse model. *Neoplasia 9*, 47-56. http://dx.doi.org/10.1593/neo.06664

Traktuev, D. O., Merfeld-Clauss, S., Li, J. et al. (2008). A population of multipotent CD34-positive adipose stromal cells share pericyte and mesenchymal surface markers, reside in a periendothelial location, and stabilize endothelial networks. *Circ Res 102*, 77-85. http://dx.doi.org/10.1161/CIRCRESAHA.107.159475

Ucuzian, A. A. and Greisler, H. P. (2007). In vitro models of angiogenesis. *World J Surg 31*, 654-663. http://dx.doi.org/10.1007/s00268-006-0763-4

van der Valk, J., Brunner, D., De Smet, K. et al. (2010). Optimization of chemically defined cell culture media – replacing fetal bovine serum in mammalian in vitro methods. *Toxicol In Vitro 24*, 1053-1063. http://dx.doi.org/10.1016/j.tiv.2010.03.016

Verseijden, F., Posthumus-van Sluijs, S. J., Pavljasevic, P. et al. (2010). Adult human bone marrow- and adipose tissue-derived stromal cells support the formation of prevascular-like structures from endothelial cells in vitro. *Tissue Eng Part A 16*, 101-114. http://dx.doi.org/10.1089/ten.TEA.2009.0106

Vuorenpää, H., Ikonen, L., Kujala, K. et al. (2014). Novel in vitro cardiovascular constructs composed of vascular-like networks and cardiomyocytes. *In Vitro Cell Dev Biol Anim 50*, 275-286. http://dx.doi.org/10.1007/s11626-013-9703-4

Yang, Z. and Xiong, H.-R. (2012). Culture conditions and types of growth media for mammalian cells. In L. Ceccherini-Nelli and B. Matteoli (ed.), *Biomedical Tissue Culture* (3-18). InTech. ISBN 978-953-51-0788-0. http://dx.doi.org/10.5772/3071

Yoder, M. C. (2012). Human endothelial progenitor cells. *Cold Spring Harb Perspect Med 2*, a006692. http://dx.doi.org/10.1101/cshperspect.a006692

Conflict of interest statement

None of the authors have any conflicts of interest.

Acknowledgements

We thank the treating staff in Tampere University Hospital as well as the donors for collaboration concerning the donations of umbilical cords and adipose tissue samples. We thank Dr Raija Sormunen at University of Oulu for EM imaging and assistance in result interpretation. We thank Dr Katriina Aalto-Setälä and Liisa Ikonen in BioMediTech for their collaboration in the project. In FICAM we want to thank Ms Paula Helpiölä, Ms Mirja Hyppönen, Ms Hilkka Mäkinen and Ms Sari Leinonen for technical assistance.

Funding for the project was provided by Pirkanmaa Centers for Economic Development, Transport and the Environment, City of Tampere, Finnish Funding Agency for Technology and Innovation, Ministry of Education and Culture, Ministry of Agriculture and Forestry, Pirkanmaa Cultural Foundation, The Diabetes Research Foundation and FinPharma Doctoral Program.

Correspondence to

Hanna Vuorenpää, MSc
FICAM, Finnish Centre for Alternative Methods,
School of Medicine
FI-33014 University of Tampere
Finland
Phone: +35 8401904105
Fax: +35 8335516170
e-mail: hanna.vuorenpaa@uta.fi

In Vitro Cell.Dev.Biol.—Animal (2014) 50:275–286
DOI 10.1007/s11626-013-9703-4

Novel in vitro cardiovascular constructs composed of vascular-like networks and cardiomyocytes

Hanna Vuorenpää · Liisa Ikonen · Kirsi Kujala · Outi Huttala · Jertta-Riina Sarkanen · Timo Ylikomi · Katriina Aalto-Setälä · Tuula Heinonen

Received: 27 June 2013 / Accepted: 3 October 2013 / Published online: 26 October 2013 / Editor: T. Okamoto

Abstract The interaction between different cardiac cells has shown to be important for critical biological properties including cell survival, proliferation, differentiation and function. The improvement of culture conditions with different cell types and to study their effects on cardiomyocyte viability and functionality is essential. For practical applications including general toxicity testing, drug development and tissue engineering it is important to study whether co-cultures have additional advantages over cardiomyocyte monoculture. Two multicellular in vitro cardiovascular constructs devoid of added biomaterial were developed in this study. In the first construct, neonatal rat cardiomyocytes (CM) were seeded on vascular-like network formed by human umbilical vein endothelial cells (HUVEC) and human adipose stromal cells (hASC). In the second construct, CMs were seeded on vascular-like network formed by HUVECs and human foreskin fibroblasts. The ability of these two vascular-like networks to support the viability and functionality of CMs was analyzed. Different culture media compositions were evaluated to support the development of optimal cardiovascular construct. Our results demonstrate that both vascular-like networks markedly improved CM viability and functionality. In the constructs, co-localization of CMs and vascular-like networks was seen. Multicellular constructs also allowed synchronized contractility of CMs. Serum-free medium supplemented with vascular endothelial growth factor and basic fibroblast growth factor was found to provide the most optimal conditions for cardiovascular construct as an entity. In conclusion, when combining a vascular-like network with CMs, the viability and functionality of CMs was markedly improved. The results suggest that the cardiovascular constructs developed provide a promising new tool for the assessment of toxicological and safety pharmacological effects of compounds in vitro.

Keywords Angiogenesis · Primary cardiomyocytes · Human adipose stromal cells, in vitro cardiotoxicity

Hanna Vuorenpää and Liisa Ikonen equally contributed to this work.

Electronic supplementary material The online version of this article (doi:10.1007/s11626-013-9703-4) contains supplementary material, which is available to authorized users.

H. Vuorenpää (✉) · O. Huttala · J.-R. Sarkanen · T. Ylikomi · T. Heinonen
FICAM, Finnish Centre for Alternative Methods, School of Medicine, University of Tampere, Medisiinarinkatu 3, 33014 Tampere, Finland
e-mail: hanna.vuorenpaa@uta.fi

L. Ikonen · K. Kujala · K. Aalto-Setälä
IBT, Institute of Biomedical Technology, University of Tampere, Biokatu 12, 33520 Tampere, Finland

L. Ikonen · K. Kujala · K. Aalto-Setälä
BioMediTech, Biokatu 10, 33520 Tampere, Finland

T. Ylikomi
Department of Cell Biology, School of Medicine, University of Tampere, 33014 Tampere, Finland

T. Ylikomi
Department of Clinical Chemistry, Tampere University Hospital, 33014 Tampere, Finland

K. Aalto-Setälä
Heart Center, Tampere University Hospital, Biokatu 6, 33520 Tampere, Finland

Introduction

The heart is a complicated organ having multiple cell types and highly organized structure and function. The major cell types present in the human heart are cardiomyocytes (CMs), smooth muscle cells, endothelial cells (ECs) and fibroblasts (Nag 1980; Banerjee et al. 2007). In adaptation to in vitro culture conditions, primary CMs have a tendency to change in morphology, dedifferentiate, and stop beating (Montessuit et al. 2004; Banyasz et al. 2008).

The interactions between coronary vasculature and myocardium are bidirectional (Bhattacharya et al. 2006) and active through the adult life affecting cardiac growth, function, and rhythmicity (Brutsaert 2003). Vascular ECs produce a variety of auto- and paracrine agents including VEGF, angiopoietin, and nitric oxide that influence cardiac metabolism, growth, contractility, and rhythmicity of the heart (Brutsaert 2003). Previously, it has been shown that ECs and fibroblasts assist the generation of a functional heart tissue construct and form vascular networks among CMs (Caspi et al. 2007; Radisic et al. 2008). Also CM proliferation has been found to increase in the presence of ECs and fibroblasts (Stevens et al. 2009; Lesman et al. 2010; Kreutziger et al. 2011). As the importance of other cardiac cells to the viability and functionality of CMs has been shown, there are recent reports of several tissue engineering constructs based on co-culture of main cell types present in heart tissue (Sekine et al. 2008; He et al. 2012; Hussain et al. 2013). However, in spite of the extensive research the effect of medium with optimal serum concentration and additional supplements to support the growth of cardiac tissue constructs has not been studied thoroughly (Sekine et al. 2008; Valarmathi et al. 2010; He et al. 2012; Hussain et al. 2013).

The heart has been shown to be particularly prone to toxic effects of both cardiac and noncardiac drugs. Cardiotoxic substances can cause severe effects on heart functions including decreased contractility and increased arrhythmia and ischemia (Lasser et al. 2002; Redfern et al. 2003; Lexchin 2005). Therefore, there is a need for reliable in vitro cardiac model for assessment of toxicological and safety pharmacological potential of human pharmaceuticals in drug development (Kettenhofen and Bohlen 2005). Functional in vitro cardiac construct would also benefit the generation of future transplantable cardiac tissue implants.

We have previously developed a three-dimensional vascular-like network comprised of co-culture of human umbilical vein endothelial cells (HUVEC) and human adipose stromal cells (hASC) (Sarkanen et al. 2012). Adipose stromal cells (ASCs) have shown to produce significant amounts of angiogenic factors and cytokines including VEGF, hepatocyte growth factor and angiopoietin (Rehman et al. 2004; Rubina et al. 2009; De Siena et al. 2010). Although several tissue engineering strategies rely on the use of scaffolds, these scaffolds may interfere the cell–cell interactions and induce inflammatory reaction (Shimizu et al. 2003; Norotte et al. 2009). The three-dimensional and intense vascular-like network of our HUVEC+hASC co-culture could serve as a natural scaffold for in vitro tissue models (Sarkanen et al. 2012). In addition, we have presented another human cell-based in vitro angiogenesis assay based on co-culture of fibroblasts and HUVECs that can be used for standardized testing of modulators of angiogenesis (Sarkanen et al. 2011).

In this study, we developed two cardiovascular constructs, consisting of two different previously developed vascular-like networks (Sarkanen et al. 2011; 2012) of different origin (HUVEC+hASC and HUVEC+fibroblast) and neonatal rat CMs. Both constructs are based on co-cultures of three cell types naturally resident in the heart, devoid of added biomaterials. The aim was to evaluate the capability of these two different vascular-like networks to support CM viability and functionality in an optimal medium. The results demonstrated that both vascular-like networks provided substantial benefit for the development of functional cardiovascular construct as the networks led to extended viability and contractile capacity of CMs.

Materials and Methods

Cells Ethics statement. This study conforms to the principles outlined in the Declaration of Helsinki. The human adipose tissue samples were obtained from surgical operations at Tampere University Hospital, Tampere, Finland with individual written informed consents. The use of human adipose tissue derived cells (hASCs) in this study was approved by Ethics Committee of the Pirkanmaa Hospital District, Tampere, Finland (permit number R03058). Human umbilical cords were received from caesarean sections at Tampere University Hospital, Tampere, Finland with individual written informed consent. The use of HUVECs in this study was approved by the Ethics Committee of the Pirkanmaa Hospital District, Tampere, Finland (permit number R08028). All animal experiments in this study were performed according to the Finnish animal protection laws and approved by the Department for Social Welfare and Health Services of State Provincial Office of Western Finland. Euthanasia was performed by decapitation, a method approved in Directive 2010/63/EU.

Isolation and culture of human adipose stromal cells. HASC were isolated from human adipose tissue by using mechanical and enzymatic procedure as described previously (Gimble and Guilak 2003; Sarkanen et al. 2012). Briefly, human adipose tissue specimens were cut into small pieces, enzymatically digested with 0.05% collagenase I (Invitrogen, Paisley, Scotland, UK) in Dulbecco's Modified Eagle's Medium Nutrient Mixture F-12 (DMEM/F-12, Gibco, Invitrogen, Carlsbad, CA) for 60 min at 37°C in a gyratory water bath. Then the digested tissue was centrifuged at 600×*g* for 10 min in room temperature (RT). Then the digested tissue was filtered through a 100 μm filter (Sarstedt, Nümbrecht, Germany), centrifuged and filtered through a 40 μm filter (Sarstedt). The Cells were seeded into 75 cm^2 flasks (Nunc EasyFlask™, Nunc, Roskilde, Denmark) in DMEM/F-12 supplemented

with 1% L-glutamine (L-glut, Gibco), 1% antibiotic–antimycotic mixture (AB/AM, Gibco) and 10% human serum (HS, Cambrex, East Rutherford, NJ). The next day, the cells were washed several times with PBS. HASC medium (Table 1) was changed three times a wk and cells were subcultured when confluent. Cells were tested for mycoplasma contamination (MycoAlert® Mycoplasma Detection Kit, Lonza Group Ltd, Basel, Switzerland) before experimental use.

Isolation and culture of human umbilical vein endothelial cells. HUVECs were isolated from human umbilical cord vein by using enzymatic procedure as described previously (Jaffe et al. 1973; Sarkanen et al. 2011). Briefly, the cord was separated from the placenta and the umbilical vein was cannulated with a 20G needle. The needle was secured by clamping the cord over the needle with a surgical clamp. The vein was perfused with PBS to wash out blood and then the opposing end of the umbilical vein was clamped with a surgical clamp. Subsequently, the vein was infused with 0.05% collagenase I. The umbilical cord was incubated in a water bath at 37°C for 15 min. After incubation, the collagenase I solution containing HUVEC was flushed from the cord by perfusion with PBS into a 50-ml polypropylene tube (Sarstedt). The cells were centrifuged at 200×*g* for 10 min, washed once with medium and centrifuged again. After last centrifugation the cells were resuspended in EGM-2 BulletKit

Table 1. Culture media used for cell culture set ups

Culture media	Basal medium	Supplements
hASC medium	DMEM/F-12 (Gibco, Invitrogen, USA)[a]	10% HS (Cambrex, USA)
		1% L-glutamine (Gibco)
		1% AB/AM (Gibco)
EGM-2 BulletKit medium (Lonza Group Ltd, Switzerland)	EBM-2 (Lonza)	SingleQuots supplements (Lonza Group Ltd, Switzerland) with unknown concentrations of:
		FBS
		hydrocortisone
		hFGF-β
		hVEGF
		IGF
		ascorbic acid
		hEGF
		GA-1000
		heparin
Fibroblast medium	Minimum Essential Medium with Earle's salts, w/o L-glutamine	10% FBS (Gibco)
		1% L-glutamine
		1% NEAA (Gibco)
		1% AB/AM
CM seeding medium (SM)	DMEM/F-12 (Sigma-Aldrich, USA)[b]	10% FBS (Invitrogen, USA)
		100 IU/ml P/0.1 mg/ml S (Lonza, Belgium)
		2.56 mM L-glutamine (Sigma-Aldrich)
CM serum-free medium (SFM)	DMEM/F-12 (Sigma-Aldrich)[b]	10% BSA (Sigma-Aldrich)
		2.8 mM NaPyruvate (Lonza)
		2.56 mM L-glutamine
		ITS (1 μM insulin, 5.64 μg/ml transferrin, 32 nM selenium, Lonza)
		100 IU/ml P/0.1 mg/ml S
		0.1 nM T_3 (Sigma-Aldrich)
Vascular-like network (HUVEC+fibroblast) medium	EBM-2	2% FBS
		0.1% GA-1000 (Lonza)
		1 mM L-glutamine
		10 ng/ml hVEGF (Sigma-Aldrich)
		1 ng/ml hFGF- β (Sigma-Aldrich)

HS human serum, *AB/AM* antibiotic–antimycotic mixture, *EBM-2* endothelial cell basal medium, *FBS* fetal bovine serum, *hFGF-β* human basic fibroblast growth factor beta, *hVEGF* human vascular endothelial growth factor, *IGF* insulin-like growth factor, *hEGF* human epidermal growth factor, *GA-1000* gentamycin, *NEAA* non-essential amino acids, *P/S* penicillin/streptomycin, *BSA* bovine serum albumin, *ITS* insulin–transferrin–sodium selenite media supplement, *T_3* 3,3′,5-triiodo-L-thyronine sodium salt

[a] *DMEM/F-12* Dulbecco's Modified Eagle's Medium Nutrient Mixture F-12

[b] Dulbecco's Modified Eagle's Medium/Ham's Nutrient Mixture F-12

medium (Lonza Group Ltd) (Table 1) consisting of EBM-2 basal medium and SingleQuots supplements including fetal bovine serum (FBS), hydrocortisone, human FGF-β, VEGF, insulin-like growth factor (IGF), ascorbic acid, human epidermal growth factor (hEGF), GA-1000 and heparin (Lonza Group Ltd) and seeded into 75 cm^2 flasks. The medium was changed three times a week and cells were subcultured when confluent. Cells were tested for mycoplasma contamination (MycoAlert® Mycoplasma Detection Kit, Lonza) before experimental use.

Isolation and culture of human foreskin fibroblasts. Human foreskin fibroblasts were purchased from American Type Culture Collection (CRL-2522; ATCC, Manassas, VA). The Cells were cultured in fibroblast medium (Table 1) consisting of Minimum Essential Medium with Earle's salts, w/o L-glutamine supplemented with 10% FBS, 1% L-glutamine, 1% NEAA, and 1% antibiotic–antimycotic mixture in 75 cm^2 flasks. Medium was changed three times a wk and cells were subcultured when confluent. Cells were tested for mycoplasma contamination (MycoAlert® Mycoplasma Detection Kit, Lonza) before experimental use.

Isolation of neonatal rat cardiomyocytes. Neonatal rat cardiomyocytes were harvested from 1- to 4-d-old Sprague–Dawley rat pups hearts as described by Uusimaa et al. (1992). Briefly, the hearts were perfused with collagenase solution and cut into 1–2-mm pieces. The heart pieces were incubated at 37°C for 5 min and the supernatant was discarded. Fresh 5 ml of collagenase solution was added and this step was repeated five times. The supernatants were collected and filtered (100 μm) into 20 ml of seeding medium [SM, DMEM/F-12 (Sigma-Aldrich, St. Louis, MO), 10% FBS (Invitrogen, USA), 100 IU/ml penicillin/0.1 mg/ml streptomycin (P/S, Lonza, Belgium), 2.56 mM L-glutamine (Sigma-Aldrich)]. The cells were preplated for 45 min to reduce the number of non-muscle cells and to achieve more pure neonatal rat cardiomyocyte (NRC) population.

Cell culture set ups Neonatal rat cardiomyocyte monoculture. After the preplating, the CMs were collected and seeded in CM seeding medium (SM, Table 1) into 48-well plates (Nunc, Thermo Fisher Scientific, Waltham, MA) at a density of $0.1–0.4\times10^6$ cells/cm^2. The serum-free medium (SFM, Table 1) consisting of DMEM/F-12, 2,5 mg/ml bovine serum albumin (BSA, Sigma-Aldrich), 2.8 mM sodium pyruvate (Lonza), 2.56 mM L-glutamine, insulin–transferrin–sodium selenite media supplement (ITS, Lonza; 1 μM insulin, 5.64 μg/ml transferring, 32 nM selenium) and 100 IU/ml P/0.1 mg/ml S 0.1 nM 3,3′,5-triiodo-L-thyronine sodium salt (T_3, Sigma-Aldrich) was changed five day after plating and thereafter every second or third day.

Vascular-like network from co-culture of hASC and HUVEC. The co-culture was constructed as described previously by Sarkanen et al. (2012). hASCs were seeded (p1–3) in EGM-2 BulletKit medium (Table 1) into 48-well plates (Nunclon™ Multidishes, Nunc, Roskilde, Denmark) at a density of 20,000 cells/cm^2. After 1–3 h HUVECs, were carefully seeded (p4) on top of hASCs at a density of 4,000 cells/ cm^2 in EGM-2 BulletKit medium (Table 1). The seeding densities of hASCs and HUVECs were chosen according to our previous study (Sarkanen et al. 2012). The control medium inducing vascular-like network formation was changed every second or third day.

Vascular-like network from co-culture of HUVEC and fibroblast. The co-culture was constructed as described previously by Sarkanen et al. (2011). Fibroblasts (p6–7) were seeded at a density of 20,000 cells/cm^2 in fibroblast medium (Table 1) and grown for 1–3 d. HUVECs were carefully seeded on top of the fibroblast culture at a density of 4,000 cells/cm^2 in EGM-2 BulletKit medium (Table 1). The seeding densities of fibroblasts and HUVECs were chosen according to our previous studies (Sarkanen et al. 2011, 2012). The following day and thereafter every second or third day vascular-like network control medium (Table 1) was changed to induce vascular-like network formation.

Cardiovascular constructs. CMs were carefully seeded on top of the co-culture of hASC+HUVEC and HUVEC+fibroblast approximately after 24 h at a density of $0.1–0.4\times10^6$ cells/cm^2. Cardiovascular construct 1 included HUVECs, hASCs and CMs and cardiovascular construct 2 included HUVECs, fibroblasts and CMs. The viability of cardiovascular constructs was assessed visually under phase contract microscope inspecting the contraction of the cardiomyocytes and tubule formation of the HUVECs, hASCs and fibroblasts three to five times a wk.

Culture media. For the cardiovascular constructs, the media were changed on the day after seeding of CMs. Altogether six different media were tested (Table 2) all in at least duplicate wells. The media were chosen to represent optimal culture media for either CMs (culture media 1–2), co-culture of HUVEC and fibroblasts (culture media 3–4) or co-culture of hASC and HUVEC (culture media 5–6) (Sarkanen et al. 2011, 2012). In addition to cardiovascular constructs, all culture media were tested also with CMs as monocultures. Cells were cultured for either 10 or 14 d and the culture media were changed three times a week.

Analysis Functionality of cardiac cell. The functionality of CMs in the cardiovascular construct was studied with micro electrode array (MEA). Cells are growing on top of the electrodes on MEA well containing 60 titanium nitride-

Table 2. Culture media (1–6) used for development of in vitro cardiovascular constructs

Culture media	Basal medium	Serum	Growth factors	Additional supplements
1	DMEM/F12	–	10 ng/ml hVEGF	T_3
			1 ng/ml hFGF-β	NaPyruvate
				BSA
				L-glutamine
				ITS
				P/S
2	DMEM/F12	–	10 ng/ml hVEGF	T_3
			1 ng/ml hFGF-β	NaPyruvate
				BSA
				L-glutamine
				ITS
				P/S
				Hydrocortisone
				Heparin
				Ascorbic acid
3	EBM-2	2% FBS	10 ng/ml hVEGF	Gentamicin
			1 ng/ml hFGF-β	L-glutamine
4	EBM-2	2% HS	10 ng/ml hVEGF	Gentamicin
			1 ng/ml hFGF-β	L-glutamine
5	EBM-2	2% HS	hVEGF[a]	Hydrocortisone
			hFGF-β[a]	Ascorbic acid
			IGF[a]	GA-1000
			hEGF[a]	Heparin
6	EBM-2	–	hVEGF[a]	Hydrocortisone
			hFGF-β[a]	Ascorbic acid
			IGF[a]	GA-1000
			hEGF[a]	Heparin

DMEM/F12 Dulbecco's modified Eagle's medium/Ham's nutrient mixture F12, *hVEGF* human vascular endothelial growth factor, *hFGF-β* human basic fibroblast growth factor beta, *T_3* 3, 3′,5-triiodo-L-thyronine sodium salt, *BSA* bovine serum albumin, *ITS* insulin–transferrin–sodium selenite media supplement, *P/S* penicillin/streptomycin, *EBM-2* endothelial cell basal medium, *FBS* fetal bovine serum, *HS* human serum, *IGF* insulin-like growth factor, *hEGF* human epidermal growth factor, *GA-1000* gentamycin

[a] Unknown concentration (SingleQuots supplements, Lonza)

coated electrodes with which the field potential can be measured (Reppel et al. 2004).

The MEA wells were first hydrophilized with FBS for 30 min at RT and then coated with 0.1% gelatin type A (Sigma-Aldrich) for 1 h at RT. The co-culture of HUVEC and hASC forms thicker vascular-like network [approximately 200 μm (Sarkanen et al. 2012)] than the co-culture of fibroblasts and HUVECs and is thus more likely to isolate the electrical signal. Therefore, the ability of this tissue construct to conduct electrical signal of CMs was analyzed. hASCs and HUVECs were first plated on MEA wells and the following d 400,000 CMs were plated on top. The culture medium 1 was used in MEA experiments.

The measurements were performed as described in Kujala et al. (2011). Briefly, an MEA1060-Inv- BC amplifier, a 20-kHz sampling rate and MC_Rack software (all from Multi Channel Systems MCS GmbH) were used. The recordings were performed at room air keeping the temperature at +37°C with MEA amplifier's heating element. To maintain the sterility of the cultures the MEAs were covered with a gas-permeable membrane (ALA Scientific, Farmingdale, NY). The field potential signals were recorded twice during each culture and for three minutes at a time. The measurements were performed with MC_Rack, files converted with MC_DataTool and signals analyzed with AxoScope.

Immunocytochemistry. The tubule formation was visualized with EC specific antibody anti-von Willebrand factor (anti-vWf, 1:100, F3520, Sigma) and CMs with an antibody against cardiac troponin T (anti-Tnt 1:500, ab33589, Abcam). The cells were washed three times with PBS, fixed with ice-cold 70% ethanol for 20 min, permeabilized with 0.5% Triton X-100 (JT Baker, Phillipsburg, NJ) for 15 min and blocked for unspecific staining with 10% BSA (Sigma) for 30 min. After blocking, the cells were incubated with the primary antibody pairs at 1 h at RT or in +4°C o/n. The cells were then washed three times with PBS, incubated 30 min with secondary antibody polyclonal anti- rabbit IgG TRITC (1:50, Sigma) for anti-vWf and polyclonal anti-mouse IgG FITC (1:100, Sigma) for anti-Tnt at RT. Fluorescence was visualized with Nikon Eclipse Ti-S microscope (Nikon, Tokyo, Japan) and the images were further processed with NIS D.2 Elements

(Nikon, Tokyo, Japan) and Adobe Photoshop CS3-software (Adobe Systems Incorporated, San Jose, CA).

Analysis of vascular-like network formation. After immunocytochemical staining, the vascular-like network formation was analyzed with Nikon Eclipse TS100 microscope (Nikon, Tokyo, Japan) from 48-well plate wells with ×40 magnification. The analysis and grading was based on vascular-like network formation, the length and the branches of tubules. The vascular-like network formation was estimated visually and compared to the control medium that gave value of 100% vascular-like network formation. The chosen control media, medium number 5 in cardiovascular construct 1 and medium number 3 in construct 2 (Table 1) induced optimal vascular-like network formation in HUVEC+hASC (Sarkanen et al 2012) and HUVEC+Fibroblast co-culture (Sarkanen et al 2011), respectively. In order to see the differences in vascular-like network formation in control versus other media a linear mixed-effect model was used. A linear mixed-effect model with estimation as a dependent variable was fitted separately for HUVEC+Fibroblast and hASC+HUVEC co-culture using function lme in R (Software environment for statistical computing and graphics, version 2.13.0, The R Foundation for Statistical Computing). Experiments and media were used as independent variables. Random intercept for parallel wells was used together with independent random errors.

Analysis of cardiomyocyte contractility. After producing the cardiovascular construct, the CM contractility was microscopically assessed three to five times a wk. The contractility was estimated as 10–30% (only few separate beating cardiomyocytes or cardiomyocyte clusters per cm^2, Electronic supplementary materials (ESM), 30–50% (at most half of the cardiomyocytes are beating per cm^2, ESM), or 50–70% (large areas of synchronously beating cardiomyocytes per cm^2, ESM).

Results

Optimal culture medium for cardiovascular construct. Different culture media (Table 2) were tested in order to primarily support CM functionality and secondarily to induce adequate vascular-like network formation. The results showed that the culture medium 1 (serum-free culture medium supplemented with 10 ng/ml VEGF and 1 ng/ml FGF) and 2 (serum-free culture medium supplemented with 10 ng/ml VEGF, 1 ng/ml FGF, ascorbic acid, hydrocortisone and heparin) improved most efficiently the cell viability in cardiovascular constructs as an entity (Table 3). Culture medium 1 provided 50–70% contractility of CMs and the vascular-like network formation was 34.7% and 68.9% in cardiovascular construct 1 and 2, respectively. Culture medium 2 provided a 111.4% and 114.3% induction for vascular-like network formation in cardiovascular construct 1 and 2, respectively, but the amount of contractile CMs was more diverse (30–70%). Since medium 1 provided a stronger, more synchronic and more repeatable cardiac contractility, it was chosen for further experiments. Media 3–6 were optimal for vascular-like network formation but only 10–30% of CMs were contractile. Moreover, the contractility decreased after 7 d in vitro culture.

Functionality of cardiomyocytes in the absence and presence of vascular-like network. In this study, two different vascular-like networks as a supporting platform for CMs were evaluated. The results demonstrated that both vascular-like networks were able to support CM viability. In the

Table 3. Cardiomyocyte contractility and vascular-like network formation in different culture media

Culture media	Cardiovascular construct 1 (HUVEC+hASC+CM)					Cardiovascular construct 2 (HUVEC+fibroblast+CM)				
	Cardiomyocyte contractility (%)[a]	Vascular-like network formation[b]			*n*	Cardiomyocyte contractility (%)[a]	Vascular-like network formation[b]			*n*
		Mean (%)	COV (%)	*p* value			Mean (%)	COV (%)	*p* value	
1	50–70	34.69	22.01	0.00	7	50–70	68.89	15.30	0.00	9
2	30–70	111.40	5.73	0.13	5	30–70	114.3	13.23	0.32	7
3	10–30	17.86	40.00	0.00	4	10–30	106.7	9.68		6
4	10–30	21.43	38.49	0.00	4	10–30	126.7	12.89	0.057	6
5	10–30	97.62	11.02		6	10–30	84.00	31.04	0.18	5
6	10–30	105.7	12.09	0.12	5	10–30	86.67	26.65	0.09	3

COV coefficient of variation

$p > 0.05$ differences are not significant

[a] 10–30% = only few separate beating cardiomyocytes or cardiomyocyte clusters/cm^2, 30–50% = at most half of the cardiomyocytes are beating/cm^2, 50–70% = large areas of synchronously beating cardiomyocytes/cm^2

[b] Compared to the control medium 5 (or 3) with value of 100% vascular-like network formation in construct 1 (or 2)

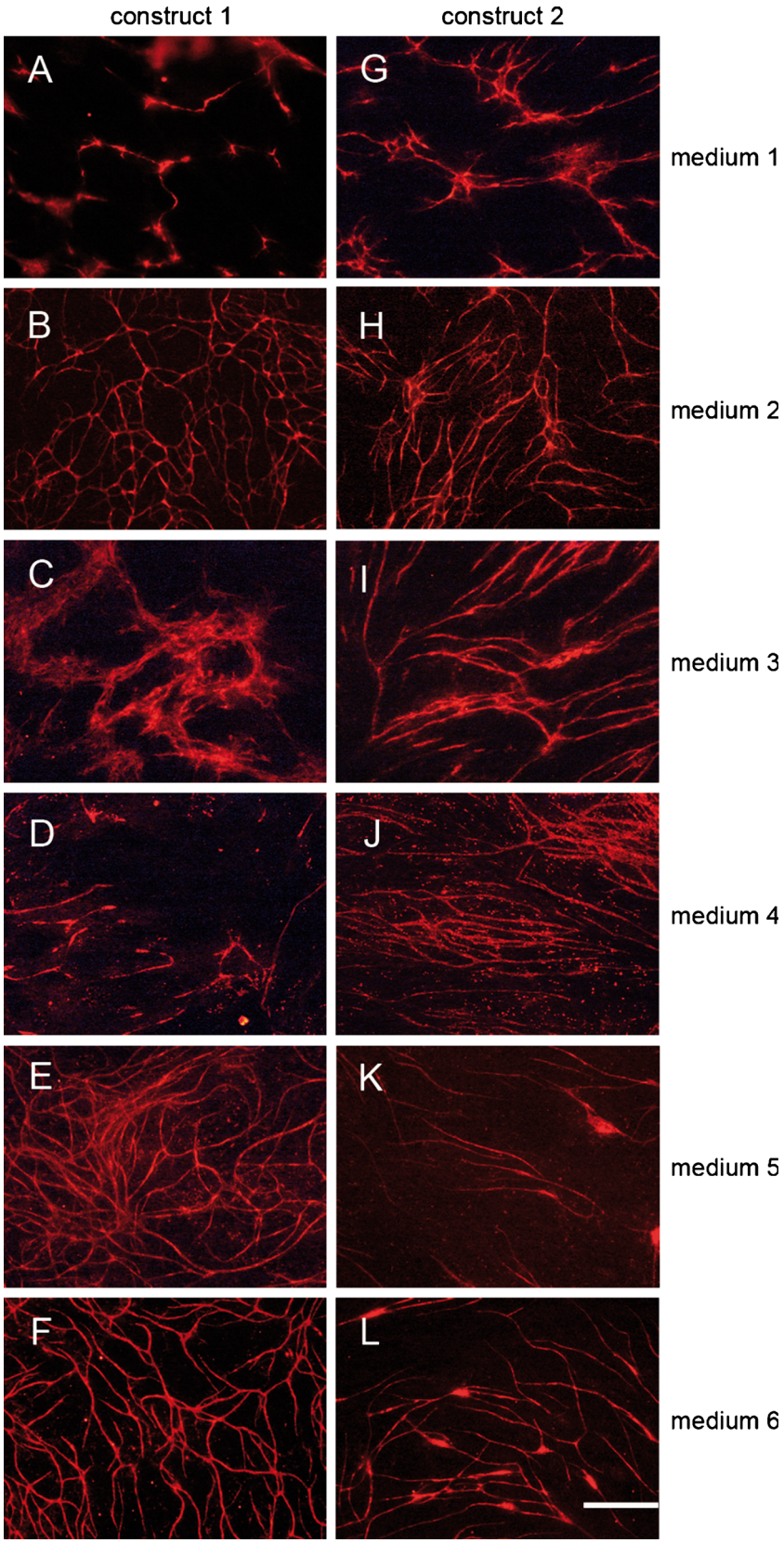

Figure 1. The formation of vascular-like network in cardiovascular construct 1 in (*A*) culture medium 1, (*B*) culture medium 2, (*C*) culture medium 3 and (*D*) culture medium 4, (*E*) culture medium 5 and (*F*) culture medium 6. The formation of vascular-like network in cardiovascular construct 2 in (*G*) culture medium 1, (*H*) culture medium 2, (*I*) culture medium 3, (*J*) culture medium 4, (*K*) culture medium 5 and (*L*) culture medium 6. The vascular-like structures were stained against von Willebrand Factor. *Scale bar* is 500 μm in each image.

cardiovascular construct 2 (HUVEC+fibroblast+CM), the formation of vascular-like structures was less dense compared to construct 1 (HUVEC+hASC+CM) (Fig. 1). The orientation of vascular-like network seemed more parallel in

Table 4 CM cell number and contractility area in the absence and presence of two vascular-like networks (HUVEC+hASC) and (HUVEC+fibroblasts)

Cell number	CM contractility in monoculture[a]	CM contractility in the presence of vascular-like network[a]
0.1×10^6	7 d, 30–50% ($n=27$)	14 d, 50–70% ($n=30$)
0.4×10^6	12 d, 50–70% ($n=13$)	14 d, 50–70% ($n=7$)

[a] Using visual inspection

cardiovascular construct 2, whereas in cardiovascular construct 1 a tight, branching 3D like network was formed (Fig. 1).

The capability of two different vascular-like networks to support the functionality of CMs was compared to CM monoculture (Table 4). In monoculture, the CMs were contractile approximately for 7 d in any of the tested media. However, in the presence of vascular-like network, the CMs were functional, and maintained their contractile capacity for at least 14 d. Differences in the time of contractility were not detected between the two constructs and a synchronized contractility was visually observed in both constructs. However, the areas which were beating were larger in co-cultures (50–70%) than in monoculture (30–50%). The number of CMs was less critical when they were cultured with the vascular-like networks compared to monoculture and the contractility was stronger even with a fewer number of CMs (Table 4).

Cardiomyocyte morphology and orientation in the absence and presence of vascular-like network. CM morphology and orientation were studied in monoculture and with the vascular-like networks. The results showed that the rod-shape morphology of mature CMs could be detected in the presence of both vascular-like networks after 14 d. However, CMs in the monoculture remained rounded and less organized in their phenotype (Fig. 2).

The results also showed that when CMs were cultured in the presence of vascular-like network they co-localized with the vascular structures in all culture media tested. Orientation of the CMs could not be detected in monoculture. Furthermore, CMs were co-localized longitudinally and parallel with the vascular-like network structure that was formed in cardiovascular construct 2. In cardiovascular construct 1, the CMs seemed more randomly oriented with the branching vascular-like structures (Fig. 2).

Electrophysiology of the cardiovascular construct. The MEA system was used to analyze the functionality of cardiovascular construct. In addition, the conductivity of the vascular-like network was proven. Vascular-like network in construct 1 (HUVEC+hASC) was chosen due to its thicker structure (Sarkanen et al. 2012) and potential to isolate the signal of CMs. However, the results showed that cardiovascular construct 1 conducted the signal and electrical activity was detectable (Fig. 3). There were no differences detected in the beating frequency in CM monoculture (Fig. 3*A*) compared to CMs in cardiovascular constructs (Fig. 3*B*). MEA measurements also showed that the contractility of CMs was synchronous in cardiovascular construct 1 (Fig. 3*C*) as already observed visually.

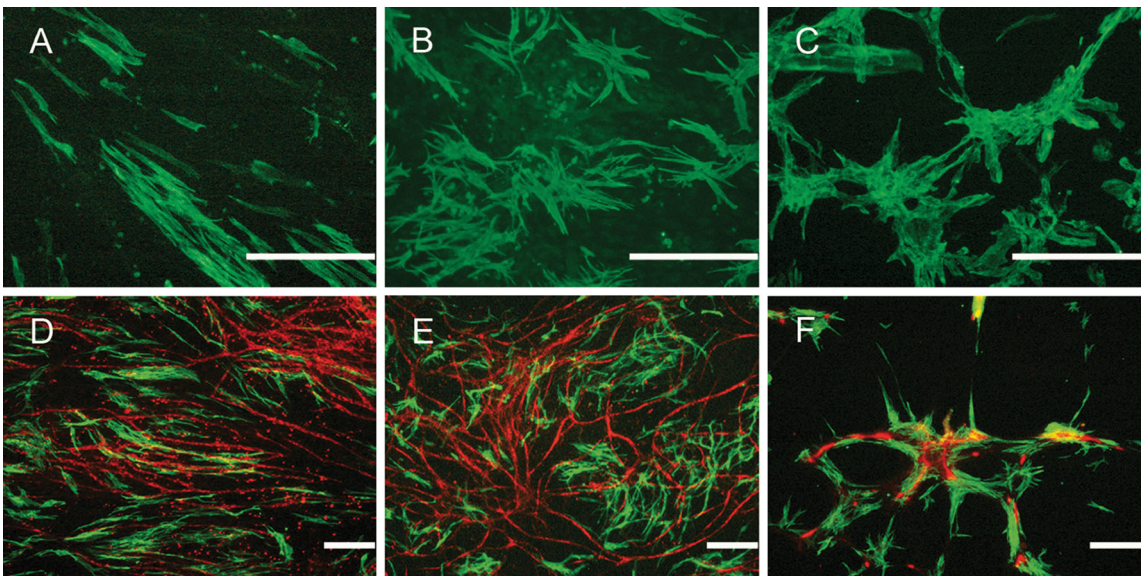

Figure 2. CM morphology at day 14 in vitro in (*A*) cardiovascular construct 2 in culture medium 1, (*B*) cardiovascular construct 1 in culture medium 1 and (*C*) monoculture in control medium (SFM). Cardiomyocytes (cardiac troponin T, *green*) were co-localized with the vascular-like network(von Willebrand Factor, *red*) in (*D*) cardiovascular construct 2 in culture medium 4, (*E*) cardiovascular construct 1 in culture medium 5 and (*F*) cardiovascular construct 1 in culture medium 1. *Scale bars* are 300 μm.

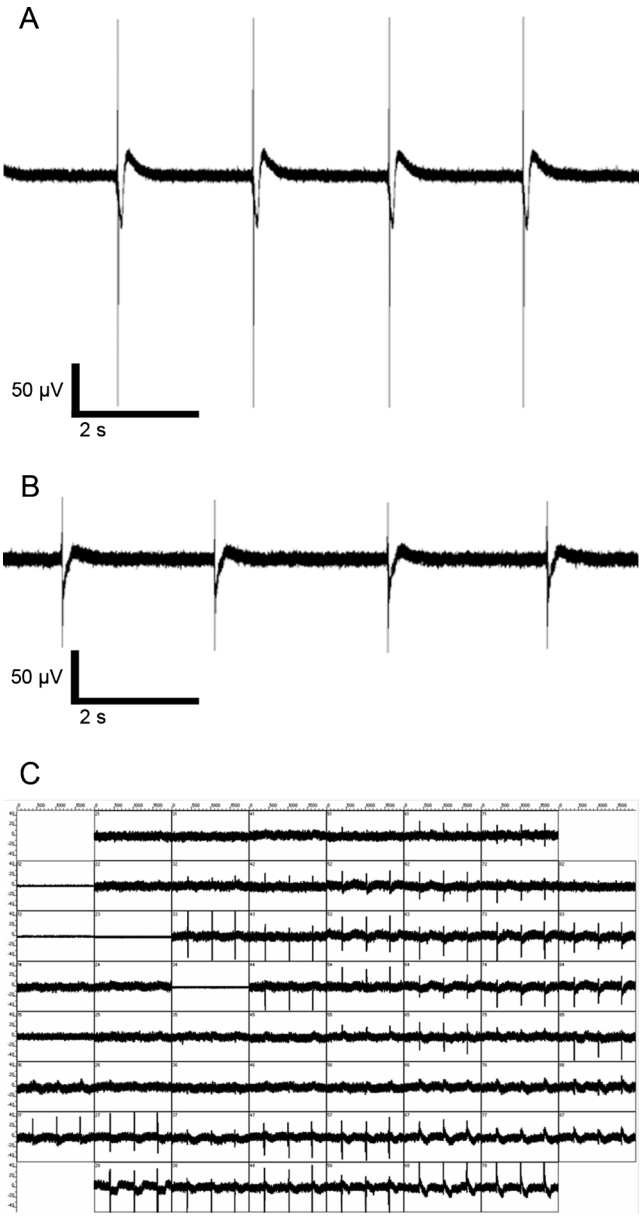

Figure 3. MEA measurements of CMs (*A*) in monoculture ($n=3$), (*B*) on top of the vascular-like network formed by HUVEC+hASC in cardiovascular construct 1 ($n=5$). (*C*) The measurements showed synchronous contraction of CMs on top of the construct 1.

Discussion

To reliably mimic the in vivo environment of heart the in vitro construct should include all critical cardiac cells including cardiomyocytes, endothelial cells and stromal cells (pericytes, smooth muscle cells, and fibroblasts). Constructs composed of single target cells are lacking the crucial microenvironment and cell–cell contacts. In addition, the cells should preferably be characterized in genotypical and phenotypical level in order to develop a high-quality in vitro construct.

In this study, two different in vitro cardiovascular constructs were developed. The constructs are based on supporting and interacting platform of vascular-like networks and NRCs. First construct is composed of NRCs, HUVECs, and human adipose stromal cells. The second construct is composed of NRCs, HUVECs, and human foreskin fibroblasts. NRCs were used in the constructs for proof of concept purposes as they can be obtained in larger amounts, and are more easily available than human CMs. Both cardiovascular constructs in this study are based on quality-controlled primary HUVECs with fixed passage (Sarkanen et al. 2011). In regards to the angiogenic and anti-apoptotic potential hASCs used in the cardiovascular constructs are well defined by us (Sarkanen et al. 2012) and others (Miranville et al. 2004; Rehman et al. 2004; Kilroy et al. 2007; Traktuev et al. 2008; Rubina et al. 2009: De Siena et al. 2010).

In the previous studies, the importance of stromal cells and endothelial cells to the viability and functionality of CMs has been shown (Narmoneva et al. 2004, Hsieh et al. 2006, Sadat et al. 2007, Tulloch et al. 2011). However, to our knowledge, the effects of premature vascular-like network formed by HUVEC+fibroblast or by HUVEC+hASC on cardiomyocyte viability and functionality without artificial scaffold has not been studied earlier. Our results showed that the contractility of rat CMs remained longer in culture with HUVEC+hASC/fibroblasts. Vascular-like network enabled a prolonged functionality of the CMs up to 14 d while the functionality of CMs in monoculture was approximately seven days with optimized cell amount. Furthermore, in both constructs, a synchronized contractility, an essential quality for properly functioning heart tissue, was visually detected also suggesting properly functioning junctional proteins.

Present tissue engineering strategies often rely on the use of scaffolds that may, however, interfere with the cell-cell interactions, cell assembly, and induce inflammatory reaction (Shimizu et al. 2003; Norotte et al. 2009). In this study, no artificial scaffolds were used. The 3D nature of HUVEC+hASC co-culture and intense vascular-like network provides mechanical support and inductive growth factors, thus acting as a natural scaffold. When the structure of the cardiovascular constructs was studied in different culture media the CMs were seen to co-localize with the vascular-like structures in both constructs. Based on earlier microscopic analysis HUVEC+hASC vascular-like network is densely branched and three-dimensional [approximately 200 μm thick (Sarkanen et al. 2012)] thus leading CMs to distribute throughout the network without organization into any major direction. HUVEC+fibroblast forms a less dense (approximately 50 μm thick, unpublished data) network and enhanced parallel organization of vascular-like structures and co-localization of CMs. In both constructs we could detect elongated phenotype of CMs resembling mature morphology. The co-localization of CMs and HUVEC+fibroblast vascular-like network may mimic more closely native heart (Kyösola et al. 1983), as we believe that cardiovascular construct 2 resembles more closely

the in vivo cardiomyocyte alignment shown by Narang et al. (2004). However, this needs to be further studied.

Our results suggest that already premature vascular-like network with short tubules, i.e., not completely matured vascular structures, is sufficient for enhanced viability and contractile capacity of CMs. Premature vascular-like network is missing some features of mature tubules, including lack of mural cells thus leading to incompletely developed basement membrane and unstable tubule structure (Rivron et al. 2008). The paracrine effects of the co-cultured cells seem to be critical. Activated hASC and HUVEC produce several angiogenic and anti-apoptotic factors (Rehman et al. 2004; De Siena et al. 2010) and may therefore increase the viability and functionality of CMs. Cell–cell contacts including endothelial–cardiomyocyte contacts are known to be crucial in maintaining the rhythmic and synchronous contraction of CMs (Brutsaert 2003). The vascular-like network in our cardiovascular construct might assist in the formation of cell-cell contacts thus enabling the formation of gap junctions. This could explain our finding that strong contractility was observed with fewer CMs in the presence of the vascular-like network than without it. The co-localization of CMs and vascular-like network may also enable better conduction of electrical signals.

There is lack of information about medium including optimal serum concentration, growth factors and additional supplement in in vitro cardiac construct (Sekine et al. 2008; Valarmathi et al. 2010; He et al. 2012; Hussain et al. 2013). In cardiomyocyte culture, the medium is essential for maintenance of cell morphology, growth characteristics, and phenotypic modulations (Li 2002). In our study, the results revealed that serum-free medium supplemented with VEGF, FGF, and additionally with ascorbic acid, heparin, and hydrocortisone provided the best results for cardiovascular construct. However, in order to get an optimal construct, a compromise between contractile function of the CMs and a mature vascular network formation was needed. VEGF and FGF are well-known angiogenic factors that stimulate ECs to form new vessels (Cao et al. 2004). Moreover, VEGF regulates the development of vascular endothelium and the endocardium by inducing multiple angiogenic cellular responses, including promotion of survival, migration, and differentiation, through the activation of Akt signaling in ECs (Ferrara et al. 1996). Therefore, the designed growth factor combination in our construct supported not only vascular-like network formation but also the prolonged functionality of CMs.

The concentration of serum in the medium plays an essential role in determining the phenotype of the cultured CMs. More mitogenic medium stimulates cell proliferation whereas CMs cultured in lower serum concentrations (0–5% FBS) maintain the cell number, phenotype, and contractile properties. (Li 2002) We tested the cardiovascular constructs in low (2%) serum as well as in serum-free conditions aiming at in vivo-like environment with mature CMs. The results showed that serum was not needed in order to produce functional cardiovascular construct. CM contractility could be maintained in serum-free conditions and, additionally, obtain more mature, rod-shaped phenotype of the cells.

Engineered cardiac tissue should have functional and morphological properties similar to that of native myocardium (Iyer et al. 2011). Cardiac grafts should be thick and compact, and contain physiologic density of metabolically active, differentiated cells (Radisic et al. 2006). The constructs developed here consisted of the cell types naturally resident in heart thus providing the essential components needed for in vitro modeling of myocardium. The results of the current study can be further utilized in development of a human heart tissue model. This is a first step towards physiologically relevant and clinically predictive in vitro cardiovascular model.

Conclusions

In this study, the ability of two different vascular-like networks to support the viability and functionality of CMs was assessed. When combining a vascular-like network with CMs the viability and functionality of CMs was markedly improved. Multicellular constructs also allowed synchronized contractility of CMs. The results suggest that the cardiovascular constructs developed provide a promising new tool for the assessment of toxicological and safety pharmacological effects of compounds in vitro.

Acknowledgments We sincerely thank Ms. Mirja Hyppönen, Ms. Sari Leinonen, Ms. Hilkka Mäkinen, and Ms. Henna Venäläinen for the excellent technical assistance. We also thank Dr. Erja Kerkelä and Mr. Mika Helminen for their contribution to this work. We would like to acknowledge the personnel of the animal facilities of University of Tampere.

Funding Funding for the project was provided by Pirkanmaa Centers for Economic Development, Transport and the Environment; City of Tampere; Ministry of Education and Culture; Ministry of Agriculture and Forestry; Finnish Cultural Foundation; Academy of Finland; Tekes—the Finnish Funding Agency for Technology and Innovation; Paavo Nurmi Foundation; Foundation of Aarne and Aili Turunen; Finnish Foundation for Cardiovascular Research and FinPharma Doctoral Program.

References

Banerjee I.; Fuseler J. W.; Price R. L.; Borg T. K.; Baudino T. A. Determination of cell types and numbers during cardiac development in the neonatal and adult rat and mouse. *Am. J. Physiol. Heart Circ. Physiol.* 293: H1883–91; 2007.

Banyasz T.; Lozinskiy I.; Payne C. E.; Edelmann S.; Norton B.; Chen B.; Chen-Izu Y.; Izu L. T.; Balke C. W. Transformation of adult rat cardiac myocytes in primary culture. *Exp. Physiol.* 93: 370–82; 2008.

Bhattacharya S.; MacDonald S. T.; Farthing C. R. Molecular mechanisms controlling the coupled development of myocardium and coronary vasculature. *Clin. Sci. (Lond.)* 111: 35–46; 2006.

Brutsaert D. L. Cardiac endothelial-myocardial signaling: its role in cardiac growth, contractile performance, and rhythmicity. *Physiol. Rev.* 83: 59–115; 2003.

Cao R.; Eriksson A.; Kubo H.; Alitalo K.; Cao Y.; Thyberg J. Comparative evaluation of FGF-2-, VEGF-A-, and VEGF-C-induced angiogenesis, lymphangiogenesis, vascular fenestration, and permeability. *Circ. Res.* 94: 664–70; 2004.

Caspi O.; Lesman A.; Basevitch Y.; Gepstein A.; Arbel G.; Habib I. H.; Gepstein L.; Levenberg S. Tissue engineering of vascularized cardiac muscle from human embryonic stem cells. *Circ. Res.* 100: 263–72; 2007.

De Siena R.; Balducci L.; Blasi A.; Montanaro M. G.; Saldarelli M.; Saponaro V.; Martino C.; Logrieco G.; Soleti A.; Fiobellot S.; Madeddu P.; Rossi G.; Ribatti D.; Crovace A.; Cristini S.; Invernici G.; Parati E. A.; Alessandri G. Omentum-derived stromal cells improve myocardial regeneration in pig post-infarcted heart through a potent paracrine mechanism. *Exp. Cell Res.* 316: 1804–15; 2010.

Ferrara N.; Carver-Moore K.; Chen H.; Dowd M.; Lu L.; O'Shea K. S.; Powell-Braxton L.; Hillan K. J.; Moore M. W. Heterozygous embryonic lethality induced by targeted inactivation of the VEGF gene. *Nature* 380: 439–42; 1996.

Gimble J.; Guilak F. Adipose-derived adult stem cells: isolation, characterization, and differentiation potential. *Cytotherapy* 5: 362–9; 2003.

He W.; Ye L.; Li S.; Liu H.; Wu B.; Wang Q.; Fu X.; Han W.; Chen Z. Construction of vascularized cardiac tissue from genetically modified mouse embryonic stem cells. *J. Heart. Lung. Transplant.* 31: 204–12; 2012.

Hsieh P. C.; Davis M. E.; Lisowski L. K.; Lee R. T. Endothelial–CM interactions in cardiac development and repair. *Annu. Rev. Physiol.* 68: 51–66; 2006.

Hussain A.; Collins G.; Yip D.; Cho C. H. Functional 3-D cardiac co-culture model using bioactive chitosan nanofiber scaffolds. *Biotechnol. Bioeng.* 110: 637–47; 2013.

Iyer R. K.; Chiu L. L.; Reis L. A.; Radisic M. Engineered cardiac tissues. *Curr Opin Biotech* 22: 706–14; 2011.

Jaffe E. A.; Nachman R. L.; Becker C. G.; Minick C. R. Culture of human endothelial cells derived from umbilical veins. Identification by morphologic and immunologic criteria. *J. Clin. Invest.* 52: 2745–56; 1973.

Kettenhofen R.; Bohlen H. Preclinical assessment of cardiac toxicity. *Drug Discov. Today* 13: 702–7; 2005.

Kilroy G. E.; Foster S. J.; Wu X.; Ruiz J.; Sherwood S.; Heifetz A.; Ludlow J. W.; Stricker D. M.; Potiny S.; Green P.; Halvorsen Y. D.; Cheatham B.; Storms R. W.; Gimble J. M. Cytokine profile of human adipose-derived stem cells: expression of angiogenic, hematopoietic, and pro-inflammatory factors. *J. Cell. Physiol.* 212: 702–9; 2007.

Kreutziger K. L.; Muskheli V.; Johnson P.; Braun K.; Wight T. N.; Murry C. E. Developing vasculature and stroma in engineered human myocardium. *Tissue Eng. Part. A* 17: 1219–28; 2011.

Kujala V. J.; Jimenez Z. C.; Väisänen J.; Tanskanen J. M.; Kerkelä E.; Hyttinen J.; Aalto-Setälä K. Averaging in vitro cardiac field potential recordings obtained with microelectrode arrays. *Comput. Methods Programs. Biomed.* 104: 199–205; 2011.

Kyösola K.; Rechardt L.; Merikallio E.; Järvinen A.; Mattila T.; Waris T.; Aalto-Setälä K. Cardioplegia versus topical cooling for cardiac protection during open-heart surgery. An electron microscopic and histochemical study of right atrial biopsies. *Ann. Clin. Res.* 15: 156–63; 1983.

Lasser K. E.; Allen P. D.; Woolhandler S. J.; Himmelstein D. U.; Wolfe S. M.; Bor D. H. Timing of new black box warnings and withdrawals for prescription medications. *JAMA* 287: 2215–20; 2002.

Lesman A.; Gepstein L.; Levenberg S. Vascularization shaping the heart. *Ann. N.Y. Acad. Sci* 1188: 46–51; 2010.

Lexchin J. Drug withdrawals from the Canadian market for safety reasons, 1963–2004. *CMAJ* 172: 765–7; 2005.

Li RK (2002) Cardiomyocytes. In: Koller MR, Palsson BO and Masters JRW, editors. Human Cell Culture: vol V: Primary Mesenchymal Cells. Kluwer. pp. 118-119.

Miranville A.; Heeschen C.; Sengenés C.; Curat C. A.; Busse R.; Bouloumíe A. Improvement of postnatal neovascularization by human adipose tissue-derived stem cells. *Circulation* 110: 349–55; 2004.

Montessuit C.; Rosenblatt-Velin N.; Papageorgiou I.; Campos L.; Pellieux C.; Palma T.; Lerch R. Regulation of glucose transporter expression in cardiac myocytes: p38 MAPK is a strong inducer of GLUT4. *Cardiovasc. Res.* 64: 94–104; 2004.

Nag A. C. Study of non-muscle cells of the adult mammalian heart: a fine structural analysis and distribution. *Cytobios* 28: 41–61; 1980.

Narang D.; Sood S.; Thomas M. K.; Dinda A. K.; Maulik S. K. Effect of dietary palm olein oil on oxidative stress associated with ischemic–reperfusion injury in isolated rat heart. *BMC Pharmacology* 4: 29–38; 2004.

Narmoneva D. A.; Vukmirovic R.; Davis M. E.; Kamm R. D.; Lee R. T. Endothelial cells promote cardiac myocyte survival and spatial reorganization. *Circulation* 110: 962–8; 2004.

Norotte C.; Marga F. S.; Niklason L. E.; Forgacs G. Scaffold-free vascular tissue engineering using bioprinting. *Biomaterials* 30: 5910–7; 2009.

Radisic M.; Malda J.; Epping E.; Geng W.; Langer R.; Vunjak-Novakovic G. Oxygen gradients correlate with cell density and cell viability in engineered cardiac tissue. *Biotechnol. Bioeng.* 93: 332–43; 2006.

Radisic M.; Park H.; Martens T. P.; Salazar-Lazaro J. E.; Geng W.; Wang Y.; Langer R.; Freed L. E.; Vunjak-Novakovic G. Pre-treatment of synthetic elastomeric scaffolds by cardiac fibroblasts improves engineered heart tissue. *J. Biomed. Mater. Res. A* 86: 713–24; 2008.

Redfern W. S.; Carlsson L.; Davis A. S.; Lynch W. G.; MacKenzie I.; Palethorpe S.; Siegl P. K.; Strang I.; Sullivan A. T.; Wallis R.; Camm A. J.; Hammond T. Relationships between preclinical cardiac electrophysiology, clinical QT interval prolongation and torsade de pointes for a broad range of drugs: evidence for a provisional safety margin in drug development. *Cardiovas. Res.* 58: 32–45; 2003.

Rehman J.; Traktuev D. O.; Li J.; Merfeld-Clauss S.; Temm-Grove C. J.; Bovenkerk J. E.; Pell C. J.; Johnstone B. H.; Considine R. V.; March K. L. Secretion of angiogenic and antiapoptotic factors by human adipose stromal cells. *Circulation* 109: 1292–8; 2004.

Reppel M.; Pillekamp F.; Lu Z. J.; Halbach M.; Brockmeier K.; Fleischmann B. K.; Hescheler J. Microelectrode arrays: a new tool to measure embryonic heart activity. *J. Electrocardiol.* 37: 104–9; 2004.

Rivron N. C.; Liu J. J.; Rouwkema J.; de Boer J.; van Blitterswijk C. A. Engineering vascularised tissues in vitro. *Eur. Cell. Mater.* 15: 27–40; 2008.

Rubina K.; Kalinina N.; Efimenko A.; Lopatina T.; Melikhova V.; Tsokolaeva Z.; Sysoeva V.; Tkachuk V.; Parfyonova Y. Adipose stromal cells stimulate angiogenesis via promoting progenitor cell differentiation, secretion of angiogenic factors, and enhancing vessel maturation. *Tissue. Eng. Part. A* 15: 2039–50; 2009.

Sadat S.; Gehmert S.; Song Y. H.; Yen Y.; Bai X.; Gaiser S.; Klein H.; Alt E. The cardioprotective effect of mesenchymal stem cells is mediated by IGF-I and VEGF. *Biochem. Biophys. Res. Commun.* 363: 674–9; 2007.

Sarkanen JR, Mannerström M, Vuorenpää H, Uotila J, Ylikomi T and Heinonen T. (2011) Intralaboratory validation of a human cell based in vitro angiogenesis assay for testing angiogenesis modulators. Front Pharmacol 1. doi: 10.3389/fphar.2010.00147

Sarkanen J. R.; Vuorenpää H.; Huttala O.; Mannerström B.; Kuokkanen H.; Miettinen S.; Heinonen T.; Ylikomi T. Adipose stromal cell tubule network model provides a versatile tool for vascular research and tissue engineering. *Cells Tissues Organs.* 196: 385–97; 2012.

Sekine H.; Shimizu T.; Hobo K.; Sekiya S.; Yang J.; Yamato M.; Kurosawa H.; Kobayashi E.; Okano T. Endothelial cell coculture within tissue-engineered cardiomyocyte sheets enhances neovascularization and improves cardiac function of ischemic hearts. *Circulation* 118: S145–52; 2008.

Shimizu T.; Yamato M.; Kikuchi A.; Okano T. Cell sheet engineering for myocardial tissue reconstruction. *Biomaterials* 24: 2309–16; 2003.

Stevens K. R.; Kreutziger K. L.; Dupras S. K.; Korte F. S.; Regnier M.; Muskheli V.; Nourse M. B.; Bendixen K.; Reinecke H.; Murry C. E. Physiological function and transplantation of scaffold-free and vascularized human cardiac muscle tissue. *PNAS* 106: 16568–73; 2009.

Traktuev D. O.; Merfeld-Clauss S.; Li J.; Kolonin M.; Arap W.; Pasqualini R.; Johnstone B. H.; March K. L. A population of multipotent CD34-positive adipose stromal cells share pericyte and mesenchymal surface markers, reside in a periendothelial location, and stabilize endothelial networks. *Circ. Res.* 102: 77–85; 2008.

Tulloch N. L.; Muskheli V.; Razumova M. V.; Korte F. S.; Regnier M.; Hauch K. D.; Pabon L.; Reinecke H.; Murry C. E. Growth of engineered human myocardium with mechanical loading and vascular coculture. *Circ. Res.* 109: 47–59; 2011.

Uusimaa P. A.; Hassinen I. E.; Vuolteenaho O.; Ruskoaho H. Endothelin-induced atrial natriuretic peptide release from cultured neonatal cardiac myocytes: the role of extracellular calcium and protein kinase-C. *Endocrinology* 130: 2455–64; 1992.

Valarmathi M. J.; Goodwin R. L.; Fuseler J. W.; Davis J. M.; Yost M. J.; Potts J. D. A 3-D cardiac muscle construct for exploring adult marrow stem cell based myocardial regeneration. *Biomaterials* 31: 3185–200; 2010.

Vascular-like Network Enhances Maturation of Pluripotent Stem Cell derived Cardiomyocytes in Cardiovascular Construct

Hanna Vuorenpää[1,3*], Kirsi Penttinen[2,3*], Tuula Heinonen[1,3], Mari Pekkanen-Mattila[2,3], Jertta-Riina Sarkanen [3,4], Timo Ylikomi [1,3,4] and Katriina Aalto-Setälä[2,3,5]

[1]FICAM, Finnish Centre for Alternative Methods, School of Medicine, University of Tampere, Tampere, Finland.
[2]BioMediTech, University of Tampere, Tampere, Finland.
[3]School of Medicine, University of Tampere, Tampere, Finland.
[4]Department of Cell Biology, School of Medicine, University of Tampere, Tampere, Finland.
[5]Heart Hospital, Tampere University Hospital, Tampere, Finland.

[*] These two authors equally contributed to this work

Hanna Vuorenpää, M.Sc., tel. +358401904105, e-mail: hanna.vuorenpaa@staff.uta.fi, mailing address: FICAM, Finnish Centre for Alternative Methods, School of Medicine, FI-33014 University of Tampere, Finland.

Kirsi Penttinen, M.Sc. (Tech.), e-mail: kirsi.penttinen@uta.fi, mailing address: BioMediTech, Institute of Biomedical Technology, Biokatu 12, FI-33014 University of Tampere, Finland.

Tuula Heinonen, PhD, e-mail: tuula.heinonen@staff.uta.fi, mailing address: FICAM, Finnish Centre for Alternative Methods, School of Medicine, FI-33014 University of Tampere, Finland.

Mari Pekkanen-Mattila, PhD, e-mail: mari.pekkanen-mattila@uta.fi, address: BioMediTech, Institute of Biomedical Technology, Biokatu 12, FI-33014 University of Tampere, Finland.

Jertta-Riina Sarkanen, PhD, e-mail: riina.sarkanen@staff.uta.fi, mailing address: Cell Biology, School of Medicine, FI-33014 University of Tampere, Finland.

Timo Ylikomi, MD, PhD, e-mail: timo.ylikomi@staff.uta.fi, mailing address: Cell Biology, School of Medicine, FI-33014 University of Tampere, Finland.

Katriina Aalto-Setälä, MD, PhD, email: katriina.aalto-setala@uta.fi, mailing address: IBT, Institute of Biomedical Technology, Biokatu 12, FI-33014 University of Tampere, Finland.

Corresponding author: Hanna Vuorenpää, M.Sc., tel. +358401904105, e-mail: hanna.vuorenpaa@staff.uta.fi, mailing address: FICAM, Finnish Centre for Alternative Methods, School of Medicine, FI-33014 University of Tampere, Finland.

This manuscript includes 6530 words (including abstract, manuscript text, references, figure legends and table).

ABSTRACT

In vitro cardiac models should include vascular structures to mimic the highly vascularized myocardium and to provide interactions between endothelial cells, stromal cells and cardiomyocytes. Currently, human pluripotent stem cell derived cardiomyocytes have been shown to present immature morphology and fetal-like electrophysiological properties that may limit their use as physiological test platform. The aim of this study was to develop multicellular *in vitro* cardiovascular construct modeling human heart tissue for cardiac safety and efficacy testing.

In the cardiovascular construct, human pluripotent stem cell-derived cardiomyocytes (CM) were cultured with vascular-like network formed by human foreskin fibroblasts and human umbilical vein endothelial cells that served as a supporting platform in the construct. CM orientation, maturation, electrophysiological properties and drug responses of the cardiovascular construct were characterized and compared to CM monoculture.

CM in cardiovascular construct showed elongated morphology and aligned with the vascular-like network. Electrophysiological properties and calcium metabolism of CM as well as response to E-4031 and adrenalin demonstrated normal physiological behavior. Gene expression studies demonstrated increased expression of cardiac structural proteins and ion channels in cardiovascular construct compared to CM monoculture.

In conclusion, vascular-like network supports the structural and functional maturation of CM. Our results suggest that cardiovascular construct presents more mature *in vitro* cardiac model compared to CM monoculture and could therefore serve as an advanced test system for cardiac safety and efficacy assessment.

INTRODUCTION

In mammalian cardiogenesis, atrial and ventricular cardiomyocytes, conduction system with pacemaker cells as well as smooth muscle and non-muscle cell types including endothelial, valvular, and endocardial cells are generated [1]. Cardiomyocytes account 20-40% of all cardiac cells in adult heart with the majority of cells being highly adaptive cells including fibroblasts, vascular smooth muscle cells and endothelial cells [2, 3]. In cardiac microenvironment, cardiomyocytes are embedded in an aligned extracellular matrix (ECM) that facilitates the coordinated contractile function of the heart [1]. Cells and ECM proteins, mainly produced by fibroblasts, are connected via cell–cell and cell–matrix interactions to maintain the structural organization and functionality of the heart [4, 5]. In mature myocardium, each cardiomyocyte has physical contact with at least one capillary blood vessel [6]. The interactions between vasculature and myocardium are bidirectional [7], and active through the adult life affecting cardiac growth, function and rhythm [3]. Vascular endothelial cells produce several angiogenic and anti-apoptotic factors including vascular endothelial growth factor (VEGF), angiopoietins and nitric oxide that influence cardiac metabolism, growth and functionality of the heart [3]. Beside to endothelial cells, also fibroblasts secrete angiogenic factors in addition to growth and differentiation factors with autocrine and paracrine effects. Fibroblasts have also been shown to give mechanical support and produce factors that promote the organization of cardiomyocytes into 3D structures in collagen matrices. [5, 8]

Cardiotoxicity is one of the leading causes of failure for new therapeutic molecules in preclinical development [9]. Presently, pharmaceutical industry relies upon animal testing although there are fundamental differences in the electrophysiological properties of animal and human cardiomyocytes [10]. In particular, the differences in ion channels and currents impact the transferability of drug screening and toxicity studies from murine to humans [11]. In addition to animal models, transfected non-cardiac cells have been used. However, these cells express usually only one cardiac ion channel of interest and all the other characteristics of human cardiomyocyte are lacking [12]. Therefore, there is a need for improved preclinical drug screening test system especially for assessment of cardiotoxic effects and for evaluation of the efficacy of new drug candidates [10, 13].

Functional cardiomyocytes derived from human pluripotent stem cells could provide a significant advantage over the previously used cardiac models. Human pluripotent stem cell derived cardiomyocytes (hPSC-CM) contract spontaneously and respond appropriately to cardioactive drugs [14]. These cells could be useful in early efficacy and toxicity screening, improving the selection of lead

candidates and the reduction of adverse outcomes in clinical stages of drug development [15]. However, since hPSC-CM have been shown to display functional properties typical to human fetal CM, the immature state of hPSC-CM may complicate their utilization [14, 16]. Ventricular cardiomyocytes in the adult human heart are large and brick-shaped whereas hPSC-CM are markedly smaller with round or triangular morphology [17]. Although the expression of cardiac structural proteins, such as α-myosin heavy chain *(*MYH6*),* is shown to be very low in undifferentiated hPSC-CM, it is strongly upregulated during *in vitro* differentiation [18]. This has been further supported by the finding that hPSC-CM do mature electrophysiologically over time *in vitro* but without reaching the adult CM maturity [19]. In addition to the increased time in culture, other methods have been utilized in the production of more mature hPSC-CMs such as electrical stimulation [20] and 3D culture environment [4, 6, 21-23]. However, the use of scaffolds to enable 3D environment has been associated with reduced cell-cell contacts, as well as incorrect deposition and alignment of extracellular matrix in cardiac constructs [24].

In this study, a multicellular *in vitro* cardiovascular construct without artificial scaffold was developed to mimic adult human heart. In the construct, hPSC-CM were co-cultured with vascular-like network composed of human fibroblasts and human umbilical vein endothelial cells (HUVEC). Vascular-like network served as a supporting platform to create natural microenvironment with cell-cell and cell-matrix interactions. The effects of the vascular-like network on cardiomyocyte morphology, gene expression and functionality were studied.

MATERIALS AND METHODS

Ethics

This study conforms to the principles outlined in the Declaration of Helsinki. The use of human umbilical cord derived cells (HUVEC) and iPSC were approved by Ethics Committee of the Pirkanmaa Hospital District, Tampere, Finland (approval numbers R08028 and R08070, respectively) and a written informed consent was obtained from all the participants.

Cell culture and differentiation

Isolation and culture of human umbilical vein endothelial cells

HUVEC were isolated from human umbilical cord vein by using enzymatic procedure as described previously by us [25]. Cells were cultured in EGM-2 medium (Lonza Group Ltd, Table 1) and tested for mycoplasma contamination (MycoAlert® Mycoplasma Detection Kit, Lonza Group Ltd) before experimental use.

Culture of human foreskin fibroblasts

Human foreskin fibroblasts were purchased from American Type Culture Collection (CRL-2522; ATCC, Manassas, VA, USA). Cells were cultured in fibroblast medium consisting of Minimum Essential Medium with Earle's salts, w/o l-Glutamine (Gibco) supplemented with 10% FBS (Gibco), 1% l-glutamine (Gibco) and 1% NEAA (Gibco). Cells were tested for mycoplasma contamination (MycoAlert® Mycoplasma Detection Kit, Lonza) before experimental use.

Generation of Patient-Specific iPSC line and Cell culture of pluripotent stem cells

Patient-specific iPSC line UTA.04602.WT was established from a healthy individual as described earlier [26]. Results of the characterization of UTA.04602.WT cell line have been described earlier [27]. H7 is a commercial hESC line purchased from WiCell Research Institute, Madison, WI, USA.

UTA.04602.WT cells and H7 hESC were cultured on mitomycin C inactivated mouse embryonic fibroblasts (MEF) in KSR medium (Table 1) which consisted of DMEM/F-12 (Invitrogen) supplemented with 20% KnockOut serum replacement (Invitrogen), 1% non-essential amino acids (Lonza), 2 mM Glutamax (Invitrogen), 50 U/ml penicillin/streptomycin (Lonza), 0.1 mM beta mercaptoethanol (Invitrogen), and 7.8 ng/ml basic fibroblast growth factor (R&D Systems). The medium was refreshed daily, and the stem cell colonies were passaged onto a new MEF layer once a week using 1 mg/ml collagenase IV (Invitrogen).

Differentiation of cardiomyocytes

Differentiation of pluripotent stem cells into cardiomyocytes was carried out with either by co-culturing hESC or iPSC with murine visceral endoderm-like (END-2) cells (Humbrecht Institute, Utrecht, The Netherlands) as described earlier [28] or with small molecule differentiation method via temporal modulation of canonical Wnt signaling [29]. Both differentiation methods formed beating cardiomyocyte aggregates. These were mechanically excised and treated with collagenase A (Roche Diagnostics) to dissociate beating aggregates to single cell level.

Development of cell models

Human cardiomyocyte monoculture

After dissociation human CM were seeded in EB 5 % medium (Table 1) at density of 0,01-0,04 x 10^6 cells/cm^2. EB 5 % medium was changed 1-2 days after cell seeding and thereafter every second or third day. CM monoculture was used as a control to cardiovascular construct throughout the study.

Vascular-like network from co-culture of HUVEC and fibroblast

The co-culture was established as described earlier [25]. Briefly, fibroblasts (p 6-7), 20 000 cells/cm^2 were seeded in fibroblast medium (Table 1) and grown for 2-3 days to confluency. HUVEC were seeded on top of fibroblasts at 4000 cells/cm^2 in EGM-2 medium (Table 1). The day after cell seeding, angiogenic stimulation medium (EBM-2, Lonza), 2 % FBS, 1 mM L-glutamine, 10 ng/ml vascular endothelial growth factor (VEGF, Sigma) and 1 ng/ml fibroblast growth factor 2 (FGF-2, Sigma) (Table 1) was changed. The angiogenic stimulation medium was changed twice during the 6 day co-culture prior to CM seeding.

Cardiovascular construct

EB 5 % medium (Table 1) was changed to HUVEC+fibroblast co-culture before seeding of CM. Dissociated human iPS- or hESC-derived CM were seeded on top of the HUVEC + fibroblast co-culture at day 6, when the vascular-like network was already formed, at a density of 0,01-0,04 x 10^6 cells/cm^2 in EB 5 % medium (Figure 1). 1-2 days after CM seeding first EB medium change was performed and thereafter three times in a week. The viability of cardiovascular constructs was evaluated visually under microscope by assessing the contraction of the cardiomyocytes and vascular-like network formation of the HUVECs and fibroblasts at least three times in a week.

Media development

In cardiovascular construct medium was designed to primarily support CM functionality and secondarily to induce vascular-like network formation. Minimum serum concentration for CM monoculture was tested due to our objective to have low-serum or serum-free culture conditions.

Immunocytochemistry

Cardiomyocytes were stained either with goat anti-cardiac-troponin-T (anti-Tnt, 1:1500, Abcam) or with mouse anti-Tnt (1:500, Abcam) and the vascular-like formation was visualized with basement membrane marker mouse collagen IV (anti-ColIV, 1:500, Sigma) for 1 hour at RT or in+ 4 °C o/n. Polyclonal IgG Alexa Fluor 568 (Abcam) for goat anti-Tnt and polyclonal IgG FITC (1:100, Sigma) for anti-ColIV and mouse anti-Tnt were used as secondary antibodies for 30 min in RT. Fluorescence was visualized with Nikon Eclipse Ti-S microscope (Nikon) or with confocal laser scanning microscope Zeiss LSM780 Laser Scanning Confocal Microscope (ZEISS) and the images were processed with Zen2009 (confocal images, Carl Zeiss) and with Adobe Photoshop software 7.0 (Adobe Systems).

Quantitative Real Time-PCR

Gene expression in CM monoculture, vascular-like network and cardiovascular construct were analyzed. The total RNA was extracted at day 1, 6, 7 and 18 (Figure 1) using using PureLink RNA Mini Kit (Life Technologies) following the manufacturer's protocol. Concentration and purity of RNA was assessed using spectrophotometry with microplate reader in Varioskan Flash Spectrophotometer (ThermoScientific) before further use. Reverse transcription of the total RNA to cDNA was performed using iScript cDNA synthesis kit (Bio-Rad) following manufacturer's instructions. qRT-PCR was performed according to standard protocols on Abi Prism 7300 instrument (Applied Biosystems) or on Bio-rad CFX96 Real Time System (BioRad). The expression of angiogenesis related genes including *VEFG-A, FGF-2, PDGFβ, TGFβ1, Angiopoietin1, Angiopoietin2* and cardiac related genes including *CACNA1C, TNNT2, KCNJ2, CX-43, MYH-6, MYH-7* were studied with SYBR chemistry. In addition, the expression of cardiac related genes *ADRB1*and *SCN5a* as well as reference genes *RPLP0* and *GAPDH* were studied using Taqman chemistry with Taqman Universal PCR Master Mix (Applied Biosystems). The following Taqman assays (x20) were used: Hs02330048_s1 for ADRB1, Hs00165693_m1 for SCN5A, Hs04189669_g1 for RPLO0 and Hs02758991_g1 for GAPDH (Applied Biosystems). SYBR primer sequences can be

found in supplemental data. The relative expression levels were determined by using the comparative method (ΔΔCt) [30].

Functional analyses

Micro electrode array (MEA) measurements

The ability of cardiovascular construct to conduct electrical signal was analyzed using the MEA system (Multi Channel Systems MCS GmbH). The MEA wells (8x8 standard MEAs or 6-well MEAs) were first hydrophilized with FBS and then coated with 0.1 % gelatin type A (Sigma-Aldrich).
Field potentials were recorded at day 10 or 18 (Figure 1) at 37°C, and signals were recorded for 2 min. The sampling frequency was 20 kHz. Field potentials were recorded during spontaneous baseline beating, and with 1µM adrenaline (Sigma-Aldrich) or 300nM E-4031(Sigma-Aldrich). Drugs were diluted and measurements performed in EB medium with 5% FBS. The field potentials were recorded with MC_Rack v.4.5.7 software (Multi Channel Systems MCS GmbH). Signals were analyzed with Cardiomyocyte MEA Data Analysis (CardioMDA) software (Pradhapan et al. 2013).

Analysis of Ca^{2+} cycling

Cardiovascular constructs were loaded with 4 µmol/L Fura-2 AM (Invitrogen, Molecular Probes) for 30 minutes in HEPES based medium. Measurements were assessed in 37°C and the extracellular solution and consisted of (in mmol/L): 137 NaCl, 5 KCl, 0.44 KH_2PO_4, 20 HEPES, 4.2 $NaHCO_3$, 5 D-glucose, 2 $CaCl_2$, 1.2 $MgCl_2$ and 1 Na-pyruvate (pH was adjusted to 7.4 with NaOH)

Ca^{2+} measurements were recorded at day 10 or 11 (Figure 1) and conducted on an inverted IX70 microscope (Olympus Corporation) with a UApo/340 x20 air objective (Olympus). Images were acquired with an ANDOR iXon 885 CCD camera (Andor Technology) synchronized with a Polychrome V light source by a real time DSP control unit and TILLvisION software (TILL Photonics). Fura-2 in CMs was excited at 340 nm and 380 nm light and the emission was recorded at 505 nm. For Ca^{2+} analysis, regions of interests were selected for spontaneously beating cells and background noise was subtracted before further processing. The Ca^{2+} levels are presented as ratiometric values of F340/F380. The changes in Ca^{2+} were recorded during spontaneous baseline beating and spontaneous beating during 1µM adrenaline (Sigma-Aldrich) perfusion.

Statistics

qPCR data is expressed as mean values +/- SD. Statistical analysis for the qPCR data was performed by IBM SPPS Statistics 22-software and by using Mann-Whitney U-test for independent samples. Bon ferroni -correction was included when more than two groups were analyzed. A *p*-value less than 0.05 was considered statistically significant.

In MEA and Ca2+ imaging data, the significance of differences between the two groups (CM monoculture and cardiovascular construct) was evaluated with the unpaired Student's *t*-test. The significance of changes within a group was evaluated with the paired Student's *t*-test. MEA and Ca2+ imaging data are expressed as average ± S.E.M. In Ca2+ imaging data n refers to the number of cells and in MEA data n refers to number of MEA chips. A *p*-value less than 0.05 was considered statistically significant.

RESULTS

Vascular-like network serves as a supporting and interactive platform for cardiovascular construct

Expression levels of angiogenesis related genes were analyzed at days 1, 6 and 18 in vascular-like network to assess the production of growth factors and maturation state of vascular structures (Figure 2). During the first six days the expression of fibroblast growth factor 2 (FGF-2), transforming growth factor β (TGF-*β)* and Angiopoietin-1 (Ang-1) had an increasing trend. Furthermore, statistically significant increase in the expression level was observed in Angiopoietin-2 (Ang-2) and platelet derived growth factor β (PDGF-β). During the days 6 - 18, the expression of aforementioned genes remained constant except for Angiopoietin-2 which had significantly increased expression level also during this time period.

The expression levels of the angiogenesis related genes were also assessed from the cardiovascular construct at day 6 and 18 (Figure 2). The expression levels of FGF-2, TGF-*β* and Angiopoietin-1 were at the similar level in cardiovascular construct compared to the vascular-like network. However, the expression levels of *VEGF* and PDGF-β were significantly higher in the cardiovascular construct.

Vascular-like network enhances mature cardiac phenotype and orientation of pluripotent stem cell derived cardiomyocytes in cardiovascular construct

Compared to the round morphology of CM in monoculture (Figure 3.A), more mature morphology with elongated CM was detected in the presence of vascular-like network (Figure 3.C-D). Moreover, 2D and 3D projections showed that CM co-localized longitudinally and parallel with tubular structures (Figure 3.E-F). On the contrary, CM in monoculture remained rounded, less organized and orientation of the cells could not be detected (Figure 3.B).

Expression levels of cardiac related genes were analyzed in cardiovascular construct on the day after CM seeding (day 7) and at day 18. The expression was similarly assessed from CM monoculture at the same time points (Figure 4). Results showed that the cardiac muscle myosin transcripts MYH6 and MYH7 as well as cardiac troponin T were significantly upregulated in cardiovascular construct over this time period whereas they remained constant or decreased in CM monoculture. Also expression level of gap junction marker connexin 43 was shown to increase significantly in cardiovascular construct while remaining low in CM monoculture. Furthermore, at day 18, MYH6,

MYH7, troponin T and connexin 43 were all expressed at significantly higher level in the cardiovascular construct compared to the CM monoculture (Figure 4).

In the cardiovascular construct, the expression levels of ion channels CACNA1C, KCNJ2 and SCN5A did not increase significantly between days 7 to 18 (Figure 4). However, similarly to structural genes, there was statistically significant difference when expression levels were compared between cardiovascular construct and CM monoculture at day 18. The expression of beta-1 adrenergic receptor (ADRB1) increased at statistically significant manner from day 7 to day 18 in the cardiac construct. Moreover, the expression was significantly higher at day 18 in the cardiovascular construct compared to CM monoculture.

Electrophysiological changes in pluripotent stem cell derived cardiomyocytes in cardiovascular construct suggest functional improvement of cardiomyocytes

The electrical activity of the cardiovascular construct was detectable with MEA and the contractility was synchronous (Figure 5.A). Adrenaline increased the beating frequency of CM (Figure 5.B-C) thus decreasing the field potential duration (FPD) in cardiovascular constructs as well as in CM monoculture (Figure 5.D). The increase in beating frequency and decrease in FPD was statistically significant between baseline and adrenaline only in cardiovascular construct.

E4031, a hERG blocker, was shown to significantly prolong the FPD in cardiovascular construct and in CM monoculture compared to the baseline but there was no significant difference between the groups (Figure 5. E-F). Prolongation of FPD due to E4031 exposure resulted in additional adverse effects including pausing beating and/or arrhythmias. These adverse effects were seen in CM monoculture as well as in cardiovascular construct (Figure 5.G).

Ca^{2+} transients of pluripotent stem cell derived cardiomyocytes in the absence and presence of vascular-like network

Cardiovascular construct and CM monoculture were shown to respond similarly to adrenaline exposure (See supplemental figure S1.A). When compared to baseline, adrenalin caused significant increase in beating frequency (Figure 6.D) and decrease in peak duration in both systems (Figure 6.B) and, additionally, a significant decrease in amplitude in cardiovascular construct (Figure 6.C). The

amplitude in cardiovascular construct was significantly lower at baseline as well as during adrenaline perfusion compared to those in CM monoculture (Figure 6.C).

The diastolic Ca^{2+} increased significantly in CM monoculture and in cardiovascular construct due to the adrenaline exposure (Figure 6.A). Ca^{2+} transient changes were also analysed separately for each cell as the ratio of adrenaline response divided by baseline response. The results showed that in cardiovascular construct adrenaline caused significant increase in beating frequency and significant decrease in amplitude when compared to CM monoculture (see supplemental figure S1.B).

DISCUSSION

Since *in vitro* assays aim at translating preclinical data into the clinical studies, it is crucial to use physiologically relevant model system [31]. In preclinical cardiotoxicity studies, the assessment of the risk for QT interval prolongation is part of the standard evaluation of new compounds as defined by the International Conference of Harmonization (ICH) Expert Working Group [9]. It has been stated that human pluripotent stem cell derived cardiomyocytes (hPSC-CM) based test systems could improve the early detection of QT prolongation with the benefit of being of human origin [32]. However, at the same time, it is widely acknowledged that hPSC-CM possess fetal-like characteristics, i.e. contractility with some proliferative capacity and with embryonic like electrophysiology. Although the factors affecting maturity remain largely unknown, cell line, time in culture, co-cultured cells and culture conditions appear to have an effect on the maturity. [14]

We have previously developed cardiovascular constructs based on co-culture of neonatal rat cardiomyocytes and two different vascular-like networks formed either by human adipose stromal cells+human umbilical vein endothelial cells (HUVEC) or HUVEC+fibroblasts. In the previous study, CM viability and functionality was maintained longer in co-culture with vascular-like network and, furthermore, morphological maturation with more elongated cardiomyocytes compared to CM monoculture was detected [33]. In the present study, vascular-like network formed by HUVEC and fibroblasts was combined with hPSC-CM to develop completely human cell based cardiovascular construct for cardiac safety and efficacy assessment.

Expression of cardiac structural protein coding genes MYH6 and MYH7 and cardiac troponin t increased markedly in cardiovascular construct whereas they remained constant or decreased in hPSC-CM monoculture. Also expression level of gap junction marker connexin 43 was shown to increase in cardiovascular construct. In CM monoculture, the overgrowth of non-cardiomyocytes may explain the decreased expression of structural transcripts MYH6, MYH7 and troponin T. However, similar overgrowth of non-cardiomyocytes was not detected in cardiovascular construct. These results suggest that vascular-like network improves the cardiac specific phenotype of hPSC-CM. Similar phenomenon has been reported previously. Genes coding structural proteins were expressed at higher level when cardiomyocytes were cultured with endothelial cells and fibroblasts with 3D biodegradable scaffold as reported by Caspi et al. [34]. Burridge et al. reported a similar kind of phenomenon in which troponin T expression at the protein level was significantly enhanced in the multicellular culture when compared to the CM monoculture [35]. In these studies, however, a 3D

matrix was used in addition to the co-culture. Our results are in line with the previous studies without hydrogel or any other external scaffold.

In heart, the extracellular matrix, mainly produced by the cardiac fibroblasts, guides cellular orientation and organization thus facilitating efficient cell contraction, force transduction and electrical transmission between the cells. The importance of alignment of CM in coordinated contraction is proven by the native cardiac structure, but also in *in vitro* studies. [4] In *in vitro* studies alignment of CM has been induced by microcontact printing demonstrating that alignment improves CM calcium handling and contractile properties when compared to randomly oriented cardiomyocyte monolayers [36, 37]. Since the use of scaffolds in cardiac constructs has been associated with reduced cell-cell contacts, as well as incorrect deposition and alignment of extracellular matrix [24], artificial scaffolds were not used in the present *in vitro* cardiovascular construct. Our result demonstrated that seeding of hPSC-CM to already formed vascular-like network orientates the CM mostly parallel with tubule structures. Moreover, as detected in 3D projection, some CM were seen to surround the tubule structures. Fibroblasts are known to produce extracellular matrix components and enhance alignment of cardiomyocytes [5]. Also in our cardiovascular construct the presence of fibroblasts was likely to enhance orientation of hPSC-CM with vascular-like structures.

As already reported in our previous study, the vascular-like network formed by HUVEC and fibroblasts served as a supporting platform for the cardiomyocytes [33]. Our new results showed that the expression of several growth factors including vascular endothelial growth factor (VEGF), fibroblast growth factor 2 (FGF-2), angiopoietin 1, platelet derived growth factor beta (PDGF-β) and transforming growth factor beta (TGF-β) was active in vascular-like network throughout the experiment. In addition, angiopoietin 2, a marker of early stage tubule formation, was shown to increase from day 1 to day 18 suggesting an ongoing tubule formation process in vascular-like network. In cardiovascular construct, expression of growth factors had a similar trend. However, expression of VEGF and PDGF-β was increased in cardiovascular construct suggesting an active production of these growth factors.

After seeding of CM (day 6), vascular-like network was shown to regress in the absence of VEGF and FGF-2. This was detected in gene expression studies with the low expression of angiopoietin 2 in cardiovascular construct compared to vascular-like network at day 18. It has been previously reported that in the absence of angiogenic stimulatory signals, such as VEGF, regression of the vessels occurs [38]. However, the regression of vascular-like structures did not seem affect to the cardiomyocyte

viability or contractility as detected in the MEA and calcium metabolism measurements that were performed 4-12 days after seeding of hPSC-CM. These results suggest that cell-cell as well as cell-matrix interactions, instead of completely developed vascular structures, are critical for cardiomyocyte viability and functionality.

Beside to cell-cell and cell-matrix contacts, the paracrine effects of the co-cultured cells are most likely important. Vascular endothelial cells have been shown to produce several angiogenic and anti-apoptotic factors compounds including VEGF and angiopoietins that influence cardiac metabolism, growth and contractility [3]. Fibroblasts also secrete angiogenic factors in addition to growth and differentiation factors that have autocrine and paracrine effects [5, 8]. Furthermore, endothelial-cardiomyocyte contacts are known to be crucial in maintaining the rhythmic and synchronous contraction of cardiomyocytes [3]. All these earlier findings support our results indicating that mature vascular-like structures are not necessary for the development of functional cardiovascular construct.

Although the major ionic currents normally present in adult CM are expressed also in hPSC-CM [14] differences are seen in the expression levels of cardiac ion channels and in calcium handling genes [39]. Our gene expression data showed that in the presence of vascular-like network the expression of transcripts of sodium (SCN5A) and calcium (CACNA1C) channels were increased during the days 7-18, while the level of a potassium channel (KCNJ2) remained constant. More importantly, all these genes were expressed at higher level in the cardiovascular construct compared to CM monoculture at the end of the experiment. SCN5A gene codes the cardiac sodium channel $Na_V1.5$ which functions in the fast depolarization phase of the cardiac action potential. The expression level of SCN5A has been reported to increase when hPSC-CM were maturated upon electrical stimulation [20]. In addition, the expression of CACNA1C, gene coding the L-type Ca^+ -channel Cav 1.2, was also shown to increase in co-culture with hESC-derived endothelial cells and human amniotic mesenchymal stem cells [35]. The expression level of KCNJ2 that codes the Kir2.1 channel responsible for the inward rectifier potassium current (I_{K1}), has been reported to significantly increase during hESC-CM maturation [19] and in culture with endothelial cells [35]. Despite the relative short co-culture time with vascular-like network, cardiomyocytes in cardiovascular construct expressed these ion channel-coding genes at higher level compared to CM monoculture. The increased expression indicates that the aforementioned currents are increasingly present in the cardiovascular construct and the hPSC-CM would therefore exhibit electrophysiologically more mature phenotype than the monoculture of CM.

MEA measurements showed that E-4031 increased significantly the field potential duration and arrhythmogenicity in the cardiovascular construct as well as in CM monoculture Calcium imaging analysis showed that Ca^{2+} transients were detectable and adrenaline responses evident in the cardiovascular construct. We detected that adrenaline increased significantly the beating frequency of cardiovascular construct compared to CM monoculture. This was evident in field potential recordings as well as in Ca^{2+} cycling measurements and further confirmed by gene expression analysis. A significantly higher expression of *ADRB1*, a gene encoding the β1-adrenoreceptor, was detected in the cardiovascular construct compared to CM monoculture which further supports the conclusion that vascular-like network has positive effect on the maturation status of the hPSC-CM.

Although earlier studies have shown that co-culture with endothelial cells and fibroblasts enhances the formation of more mature-like morphology of cardiomyocytes, increases the expression of cardiac specific genes and their electromechanical properties [34, 35, 40], they are based on the utilization of different artificial scaffolds. In the present study, vascular-like network served as a natural, supporting and interactive platform for the hPSC-CM. Enhanced maturation of hPSC-CM detected in already 12 days suggests that the cardiovascular construct provides more rapid test system. In addition, we detected increased sensitivity in response to adrenalin that is likely due to higher expression of the β1-adrenoreceptor in cardiovascular construct compared to CM monoculture.

The specific mechanism which vascular-like network enhances the maturation state of hPSC-CM remains unknown. However, it can by hypothesized that neighboring non-myocytes could enhance the electrical maturation of hPSC-CM in cardiovascular construct by secreting paracrine factors or non-cardiac cells might enhance CM signal propagation through cell-to-cell contacts as also suggested by others [41, 42].

In conclusion, the vascular-like network composed of HUVEC and fibroblasts improves the morphological and electrophysiological maturation state of hPSC-CM. Optimal microenvironment for CM is likely essential for proper functioning of the cells and the cardiovascular construct could serve as a more mature and advanced test systems in the cardiac safety and efficacy assessment.

Funding

This study was supported by the Finnish Funding Agency for Innovation, Ministry of Agriculture and Forestry and Finnish Cardiovascular Foundation. In addition, FinPharma Doctoral Programme, Orion Pharma, Pirkanmaa Hospital District Foundation and Finnish Cultural Foundation supported this work.

Acknowledgments

We sincerely thank Ms Mirja Hyppönen, Ms Paula Helpiölä, Ms Sari Leinonen, Ms Hilkka Mäkinen and Ms Henna Venäläinen for the excellent technical assistance. We also want to thank Dr Erja Kerkelä for her contribution to this work.

Conflict of Interest: none declared.

REFERENCES

1. Chien KR, Domian IJ, Parker KK. Cardiogenesis and the complex biology of regenerative cardiovascular medicine. *Science* 2008;**322**:1494-7.

2. Soonpaa MH, Field LJ. Survey of studies examining mammalian cardiomyocyte DNA synthesis. *Circ Res* 1998;**83**:15-26.

3. Brutsaert DL. Cardiac endothelial-myocardial signaling: Its role in cardiac growth, contractile performance, and rhythmicity. *Physiol Rev* 2003;**83**:59-115.

4. van Spreeuwel AC, Bax NA, Bastiaens AJ, Foolen J, Loerakker S, Borochin M, van der Schaft DW, Chen CS, Baaijens FP, Bouten CV. The influence of matrix (an)isotropy on cardiomyocyte contraction in engineered cardiac microtissues. *Integr Biol (Camb)* 2014;**6**:422-9.

5. Pfannkuche K, Neuss S, Pillekamp F, Frenzel LP, Attia W, Hannes T, Salber J, Hoss M, Zenke M, Fleischmann BK, et al. Fibroblasts facilitate the engraftment of embryonic stem cell-derived cardiomyocytes on three-dimensional collagen matrices and aggregation in hanging drops. *Stem Cells Dev* 2010;**19**:1589-99.

6. Garzoni LR, Rossi MID, de Barros APDN, Guarani V, Keramidas M, Balottin LBL, Adesse D, Takiya CM, Manso PP, Otazú IB, et al. Dissecting coronary angiogenesis: 3D co-culture of cardiomyocytes with endothelial or mesenchymal cells. *Exp Cell Res* 2009;**315**:3406-18.

7. Bhattacharya S, Macdonald ST, Farthing CR. Molecular mechanisms controlling the coupled development of myocardium and coronary vasculature. *Clin Sci (Lond)* 2006;**111**:35-46.

8. Wong T, McGrath JA, Navsaria H. The role of fibroblasts in tissue engineering and regeneration. *Br J Dermatol* 2007;**156**:1149-55.

9. Braam SR, Tertoolen L, van de Stolpe A, Meyer T, Passier R, Mummery CL. Prediction of drug-induced cardiotoxicity using human embryonic stem cell-derived cardiomyocytes. *Stem Cell Res* 2010;**4**:107-16.

10. Feric NT, Radisic M. Towards adult-like human engineered cardiac tissue: Maturing human pluripotent stem cell-derived cardiomyocytes in human engineered cardiac tissues. *Adv Drug Deliv Rev* 2015. Epub ahead of print.

11. Polini A, Prodanov L, Bhise NS, Manoharan V, Dokmeci MR, Khademhosseini A. Organs-on-a-chip: A new tool for drug discovery. *Expert Opin Drug Discov* 2014;**9**:335-52.

12. Martin RL, McDermott JS, Salmen HJ, Palmatier J, Cox BF, Gintant GA. The utility of hERG and repolarization assays in evaluating delayed cardiac repolarization: Influence of multi-channel block. *J Cardiovasc Pharmacol* 2004;**43**:369-79.

13. Kettenhofen R, Bohlen H. Preclinical assessment of cardiac toxicity. *Drug Discov Today* 2008;**13**:702-7.

14. Robertson C, Tran DD, George SC. Concise review: Maturation phases of human pluripotent stem cell-derived cardiomyocytes. *Stem Cells* 2013;**31**:829-37.

15. Davila JC, Cezar GG, Thiede M, Strom S, Miki T, Trosko J. Use and application of stem cells in toxicology. *Toxicol Sci* 2004;**79**:214-23.

16. Snir M, Kehat I, Gepstein A, Coleman R, Itskovitz-Eldor J, Livne E, Gepstein L. Assessment of the ultrastructural and proliferative properties of human embryonic stem cell-derived cardiomyocytes. *Am J Physiol Heart Circ Physiol* 2003;**285**:H2355-63.

17. Hartman ME, Dai DF, Laflamme MA. Human pluripotent stem cells: Prospects and challenges as a source of cardiomyocytes for in vitro modeling and cell-based cardiac repair. *Adv Drug Deliv Rev* 2015. Epub ahead of print.

18. Gupta MK, Illich DJ, Gaarz A, Matzkies M, Nguemo F, Pfannkuche K, Liang H, Classen S, Reppel M, Schultze JL, et al. Global transcriptional profiles of beating clusters derived from human induced pluripotent stem cells and embryonic stem cells are highly similar. *BMC Dev Biol 2010*;**10**.

19. Sartiani L, Bettiol E, Stillitano F, Mugelli A, Cerbai E, Jaconi ME. Developmental changes in cardiomyocytes differentiated from human embryonic stem cells: A molecular and electrophysiological approach. *Stem Cells* 2007;**25**:1136-44.

20. Chan YC, Ting S, Lee YK, Ng KM, Zhang J, Chen Z, Siu CW, Oh SK, Tse HF. Electrical stimulation promotes maturation of cardiomyocytes derived from human embryonic stem cells. *J Cardiovasc Transl Res* 2013;**6**:989-99.

21. Schaaf S, Shibamiya A, Mewe M, Eder A, Stohr A, Hirt MN, Rau T, Zimmermann WH, Conradi L, Eschenhagen T, et al. Human engineered heart tissue as a versatile tool in basic research and preclinical toxicology. *PLoS One* 2011;**6**:e26397.

22. Valarmathi MT, Goodwin RL, Fuseler JW, Davis JM, Yost MJ, Potts JD. A 3-D cardiac muscle construct for exploring adult marrow stem cell based myocardial regeneration. *Biomaterials* 2010;**31**:3185-200.

23. Pontes Soares C, Midlej V, de Oliveira ME, Benchimol M, Costa ML, Mermelstein C. 2D and 3D-organized cardiac cells shows differences in cellular morphology, adhesion junctions, presence of myofibrils and protein expression. *PLoS One* 2012;**7**:e38147.

24. Norotte C, Marga FS, Niklason LE, Forgacs G. Scaffold-free vascular tissue engineering using bioprinting. *Biomaterials* 2009;**30**:5910-7.

25. Sarkanen JR, Mannerstrom M, Vuorenpaa H, Uotila J, Ylikomi T, Heinonen T. Intra-laboratory pre-validation of a human cell based in vitro angiogenesis assay for testing angiogenesis modulators. *Front Pharmacol* 2011;**20**;1:147.

26. Takahashi K, Tanabe K, Ohnuki M, Narita M, Ichisaka T, Tomoda K, Yamanaka S. Induction of pluripotent stem cells from adult human fibroblasts by defined factors. *Cell* 2007;**131**:861-72.

27. Lahti AL, Kujala VJ, Chapman H, Koivisto AP, Pekkanen-Mattila M, Kerkela E, Hyttinen J, Kontula K, Swan H, Conklin BR, et al. Model for long QT syndrome type 2 using human iPS cells demonstrates arrhythmogenic characteristics in cell culture. *Dis Model Mech* 2012;**5**:220-30.

28. Mummery C, Ward-van Oostwaard D, Doevendans P, Spijker R, van den Brink S, Hassink R, van der Heyden M, Opthof T, Pera M, de la Riviere AB, et al. Differentiation of human embryonic stem cells to cardiomyocytes: Role of coculture with visceral endoderm-like cells. *Circulation* 2003;**107:**2733-40.

29. Lian X, Zhang J, Azarin SM, Zhu K, Hazeltine LB, Bao X, Hsiao C, Kamp TJ, Palecek SP. Directed cardiomyocyte differentiation from human pluripotent stem cells by modulating wnt/beta-catenin signaling under fully defined conditions. *Nat Protoc* 2013;**8**:162-75.

30. Livak KJ, Schmittgen TD. Analysis of relative gene expression data using real-time quantitative PCR and the 2(-delta delta C(T)) method. *Methods* 2001;**25**:402-8.

31. Engle SJ, Puppala D. Integrating human pluripotent stem cells into drug development. Cell *Stem Cell* 2013;**12**:669-77.

32. Pfannkuche K, Hannes T, Khalil M, Noghabi MS, Morshedi A, Hescheler J, Droge P. Induced pluripotent stem cells: A new approach for physiological research. *Cell Physiol Biochem*;**26**:105-24.

33. Vuorenpaa H, Ikonen L, Kujala K, Huttala O, Sarkanen JR, Ylikomi T, Aalto-Setala K, Heinonen T. Novel in vitro cardiovascular constructs composed of vascular-like networks and cardiomyocytes. *In Vitro Cell Dev Biol Anim* 2014;**50**:275-86.

34. Caspi O, Lesman A, Basevitch Y, Gepstein A, Arbel G, Habib IH, Gepstein L, Levenberg S. Tissue engineering of vascularized cardiac muscle from human embryonic stem cells. *Circ Res* 2007;**100**:263-72.

35. Burridge PW, Metzler SA, Nakayama KH, Abilez OJ, Simmons CS, Bruce MA, Matsuura Y, Kim P, Wu JC, Butte M, et al. Multi-cellular interactions sustain long-term contractility of human pluripotent stem cell-derived cardiomyocytes. *Am J Transl Res* 2014;**6**:724-35.

36. Pong T, Adams WJ, Bray MA, Feinberg AW, Sheehy SP, Werdich AA, Parker KK. Hierarchical architecture influences calcium dynamics in engineered cardiac muscle. *Exp Biol Med (Maywood)* 2011;**236**:366-73.

37. Feinberg AW, Alford PW, Jin H, Ripplinger CM, Werdich AA, Sheehy SP, Grosberg A, Parker KK. Controlling the contractile strength of engineered cardiac muscle by hierarchal tissue architecture. *Biomaterials* 2012;**33**:5732-41.

38. Liekens S, De Clercq E, Neyts J. Angiogenesis: Regulators and clinical applications. *Biochem Pharmacol* 2001;**61**:253-70.

39. Synnergren J, Giesler TL, Adak S, Tandon R, Noaksson K, Lindahl A, Nilsson P, Nelson D, Olsson B, Englund MC, et al. Differentiating human embryonic stem cells express a unique housekeeping gene signature. *Stem Cells* 2007;**25**:473-80.

40. Radisic M, Park H, Martens TP, Salazar-Lazaro JE, Geng W, Wang Y, Langer R, Freed LE, Vunjak-Novakovic G. Pre-treatment of synthetic elastomeric scaffolds by cardiac fibroblasts improves engineered heart tissue. *J Biomed Mater Res A* 2008;**86**:713-24.

41. Sekine H, Shimizu T, Hobo K, Sekiya S, Yang J, Yamato M, Kurosawa H, Kobayashi E, Okano T. Endothelial cell coculture within tissue-engineered cardiomyocyte sheets enhances neovascularization and improves cardiac function of ischemic hearts. *Circulation* 2008;**118**:S145-52.

42. Narmoneva DA, Vukmirovic R, Davis ME, Kamm RD, Lee RT. Endothelial cells promote cardiac myocyte survival and spatial reorganization: Implications for cardiac regeneration. *Circulation* 2004;**110**:962-8.

Tables

Table 1. Culture media used for development of cell models.

Acronym	Basal medium	Serum	Growth factors	Supplementation
Fibroblast medium	MEM	10 % FBS	-	1% l-glutamine, 1% NEAA
EGM-2 medium	EBM-2	2 % FBS	VEGF, FGF-2, IGF, EGF	hydrocortisone, ascorbic acid, heparin
Angiogenic stimulation medium	EBM-2	2 % FBS	10 ng/ml VEGF, 1 ng/ml FGF-2	1 % l-glutamine
EB 5%	DMEM/F12	5% FBS	-	1 % NEAA, 1 % Glutamax, 0,5 % Pen/Strep

VEGF, Vascular Endothelial Growth Factor
FGF-2, Fibroblast Growth Factor 2
IGF, Insulin-like Growth Factor
EGF, Epidermal Growth Factor

Figures

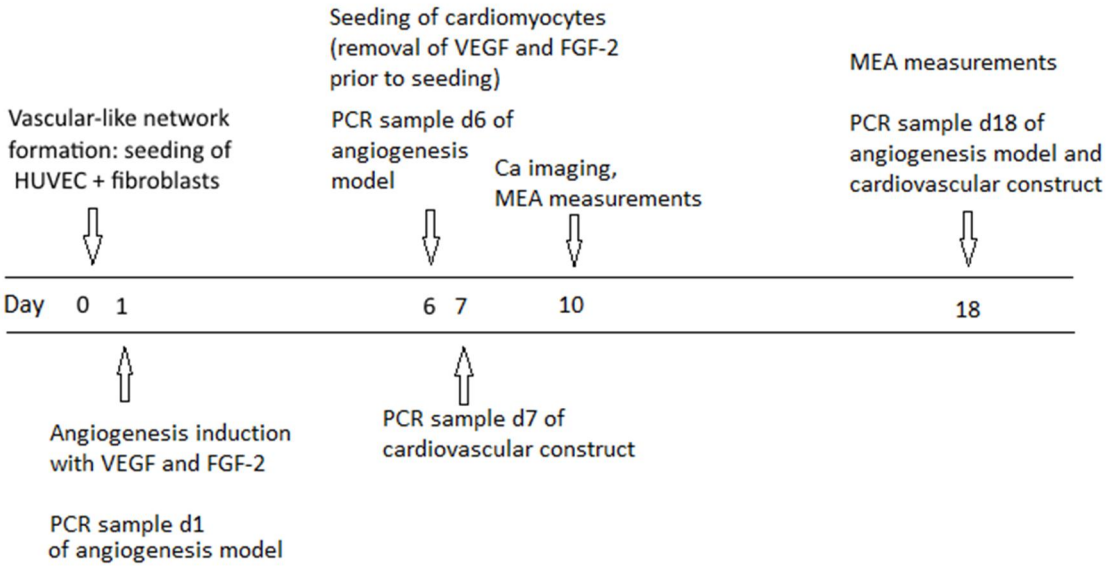

Figure 1. Establishment of cardiovascular construct and different end points.

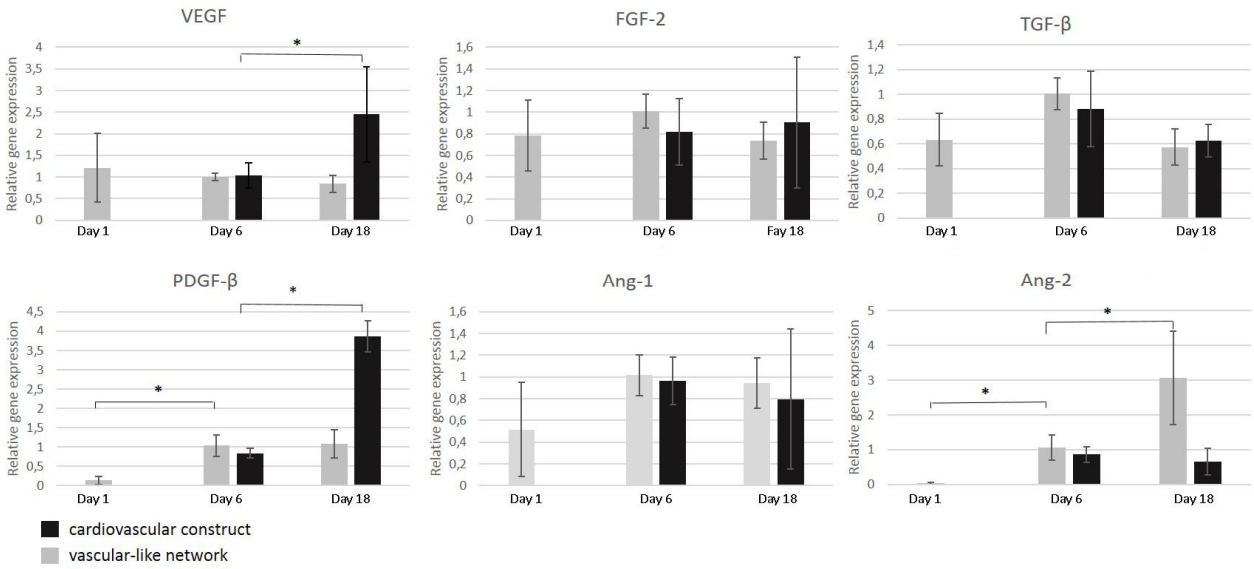

Figure 2. Expression levels of angiogenesis related genes vascular endothelial growth factor (*VEGF*), fibroblast growth factor 2 (*FGF-2*), transforming growth factor beta (*TGF-β*), angiopoietin 1 (*ANG-1*), angiopoietin 2 (*ANG-2*) and platelet derived growth factor beta (*PDGF-β*) in cardiovascular construct and in vascular-like network at time points 0, 6 and 18. * $p<0.05$.

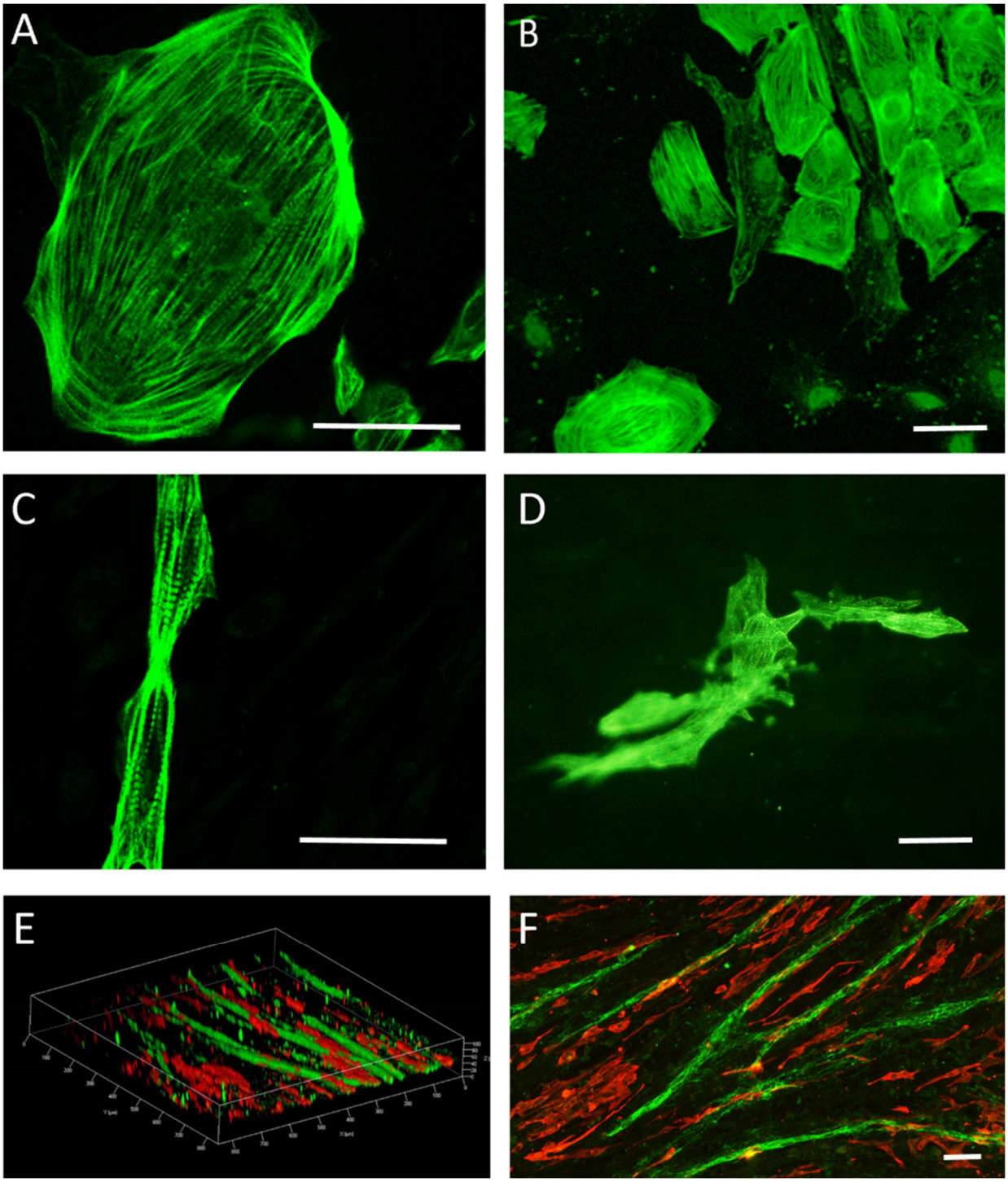

Figure 3. Morphology of human stem cell derived cardiomyocytes in (A-B) cardiomyocyte monoculture and in (C-D) cardiovascular construct. (E-F) Orientation of human stem cell derived cardiomyocytes (troponin t, red) with vascular-like network (collagen IV, red) in cardiovascular construct. Scale bars 50 µm.

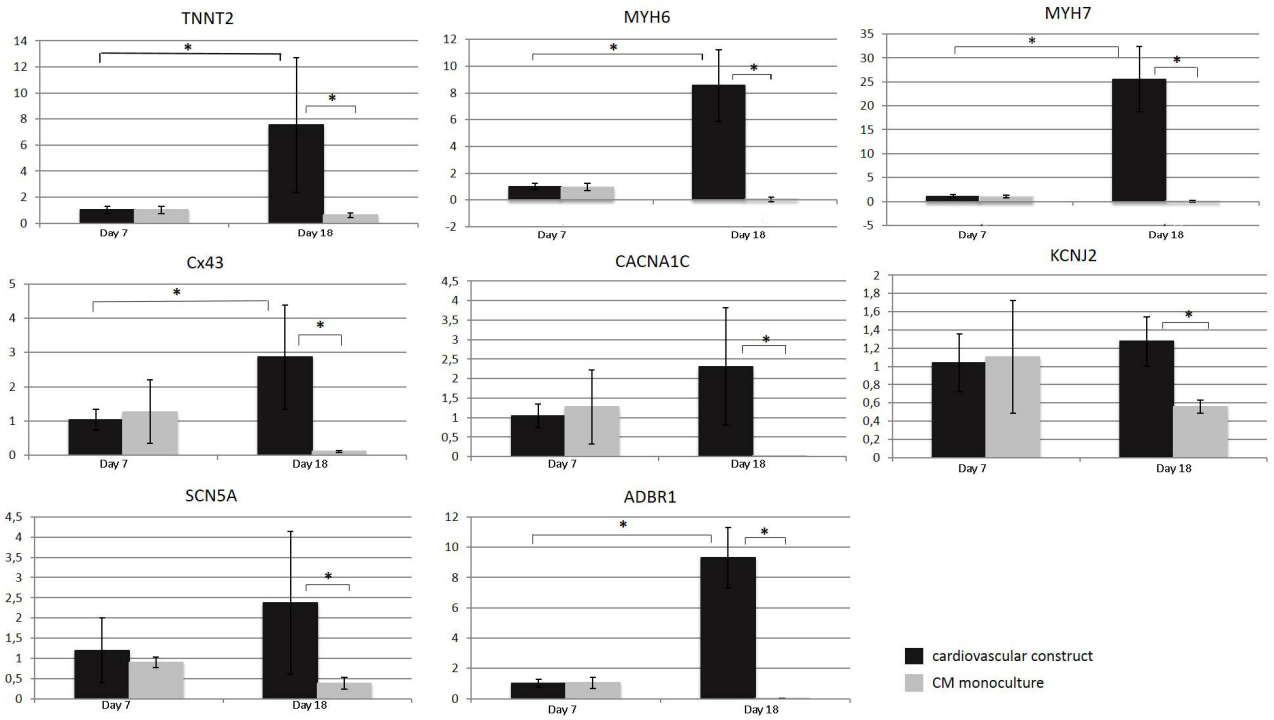

Figure 4**.** Expression of levels of cardiac related genes troponin t (*TNNT*), cardiac muscle myosins (*MYH6*, *MYH 7*), connexin 43 (*Cx43*), calcium channel (*CACNA1C*), potassium channel (*KCNJ2*), sodium channel (*SCN5A*) and beta-1-adrenergic receptor (*ADBR1*) at time points 7 and day 18 in cardiomyocyte monoculture and in cardiovascular construct.* $p<0.05$.

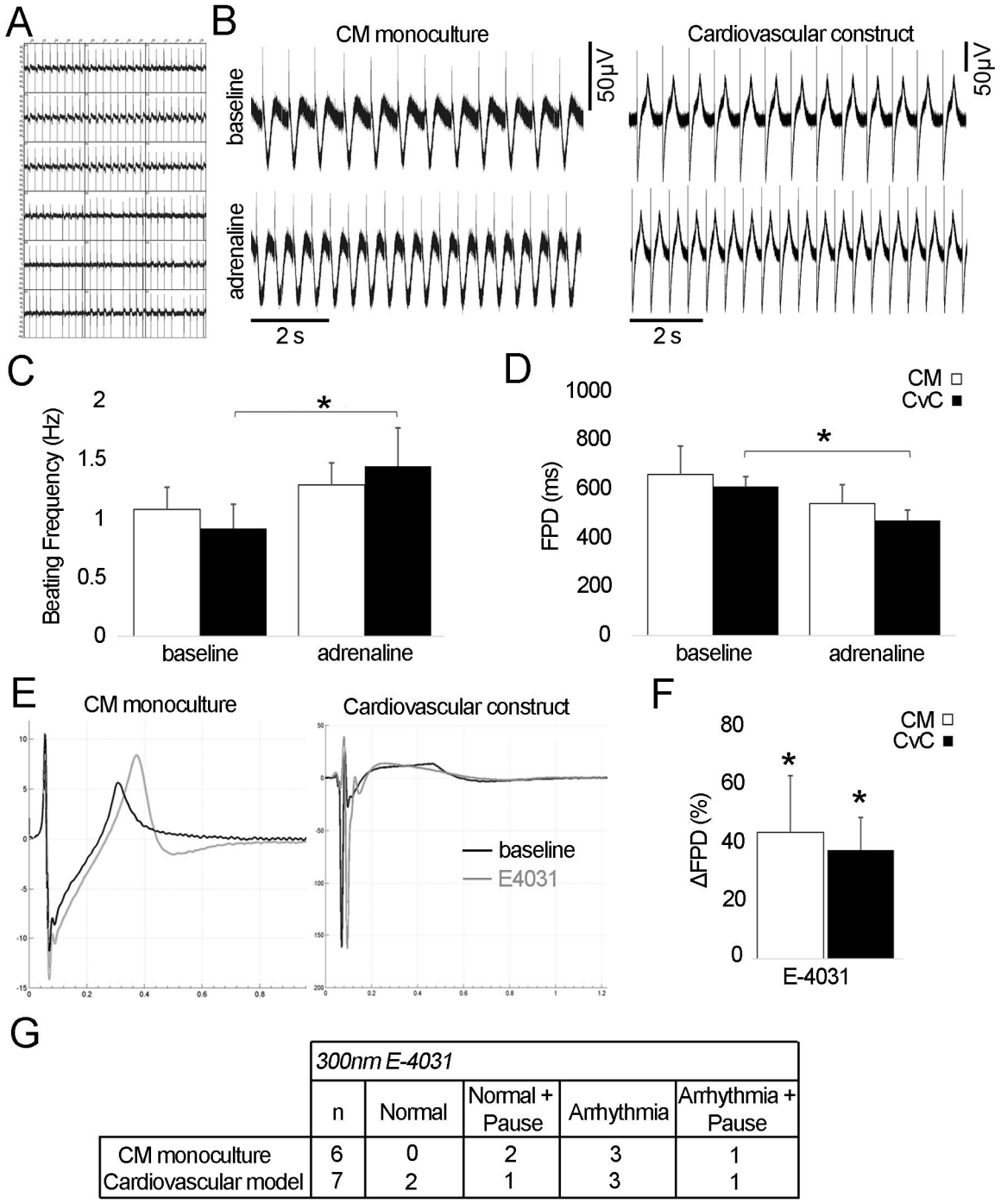

	300nm E-4031				
	n	Normal	Normal + Pause	Arrhythmia	Arrhythmia + Pause
CM monoculture	6	0	2	3	1
Cardiovascular model	7	2	1	3	1

Figure 5. MEA measurements of the cardiovascular construct. (A) The electrical activity of the cardiovascular construct was detectable with MEA and the contractility was synchronous. (B) Representative field potential traces of the effect of β-adrenergic agonist adrenaline (1 uM). (C) Beating frequencies and (D) field potential durations in MEA measurements. In (C) and (D) n=5 in CM monoculture and in cardiovascular construct. (E) Overlay plot showing the effect of 300nM E-4031 on field potential duration. (F) E-4031 responses in CM monoculture (n=6) and cardiovascular construct (n=7). Change in the field potential duration was calculated as relative change from the baseline. No significant difference between CM monoculture and cardiovascular construct. (G) Adverse effects of E-4031. The number indicates how many replicates were affected. Normal: no arrhythmias, Normal+Pause: no arrhythmias but field potential activity terminates, Arrhythmia: arrhythmias affecting amplitude and frequency, Arrhythmia+Pause: arrhythmias leading to termination of beating activity. CM=cardiomyocytes; CvC=cardiovascular construct. * $p<0.05$.

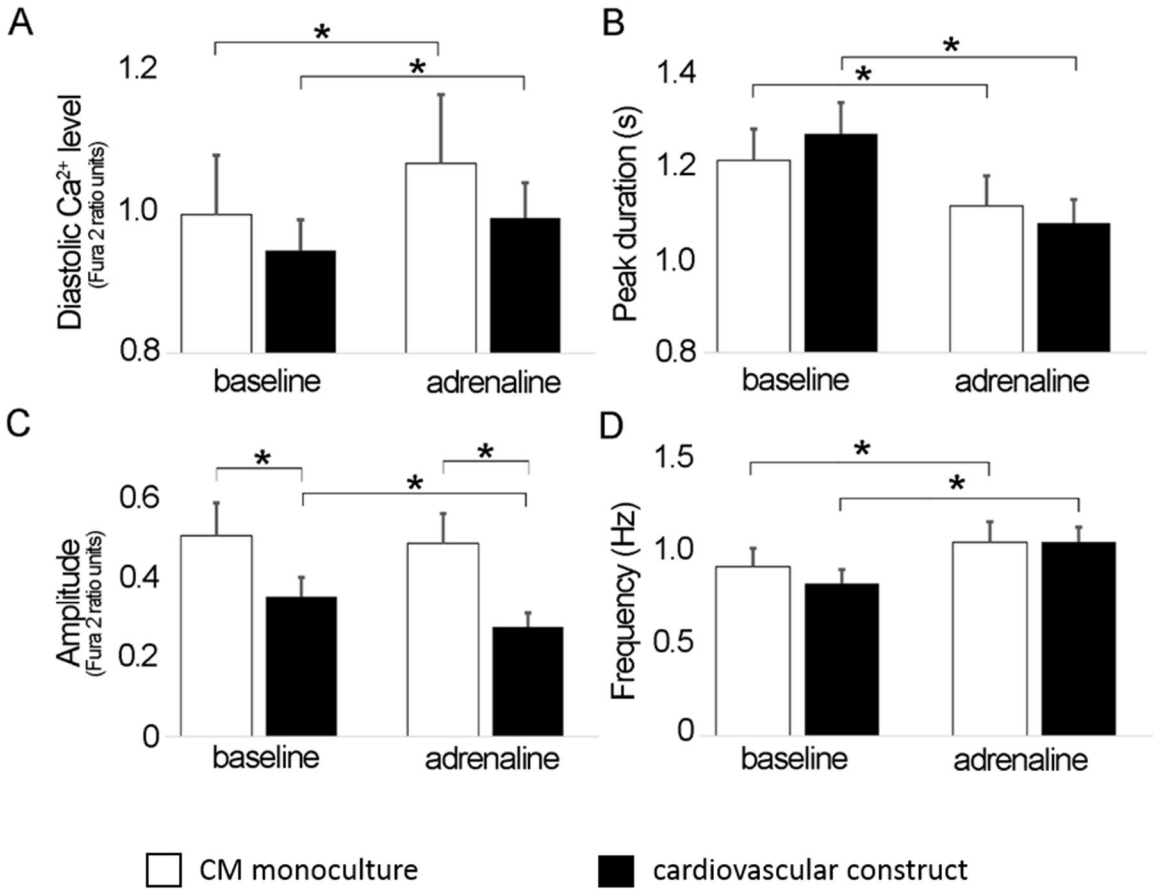

Figure 6. Ca^{2+} measurements of the cardiovascular construct and cardiomyocyte monoculture in baseline and after adrenalin exposure represented as (A) diastolic Ca^{2+} levels; (B) peak duration; (C) amplitude and (D) frequency. CM monoculture n=16, cardiovascular construct n=26. * $p<0.05$.

Supplemental data

Primer sequences for SYBR green qPCR.

Gene	Forward Primer	Reverse Primer
VEFG-A	AGGGCAGAATCATCACGAAGT	AGGGTCTCGATTGGATGGCA
FGF-2	AGAAGAGCGACCCTCACATCA	CGGTTAGCACACACTCCTTTG
PDGFβ	CTCGATCCGCTCCTTTGATGA	CGTTGGTGCGGTCTATGAG
TGFβ1	CAATTCCTGGCGATACCTCAG	GCACAACTCCGGTGACATCAA
Angiopoietin1	AGCGCCGAAGTCCAGAAAAC	TACTCTCACGACAGTTGCCAT
Angiopoietin2	ACCCCACTGTTGCTAAAGAAGA	CCATCCTCACGTCGCTGAATA
CACNA 1C	TGACATCGAGGGAGAAAACT	ACATTAGACTTGACTGCGGC
TNNT2	TTCACCAAAGATCTGCTCCTCGCT	TTATTACTGGTGTGGAGTGGGTGTGG
KCNJ2	GAGCACAGCTCCTCAAATCC	TTCCACTGTCAAACCCAACA
CX-43	GGTCTGAGTGCCTGAACTTGCCT	TGCCTGGGCACCACTCTTTTGC
MYH6	AGGGATAACCAGGGGAAGCACC	TGCGAATGTCAAAGGGCCGGG
MYH7	GGCAAGACAGTGACCGTGAAG	CGTAGCGATCCTTGAGGTTGTA

Figures

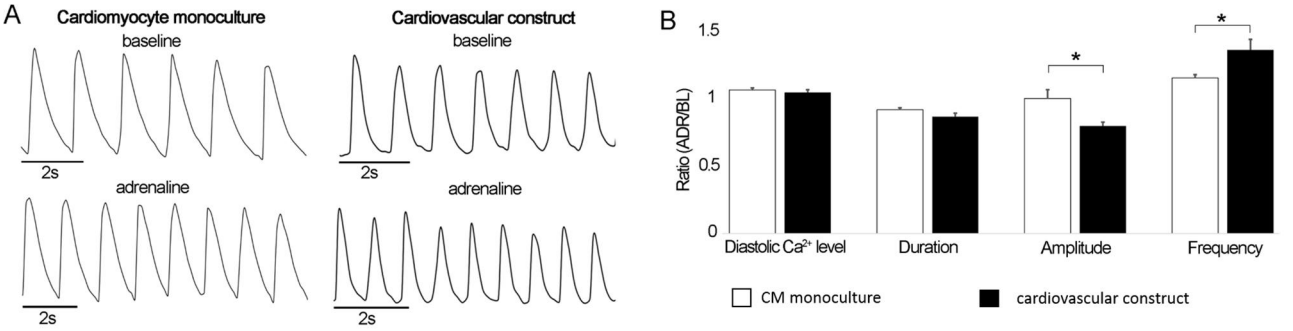

Figure S1. Ca^{2+} measurements of the cardiovascular construct and cardiomyocyte monoculture (A) Ca^{2+} traces of cardiomyocyte monoculture and cardiovascular construct at baseline and after adrenalin exposure. (B) Diastolic Ca^{2+} level and duration, amplitude and frequency of calcium transients in cardiomyocyte monoculture and in cardiovascular construct were analyzed separately for each cell as the ratio of adrenaline response divided by baseline response. CM monoculture n=16, cardiovascular construct n=26. * $p<0.05$.